Investigation of the Structure-Function Relationship of the PDZ G-Nucleotide Exchange Factor (PDZ-GEF) Dizzy in *Drosophila*

Dissertation

der Mathematisch-Naturwissenschaftlichen Fakultät

der Eberhard Karls Universität Tübingen

zur Erlangung des Grades eines

Doktors der Naturwissenschaften

(Dr. rer. nat.)

vorgelegt von

Annemarie Witz (M.Sc.)

aus Neumarkt (Rumänien)

Tübingen

2023

*"Science, my lad, is made up of mistakes,
but they are mistakes which it is useful to make,
because they lead little by little to the truth."*

Jules Verne, A Journey to the Center of the Earth

Abbreviations

aa	amino acids	GDP	guanosine diphosphate
ABC	Avidin Biotin Complex	GTP	guanosine triphosphate
bp	nucleotide base pairs	hs	heat shock
C3G	Crk SH3-domain-binding guanine nucleotide releasing factor	kb	kilo base pair
		MAGI	membrane-associated guanylate kinase
cDNA	complementary DNA	min	minute
cNMP	cyclic nucleotide monophosphate-binding-domain	NGS	normal goat serum
		ORF	open reading frame
		PBM	PDZ binding motif
Cy	Cyanine	PDZ	PSD-95/DISC-large/ZO-1
CyO	Curly of Oster	PRM	proline-rich motif
DAB	3,3'-diaminobenzidine	RA	Ras association or Ral-GDS/AF6
ddH$_2$O	double-distilled water		
DIG	dioxygenin	Rap1	Ras-related protein 1
DNA	deoxyribonucleic acid	RasGEF	Ras guanine-nucleotide-exchange factor domain
dNTPs	deoxynucleotide triphosphates		
Dzy	Dizzy	RNA	ribonucleic acid
ECM	extracellular matrix	Sb	Stubble
egfp	enhanced green fluorescent protein	sec	second
		srp	serpent
EP-element	enhancer promotor element	srph	serpent hemocyte enhancer
Epac	exchange protein activated by cAMP	tub	tubulin
		UAS	upstream activating sequences
EST	expressed sequence Tag		
GAP	GTPase-activating protein	V	volt
GEF	guanine-nucleotide-exchange factor	VNC	ventral nerve cord
		wt	wild-type
GFP	Green fluorescent protein		

Abstract

The migration of embryonic macrophages in the fruit fly is an ideal system to investigate the regulation and the mechanisms of cell movement *in vivo*. The macrophages originate from the cephalic mesoderm and perform a complex migration throughout the entire embryo. The *Drosophila* PDZ G-nucleotide exchange factor (PDZ-GEF) Dzy was identified as an essential component in macrophages for proper migration and cell shape regulation. In mutants lacking *dzy* function, macrophages have smaller cellular protrusions and migrate less efficiently. In contrast, macrophages overexpressing *dzy* are vastly enlarged and form multiple long protrusions. Additionally, *dzy* is known to play a role in adult morphogenesis. Homozygous *dzy* mutants are lethal, but "escaper" flies are occasionally observed, showing a characteristic phenotype with bent downward wings, rough eyes and distorted genitalia. The Dzy protein contains several conserved domains found in PDZ-GEFs and is expressed in three isoforms (*dzyA*, *dzyB* and *dzyC*) due to alternative splicing of the mRNA. While all domains typical of PDZ-GEFs are equally present in all isoforms, the variable regions have three proline-rich motifs (PRMs), of which DzyA and DzyB have all three and DzyC only one. Here we explore the function of the N-terminal PDZ domain and of the different isoforms which are distinguished by their unique C-termini and the presence or absence of two proline-rich motifs (PRMs). Both structural features, the PDZ domain and PRMs, are often involved in protein-protein interactions. Here we tested the relevance of the PDZ domain and PRMs for the function of Dzy in macrophage migration. We investigated the impact of the ΔPDZ form and the different splice forms on the migration of macrophages by analysing their overexpression phenotypes. Furthermore, we examined the ability of the various forms to provide full wild-type *dzy* function. Our findings on the function of *dzy* revealed that *dzyC* is the only splice form capable of causing cell shape changes when expressed in macrophages. Furthermore, we found that the *dzyC* splice form is also sufficient to partially rescue the phenotype of homozygous *dzy* mutant adult escapers. The only difference between *dzyC* and the other two splice forms (*dzyA* and *dzyB*) is the presence or absence of exon 5 in the different splice forms. Therefore, the domain encoded by exon 5 is the key component in regulating the activity of the different splice forms. We hypothesised that the PRMs encoded by exon 5 interact intramolecularly with the Dzy PDZ domain and have a function-inhibiting effect. This suggests a novel PDZ-GEF regulatory mechanism which is dependent on alternative splicing. Thus, extending this model is a promising endeavour to elucidate the molecular mechanisms that cause and control the process of cell migration in all organisms.

Zusammenfassung

Die Wanderung embryonaler Makrophagen in der Fruchtfliege ist ein ideales Modellsystem, um die Mechanismen und die Regulation der Zellbewegung *in vivo* zu untersuchen. Während der Embryogenese von *Drosophila melanogaster* wandern Makrophagen, die aus dem Kopfmesoderm stammen, entlang stereotyper Routen, um den gesamten Embryo zu besiedeln. Eine wichtige Komponente, die diesen Wanderungsprozess beeinflusst, ist der *Drosophila*-PDZ-G-Nukleotidaustauschfaktor (PDZ-GEF) Dzy. Neben vielen weiteren Funktionen hat PDZ-GEF Dzy Auswirkungen auf das Wanderungsverhalten und die Zellform der embryonalen Makrophagen. In Mutanten, die einen Funktionsverlust von Dzy aufweisen, ist die Makrophagenwanderung beeinträchtigt, die Zellen wandern weniger effizient und ihre zellulären Ausläufer sind verkürzt. Im Gegensatz dazu zeigen Makrophagen nach einer Überexpression von *dzy* mehrere verlängerte Zellfortsätze, die sich berühren und Netzwerke bilden können. Darüber hinaus ist bekannt, dass *dzy* eine Rolle bei der Morphogenese von adulten Fliegen spielt. Homozygote *dzy*-Mutanten sind letal, aber gelegentlich werden "Escaper"-Fliegen beobachtet, die einen charakteristischen Phänotyp mit nach unten gebogenen Flügeln, rauen Augen und verformten Genitalien aufweisen. Dzy enthält mehrere konservierte Proteindomänen und wird durch alternatives Spleißen der mRNA in drei Isoformen (*dzyA*, *dzyB* und *dzyC*) exprimiert. Während alle für PDZ-GEFs typischen Domänen in allen Isoformen gleichermaßen enthalten sind, weisen die variablen Regionen drei prolinreiche Motive (PRMs) auf, von denen DzyA und DzyB alle drei besitzen und DzyC nur eines besitzt. Der Schwerpunkt dieser Arbeit liegt auf der Analyse der Funktion der N-terminalen PDZ-Domäne und der verschiedenen *dzy*-Spleißformen, die sich durch ihre individuellen C-Termini und das Vorhandensein oder Fehlen von zwei PRMs unterscheiden. Die beiden strukturellen Komponenten des Dzy-Proteins, die PDZ-Domänen und die PRMs, sind häufig an Protein-Protein-Wechselwirkungen beteiligt. Das vordergründige Ziel dieser Arbeit ist es, die Bedeutung der beiden Domänen für die Funktion von Dzy bei der Makrophagenwanderung zu untersuchen. Dabei haben wir die Auswirkungen der ΔPDZ-Form und der verschiedenen Spleißformen auf die Wanderung der Makrophagen untersucht, indem wir ihre Überexpressionsphänotypen analysierten. Ein weiterer wichtiger Punkt war die Klärung der Frage, inwieweit die verschiedenen Formen in der Lage sind, die *dzy*-Mutanten und deren Defekte zu beheben und die volle Funktion des Wildtyps wiederherzustellen. Unsere Ergebnisse zur Funktion von *dzy* zeigen, dass *dzyC* die einzige Spleißform ist, die Zellformveränderungen hervorrufen kann, wenn sie in Makrophagen exprimiert wird. Des Weiteren haben wir festgestellt, dass die *dzyC*-Spleißform ebenfalls ausreicht, um den Phänotyp homozygoter adulter *dzy*-Mutanten Escaper zumindest teilweise zu retten. Da der einzige Unterschied zwischen *dzyC* und den anderen Spleißformen (*dzyA* und *dzyB*) das

Vorhandensein oder Fehlen von Exon 5 ist, konnte die von Exon 5 kodierte Domäne als eine Schlüsselkomponente bei der Regulation der Aktivität der verschiedenen Spleißformen identifiziert werden. Wir stellten die Hypothese auf, dass die durch Exon 5 kodierten PRMs intramolekular mit der PDZ-Domäne von Dzy interagieren und somit eine funktionshemmende Wirkung auf das Protein haben. Dies deutet auf einen neuartigen PDZ-GEF-Regulationsmechanismus hin, der vom alternativen Spleißen abhängig ist. Daher ist die Erweiterung dieses Modells ein vielversprechendes Unterfangen, um die molekularen Mechanismen aufzuklären, die den Prozess der Zellwanderung in allen Organismen verursachen und steuern.

Contents

VI

1. Introduction

1.1 Cell migration

From worms to humans, cell migration is a fundamental cellular process throughout the entire lifetime of many organisms. During embryonic development, cells migrate to specific places where they differentiate and form various tissues and organs. Later in adult organisms, cell migration is involved in tissue renewal, tissue repair and immune response (Ridley 2001; Huelsmann *et al.* 2006). Disrupted or anomalous cell migration can lead to developmental and pathological defects such as cancer, atherosclerosis and chronic inflammatory diseases. Therefore, understanding the mechanisms that control cell migration may be essential for effective therapeutic approaches to treat diseases (Ridley *et al.* 2003).

<u>The process of cell migration</u>

In general, cell migration is a complex multistep process involving (1) the reorganisation of the actin cytoskeleton and the formation of protrusions, (2) the assembly of new adhesion sites, (3) the contraction and forward movement of the main cell body and (4) the detachment of the tail (Lauffenburger & Horwitz 1996; Ridley 2001; Ridley *et al.* 2003; Paladi & Tepass 2004). The process of cell movement is initiated by migration-promoting cues that release an intracellular response leading to the polarisation of the cell and the formation of actin-based protrusions in the direction of migration. The extension of the protrusions is accompanied by the assembly of molecular structures called focal adhesions that connect the actin cytoskeleton to the ECM. The adhesion sites attach the protrusions to the substrate, provoke a traction force and move the cell body forward by actomyosin-mediated contraction. Finally, the adhesion sites at the rear of the cell are disassembled, allowing the cell tail to detach and migrate towards the guidance cues. The migratory cycle can begin anew by the next extension of the protrusions (Lauffenburger & Horwitz 1996; Mitchison & Cramer 1996; Ridley 2001; Ridley *et al.* 2003; Paladi & Tepass 2004). Therefore, cell adhesion and its regulation is fundamental for cell migration.

<u>Cell migration in the fruit fly *Drosophila melanogaster*</u>

Many cellular and molecular mechanisms have been discovered to be highly conserved between *Drosophila* and mammals (Wang *et al.* 2014). The fruit fly *Drosophila melanogaster* is therefore undoubtledly a powerful model organism for studying almost all essential and fundamental biological processes. It is therefore not suprising that the migration of embryonic macrophages in the fruit fly *Drosophila melanogaster* represents an ideal system for analysing the process of cell migration and its control mechanisms. *Drosophila* generally has the advantages of an intensively researched model organism, including a completely sequenced

genome and the availability of a wide range of genetic tools. In particular, regarding the study of embryonic macrophage migration, *Drosophila* has additional practical features: embryonic macrophages undergo a large-scale migration, they migrate throughout embryogenesis (+/- 20 hours) and their complex migration stereotypically follows some major routes through the fly embryo, suggesting a precise regulation of this process.

1.2 Migration of macrophages in *Drosophila melanogaster*

Many parallels can be drawn between the development of blood cells in vertebrates and haematopoietic processes in *Drosophila* (Evans *et al.* 2003; Evans & Wood 2014; Gold & Brückner 2014), as both processes share many conserved components. Compared to the complexity of blood cell lineages in mammals, the *Drosophila* system is rather simple, as only three types of haemocytes can be distinguished (Crozatier & Meister 2007; Fauvarque & Williams 2011).

<u>The different blood cell types</u>

The blood cells or haemocytes of *Drosophila* belong to three lineages: plasmatocytes, crystal cells and lamellocytes. These three cell types form the cellular part of the embryonic immune system (Meister & Lagueux 2003). *Drosophila* plasmatocytes are phagocytes, similar to the mammalian monocyte/macrophage lineage. The main known functions of these embryonic macrophages are to model and promote organogenesis by phagocytosing apoptotic cell corpses and producing extracellular matrix (ECM) components (Brückner *et al.* 2004; Huelsmann *et al.* 2006; Comber *et al.* 2013). Crystal cells have crystalline inclusions that contain enzymes for melanisation of pathogenic material in the haemolymph. The production of melanin generates cytotoxic free radicals that are involved in killing pathogens (Crozatier & Meister 2007). The embryonic precursors of macrophages and crystal cells have a common origin. This part of the head mesoderm is specified as the haemocyte primordium by the expression of the GATA transcription factor Serpent (Srp), which plays a crucial role in the haemotopoetic development (Rehorn *et al.* 1996; Lebestky *et al.* 2000; Fossett *et al.* 2003; Spahn *et al.* 2014). The differentiation of the blood cells depends on specific transcription factors such as AML-1 protein Lozenge (Lz) and Glia cell missing (Gcm). Serpent is expressed earliest in the haemocyte precursors. Most of the Srp-expressing cells begin to express Gcm and differentiate as macrophages. A small subset of the Srp-expressing cells begins to express Lz; these cells give rise to all crystal cells and a very small proportion of macrophages (Tepass *et al.* 1994; Lebestky *et al.* 2000; Evans *et al.* 2003; Fossett *et al.* 2003; Holz *et al.* 2003). The third lineage, the lamellocytes, differentiate in response of parasitism of the *Drosophila* larvae. The primarily function of these cells is to encapsulate and neutralise objects that are too large

2

to be engulfed by macrophages. Lamellocytes form a multilayered capsule around the invader, accompanied by blackening due to melanisation. Within the capsule, the parasite is eventually killed by a series of cytotoxic intermediates formed during melanin synthesis (Evans *et al.* 2003; Holz *et al.* 2003; Meister & Lagueux 2003).

<u>The haemocyte migration</u>

Blood cell developement in *Drosophila melanogaster* occurs in two waves: A first haematopoetic wave takes place during embryogenesis. In the *Drosophila* embryo, haemocytes originate from the cephalic mesoderm and disperse along invariant migratory paths throughout the embryo (Tepass *et al.* 1994). Beginning with the invagination of the mesoderm during gastrulation (late stage 10), the first haemocytes leave the head and infiltrate the posterior part of the extended germ band (Fig. 1). The germ band of the embryo is extended so that the tail is located next to the head. So, during stage 12, haemocytes enter the tail and are then transported with the retracting germband to populate the posterior of the embryo. Meanwhile, more and more cells leave the head and migrate along the dorsal side of the embryo (Paladi & Tepass 2004; Wood & Jacinto 2007). In the following stages (stage 13 and 14), the haemocytes from the anterior and posterior ends of the embryo migrate towards each other along the nerve cord and the developing gut until the anterior and the posterior populations meet. At these stages, the haemocytes also continue to migrate posteriorly on the dorsal side of the embryo along the developing dorsal vessels and finally disperse throughout the entire embryo. In late stage 14, most parts of the embryo are fairly evenly populated with haemocytes (Tepass *et al.* 1994). These circulating haemocytes are macrophages and account for 95 % of all haemocytes in the embryo. In contrast, the second haemocyte population, the cristal cells, do not migrate but instead remain associated with the foregut (Lebestky *et al.* 2000; Evans *et al.* 2003; Paladi & Tepass 2004; Wood & Jacinto 2007). The molecular mechanisms that regulate this cell migration remain largely unknown (Wood & Jacinto 2007). Embryonic macrophages persist in postembryonic stages and form a significant part of the adult blood cell population, which is supplemented by haemocytes that derive from the larval lymph gland (Evans *et al.* 2003; Paladi & Tepass 2004).

The second wave of haematopoesis, the so called larval haematopoesis, takes place in a specialised organ, the lymph gland. The lymph gland, which is of mesodermal origin, consists of a dedicated number of pairs of haemocyte-containing lobes and is located along the dorsal vessel. Fully differentiated haemocytes are released into the circulation. The mature macrophages are part of the *Drosophila* immune system, phagocytosing debris and dead cell bodies and contributing to the secretion of the extracellular matrix. In pupae and adults, the

haemocyte population is composed of a mixture of both embryonic and lymph gland-derived haemocytes (Brückner *et al.* 2004; Huelsmann *et al.* 2006; Crozatier & Meister 2007).

So, in *Drosphila* embryos, macrophages originate from the cephalic mesoderm and follow specific migration patterns through the entire embryo. The molecular mechanisms regulating the process of cell migration remain largely unknown. However, a number of key factors involved in the regulation of this process are already known: (a) One of the key factors identified in this process is the *Drosophila* PDGF/VEGF receptor Pvr, which is required for proper migration and the survival of the macrophages (Cho *et al.* 2002; Brückner *et al.* 2004; Wood *et al.* 2006; Parsons & Foley 2013). The Pvr receptor, which is expressed in the haemocytes, is attracted to the ligands Pvf2 and Pvf3, which are expressed in the different tissues of the embryo. So, the migration of macrophages is guided by the Pvr/Pvf guidance system. (b) Other components involved in the process of cell migration are members of the Rho family of small GTPases. These small GTPases have been identified as key regulations of adhesion and cytoskeletal dynamics during migration (Ridley 2001). *Drosophila* Rho proteins, especially Cdc42, Rac1 and RhoA, are associated with processes such as cell adhesion, cytoskeletal reorganisation and cell migration (Etienne-Manneville & Hall 2002). During cell migration, Cdc42 is a master regulator of the

Fig. 1 Haemocyte migration in the *Drosophila* embryo.
Embryonic haemocytes migrate along invariant pathways to populate the embryo. Haemocytes leave the head and infiltrate the posterior part of the extended germ band (1). Germ-band retraction carries the haemocytes to the posterior end of the egg. Cells from the head migrate along the dorsal side of the embryo (2). Haemocytes from the anterior and the posterior end migrate towards one another along the ventral nerve cord (3). The anterior and the posterior population meet (4). The haemocytes continue to migrate posteriorly on the dorsal side of the embryo (5) (figure from Wood & Jacinto 2007).

initiation and maintenance of cell polarity. Rac1 is required for the initiation and maintenance of protrusion at the leading edge. On the opposite side of the migrating cell, RhoA has a function in the disassembly of the rear adhesion sites and the tail retraction (Etienne-Manneville & Hall 2002; Ridley *et al.* 2003; Paladi & Tepass 2004). (c) The third group of important components relevant to macrophage migration are molecules that play a central role in regulating cell adhesion. Many different factors are involved in regulating cell adhesion during cell migration, including cell surface receptors that mediate cell adhesion. An important
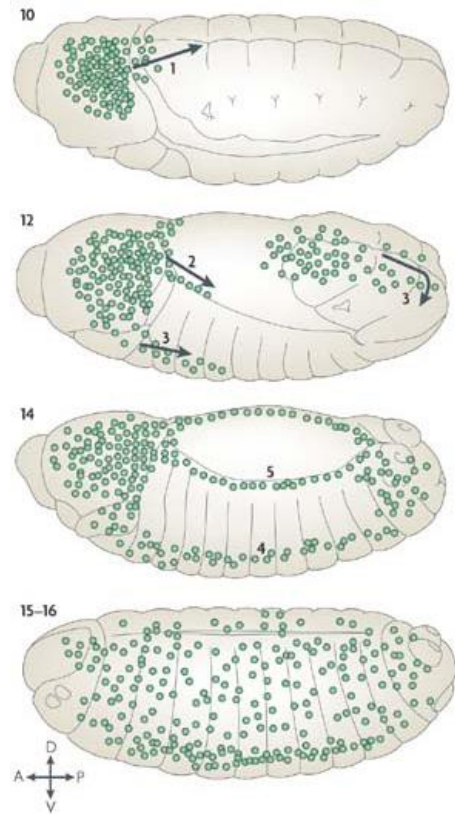
family of these receptors are the integrins (Hynes 1992; Katagiri *et al.* 2003; Huelsmann *et al.* 2006).

1.3 Regulation of migrating macrophages

1.3.1 Integrins and cell migration

Cell adhesion is a very important part of cell migration, and cell surface receptors play an important role in this process. Many different receptors are involved in the migration process of different cell types, and an important family of these migration-promoting receptors are the integrins (Ridley *et al.* 2003; Huelsmann *et al.* 2006). Integrins are heterodimeric intracellular adhesion molecules (ICAMs), consisting of an α- and a β-subunit. Most multicellular organisms have several variants of the two subunits: *C. elegans* has two distinct α-subunits and a single β-subunit, while *Drosophila* has five α-subunits (αPS1-5) and two β-subunits (βPS and βv). In comparison, vertebrates have up to 18 α- and 8 β- subunits (Kinbara *et al.* 2003; Huelsmann *et al.* 2006; Comber *et al.* 2013). So, the two glycoprotein chains occur in different combinations, resulting in a whole repertoire of distinct integrins (Brown *et al.* 2000; Hynes & Zhao 2000). Each of these integrin heterodimers has different ligand-binding and signaling properties.

Integrin-mediated adhesion can be regulated by modulation of integrin affinity to ligands or by changing the local concentration of integrins at the membrane. This regulation of integrin function occurs either at the outside of the cell by the binding of extracellular ligands (outside-in signaling) or from inside the cell by cytoplasmatic signals (inside-out signaling) (Bökel & Brown 2002). The two directions of integrin signaling have different biological consequences: "Inside-out" signaling involves an intracellular molecule binding to the short cytoplasmatic β integrin tail, resulting in conformational changes that regulate affinity to extracellular ligands. "Inside-out" signaling controls processes such as cell adhesion, cell migration and ECM assembly (Kinbara *et al.* 2003; Ginsberg 2014). Integrins also behave like conventional signaling receptors by transmitting information into cells through "outside-in" signaling. Binding of the large extracellular part of the integrin to its extracellular ligands leads to conformational changes and integrin clustering. The combination of these two events initiates intracellular signals that control cell polarity, cytoskeletal structure, cell survival, cell proliferation and gene expression (Bökel & Brown 2002; Hynes 2002; Kinbara *et al.* 2003; Ridley *et al.* 2003; Ginsberg 2014). Many candidates are involved in the process of integrin activation, including small GTPases as important mediators of the signal to integrins. For instance, the small GTPase Rap1 is involved in the regulation of integrin-mediated cell adhesion in several cases during cell migration (Caron *et al.* 2000; Katagiri *et al.* 2000; Reedquist *et al.* 2000; Arai *et al.* 2001; Huelsmann *et al.* 2006).

1.3.2 Small GTPases and cell migration

Small GTPases

Small guanosine triphosphatases (GTPases) are monomeric GTP-binding proteins of 20-25 kDa that act as molecular switches in various cellular and developmental processes, including cell proliferation, differentiation, apoptosis and control of the cytoskeleton (Lee *et al.* 2002; Pannekoek *et al.* 2009; Shirinian *et al.* 2010). There are hundreds of different G-proteins, which are divided into several superfamilies based on their sequence homology and functionality (Zwartkruis & Bos 1999; Wennerberg *et al.* 2005). The Ras superfamily of small GTPases is divided into five subfamilies, including Rho, Rab, Ran, Arf and Ras. Each subfamily is thought to control an important cellular process. In general, the Ras subfamily is dedicated to cell proliferation and differentiation, Rho to cytoskeleton regulation, Rab to membrane trafficking, Ran to nuclear transport and Arf to vesicle transport (Etienne-Manneville & Hall 2002; Caron 2003; Wennerberg *et al.* 2005).

Small GTPases and their function as molecular switches

Thus, small GTPases are master regulators for many aspects of cell biology. Due to their function as binary molecular switches and their interaction with several effector proteins, they are involved in the regulation of a multitude of cellular processes (Ridley 2001). With such a prominent role, it is not suprising that GTPases are tightly regulated (Schmidt & Hall 2002). Small GTPases cycle between an inactive GDP-bound and an active GTP-bound conformation. The activation occurs through the stereotypic GTPase cycle, which is initiated by an upstream signal that induces a target G-protein to exchange a bound GDP molecule for GTP. GTP binding switches the GTPase to its "on" state, which facilitates interaction with downstream signaling effectors. The cycle is completed by GTP hydrolysis to return the G-protein to the GDP-bound "off" state (Etienne-Manneville & Hall 2002; Wennerberg *et al.* 2005). These processes can be accelerated by GTP exchange factors (GEFs), which promote the release of GDP release, and by GTPase-activating proteins (GAPs), which promote GTP hydrolysis (Zwartkruis & Bos 1999; Wennerberg *et al.* 2005). Generally, GTPases are ubiquitously expressed, so that the specification of their signal transduction and their cellular effects depend on the presence and the type of GEFs and GAPs in the cell (Ridley 2001).

Rap1 and Ras

The Ras-like small GTPase Rap1 (Ras related protein-1) belongs to the Ras family of small molecular weight GTPases. The Ras subfamily consists of 19 members, the best characterized of which are further divided into the classic Ras (H-, K- und N-Ras), R-Ras, Ral and Rap groups. The Ras subfamily is known to regulate many physiological responses, including cell adhesion, cell growth, apoptosis, cytoskeletal remodelling, motility and intracellular vesicle transport (Jaśkiewicz *et al.* 2018). In addition to controlling physiological processes, the Ras subfamily also plays an active role in pathological processes. Due to their mutational activation in over 20 % of human cancers, much research has focused on the prototypic Ras family members H- K- and N-Ras. In the shadow of these oncoproteins, there are additionally over 30 Ras-related proteins, that include the Rap proteins, Rap1A, Rap1B, Rap2A, 2B and 2C (Pannekoek *et al.* 2009; Nguyen & Quilliam 2012). Rap1 and Rap2 proteins are only 60 % identical to each other (Gloerich & Bos 2011), showing noticeable variations at their C-terminus. These variations could impact their subcellular localisation and, also explain their different sensitivities to RapGEFs or their distinct profiles of downstream targets (Caron 2003). Rap1, a 21 kDa monomeric G-protein, was discovered in 1989 in a genome-wide screen for proteins able to suppress the oncogenic effect of the mutated Ras gene K-Ras. Described as Kristen-ras reverant-1 (Krev-1) the protein was found to have high sequence similarity (53 % identical) to Ras proteins (Kitayama *et al.* 1989; Asha *et al.* 1999). The initial hypothesis was that Ras and Rap1 compete for a common target, but none has been found. Initial studies mainly focused on the possibility that Rap1 interferes with Ras signaling by directly interacting with Ras effectors, but more recent results indicate that Rap1 functions in independent signaling pathways that control diverse processes, such as cell adhesion, cell-cell junction formation and cell polarity (Knox & Brown 2002; Katagiri *et al.* 2003; Bos 2005; Kooistra *et al.* 2007; Pannekoek *et al.* 2009). Nowadays, the mammalian Rap1 proteins Rap1A and Rap1B are generally regarded as acting independently of Ras (Frische & Zwartkruis 2010; Wittchen *et al.* 2011).

Rap1 acts as a molecular switch

Similar to the other GTPases from the Ras subfamily, the Rap1 protein acts as a molecular switch by cycling between two states – an inactive GDP-bound form and an active GTP-bound form (Fig. 2). These modifications are strictly controlled by GEFs and GAPs (Ridley 2001). In general, GEFs turn on signaling by catalyzing the exchange from G-protein bound GDP to GTP, whereas GAPs terminate signaling by inducing GTP hydrolysis (Bos *et al.* 2007). The small GTPase Rap1 is activated by various extracellular signals, which induce the conversion of the inactive GDP-bound form into the active GTP-bound form by stimulating different GEFs.

Many of these GEFS are regulated by common second messengers, such as Ca^{2+}, DAG and cAMP. Inactivation of Rap1 is mediated by several specific GAPs.

Rap1 effectors

Downstream of Rap1, there is a variety of proteins that interact with its GTP-bound form and serve as effectors in Rap1 mediated processes, such as integrin activation, vesicle trafficking, neuronal polarity and phagocytosis (Caron 2003; Bos 2005; Kooistra *et al.* 2007). Furthermore, Rap1 is involved in the regulation of cadherin-based cell-cell junctions (Bos 2005). So, the small GTPase Rap1 has been shown to play multiple roles including a variety of integrin-mediated "inside-out" signaling events (Katagiri *et al.* 2000; Reedquist *et al.* 2000; Bos *et al.* 2001). In particular, Rap1 controls integrin β1, β2 and β3 subunits to affect both integrin activity (affinity) and integrin clustering (avidity), depending on the intergin and the cell type (Bos 2005). Rap1 also localises to adherens junctions where it influences cell-cell adhesion and plays a number of other roles in cell signaling (Knox & Brown 2002; Bos *et al.* 2003; Nguyen & Quilliam 2012). Although many functions of Rap1 signaling have been proposed, the most consisting findings are its involvement in cadherin- and integrin-mediated adhesion processes. These adhesion processes occur through downstream effectors such as AF-6/Afadin, Krit-1 (Krev Interaction Trapped1), RIAM (Rap1-GTP-interacting adapter molecule) and RapL (regulator of adhesion and cell polarity enriched in lymphoid tissues/Rassf5) (Bos 2005; Kooistra *et al.* 2007; Boettner & van Aelst 2009). So, the complexity and diversity of Rap1 functions are tightly regulated by Rap-interacting proteins such as GEFs, GAPs and Rap effectors (Guo *et al.* 2016).
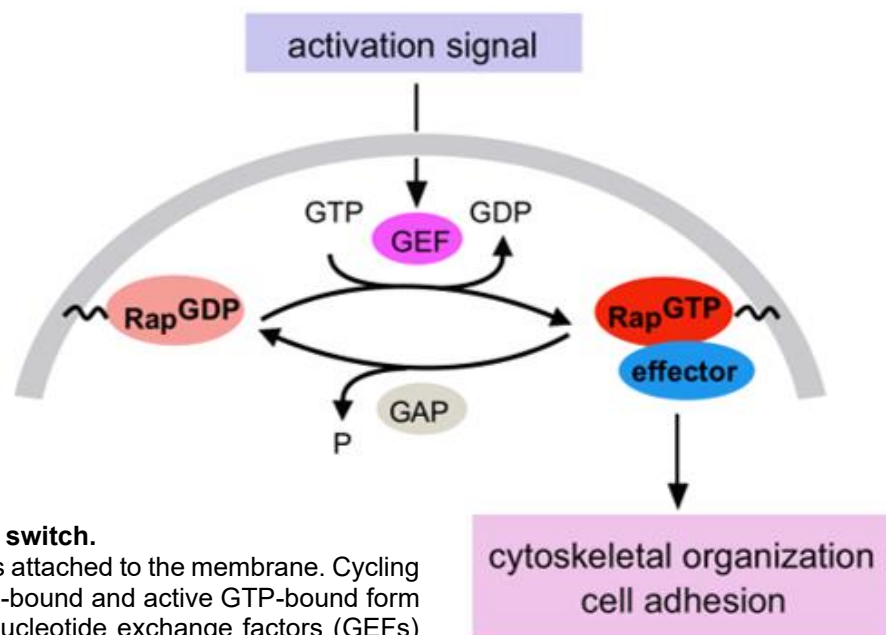

Fig. 2 The small GTPase switch.
The small GTPase Rap1 is attached to the membrane. Cycling between the inactive GDP-bound and active GTP-bound form is regulated by guanine nucleotide exchange factors (GEFs) and GTPase-activating proteins (GAPs). Active GTP-bound GTPases interact with Rap1 effector molecules to mediate many cellular processes (*cf.* Schmidt & Hall 2002).

Rap activators (RapGEFs) catalyse the dissociation of the nucleotide from the inactive G-protein by modifying the nucleotide-binding site. The affinity of the nucleotide is decreased and, thus, the nucleotide is released and subsequently replaced. In general, the affinity of the G-protein for GTP and GDP is similar, and the GEF does not favor rebinding of GDP or GTP. Thus, the resulting increase in the GTP-bound form compared to the GDP-bound form is due to the approximately ten times higher cellular concentration of GTP compared to GDP (Bos *et al.* 2007). So, GEFs induce the release of the bound GDP to be replaced by the more abundant GTP. GTP can then bind and induce a conformational change that permits interaction with downstream effectors (Quilliam *et al.* 2002). The activated GTPase undergoes conformational change that enables it to interact with so-called downstream "Rap effectors", which ultimately produce a biological response (Guo *et al.* 2016). RapGEFs are multidomain proteins and regulated in a highly complex fashion. The activation of GEFs includes protein-protein or protein-lipid interactions, binding of second messengers and posttranslational modifications. These interactions and modifications induce either one or more of three major events: the translocation to specific compartments of the cell where the small G-protein is located, the release from autoinhibition by a flanking region, which covers the binding site for the small G-protein, or the induction of allosteric changes in the catalytic domain (Bos *et al.* 2007). Rap family GEFs are characterised by the presence of two specific domains, a Cdc25 homology domain and a Ras exchange motif (REM), which is located N-terminal to the Cdc25 domain. The Cdc25 homology domain (also RasGEF domain) mediates the guanine nucleotide exchange activity of RapGEFs, while the REM domain is thought to be involved in the catalytic activity of the exchange factor (Guo *et al.* 2016). Beyond these two characteristic domains, RapGEFs vary in their domain composition and contain several other domains that regulate either activity, localisation, or both (Wittinghofer 2014). Several GEFs have been identified that mediate the activation of the small GTPase Rap1 and are implicated in the regulation of adhesion complexes: C3G, and members of the Epac, CalDAG-GEF and PDZ-GEF subfamilies have been implicated in the regulation of adhesion complexes (Kuiperij *et al.* 2003; Boettner & van Aelst 2007).

C3G

The first RapGEF to be identified, C3G (Crk SH3-domain-binding-guanine-nucleotide releasing factor) mediates the activation of Rap1 triggered by receptor thyrosine kinases. C3G consists largely of three regions: A GEF catalytic unit at the C-terminal region, that includes the REM and the catalytic Cdc25 homologous domain which in turn is responsible for the guanine-nucleotide exchange reaction of Rap1. The central region of C3G contains several proline-rich

sequences which are capable of interacting with the first Src homology 3 (SH3) domain of members of the Crk (cell cycle related kinase) adapter proteins (Tanaka *et al.* 1994; Kiyokawa *et al.* 1997; Ichiba *et al.* 1999; Shirinian *et al.* 2010). Many types of stimulations induce binding of the Crk-C3G complex to a variety of phosphotyrosine-containing proteins, such as receptor tyrosine kinases. Following translocation from the cytosol to the cell membrane, C3G becomes phosphorylated of on Tyr 504 (Ichiba *et al.* 1999; Bos *et al.* 2001). So, this association of Crk-C3G with phosphotyrosine-containing proteins enhance the GEF activity of C3G. In the absence of stimulation, the N-terminal region of C3G negatively regulates its GEF activity (Ichiba *et al.* 1999). The phosphorylation of C3G on Tyr 504 represses the negative N-terminal regulation of its GEF activity (Ichiba *et al.* 1999; Quilliam *et al.* 2002). So, C3G is a RapGEF that is activated by receptor tyrosine kinases and membrane recruitment (Ichiba *et al.* 1999; Bos *et al.* 2001; Kuiperij *et al.* 2003; Guo *et al.* 2016).

Epac

Another RapGEF family is the Epac (Exchange protein directly activated by cAMP) family, which consists of three members: Epac1, Epac2 and Repac (related to Epac). In addition to the GEF catalytic region in the C-terminus, Epac proteins have a cyclic nucleotide-binding domain (cNBD), a docking site for cAMP, in the N-terminal region, which is necessary for its allosteric regulation (Guo *et al.* 2016). The activation of Rap by Epac requires the assistance of the second messenger cAMP (Rooij *et al.* 1998). These Rap-specific GEFs contain either one (Epac1) or two (Epac2) cyclic nucleotide-binding domains. Epac2 contains a second cAMP-binding site closer to its N-terminus. The isolated N-terminal domain possesses only low affinity for cAMP (Quilliam *et al.* 2002). The N-terminal cAMP domain is an autoinhibitory region that can inhibit the GEF activity of Epac: In the absence of cAMP, the cAMP-binding domains bind with high affinity to the C-terminal GEF catalytic domain and repress its catalytic activity; the binding of cAMP releases this autoinhibition, leading to the activation of the GEF (Rooij *et al.* 2000). For this reason, Epac1 and Epac2 are also referred to as cAMP-GEFs. They both bind cAMP and activate Rap1 (Guo *et al.* 2016). So, Epac family proteins have autoinhibitory regions capable of binding cAMP, and the binding of cAMP results in the activation of their GEF activity via conformational changes (Rooij *et al.* 1998; Bos *et al.* 2007). Epacs also contain a Dishevelled, Egl-10, Pleckstrin (DEP) domain that is involved in membrane localisation (Rooij *et al.* 2000). This is not regulated by cAMP, indicating that localisation to the membrane is not, like in adapter protein regulated GEFs, a mechanism of activation in Epacs (Quilliam *et al.* 2002).

CalDAG

Epac proteins are not the only members of the RapGEF family that are regulated by second messengers. CalDAG-GEF, also known as Ras guanine nucleotide releasing proteins (RasGRPs) are another family member regulated by second messengers. The four CalDAG-GEFs contain an N-terminal catalytic region composed of a REM and a Cdc25 homolgy domain. This catalytic region is followed by a pair of calcium (Ca^{2+}) binding EF hands and a domain that resembles the C1-type diacylglycerol (DAG) binding motifs (de Rooij 2000). So, the activation of Rap by CalDAG-GEF is regulated by one or both second messengers (Bos *et al.* 2001; Bos *et al.* 2007; Guo *et al.* 2016). Members of the CalDAG-GEF family have different GTPase specificities: CalDAG-GEF1, CalDAG-GEF2, CalDAG-GEF3 and CalDAG-GEF4 activate either Ras, Rap or both (Bos *et al.* 2007). CalDAG-GEF1 and CalDAG-GEF3 act as GEFs for Rap proteins. CalDAG-GEF1 is the main mediator of Rap activation by Ca^{2+}, and CalDAG-GEF3 is the main mediator of Rap activation by DAG (Nguyen & Quilliam 2012).

PDZ-GEF

The Rap activator PDZ-GEF (Ras/Rap1a associating GEF) was independently identified by numerous groups and so has accrued multiple names: PDZ-GEF1, RA-GEF, nRAPGEP or CNrasGEF (Liao *et al.* 1999; Ohtsuka *et al.* 1999; Rooij *et al.* 1999; Quilliam *et al.* 2002). It was identified by the Bos and Quilliam labs by searching the EST (Expressed Sequence Tag) database for genes sharing sequence homology with Cdc25 (Rooij *et al.* 1999; Quilliam *et al.* 2002). de Rooij *et al*., who identified two PDZ-GEF isoforms (PDZ-GEF1 and PDZ-GEF2), was searching for GEFs that might be regulated by second messengers. They noted the presence of a putative N-terminal cAMP-binding domain similar to that present in the regulatory subunits of cAMP dependent proteins. PDZ-GEFs contain the characteristic Ras exchange motif and GEF sequence present in all GEFs for Ras-like small GTPases, as well as a proline-rich motif, a PDZ domain and a structure that is related to the cAMP-binding domain in Epac (Rooij *et al.* 1999). However, several groups have reported that PDZ-GEF does not bind cyclic nucldeotides with a physiologically relevant affinity and it is therefore probably regulated by other signals (Rooij *et al.* 1999; Kuiperij *et al.* 2003). Similar to Epac1, deletion of the N-terminal cAMP-binding domain activates PDZ-GEF1 (Rooij *et al.* 2000; Bos *et al.* 2001), suggesting that even though PDZ-GEF lacks regulation by cyclic nucleotides, the autoinhibitory role of this domain is conserved (Quilliam *et al.* 2002). Even though PDZ-GEF proteins contain regions homologous to cyclic nucleotide domains and have an autoinhibitory function similar to Epac, their activation is not regulated by cAMP (Rooij *et al.* 2000). As may be expected from its name, PDZ-GEF possesses a PDZ domain, a protein interaction module that typically mediates protein-protein interactions via the binding of specific C-terminal peptides (Rooij *et al.* 1999;

Quilliam *et al.* 2002). So, PDZ-GEFs have two putative regulatory domains, a domain with an amino acid sequence related to cAMP-binding domains and a PDZ domain. Interestingly, PDZ-GEF also contains a Rap/Ras-associated domain (RA) close to the Cdc25 homology domain that is commonly observed in downstream Rap effectors (Liao *et al.* 1999; Rooij *et al.* 2000), suggesting that PDZ-GEF serves not only as a Rap activator but also as a positive feedback control factor (Liao *et al.* 2001). This domain has been found to bind to GTP-bound Rap1 and Rap2 (Liao *et al.* 1999; Quilliam *et al.* 2002; Guo *et al.* 2016).

1.3.3 The PDZ-GEF Dzy and macrophage migration

Cell migration is an essential element of morphogenesis during embryonic development of the animal organism and contributes significantly to the formation of its organs. In Prof. Reuter's lab, we focussed our attention on many aspects of development and organogenesis. We aimed to help elucidate the molecular mechanisms that cause and control cell migration in the organism using the migration of mature macrophages in the *Drosophila* embryo as a model. In particular, our goal was to isolate and characterise genes involved in macrophage differentiation and migration. The central theme of this analysis is the function of the G-nucleotide exchange factor Dizzy (Dzy).

To identify genes involved in the regulation and execution of cell migration of embryonic macrophages in *Drosophila*, an EP misexpression screen (Rørth 1996) was performed. This gain-of-function screen allowed the testing of the ability of various genes to influence certain biological processes when overexpressed. In this case, a Gal4 driver was expressed in haemocytes under the control of the *srp* enhancer (driver). The genes to be tested were under the control of EP-elements that were randomly integrated into the genomes of the EP lines. A significant change was observed when the driver was crossed with an EP line that had an insertion upstream of the gene *dizzy* (termed *dzy^{EP}* hereafter) (Huelsmann *et al.* 2006).

The PDZ-GEF Dzy in macrophage migration

In *Drosophila* embryos, macrophages originate from the cephalic mesoderm and perform a complex migration throughout the entire embryo. The molecular mechanisms regulating this cell migration remain largely unknown. Huelsmann et al. identified the gene *dizzy* (*Gef26* – FlyBase) encoding the *Drosophila* PDZ G-nucleotide exchange factor (PDZ-GEF) Dzy as a component essential for proper cell shape and normal macrophage migration in the *Drosophila* embryo. In mutants lacking Dzy, macrophages show smaller cellular protrusions, and their migration is slowed down significantly. In a complementary fashion, macrophages overexpressing Dzy are vastly extended and form very long protrusions (Fig. 3).

12

sagittal view   lateral view

A   A′

wild-type

B   B′

dzy^EP

C   C′

dzy^Δ1
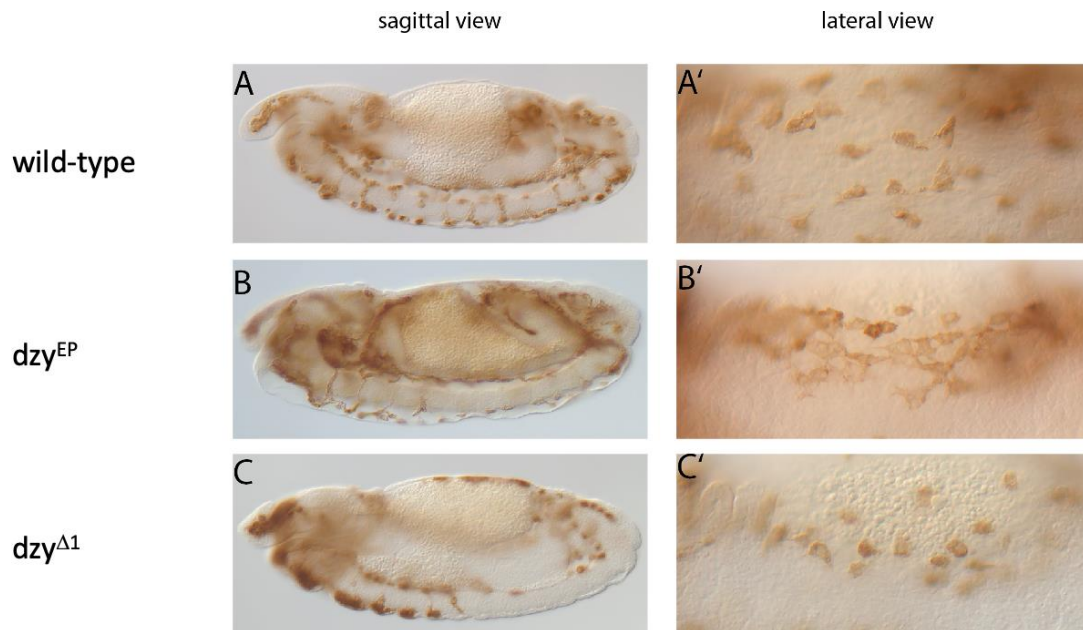
Fig. 3 *dzy* is required for proper cell migration and cell shape of embryonic macrophages.
(A-C) Migrating macrophages at stage 14. Macrophages overexpressing *dzy* (B) migrate similarly to *wt* (A). Mutations in *dzy* (C) affect the migration of macrophages. The posterior part of the ventral nerve cord lacks macrophages. (A'-C') Cell shape of macrophages at lateral positions. Macrophages of *dzy^EP* embryos (B') show longer protrusions, which contact each other and form networks. In contrast, *dzy* mutant embryos (C') have smaller protrusions (*cf.* Huelsmann *et al.* 2006).

The PDZ-GEF Dzy is fundamental for proper migration and cell shape of embryonic macrophages

In mutants lacking Dzy, macrophages form smaller cellular protrusions, and their migration is slowed down significantly. The lack of *dzy* function results in a relatively subtle phenotype in the embryo where macrophage migration is severely delayed, macrophages failed to reach the posterior end of the germ band in time (2), and the cellular protrusions are smaller than in the wild-type (1).

(1) In *dzy* mutants, macrophages have smaller cellular protrusions than those in wild-type embryos. The macrophages in *dzy* mutants have cellular protrusions about half the size of wild-type cells on average in fixed preparations. The size difference in the protrusions was surprisingly not obvious in live *dzy* macrophages. This oberservation suggests that the difference in fixed preparations is caused by reduced stability of the protrusions in *dzy* mutants, resulting in decreased preservation during fixation (Huelsmann *et al.* 2006). One hypothesis is that Dzy normally stabilizes the protrusions which explains the smaller protrusions in fixed preparations of *dzy* mutants.

(2) In *dzy* mutants, the migration of the macrophages is disturbed, especially the migration along the ventral nerve cord (VNC). Macrophages from the anterior and the posterior part of the embryo migrate towards each other along the midline of the VNC. At stages 13 and 14, wild-type macrophages have migrated over the entire ventral nervous system, whereas macrophages in embryos homozygous for *dzy* loss-of-function alleles have not reached most of the posterior nervous system. Macrophages of *dzy* mutant embryos cannot migrate properly and fail to completely surround the midline of the VNC at this time. In some embryos, the resulting ventral gap persists into later stages, while in others the defect disappears (Huelsmann *et al.* 2006). The loss-of-function phenotypes demonstrates that *dzy* is required for proper migration and normal cell shape of migrating macrophages during *Drosophila* embryogenesis and indicates a function of *dzy* in cell adhesion. These phenotypes appear to be cell-autonomous, as it is also observed in embryos with a dsRNA-induced down-regulation of *dzy* function in macrophages (Huelsmann *et al.* 2006).

Overexpression of *dzy* in macrophages leads to cell shape changes that are complementary to the loss-of-function phenotype of *dzy*. Macrophages overexpressing *dzy* display longer cellular protrusions and form a characteristic network of cells in contact with each other and with the substrate. The length of the protrusion per cell is increased fourfold and more protrusions per cell can be identified (Huelsmann *et al.* 2006). These protrusions are formed in addition to the normal tails and leading edges, resulting in an increased number of protrusions per cell. In live cells, it appears that the protrusions stem from lamellopodia that are incompletely retracted or from cell tails that do not retract properly. It is thought that Dzy plays a role in stabilizing the protrusions, which explains the smaller protrusions in fixed preparations of *dzy* mutants. When overexpressed, *dzy* could hinder the proper disassembly of cellular protrusions, which explains the pronounced enlargement and persistence of these protrusions. Macrophages overexpressing *dzy* start their migration as usual, but form very long protrusions during the migration process, in the range of 20 µm per cell. In addition, the long and stable protrusions of various macrophages are able to connect with each other to form a network that spans the nervous system. The formation of this network can also be seen in a lateral position under the epidermis. In wild-type embryos, macrophages migrating along the midline of the VNC or beneath the dorsal edge of the epidermis show smaller protrusions and form fewer or no connections with each other. Surprisingly, when *dzy* is overexpressed from one copy of *dzy^{EP}*, macrophage motility is not significantly affected, although dramatic changes in cell shape do occur. The cells migrate along their invariant migration paths and come in contact with each other and with their normal substrates. However, as the expression level of *dzy* is further increased by expressing two copies of *dzy^{EP}*, macrophage migration is slowed down. In embryos after stage 13, a significant gap remains at the VNC, which is not closed even in the further course of embryogenesis. Complementary to the loss-of-function

14

phenotype, the gain-of-function phenotype demonstrates the role of Dzy in regulation cell shape and cell migration: macrophages overexpressing *dzy* from a single copy of the gene have large protrusions, and macrophages overexpressing from two copies of *dzy* cannot migrate efficiently (Huelsmann *et al.* 2006).

Dzy acts via the small GTPase Rap1

PDZ-GEFs are highly conserved in metazoans and have been recognised as GEFs for Rap in several model systems. Reports from mammalian cell culture experiments demonstrate that PDZ-GEFs specifically activate the small GTPases Rap1 and Rap2 (Rooij *et al.* 1999; Rebhun *et al.* 2000; Gao *et al.* 2001; Liao *et al.* 2001; Kuiperij *et al.* 2003). Further data from *C.elegans* and *Drosophila* place PDZ-GEFs upstream of Rap1 (Rooij *et al.* 1999; Rebhun *et al.* 2000; Gao *et al.* 2001; Liao *et al.* 2001; Lee *et al.* 2002; Kuiperij *et al.* 2003; Huelsmann *et al.* 2006). The PDZ-GEF Dzy behaves like a GEF for the small GTPase Rap1 during macrophage migration in *Drosophila*. In wild-type embryos, the migrating macrophages have small protrusions and are clearly separated from each other. When *dzy* is overexpressed (*srph>dzy^{EP}*), the protrusions are enlarged, and the cells form a network. These changes in cell shape depend on the function of the small GTPase Rap1: Thus, Dzy goes through Rap1 for two reasons: (1) in *rap1* mutants, cell shape changes are not visible, and Dzy is not able to induce the large protrusions phenotype. Overexpression of *dzy* is only effective in *rap1^{+}* embryos. This leads to the assumption that *rap1* is epistatic to *dzy*. (2) Furthermore, a constitutively active form of *rap1* (*rap1^{CA})* in macrophages shows the same effect on cell shape and distribution as *dzy* overexpression. The appearance of macrophages from *dzy* overexpressing embryos and from embryos overexpressing a constitutively active form of *rap1* are very similar. So, *rap1* mutants do not respond to *dzy* overexpression with cell shape changes, whereas a constitutively active form of *rap1* can induce these same cell shape changes. These findings suggest that Dzy acts via Rap1 (Fig. 4).
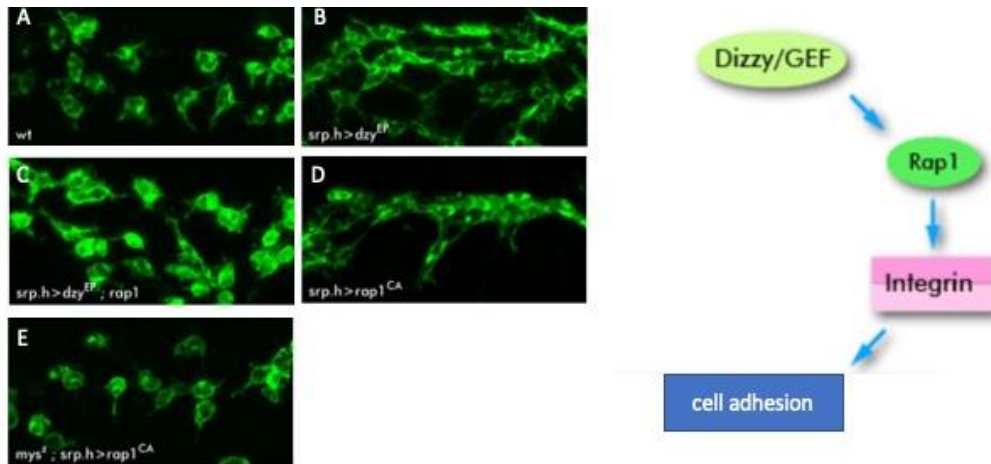
Fig. 4 Dzy acts via Rap1 on integrins to regulate the cell shape.
(A) In wild-type embryos (wt) lateral haemocytes have small protrusions and are clearly separated. (B) Upon *dzy* overexpression (*srph>dzy^EP^*) the protrusions are enlarged and the cells form a network. (C) The cell shape changes are not seen in *rap1* mutants. Thus, *rap1* is epistatic to *dzy*. (D) A constitutively active form of *rap1* (*rap1^CA^*) exerts the same effect on cell shape and distribution as *dzy*. (E) The changes induced by *rap1^CA^* or by *dzy* are not seen in integrin mutants (*mys*) This suggests the model that Dzy acts via Rap1 on integrins to regulate the cell shape (Website Genetik der Tiere).

Dzy modulates integrin activity via Rap1

The cell shape changes induced by *rap1^CA^* or *dzy* overexpression are not observed in integrin mutants (*mys*). Thus, these effects in macrophages are dependent on the function of βPS integrins. In *mys* mutants, which lack the zygotic contribution of βPS integrin, neither Dzy overexpression nor constitutively active Rap1 are able to trigger the formation of long cellular protrusions. This suggests the model that the PDZ-GEF Dzy in *Drosophila* acts on integrins via Rap1 to regulate cell migration and changes in cell shape. Integrin-dependent cell adhesion is a Rap1-mediated target of Dzy activity (Fig. 4). These data represent the first link between a PDZ-GEF, the corresponding small GTPase and integrin-dependent cell adhesion during cell migration in embryonic development (Huelsmann *et al.* 2006).

Function of Dzy

The Dzy protein is ubiquitously expressed in the embryo and has a variety of functions during *Drosophila* development. As already mentioned, Dzy is a component involved in haemocyte cell migration and the regulation of the normal cell shape of macrophages in the *Drosophila* embryo (Huelsmann *et al.* 2006). In addition, Dzy is involved in wing, eye and ovary development and is required for stem cell niche maintenance, ventral furrow formation (VFF) and dorsal closure (DC), thereby affecting cell adhesion via E-cad and integrins (Lee *et al.* 2002; Huelsmann *et al.* 2006; Wang *et al.* 2006; Boettner & van Aelst 2007; Spahn *et al.* 2012). Recently, Dzy has also been shown to be important for synapse development and function (Heo *et al.* 2017; Ou *et al.* 2019).

16

Domains of the Dzy protein

PDZ-GEF proteins are characterised by the presence of the same conserved domains. Dzy consists of a PSD-95/DlgA/ZO-1 (PDZ) domain, a Ras-associated (RA) domain and a nucleotide monophosphate-binding (cNMP) domain (Fig. 5). In addition to these domains, Dzy contains a Ras-exchange (RasGEFN) motif and a RasGEF domain characteristic of GEFs for Ras-like small GTPases. The GEF domain of the PDZ-GEF leads to the nucleotide exchange of the Rap1 effector protein. The other domains may play a role in regulating the activity or localisation of the protein (Kuiperij *et al.* 2003). PDZ domains are modular protein interaction domains that play a role in protein targeting and protein complex assembly (Hung & Sheng 2002; Nourry *et al.* 2003). Many cellular functions, especially those related to signal transduction complexes, are influenced by PDZ-mediated interactions. PDZ domains act as scaffolds to concentrate signaling molecules to multiprotein complexes in specific regions of the cell (García-Mata & Burridge 2007).
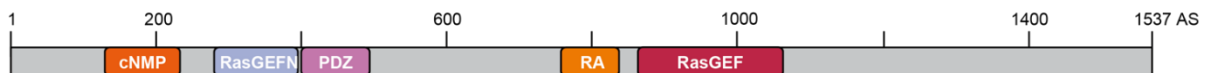
Fig. 5 Domain arrangement of Dzy.
Dzy encodes a PDZ-GEF carrying five protein domains: a cyclic NMP binding (cNMP), a N-terminal RasGEF (RasGEFN), a PDZ, a Ras association (RA) and a RasGEF domain, in an arrangement typical for PDZ-GEFs

In addition to the aforementioned domains, there are three proline-rich motifs (PRMs) at the C-terminus of Dzy. All domains have been reported in an arrangement typical for PDZ-GEFs, with the exception of these proline-rich regions, which are not found in all PDZ-GEFs. The occurrence of the proline-rich region at the C-terminus can vary within PDZ-GEFs and within different isoforms of a protein (Kuiperij *et al.* 2003).

The different isoforms

To characterise the molecular structure of the *dzy* gene and obtain the tools to further investigate its function, full-length cDNAs of *dzy* were isolated by RACE in Professor Reuter's lab. Thus, we found that in addition to the exons 1 to 7 described in Flybase, there are two other exons: an additional exon 0 with an alternative transcription start located 5' from exon 1, and an alternative exon 7* between exons 6 and 7.
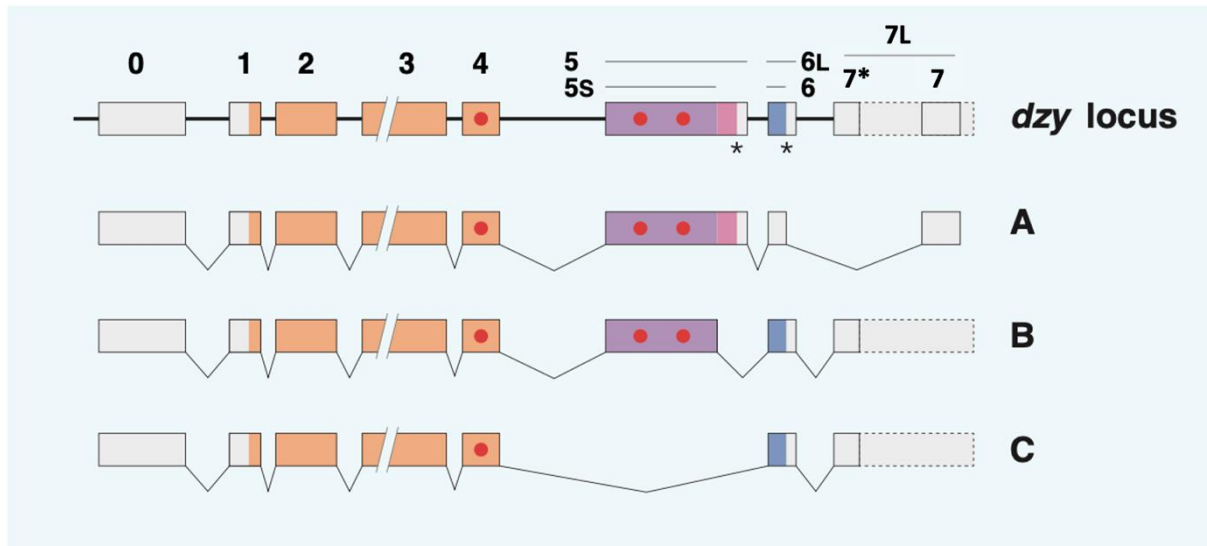
Fig. 6 The different *dzy* splice forms.
The *dzy* genomic locus comprises nine exons. All PDZ-GEF conserved domains reside in exon 3. Based on ESTs, *dzy* gives rise to three different mRNA splice variants *dzyA*, *dzyB*, *dzyC*. Exons 0 - 4 are present in all isoforms. Exon 5 is either included entirely (splice form *dzyA*), shortened (*dzyB*) or spliced out (*dzyC*). Three proline-rich domains (red dots), which are usually responsible for protein-protein interactions, are encoded by parts of exon 4, 5S and 5. Accordingly, the different splice forms *dzyA* and *dzyB* feature all three and splice form *dzyC* only one proline rich domain. The coloured areas in the splice forms represent the ORF.

The *dzy* locus comprises nine exons: exon 0 - 6, 7* and 7. All conserved domains characteristic for PDZ-GEFs are encoded by exon 3. The three proline-rich motifs are located in exon 4 (PRM1) and exon 5 (PRM2 and PRM3) (Fig. 6). Like many other genes encoding a GEF, *dzy* also exhibits alternative splicing. Based on ESTs from the *Drosophila Genome Resource Center*, three different splice forms arise from the gene *dzy*: *dzyA*, *dzyB* and *dzyC*. The cDNAs belonging to these ESTs are only short fragments. Exons 0 - 4 are present in all three isoforms, no variability was observed concerning the 5' part of the cDNA. The three transcripts share a common structure from exon 0 to exon 4. All conserved domains that are typical for PDZ-GEFs reside in exon 3, so all splice forms contain these domains. In addition, the splice forms share a proline-rich motif (PRM1) encoded by exon 4 (Fig. 6). However, the three splice forms are distinguished by their different C-termini and the presence or absence of two additional PRMs, PRM2 and PRM3, encoded by exon 5/5S. So, the differences found during splicing mainly affect the 3' region of the gene, including the proline-rich motifs.

Firstly, three different splicing forms can be distinguished concerning exon 5 (Fig. 6). Exon 5 is either included entirely in the mRNA (*dzyA*), truncated and named 5S (*dzyB*), or absent (*dzyC*). In splice form C, the entire exon 5 is spliced out. Concerning PRM2 and PRM3, the splice forms A and B contain exon 5 or exon 5S, respectively, and therefore include both motifs. Only splice form C lacks this pair of PRMs, since exon 4 is spliced directly to exon 6L. Furthermore, the mRNA from exon 5 can be contined with exon 6 and exon 7 (*dzyA*) or with the extended exon 6L (a longer version of exon 6) and exon 7L, including exon 7*/exon 7 and

18

the intron region (*dzyB* and *dzyC*). PRMs are predicted to play a role in protein-protein interactions (Kay *et al.* 2000). What functions the protein regions encoded by exon 6/6L and exon 7/7L might have is not known yet.

So, Dzy is alternatively spliced, resulting in the formation of three different proteins with unique C termini. There are two different stop codons in the *dzy* locus (asterices in Fig. 6). A stop codon in exon 5 terminates translation for the A splice form. The A form is the only splice form that contains the entire exon 5. For the A form, a stop codon in exon 5 terminates the translation, and the ORF of the A form ends in the 3' region of exon 5. The DzyA protein contains a C-terminal stretch of 26 amino acids which is encoded by the 3' part of exon 5, that is not included in in exon 5S. The second stop codon is located in exon 6L and stops translation of the B and the C form, since their mRNAs do not contain the stop within exon 5 (Fig. 6). In comparison, the B splice form has a truncated version of exon 5 (5S). At the protein level, the B form is the longest, which is due to the loss of the stop codon in the spliced sections of exon 5. Therefore, the DzyB and DzyC (without exon 5) forms use another stop codon in exon 6L. The different splice variants may lead to differences in interaction domains and specific features that could be important for the use of the gene in different processes, developmental stages and tissues (Kuiperij *et al.* 2003; Sierralta & Mendoza 2004). It is very likely that the different splice forms have different effects on the cell shape and migration of haemocytes (Sierralta & Mendoza 2004).

1.4 The focus of the research

The migration of embryonic macrophages in the fruit fly is an ideal system to study the regulation and mechanism of cell movement *in vivo*. PDZ-GEF Dzy is involved in the process of cell migration by acting through the small GTPase Rap1 (Rooij *et al.* 1999) and integrins (Huelsmann *et al.* 2006). The aim of this work is to analyse the structure-function relationship of the Dzy PDZ-GEF protein during macrophage migration in the *Drosophila* embryo. We want to investigate on a molecular and cellular level how the PDZ-GEF Dzy acts in cell migration, which processes it controls and how it is regulated. To this end, it is important to understand the complex relationship between the structure and function of Dzy, the link between genotype and phenotype and the relevance of alternative splicing.

The focus of this PhD thesis is mainly on exploring the function of the N-terminal PDZ domain and the different splice variants, which are distinguished by their C-termini and the presence or absence of two proline-rich motifs (PRMs). The two structural features, the PDZ domain and the PRMs, are often involved in protein-protein interactions. It is also assumed that these two regions can interact with each other and therefore influence the functionality of the protein. In order to investigate the relevance of these domains, deletion variants of Dzy either with an inoperative PDZ domain or non-functional PRMs are generated. These Dzy isoforms will allow

us to test which functions of Dzy, for instance during haemocyte migration, are PDZ- or PRM-dependent. The main questions that arise are: (1) What parts of the Dzy sequence are relevant to its function? (2) Are the conserved PDZ domain and the PRMs relevant for macrophage migration and cell shape changes? Furthermore, in order to elucidate the relationship between the structure and function of PDZ-GEF Dzy, the different isoforms DzyA, DzyB and DzyC are also investigated. The various isoforms are formed by alternative splicing and differ in their C-termini and the varying number of PRMs. The different splice forms are to be introduced into the fly as Gal4-controllable transgenes to clarify the following questions: (3) Can the overexpression of one or more isoforms in haemocytes produce the same Rap1-dependent cell shape changes as observed with the *dzy*[EP] allele? Furthermore, do the various isoforms of Dzy have different effects on the cell form and the migration behaviour of macrophages? (4) Is the overexpression of one isoform or several isoforms within the macrophages sufficient to rescue the migration phenotype of *dzy* mutants? (5) Which of the individual splice variants is able to rescue the semi-lethality of *dzy* mutants or their defects in eye, wing and genital apparatus development? Answers to all of these questions can be found through functional studies on Dzy during *Drosophila* development, by studying the overexpression phenotypes of the different isoforms and their ability to provide full wild-type *dzy* function.

2. Materials & Methods

2.1 Materials

2.1.1 Fly stocks

The following fly stocks were used in this work: *dizzy*^{EP} *(dzy*^{EP}*)*, EP line EP(2)388 of the Szeged stock collection (*pdz-gef*², (Lee *et al.* 2002); *dzy*^{Δ8}, allele of *dzy* obtained by imprecise excision of the P-element of *dizzy*^{EP} (Huelsmann *et al.* 2006); *dzy-GFP* (*dPDZ-GEF*^{EGFP}) and *UAS-dzyGFP* (UAS-*dPDZ-GEF*^{EGFP}) (Boettner & van Aelst 2007); *Df(2L)ED380*, breakpoints 26C2-26D7 (DrosDel deletion collection)) deficient for the genomic region of *dzy* (Ryder *et al.* 2007); *UAS-cd2* (3rd chromosome), heterologous cell surface marker under the control of UAS (Dunin-Borkowski & Brown 1995); *srph-Gal4 (3rd chromosome)*, *srp* haemocyte enhancer (Huelsmann *et al.* 2006) in the Gal4 vector (Brand & Perrimon 1993); *srph>cd2* (3rd chromosome) recombinant of *srph-Gal4* and *UAS-cd2*, kept as homozygous stock; *tub-Gal4* (Fly strain collection stock 746); *da-Gal4* (Hinz *et al.* 1994); *ey-Gal4* (Hazelett *et al.* 1998); *GMR-Gal4*, *Glass-Multimer Reporter-Gal4* (Dr. Denise Dewald); *hs-Gal4* (*heat shock-Gal4*), expression of a Gal4 driver, driven by a heat-inducible promotor (Brand *et al.* 1993); *prd-Gal4* (Fly strain collection stock 334); *h:Gal4* (Fly strain collection stock 171)*; UAS-StingerGFP* (Barolo et al. 2000); *UAS-srp* (Fly strain collection stock 260); *pdzy* promotor, *pdzy(1)-Gal4* and *pdzy(3)-Gal4* (Fly strain collection stock 1241 and 1229, respectively); *PhiC31-attP-86FB,* fly strain with attP-site on the third chromosome, endogenous PhiC31 activity (Bischof *et al.* 2007), Fly strain collection Sven Huelsmann; multibalancer stocks *Gla/CyO; eE/TM3* (Fly strain collection stock 977) and *Gla/CyO; eE/TM6B* (Fly strain collection stock 608), balancer chromosomes (Lindsley & Zimm 1992).

For the expression of the splice forms in the macrophages, we generated and used *UAS-dzyA*; *UAS-dzyB*; *UAS-dzyC*; *UAS-dzyCΔPDZ*; *UAS-dzyB_GFP* and *UAS-dzyC_GFP.* A complete listing of the *UAS-dzy* strains produced can be found in the Appendix. These stocks were crossed with a fly strain harbouring the macrophage-specific driver (*srph*) and the *UAS-cd2* transgene recombined on the same chromosome: *w; srph-Gal4 UAS-cd2* (Huelsmann et al. 2006). For the rescue experiments, the mutant allele *dzy*^{Δ8} was recombined with *srph-Gal4* (*dzy*^{Δ8}/*srph-Gal4*, embryo rescue) or *hs-Gal4* (*dzy*^{Δ8}/*hs-Gal4*, adult rescue). These stocks were further crossed with *Df(2L)ED380/UAS-dzy* strains: *Df(2L)ED380/UAS-dzyA, Df(2L)ED380/UAS-dzyB, Df(2L)ED380/UAS-dzyC, Df(2L)ED380/UAS-dzyCΔPDZ* and *Df(2L)ED380/UAS-dzyGFP.* A detailed explanation of the individual crossing schemes can be found in the Results section and in the Appendix.

2.1.2 Antibodies & dyes

The following primary antibody was used for this study: mouse anti-CD2 (1:4000, Serotec). Secondary antibodies used for the detection of the primary antibodies were either directly fluorescently labelled (1) or coupled with biotin (2). (1) We detected the primary antibody with secondary antibodies, labeled with the fluorescent dye Cyanine (Cy3, Molecular Probes). Secondary antibodies, labeled with goat anti mouse GAM Cy3 were used at 1:250. Embryos stained with fluorescent dyes were in many cases counterstained with 4',6-diamidino-2-phenylindole (DAPI 1:1000 of a 1mg/ml stock; Sigma) to visualize nuclei. (2) Biotinylated secondary antibodies were used for the detection of the primary antibodies: goat anti-mouse (GAM-BIO, 1:500, Jackson ImmunoResearch Laboratories). The signal of the biotinylated secondary antibody was enhanced using peroxidase-coupled Vectastain ABC Elite Kit (1:100; Vector Laboratories). After preincubation of the Avidin Biotin Mix, the peroxidase was visualized with H_2O_2 (0.003 %; Fluka) and 3,3'-diaminobenzidine (DAB 25 mg/ml Sigma) for a brown staining.

2.1.3 Chemicals, enzymes and kits

Chemicals used in this work were supplied from Roth or different suppliers as labelled.

Chemicals

1kb DNA Ladder (1,0 µg/µl)	NEB
10x BlueJuiceTM Gel Loading Buffer	NEB
Acetone	Sigma-Aldrich
Agar	Sigma-Aldrich
Agarose	Sigma-Aldrich
Ampicilin	Sigma-Aldrich
AquaPolyMount	Polysciences
Araldite	Honeywell Fluka^{TM}
Chloroform	Sigma-Aldrich
Ethidium bromide	Roche
Ethanol	Honeywell Research Chemicals
H_2O_2	Honeywell Fluka^{TM}
Heptane	Sigma-Aldrich
Isopropanol	Fisher Chemicals
Klorix®	Colgate-Palmolive
Methanol	Sigma-Aldrich
dNTPs Mix 10mM	NEB
NBT/X-phosphate	Roche

Phenol	AppliChem
Tris-base	Sigma-Aldrich
Triton X-100	Serva
Tween 20	Sigma-Aldrich
Vectashield, Mounting Medium	Vector Labs Inc.
Voltalef® oil 3S and 10S	BDH Prolabo Chemikalien

Enzymes

DNase I	NEB
RNase (DNase-free)	Sigma-Aldrich
OneTaq® DNA Polymerase	NEB
HotStar HiFidelity Polymerase	Qiagen
Phusion® High-Fidelity Polymerase	NEB
rAPid Alkaline Phosphatase	Roche
Lysozyme	Merck
Restriction endonucleases: BamHI, BglII, EcoRI, KpnI, NotI, SpeI, XbaI, XhoI	NEB
Buffer: NEB 1 - 4, T4 Ligase Buffer and Cut smarter	NEB
T3/T7 Reverse Transcriptase	NEB
T4 DNA Ligase	NEB
Proteinase K	NEB

Reagent kits

Macherey Nagel® NucleoBond® Xtra Midi Kit	Macherey Nagel
Nucleospin® Gel and PCR Clean-up Kit	Macherey Nagel
Monarch® DNA Gel Extraction Kit	NEB
Transcriptor First Strand cDNA Synthesis Kit	Roche
DIG RNA Labeling Kit	Roche
TOPO® TA Cloning® Kit	Invitrogen
peqGold Plasmid Miniprep Kit	Peqlab Biotechnologie
E.Z.N.A® Gel Extraction Kit	Omega
LunaSkript^{TM} RT SuperMix Kit	New England BioLabs
QIAzol® Lysis Reagent	Qiagen
miRNeasy Micro Kit	Qiagen
RNeasy® Plus Mini Kit	Qiagen
NEBuilder HiFi DNA Assembly Cloning Kit	NEB
VECTASTAIN Elite ABC kit	Vector Laboratories
peqGold RNA Pure^{TM} Kit	Peqlab Biotechnologie

Direct-zol™ RNA Miniprep Plus	Zymo Research
Zymoclean Gel DNA Recovery Kit	Zymo Research

2.1.4 Buffer and solutions

Ampicillin stock solution	20/50/75 mg/ml in ddH$_2$O
Apple juice agar	45 g agar 1.5 l ddH$_2$O 50 g sugar 0.5 l apple juice 20 ml Nipagin (14 % in ethanol)
Blocking solution	PBST with 2 % NGS
EDTA	0.5 M Ethylenediaminetetraacetic acid in ddH$_2$O pH 8.0
Ethidium bromide stock solution	Ethidium bromide (Sigma-Aldrich) 10 mg/ml in ddH$_2$O
DAB staining solution	0.25 mg/ml 3,3'-diaminobenzidine 0.003 % H$_2$O$_2$
Fly food	20 l H$_2$O 170 g agar 1.5 kg cornmeal 200 g soybean flour 360 g dry yeast 820 g sugar beet molasses 1.6 kg malt extract 90 ml propionic acid 300 ml Nipagin (14 % in Ethanol)
Fixative A	3.7 % formaldehyde (Sigma-Aldrich) in pBS
Hybridization buffer HybA (Hyb-5.5-)	25 ml deionized formamide 12.5 ml 20x SSC 50 µl Tween20 fill up to 50 ml with ddH$_2$O
Hybridization buffer HybB (Hyb-5.5+)	25 ml deionized formamide 12.5 ml 20x SSC 1 ml salmon testis DNA (10 mg/ml) 250 µl tRNA (20 mg/ml) 25 µl heparine (100 mg/ml) 50 µl Tween20 fill up to 50 ml with ddH$_2$O
In Situ Staining Solution B	2 ml 1 M Tris pH 9.5

	1 ml 1 M MgCl$_2$
	400 µl 5 M NaCl
	20 µl Tween20
	fill up to 20 ml with ddH$_2$O
LB medium	4 g peptone
	4 g NaCl
	2 g Yeast extract
	fill up to 400 ml with ddH$_2$O
	pH 7.5 (using NaOH)
LB agar plates	4 g peptone
	4 g NaCl
	2 g Yeast extract
	6 g agar agar
	fill up to 400 ml with ddH$_2$O
Lysis buffer A	100 mM Tris-HCL (pH 7.5)
	100 mM EDTA
	100 mM NaCl
	0.5 % SDS
NBT	Nitro blue tetrazolium in 70 % dimethylformamide
PBS	130 mM NaCl
	20 mM KP$_i$ pH 7.4
PBST	0.1 % Triton X-100 in PBS
PBSTw	0.1 % Tween 20 in PBS
SOC medium	2 g peptone
	0.5 g Yeast extract
	0.860 ml 1 M NaCl
	1 ml 0.25 M KCl
	0.5 ml 2 M MgCl$_2$
	0.36 g glucose
	fill up to 100 ml with ddH$_2$O
	pH 7.0 (NaOH)
SQ buffer	10 µl 1 M Tris pH 8.2
	2 µl 0.5 M EDTA pH 8.0
	5 µl 5 M NaCl
	10 µl Proteinase K (Roche)
	fill up to 1 ml with ddH$_2$O
TAE buffer (50x)	242 g Tris in 500 ml water
	100 ml 0.5 M EDTA
	57.1 ml acetic acid

	fill up to 1 l with ddH$_2$O
TE buffer	200 µl 1 M Tris-HCl, pH 7.4
	40 µl 0.5 M EDTA, pH 8.0
	fill up to 20 ml with ddH$_2$O
TELT buffer	5 µl 1 M Tris pH 8.0
	12.5 µl 0,5 M EDTA pH 8.0
	31 µl 8 M LiCl
	41.5 µl 10 % Triton X-100
	10 µl lysozyme (50 mg/ml)
X-phosphate	(BCIP) 5-Bromo-4-chloro-indolyl phoshate in dimethylformamide

2.1.5 Synthesized oligonucleotides (primers)

The primers were produced exclusively by the company Metabion and supplied in lyophilized form. The stock solutions were prepared in a concentration of 100 µM. Primers used in this thesis for sequencing or in PCR reactions were designed with PrimerSelect (Lasergene, DNASTAR) and synthesised by Metabion (https://www.metabion.com).

Primer/ Denotation	Nucleotide Sequence 5`- 3` direction	Annealing temp. (°C)
PR51 (M13-20 long)	GTAAAACGACGGCCAGTGA	54.0
PR99 (pUAST U 5540)	TCTCTGTAGGTAGTTTGTC	52.4
PR100 (pUAST start (3))	GTAAATAGCAAAGCAAGCAAGAGT	57.6
PR101 (pUAST stop (4))	AAGTAACCAGCAACCAAGTAAATC	57.6
PR159 (3'EP388-3474)	TTCCGGCCGGTTGATTGTAGTC	62.1
PR160 (3'EP388-3478)	GCAGTTCCGGCCGGTTAGTTGTAGTC	68.0
PR164 (5'end up 1535)	TTTCGAGGCGGACTATGAGATGATGGAG	61.0
PR166 (5'end up)	TTCCAACAATGCGCACCACAATACCAATACACA	67.0
PR169 (5'end down 2232)	AGGCCATGTTACCGCTCCCACTCACTG	69.5
PR181 (3'end up nested)	GCTCCGCCGCCGCCTCTA	65.1
PR183 (3'end down)	ACTCCCGCTTTGCATTTGTTGTTTTGTC	63.7
PR188 (3'end down Ex6 5273)	GGCATGGGACATATGGTACACTTGGTGCTATCC	70.7
PR189 (3'end down Ex7 5362)	GTGGCTTCGAGTTGATTCCGTTTGCGTTTCTAT	68.3
PR190 (alt 3'end down Ex7)	CTGATTGCTGGCGAAATTGAAACCACAACC	66.8
PR219 (5'Ex4 Start)	GCAACATTATTCCCTCTCGCGCAATACACG	68.1
PR221 (BglII up PDZ)	AGATCTGTGTTTGTGTGTGTGAGTGAA	57.5
PR222 (XhoI down PDZ)	CTCGAGACGTGACGATCGAGTG	57.5
PR224 (End down Eco Not)	CCACAGAAGTAAGGTTCCTTCACAAAG	57.7
PR225 (PR2 BglII down rev II)	AGATCTGCTGGGTGGTTGTGTTTGTGCTTTGAC	70.3

PR226 (PR2 BamHI up)	CACCGGATCCAGCACACAGCAACCATT	68.7
PR227 (PR3 XhoI down rev)	CTCGAGCGGTGGTGGTCATGGCCAAAGATTGC	76.4
PR228 (PR3 SalI up)	TGTCGACACCTGGGCAGTATCTACAGCC	65.8
PR229 (Upper Primer CII)	TTGCGCAAATCCGTGACTTC	56.0
PR230 (Lower Primer CII)	GCAGCTTTTTCCTTTGTGGTGTAA	62.0
PR231 (Start up Spe 25 II)	CCTCGCGCAACATGAGCAAGTATC	67.0
PR247 (M13fw)	GTTGGTAAAACGACGGCCAGT	59.8
PR248 (M13rev)	ACAGGAAACAGCTATGACCATG	58.4
PR296 (dzy iso I)	AGCGTTTAAAGGAGTATGCTTG	58.0
PR297 (dzy iso II)	TTTTTGCAGCTCCGTAAAGG	56.0
PR298 (dzy iso III)	CTGCCTGCAGACGTTTTCTT	58.0
PR1a BottomA	AAAATCTAGAAGCGTTTAAGGGAGTATGCTTG	69.0
PR1b BottomBC	AAAATCTAGATTCTGATTGCTGGCGGAATTG	67.0
PR2 TopABC	AAAAGCGGCCGCTATGGATCCGTATCACCATATC	75.0
PR3 BottomGFP	AAAAGCGGCCGCGGAAGAGGAAG	68.0
PR4 TopGFP	AAAAGGTACCCAACATGAGTAAAGGAGAAGAACT	70.0
PR1 GFPfw	ACTCTGAATAGGGAATTGGGCAACATGAGTAAAGGAGAA GAACTTTTCACTGGAGTTG	70.7
PR2 GFPrev	CGGATCCATAGCGGCCGCGGAAGAGGAA	75.5
PR3 dzyABCfw	CCGCGGCCGCTATGGATCCGTATCACCATATC	60.3
PR4a dzyArev	CGGCCGCAGATCTGTTAACGAGCGTTTAAGGGAGTATG	58.1
PR4b dzyBCrev	CGGCCGCAGATCTGTTAACGTTCTGATTGCTGGCGAAAT TG	63.6

2.1.6 Vectors and bacteria strains

Vectors

pCR®2.1 TOPO®	Invitrogen
pCR®4 TOPO®	Invitrogen
pBlueScript II SK/KS (+)	Fermentas
pUAST	DGRC
pUASTattB	DGRC

The generated constructs are in the Results section with the corresponding cloning schemes.

Strain of bacteria

E.coli DH5α	Lab resources Genetik der Tiere
E.coli One Shot Top10	Invitrogen

2.1.7 Computer software

Adobe Photoshop CS5	Adobe

Adobe Illustrator CS5	Adobe
4Peaks	Mekentosj.com
SeqBuilder	Lasergene ®8 DNAStar
Megalign	Lasergene ®8 DNAStar
PrimerSelect	Lasergene ®8 DNAStar
Amira 5.4	Thermo Fisher Scientific
SnapGene Viewer	GSL Biotech LLC

2.2 Methods

<u>Work with *Drosophila melanogaster*</u>

2.2.1 Fly culture

The flies were kept at 18 °C in small (28 ml) and large (68 ml) vials. The vials were filled about a quarter with standard fly food on the bottom and closed with a foam plug on the top. For mating, the flies were maintained at 25 °C.

2.2.2 Collection of staged *Drosophila* embryos

For egg harvesting, the flies were kept in a cage made of acrylic glass. The tops of the cages were closed using a fine wire mesh. The bottom opening fit onto plates containing apple juice agar with fresh yeast. In order to obtain a sufficient amount of stage 13 - 14 embryos, the plates were placed at 25 °C overnight and exchanged the next morning. The resulting plate covered with fly eggs could then be dechorionated and fixed. Developmental stages were distinguished following Campos-Ortega & Hartenstein (1985).

2.2.3 Fixing of *Drosophila* embryos with formaldehyde and methanol

<u>Dechorionating embryos</u>

Before the fixation step, the embryos were dechorionated. To remove the chorion, the collected embryos were incubated with a 1:1 bleach (Klorix®) and water solution. After an incubation period of 2 minutes, the dechorionated embryos were transferred into a thin, fine-meshed plastic sieve and thoroughly rinsed with running tap water. The sieve was removed from the plastic cylinder to transfer the embryos into the fixing solution.

<u>Fixation of *Drosophila* embryos</u>

The dechorionated embryos were transferred from the sieve into a mixture of 3.7 % formaldehyde in posphate buffer saline (PBS) (Fixative A solution) and heptane (at 1:1 v/v ratio). The embryos were vigorously shaken in the fixative:heptane mix for 20 minutes at 37 °C. The aqueous layer at the bottom consisting of Fix A solution was removed with a pipette and

replaced by the same volume of methanol. The embryos were further devitellinised using a mixture of 1:1 (v/v) methanol:heptane.

<u>Devitellinisation</u>

After formaldehyde fixation, the embryos were placed in a 1:1 mixture of heptane and methanol and vortexed for 30 seconds. Devitellinised embryos then start to settle at the bottom of the tubes. The heptane phase was discarded and the tube filled with the same amount of methanol. After renewed vortexing, the embryos were washed twice with methanol and stored at -20 °C until further treatment.

2.2.4 Antibody staining of *Drosophila* embryos

2.2.4.1 Antibody staining with Avidin Biotin complex (ABC) amplification and DAB

After the previous fixation and devitellinisation process, the embryos were freed from methanol and rehydrated in PBST (0.1 % Triton X-100 in PBS). The first part of the ABC staining involved the saturation of unspecific binding sites by incubation with blocking solution (PBSTG: 2 % NGS in PBST) for 45 minutes. After this step, the primary antibody of choice (see Materials & Methods) was added to the blocking solution and the embryos were slowly rotated over night at 4 °C. Afterwards the embryos were washed three times for 10 minutes in PBST and incubated for 90 minutes at RT with the biotinylated secondary antibody (1:500 GAM-BIO in PBST). Embryos were then washed with PBST twice for 20 min and one last time for 30 minutes. During the final, 30-minute washing step, Reagent A (Avidin) and Reagent B (Biotinylated HRP (Horseradish peroxidase)) (VECTSTAIN Elite ABC kit, Vector laboratories), were mixed in a separate microcentrifuge tube to allow the formation of complexes (**A**vidin-**B**iotin-PO Amplification **C**omplex). Embryos were incubated with the AB-Complex solution for 45 minutes slowly rotating at RT. After the incubation the embryos were washed three times for 20 minutes and incubated with the 3,3'-diaminobenzidine (DAB, Sigma) staining solution for a brown staining. The coupled peroxidase served as a detection enzyme. The enzyme substrate was 3,3'-diaminobenzidine (DAB) staining solution. To quench the peroxidase (HRP) activity H_2O_2 diluted 1:100 in PBST were added. The reaction started by adding the 0.003 % H_2O_2 solution and resulted in a visible brown color reaction. The stopping was achieved by replacing the solution with PBST.

2.2.4.2 Antibody staining with fluorescently conjugated secondary antibodies

Embryos for histochemistry were fixed in formaldehyde/methanol. For antibody staining, the embryos were rehydrated in PBST. The embryos were blocked with 2 % normal goat serum (NGS, Sigma) in PBST for 30 minutes at room temperature (RT) and then incubated with one

or more primary antibodies from different species overnight at 4 °C. The primary antibodies were added to the 2 % NGS solution to the final concentration specified. After this step, the embryos were washed with PBST and incubated for 90 minutes at room temperature with the corresponding secondary antibodies conjugated to different fluorescent dyes, for example GAM-Cy3. The samples must be stored in the dark from this point onwards, otherwise the fluorescent dye will be affected. Embryos were washed twice in PBST, mounted in methylsalycylate or araldite and analyzed under the confocal microscope.

2.2.5 *In situ* hybridization of *Drosophila* embryos

The *in situ* hybridization protocol is based on the method described by Tautz & Pfeifle (Tautz & Pfeifle 1989).

2.2.5.1 *dzy*-RNA probe preparation

<u>Sample preparation</u>

The DNA template (RH54455 in Vector pFLC1, 4559 bp) was linearised by cutting at a restriction enzyme site (Not-HF) downstream of the cloned insert. After the 30-hour restriction digest with Not-HF the linearised DNA was phenol-chloroform extracted and ethanol precipitated (see section 2.2.26).

<u>RNA labeling reaction</u>

For an *in vitro* transcription reaction, 500 ng purified template DNA were added to an RNAse free reaction vial (500 ng DNA + H_2O = 6 µl). The DIG RNA Labeling Kit (Roche) was used according to the manufacturer's specifications to generate the single-stranded RNA probe. The reaction vial was placed on ice and the following reagents were added: 1 µl 10x rNTP labeling mixture, 1 µl transcription buffer, 1 µl RNase inhibitor and 1 µl 25 U RNA polymerase T3. The transcription reaction was incubated for 4 hours at 37 °C. Extra template DNA was removed by digesting the products with DNAse (NEB) at 37 °C for 15 minutes. After incubation, 90 µl of Serapur H_2O with 0.1 % DEPC was added to the transcription reaction and the resulting solution was divided into 15 µl aliquots. The labeled probes were stored at -80 °C.

2.2.5.2 Hybridization

The embryos were collected and treated as described in 2.2.2 Collection of staged *Drosophila* embryos and 2.2.3 Fixing of *Drosophila* embryos with formaldehyde and methanol. The fixed embryos were rehydrated with PBSTw and transferred via a 1:1 step (50 % HybA (Hyb-5.5-) and 50 % PBSTw) into the hybridization solution HybA (Hyb-5.5-). Embryos were pre-hybridized to block unspecific binding sites for at least one hour at 68 °C. After pre-

hybridization, the embryos were incubated with the digoxigenin (DIG)-labeled RNA probe (1 - 5 µl) in 20 µl of the hybridization solution HybB (Hyb-5.5+). The hybridization was performed at 68 °C in a heat block overnight. Finally, embryos were washed at 68 °C with the hybridization solution HybA and were transferred via a 1:1 step (HybA (Hyb-5.5) and PBSTw) into PBSTw.

2.2.5.3 Detection

An anti-DIG antibody conjugated to AP (1:2000 dilution in PBSTw (0.1 % Tween 20 in PBS)) was used to detect the probe. Embryos were incubated with the antibody for 1 hour at RT. After further washing steps with PBSTw, the embryos were transferred into a 24-well plate. For detecting the probe, PBSTw was removed, and the embryos were placed in 400 µl freshly prepared staining buffer B. The supernatant was discarded and replaced with 200 µl of the staining buffer B mixed with 2 µl NBT (10 mg/ml) and 2 µl X-phosphate (10 mg/ml) to initiate a colour reaction, where anti-DIG-AP was present. When the desired intensity was reached, the reaction was stopped by rinsing and washing several times with PBSTw. The embryos were then dehydrated through a graded ethanol series (40 % ethanol, 70 % ethanol and three times 100 % ethanol) and rinsed twice with dehydrated acetone before being mounted in araldite.

2.2.6 Mounting of embryos

2.2.6.1 Mounting in methyl salicylate

Mounting in methyl salicylate (Sigma-Aldrich) was performed when a large number of embryos needed to be analysed, for example in order to study a phenotype. Methyl salicylate is a visually excellent embedding medium, but does not allow permanent mounting of the embyos. The embryos were dehydrated through a graded ethanol series (40 % ethanol, 70 % ethanol and three times 100 % ethanol). After dehydration, the ethanol was removed and 800 µl methyl salicylate was added to the embryos. Within 15 minutes the embryos were settled at the bottom of the tube. The methyl salicylate was removed, the embryos were resuspended in 120 µl of new methyl salicylate and transferred directly to a slide.

2.2.6.2 Mounting in araldite-acetone

Mounting in araldite was done when embryos were to be photographed. Araldite has a high viscosity and protects the embryo from damage while they are being manipulated. Araldite polymerizes after some time and is therefore suitable for making permanent preparations. After alcohol dehydration (40 % ethanol, 70 % ethanol and three times with 100 % ethanol) the embryos were washed twice in dehydrated acetone and resuspended in a 1:1 araldite-acetone solution. The embryos were transferred into a polyethylene snap lid and stored overnight at -20 °C. The initially thin solution condensed within a few hours due to evaporation of the

acetone until the desired viscosity was reached. Embryos were mounted individually in araldite drops, whereby it was possible to rotate the embedded embryos with a wolfram-needle or by moving the cover slip.

2.2.6.3 Mounting in Vectashield or AquaPolyMount

All fluorescently labelled embryos were mounted in Vectashield (Vector Laboratories) or AquaPolyMount (Polyscience). Compared to AquaPolyMount, Vectashield remains liquid so that the mounted embryos can still be rotated. The embryos were transferred to a drop of mounting medium (Vectashield or AquaPolyMount) immediately after staining without using the alcohol series to prevent fading.

2.2.7 Imaging *Drosophila* embryos

Confocal images were taken with a Leica TCS SP2 confocal system (Leica Microsystems) and on an inverted laser-scanning Leica DM IRBE microscope. For bright-field microscopy, embryos were mounted in araldite and analyzed on a Zeiss Axioplan 2 microscope equipped with a ProgRes C14 camera (Jenoptik) or SPOT Insight camera (spotimaging). The images were processed by using the programs Photoshop CS5 and ImageJ.

2.2.8 P-element mediated germ line transformation of *Drosophila melanogaster*

P-element transformation is a method for the generation of transgenic *Drosophila* strains, in which foreign DNA is stably introduced into the germ line of *D. melanogaster* (Rubin & Spradling 1982; Spradling & Rubin 1982). The integration into the fly genome is random and undirected.

Preparing the DNA

All constructs were sequenced prior to injection into *Drosophila* embryos. Highly-purified DNA of the transformation construct was incorporated into ddH_2O (approx. 3 µg DNA construct). The injection solution additionally contained 1 µg of the Δ2-3 helper plasmid. If transformation vector and helper plasmid are co-injected, a stable integration of the vector into the fly genome can be achieved. Before injection, the solution was centrifuged for 15 minutes at 13,000 rpm to pellet insoluble particles.

Preparing the flies

The DNA constructs were injected into w^- embryos, the flies were maintained in cages with a fine wire mesh on apple juice agar plates (see section 2.2.2). Before injection, hourly changes of apple juice agar plates on the cages were done for 2-3 hours and then every 30 minutes for at least two hours. During this time, accessories for the injection were prepared (coverslips

with glue, desiccation chamber, needles, needles with loaded DNA, agar block for lining up the eggs). For the injection fertilized eggs from a 30-minute collection were dechorionated with 1:1 Klorix®-water solution for 2 min, rinsed with water and transferred to an agar bloc for lining up. The embryos were lined up with their anterior end pointed towards the edge of the apple juice agar bloc. Using heptane glue, the resulting row of embryos was transferred to a coverslip and dried for 7-10 minutes in desiccation chambers with silica gel (blue or orange).

<u>Injection</u>

The dried embryos were covered with Voltalef® 10S oil (BDH Prolabo Chemikalien) and the P-element construct together with the helper plasmid were injected into the posterior pole of the embryo. The injection was performed under a microscope (Zeiss), combined with a micromanipulator. Glass capillaries were used as injection needles. The injection needle was filled with 4.5 µl of the injection solution and inserted into the micromanipulator. Injection volume was regulated by the built-up pressure of the injection equipment (FemtoJet, Eppendorf) so that a regulated amount of DNA was injected into the embryos. After the injection, the embryos were placed on an apple juice agar plate with dry yeast and allowed to recover for 1 - 2 days at 25 °C.

<u>Recovery of the injected embryos</u>

After the recovery period, the hatched larvae were collected and transferred into a vial with fresh food and developed at 25 °C until the pupae or adult stage. The enclosed adults were mated with *w⁻* flies of the opposite sex and the offspring were selected for the presence of the inserted P-element (eye colour: red). The red-eyed flies (white⁺) were backcrossed with flies from balancer stocks to produce a stable strain and determine the chromosomal localisation of the P-element. Crosses were made with 2nd and 3rd chromosomal balancers (R104, *w; Bl/SM1,CyO; +* and R24, *w; +; TM3,Sb/TM6B,Tb*) The established strains were kept either homozygous or balanced.

2.2.9 Germline transformation using the PhiC31 integrase system

A disadvantage of the P-element-mediated germline transformation (see section 2.2.8) is the random and undirected integration of the transformation construct into the fly genome. The location of the insert cannot be selected and sometimes the transgene can be inserted within a regulatory or coding region of another gene and disrupt its function. Another method to target specific localisations in the genome is the PhiC31 system, which uses the bacteriophage PhiC31 integrase and allows an efficient, directed integration of the transgene at a specific recognition site (Groth *et al.* 2004). The PhiC31 integrase is an enzyme that recognizes specific "attachment sites" in both the bacteriophage genome (attP) and in its bacterial host's genome

(attB) and catalyzes stable recombination between the two to insert itself into the bacteria's genome (Thorpe & Smith 1998). A large selection of fly strains is available that carry "attP sites" at different positions in the genome and have an endogenous PhiC31 integrase source (Bischof *et al.* 2007). A helper plasmid is therefore not necessary. Transformation into these fly strains was carried out using special transformation vectors that contained both an attB site and a selectable marker. With this technique, it is possible to introduce large pieces of DNA at a specific location in the genome. The injection of the transformation vector was performed as in the P-element-mediated germline transformation (see section 2.2.8).

2.2.10 UAS-Gal4 system

The UAS-Gal4 system is a genetic tool allowing the ectopic expression of a gene in a particular place and time during development (Brand & Perrimon 1993). It is a powerful method used to study gene expression and function in organisms. In *Drosophila*, the two components are carried in separate lines allowing for numerous combinatorial possibilities. The driver lines provide tissue-specific Gal4 expression under the control of a selected promoter or enhancer. The effector lines carry the coding sequence for the gene of interest under the control of five sequential Gal4-binding UAS sites (upstream-activating sequences). The two components are brought together in a simple genetic cross. When the driver line is crossed to the effector line, the "gene of interest", in our case the gene *dzy*, is only expressed in those cells or tissues expressing the Gal4 protein. The UAS-Gal4 system was used for the gain-of-function (gof) and rescue experiments. In gof experiments, tissue-specific Gal4 drivers were used to overexpress genes of interest. In rescue experiments, a UAS construct containing full-length or mutated cDNA of the gene was overexpressed in the respective genetic mutant background.

<u>Work with DNA</u>

2.2.11 Preparation of chemically competent cells

Bacterial cells of *E. coli* strains were treated with the following method to give them the ability to absorb plasmid DNA from the surrounding solution. 10 ml of LB medium were inoculated with a single colony from a LB agar plate and incubated and shaken overnight at 37 °C. With 2 ml of this culture, 250 ml of LB medium were inoculated and incubated under identical conditions up to an optical density OD_{650} of 0.2, corresponding to the logarithmic growth phase of the bacteria. After the culture was transferred into pre-cooled centrifuge tubes, the cells were cooled on ice for 5 minutes and harvested by centrifugation at 5,000 rpm for 5 minutes at 4 °C. All subsequent procedures were completed at 4 °C with minimal agitation to the cells to preserve their viability. The supernatant was discarded, the bacteria pellet was gently resuspended in 1/4 volume ice-cold 100 mM $MgCl_2$ and incubated for 3 - 5 minutes. The treated

cells were collected by centrifugation at 4,000 rpm for 10 minutes at 4 °C. The supernatant was discarded, and the pellet resuspended in 1/20 volume ice-cold 100 mM $CaCl_2$, then 9/20 volume ice-cold 100 mM $CaCl_2$ was added. The suspension was kept on ice for 20 minutes and was centrifuged at 4,000 rpm for 10 minutes at 4 °C. After centrifugation, the cells were resuspended in 1/100 volume ice-cold 85 % (v/v) 100 mM $CaCl_2$ and 15 % glycerol. For storage, 50 - 100 µl aliquots of competent cells were immediately frozen in liquid nitrogen and stored at -80 °C for use in bacterial transformations.

The transformation efficiency of the bacteria was measured in number of colonies per µg DNA. 50 µl of the chemically competent cells were incubated with 1 µl of the different dilution levels (100 ng, 10 ng, 1 ng, 0.1 ng and 0.01 ng) of plasmid DNA, heat-shocked at 42 °C for 30 seconds and plated out on antibiotic-containing agar plates (according to the resistance of the plasmid). Further 50 µl cells were carried along without plasmid DNA as negative control. The colonies were counted on the following day.

2.2.12 Restriction digest of DNA

Restriction digestions of PCR products or DNA plasmids were performed with restriction enzymes purchased from New England Biolabs (NEB) using the buffer provided according to the manufacturer's instructions for the respective restriction enzyme. The digestion was done in a total volume of 20 µl and contained the following reaction mixture: 5 - 10 µl of the plasmid DNA or PCR products were mixed with ddH_2O and the corresponding NEB restriction buffer was added in a 10 times concentration. The mixture was digested with 1 µl of the respective restriction enzyme or enzymes. Each tube was vortexed to thoroughly mix the contents and centrifuged for 5 seconds to ensure all of the reactants were in contact.

Amounts inserted in a digestion reaction:

DNA	5 µl
10x NEB buffer	2 µl
Enzyme 1	1 µl
Enzyme 2	1 µl
ddH_2O	11 µl
Total volume	20 µl

Digestion was carried out for 1 hour for test digests and 2 - 3 hours for preparative digests at 37 °C. An exception in temperature should be considered for some enzymes. The samples were separated on a 0.8 % agarose gel and gel purified using the Nucleospin® Gel and PCR Clean-up Kit (Macherey Nagel), Monarch® DNA Gel Extraction Kit (NEB) or the E.Z.N.A® Gel Extraction Kit (Omega) (see section 2.2.13).

Digestion of plasmids and DNA fragments for ligation

PCR products were digested prior to ligation in the appropriate plasmids. Larger scale digests were done in a total of 50 µl. In general, the total amount from a PCR reaction, following a purification step, was used in the digestion. The plasmids were digested with the same enzymes as the PCR fragment. Both the plasmid and fragment were digested with 1.5 µl of each NEB enzyme for 2 - 3 hours at 37 °C. Afterwards, the digests were analysed on an agarose gel.

2.2.13 Electrophoretic separation of DNA fragments in agarose gels

Agarose gel electrophoresis is a method used to separate DNA on the basis of their size and rate of movement through a gel under the influence of an electric field. The electrophoretic separation of DNA was performed in 0.8 % agarose gels. For gel production 1.3 g agarose was boiled in 160 ml 1xTAE, slightly cooled, provided with 8 µl ethidium bromide (10 mg/ml stock solution, Sigma) and poured into a prepared chamber. After polymerization, the gel was coated with 1xTAE gel running buffer and loaded with the prepared DNA samples (DNA + 1/4 volume 10x BlueJuice™ Gel Loading Buffer, NEB) and the 1kb DNA ladder (NEB). Electrophoresis was performed at constant voltage (Bio Rad Power PAC 200), which was selected between 100 V and 120 V depending on the size of the gel. The ethidium bromide-stained DNA was visualised under UV light and photographed with a gel documentation system (Gel doc, Phase).

DNA isolation from agarose gels

DNA fragments were isolated from agarose gels after gel electrophoresis using the Nucleospin® Gel and PCR Clean-up Kit (Macherey Nagel), Monarch® DNA Gel Extraction Kit (NEB) or the E.Z.N.A® Gel Extraction Kit (Omega) as described in the manufacturer's instructions.

2.2.14 Quantification of DNA and RNA with the spectrophotometer

The amount (ng) of isolated DNA (plasmid DNA, digested DNA or PCR fragments) and RNA was measured by the NanoDrop™ spectrophotometer (Thermo Scientific). The ratio of absorbance at 260 nm and 280 nm was used to assess the purity of the DNA and RNA. A 260/280 ratio of between 1.8 and 2.0 was accepted as "pure" for DNA and RNA.

2.2.15 De-phosphorylation of DNA fragments with rAPid Alkaline Phosphatase

In order to avoid a re-ligation of the linearized vector DNA during the ligation process (see 2.2.16) the vector DNA was dephosphorylated. The 20 µl dephosphorylation reaction was prepared as follows: up to 1 µg digested vector DNA, 2 µl 10x rAPid Alkaline Phosphatase buffer (Roche), 1 µl rAPid Alkaline Phosphatase (1 U, bovine intestinal Alkaline Phosphatase (Roche)) and ddH$_2$O. After an incubation period of 30 minutes at 37 °C the reaction was stopped by heating to 75 °C for 2 minutes to deactivate the Alkaline Phosphatase. The dephosphorylated DNA was directly used for ligation reactions or stored at -20 °C until further use.

2.2.16 Ligation

For the enzymatic ligation of the DNA fragments, the linearized and purified vector DNA was mixed with purified foreign DNA, 0.1 volume of 10x ligase buffer and 1 µl T4 DNA ligase. The ligation reaction was performed with a digested vector concentration of 50 ng and a total volume of 20 µl, using the supplier's buffer condition. The ligation reaction was prepared using an approximately 3:1 molar ratio of the insert and the vector. The amount of the insert to include in the ligation reaction was calculated as followed (Formula: Der Experimentator, C. Mühlhardt-Molekularbiologie/Genomics): ng of insert = 3 (ratio 3:1)* ng of vector (50 ng)* size of insert (bp) / size of vector (bp). The mixture was incubated for 2 hours at 37 °C or overnight at room temperature. After inactivation of the ligase for 15 minutes at 65 °C the ligated plasmid was used for transformation of chemically competent bacteria (see section 2.2.17).

Contents of the ligation reaction:

Vector (50 ng)	1 µl
10x ligase buffer	2 µl
Insert (3:1 ratio)	3 µl
Ligase	1 µl
ddH$_2$O	13 µl
Total volume	20 µl

2.2.17 Transformation of chemically competent cells

Transformation is the introduction of plasmid DNA into competent cells. The competent cells are chemically treated to allow their membranes to be permeated by plasmids (see section 2.2.11). Chemically competent bacterial cells were thawed on ice for 10 minutes. The DNA of interest was added, and the cells were incubated for 30 minutes on ice. Afterwards, the cells were heat-shocked at 42 °C for 2 minutes to introduce the DNA, following by a 5-minute recovery period on ice. After the addition of 200 µl SOC medium or LB medium, the cells were

incubated for a further 90 minutes at 37 °C on a shaker. 100 µl of the transformed cells was plated on LB agar plates containing the appropriate antibiotic and incubated overnight at 37 °C in an incubator. The next day single clones could be grown in liquid culture and subsequently analysed.

2.2.18 Cloning using TOPO® TA Cloning® Kit

The TOPO® TA Cloning® Kit from Invitrogen allows the cloning of PCR products with 3'-A-overhangs directly from the PCR reaction into the linearized TOPO vectors pCR®2.1 or pCR®4 without further modification or purification. PCR reaction was carried out using OneTaq® DNA Polymerase (NEB), Phusion® High-Fidelity (NEB) or HotStar HiFidelity (Qiagen) DNA polymerase, and the resulting PCR product was ligated into the pCR®2.1-TOPO® vector or pCR®4-TOPO® vector (Invitrogen) according to the manufacturer's protocol. For this purpose, the following ligation mixture was prepared: 4 µl PCR amplification product, 1 µl vector pCR®2.1-TOPO® or pCR®4-TOPO® (25 ng/µl), 1 µl salt solution and incubated for 30 minutes at RT. Transformation was carried out as described in section 2.2.17 Transformation of chemically competent cells. 6 µl of the ligation product was added to 50 µl chemically competent *DH5α* cells, gently mixed and incubated on ice for 30 minutes. After a 30-second heat shock at 42 °C, the cells were cooled down on ice, 100 µl SOC medium was added and the cells were shaken for 1 hour at 37 °C. Afterwards the ligation mixture was plated out on Ampicillin-containing agar plates (50 µg/ml) and incubated inverted overnight at 37 °C.

<u>Blue-White Screening</u>

When the selection plates were prepared with 10 µl IPTG solution (0.5 M (1 g/8.4 ml in ddH$_2$O), 10 µl X-Gal solution (100 mg/ml (240 mM) in DMF) and 100 µl ddH$_2$O, the specification of the pCR®2.1-TOPO® vector or pCR®4-TOPO® vector allow a colour selection in which clones with integrated foreign DNA appear light blue to white, while vectors without foreign DNA lead to a strong blue coloration of the bacterial colony. Therefore, only white (light blue) clones were used for further analyses. Clones obtained from the TOPO cloning were characterized by sequencing.

2.2.19 Cloning using NEBuilder HiFi DNA Assembly Cloning Kit

For the overlap-based in vitro DNA assembly method NEBuilder HiFi DNA Assembly (NEB), DNA fragments containing 25 - 36 bp long overlap regions were generated by PCR amplification and were assembled with a linerazied plasmid. The NEBuilder HiFi DNA Assembly cloning method was performed according to the manufacturer's recommendations. Briefly, DNA fragments with 15 to 20 bp long homology regions were prepared by PCR and assembled with linearized and dephosphorylated plasmids. Primers were designed using the

NEBuilder Assembly Tool, available at nebuilder.neb.com, adjusting the settings to Phusion® High-Fidelity Polymerase and 2 - 3 fragment cloning. The ligation reaction was performed using the DNA fragments with 15 - 20 bp overlapping regions and the digested vector backbone (50 - 100 ng). Fragments were incubated in a 1:2 vector:insert molar ratio, in a maximum volume of 10 µl and a maximum molarity of 0.2 pmol. The calculation performed to determine the total amount of fragments to be used with its corresponding backbone amount was done according to the manufacturer's formula (pmols = (weight in ng) x 1000/ (basepairs x 650 Daltons) or the NEB Ligation Calculator. To this, 10 µl NEBuilder HiFi DNA Master Mix was added and the volume was brought up to 20 µl with ddH$_2$O. The NEBuilder Assembly Master Mix reaction contained different enzymes working together in the same reaction mixture: the exonuclease created single-stranded 3' overhangs that facilitated the annealing of the overlap regions, the polymerase filled in the gaps within the annealing fragment, and the DNA ligase sealed the nicks in the assembled DNA. The mixture was incubated in a thermocycler at 50 °C for 1 hour. 2 µl of the reaction mixture was used to transform chemically competent bacterial *DH5a* cells, following the standard procedure described in section 2.2.17 Transformation of chemically competent cells.

2.2.20 Plasmid isolation

2.2.20.1 Plasmid isolation by TELT Miniprep (Lithium-chloride method)

3 ml LB medium with appropriate antibiotic were inoculated with a single bacterial colony and incubated overnight at 37 °C (shaking at 250 - 300 rpm). 1.5 ml of the overnight culture was transferred to a reaction tube and the cells were harvested by centrifuging for 5 minutes at 4,000 rpm. The supernatant was completely discarded, and the cells were resuspended in 100 µl of TELT+L-buffer (see section 2.1.4). After thorough mixing until the solution was homogeneous, the cells were incubated for 5 minutes at RT to break up the bacterial cell walls and release the DNA. Thereupon the preparation was heat-shocked for 2 minutes at 100 °C, incubated on ice for 5 minutes and centrifuged for 10 minutes at 10,000 rpm in a benchtop centrifuge. The precipitate pelleted by the centrifugation step (softpellet) was removed completely with a sterile toothpick. Afterwards the DNA was purified with an alcohol precipitation (see section 2.2.26.2).

2.2.20.2 Plasmid isolation using peqGold Plasmid Miniprep Kit

To obtain pure DNA, it was isolated from 3 ml of an overnight culture using the peqGold Plasmid Miniprep Kit (Peqlab) according to manufacturer's instructions.

2.2.20.3 Plasmid isolation using Macherey Nagel Plasmid Midiprep Kit

To obtain large amounts of pure DNA, the plasmid DNA isolation from 50 ml of an overnight culture was performed as described in the Macherey Nagel® NucleoBond® Xtra Midi Kit protocol.

2.2.21 Isolation of genomic DNA from *Drosophila melanogaster*

2.2.21.1 Isolation of genomic DNA from *Drosophila* adult flies

Per batch, 15 to 20 flies, anaesthetized with CO_2, were collected in a 1.5 ml reaction tube and frozen at -80 °C for 10 minutes. The frozen flies were homogenized gently with a Kontes pestle in 200 µl of extraction buffer (0.1 M Tris-HCl, pH 9.0, 0.1 M EDTA and 1 % SDS). The homogenate was incubated at 70 °C for 30 minutes to denature proteins. 30 µl of 8 M potassium acetate was added, mixed thoroughly, incubated for 30 minutes on ice and centrifuged at 4 °C for 15 minutes at 13,000 rpm in a microcentrifuge. 100 µl supernatant was transferred into a fresh reaction tube and precipitated by adding 0.1 volumes 3 M sodium acetate (pH 5.2) and 0.8 volumes isopropanol for 5 minutes at room temperature. Following centrifugation for 15 minutes at 13,000 rpm, the DNA pellet was washed with 70 % EtOH for 5 minutes at room temperature and resuspended in 50 µl ddH$_2$O. RNA was removed by adding DNase-free RNAse to a final concentration of 50 µg/ml and incubating at 37 °C for 15 minutes.

2.2.21.2 Genomic DNA isolation from a single fly -"quick n dirty" protocol

Single flies of the strains to be tested were anesthetized, collected and transferred to a 0.5 ml reaction tube. The single flies were briefly stored at -20 °C and then mashed for 5 - 10 seconds with a pipette tip containing 50 µl of squishing buffer (SQ-Buffer), without expelling any liquid. The required amount of SQ-Buffer was automatically dispensed from the tip when crushed. Then the remaining 50 µl of SQ Buffer was expelled. The mixture was incubated at 37 °C for 30 minutes and the enzyme Proteinase K was deactivated by heating to 85 °C for 10 minutes. Finally, the solid junk was briefly spin down by centrifugation at 13,000 rpm for 1 minute and the preparation was stored on ice.

2.2.22 RNA isolation

RNA was extracted either with the RNeasy® Plus Mini Kit (Qiagen) according to the manufacturer`s instruction or using the miRNeasy Micro Kit in combination with the QIAzol® Lysis Reagent.

2.2.22.1 RNA extraction using RNeasy® Plus Mini Kit (Qiagen)

<u>Sample preparation</u>

Embryos were dechorionated with a 1:1 Klorix® and water solution. After an incubation period of 5 minutes, the dechorionated embryos were transferred into a thin, fine-meshed plastic sieve and thoroughly rinsed with running tap water (see section 2.2.3). The sieve was removed from the plastic cylinder to transfer the embryos onto an apple juice agar plate. 5 - 25 mg of the embryos were collected with a preparation needle or spatula from the agar plate and transferred into a 1.5 ml reaction tube. Embryos were frozen in liquid N_2 and stored at -80 °C prior to use.

<u>RNA extraction</u>

Total RNA was isolated from w^- embryos of *Drosophila* using RNeasy Plus Mini Kit (Qiagen) according to the manufacturer's instruction. The RNeasy® Plus Mini Kit isolates total RNA from up to 30 mg tissue. Briefly, samples were first lysed and homogenized. The lysate was passed through a gDNA Eliminator spin column, 70 % ethanol was added to the flow-through, and the sample was applied to a RNeasyMini spin column. The mixed solution was centrifuged, the flow-through was discarded and the column containing the RNA was washed with various RNA-Wash buffers from the RNeasy® Plus Mini Kit. RNA binds to the membrane and contaminants are washed away. The RNeasyMini spin column was inserted into a fresh 1.5 ml reaction tube and RNA was eluted in 30 µl RNAse-free water. RNA concentration and purity was measured with the NanoDrop (260/280 = 2.0) and the RNA samples were stored at -20 °C for later use.

2.2.22.2 RNA extraction with miRNeasy Micro Kit and QIAzol® Lysis Reagent

The miRNeasy Micro Kit (Qiagen) in combination with QIAzol® Lysis Reagent (Qiagen) were used to isolate RNA from difficult-to-lyse tissues. Total RNA was isolated from w^- embryos, larvae, pupae and adults of *Drosophila* using miRNeasy Micro Kit with QIAzol® Lysis Reagent according to the manufacturer`s instructions.

<u>Sample preparation and RNA extraction</u>

Embryos were incubated with a 1:1 bleach (Klorix®) and water solution for 2 minutes and transferred into a sieve. Embryos were transferred with a preparation needle or spatula into a reaction tube. For whole fly RNA extraction, 5 mg of larvae, pupae and anaesthetized adult flies were collected directly from the w^- fly vials and transferred in a reaction tube. For isolation, the tubes were stored in liquid nitrogen for 3 minutes prior to use. The samples were disrupted and homogenized in a 1.5 ml tube using a plastic mortar in the presence of 700 µl of the

QIAzol® Lysis Reagent. The homogenate was proceeded further using the miRNeasy Micro Kit from Qiagen according to the manufacturer's instructions. RNA was eluted in 14 µl RNAse-free water.

2.2.23 Reverse transcription

2.2.23.1 cDNA synthesis using Transcriptor First Strand cDNA Synthesis Kit

Reverse transcription was performed using the Transcriptor First Strand cDNA Synthesis Kit (Roche) with specific reverse primer or anchored-oligo-(dT) primer, following the manufacturer's instructions. 1 µg of total RNA was subjected to cDNA synthesis.

The PCR was set up using the following mixture:

RNA template (1 µg total RNA)	variable
Primer 1 (10 µM)*	1 µl
5x Reverse Transcriptase Buffer	4 µl
Protector Rnase Inhibitor (40 U/µl)	0.5 µl
dNTP Mix (10 mM)	2 µl
Transcriptor Reverse Transcriptase (20 U/µl)	0.5 µl
ddH$_2$O	to 20 µl
Total volume	20 µl

* reverse primer or oligo-(dT) primer

The reagents were gently mixed by pipetting and centrifuged briefly to collect the sample on the bottom of the reaction tube. Afterwards, the sample (total volume 20 µl), was placed in a thermal block cycler (FlexCycler^2, analytikjena) with a heated lid and incubated for either 30 minutes at 55 °C (up to 4 kb target RNA) or 60 minutes at 50 °C (> 4 kb target RNA). The Transcriptor Reverse Transcriptase was inactivated by heating to 85 °C for 5 minutes. To stop the reaction, the reaction tube was placed on ice. The cDNA was then stored at -20 °C.

2.2.23.2 cDNA Synthesis using LunaSkript™ RT SuperMix Kit

LunaSkript™ RT SuperMix (NEB) is an optimized Master Mix containing all necessary components for first strand cDNA synthesis: Luna™ Reverse Transcriptase, Murine RNase Inhibitor, dNTPs and oligo-(dT) primers.

The cDNA synthesis was set up using the following mixture (20 µl total volume):

LunaScript RT SuperMix (5x)	4 µl
RNA Sample (up to 1 ug total RNA)	variable
Nuclease-free Water	to 20 µl
Total volume	20 µl

The cDNA synthesis was performed in a thermal cycler (FlexCycler2, analytikjena) under the conditions listed below. The cDNA products were used directly in the PCR reaction or stored at -20 °C for later use.

PCR incubation steps of the thermal cycler during cDNA synthesis with LunaSkript™ RT SuperMix:

Step	Temp.	Time
Primer Annealing	25 °C	2 min
cDNA Synthesis	55 °C	10 min
Heat Inactivation	95 °C	1 min

*Heat lid to 95 °C

2.2.24 Polymerase Chain Reaction (PCR)

PCR reactions were carried out using OneTaq® DNA Polymerase (NEB), Phusion® High-Fidelity DNA Polymerase (NEB) or HotStar HiFidelity DNA Polymerase (Qiagen).

2.2.24.1 PCR using OneTaq® DNA Polymerase with Standard Buffer (NEB)

Specific DNA sections were amplified *in vitro* using the polymerase chain reaction. Unless otherwise indicated, the heat stable Taq-polymerase from the thermophilic bacterium *Thermus aquaticus* was used as DNA polymerase.

Contents of the OneTaq® DNA Polymerase with Standard Buffer (NEB) approach:

OneTaq® 2x MasterMix	12.5 µl
(dNTPs, polymerase buffer, Taq-polymerase)	
Primer 1 (10 µM)	1 µl
Primer 2 (10 µM)	1 µl
Template DNA*	1 µl
ddH$_2$O	9.5 µl
Total volume	25 µl

* Amount used for standard PCR: 50-100 ng

Steps of the PCR reaction:

Steps of the procedure	temperature	time
Initial denaturation	94 °C	30 sec
Loop: (25 - 30x)		
Denaturation	94 °C	20 sec
Annealing	Primer specific	45 sec
Extension	68 °C	1 min/kb
Final-Extension	68 °C	5 min
Hold	8 °C	-

The PCR process is composed of 25 - 30 cycles. Each individual cycle consists of three precisely time-controlled and temperature-controlled steps: denaturation, annealing and extension. The annealing temperature is primer specific and depends on the melting temperature of the used primers. Primers used in this work are listed above (see section 2.1.5). Specific primers for the individual experiments were designed using the PrimerSelect Lasergene software (DNASTAR). For primers with specific base mismatches, a low stringency annealing temperature of 58 °C - 60 °C was chosen to ensure adequate primer deposition. To perform the reactions either the FlexCycler[2] (analytikjena) or the Peqstar 96 Universal Gradient (Peqlab) thermal cycler were used.

2.2.24.2 PCR using Phusion® High-Fidelity DNA Polymerase (NEB) and HotStar HiFidelity DNA Polymerase (Qiagen)

The Taq-polymerase used in standard PCR has a comparatively high error rate of 2×10^{-4}/ base. Therefore, High-Fidelity PCR enzymes were used for applications requiring high accuracy during DNA amplification. Phusion® High-Fidelity DNA Polymerase (NEB) and HotStar HiFidelity DNA Polymerase (Qiagen) were used for cloning experiments, as both have a proofreading function and therefore extremely low error rates. Both polymerases were used, according to the supplier's recommendations.

Contents of the Phusion® High-Fidelity Polymerase PCR approach:

5x Phusion HF Buffer	4 µl
dNTPs (10 mM)	0.4 µl
Primer 1 fw (10 µM)	1 µl
Primer 2 rev (10 µM)	1 µl
Template DNA (< 250 ng)	variable
Phusion DNA Polymerase	0.2 µl
ddH$_2$O	to 20 µl
Total volume	20 µl

Steps of the Phusion® High-Fidelity Polymerase PCR reaction:

Steps of the procedure	temperature	time
Initial denaturation	98 °C	30 sec
Loop: (25 - 35x)		
Denaturation	98 °C	5 - 10 sec
Annealing	Primer specific (45 - 72 °C)	10 - 30 sec
Extension	72 °C	15 - 30 sec/kb
Final-Extension	72 °C	5 - 10 min
Hold	4 - 10 °C	-

Contents of the HotStar HiFidelity DNA Polymerase PCR approach:

5x HotStar HiFidelity PCR Buffer (contains dNTPs)	10 µl
Primer 1 (20 µM)	1 µl
Primer 2 (20 µM)	1 µl
Template DNA (50 ng)	1 µl
HotStar HiFidelity DNA Polymerase	1 µl*, 2 µl*
ddH$_2$O	to 20 µl
Total volume	20 µl

*Depending on expected PCR product length. 1 µl enzyme was used when amplifying PCR products <2 kb and 2 µl when amplifying PCR products 2 - 5 kb

Steps of the HotStar HiFidelity DNA Polymerase reaction:

Steps of the procedure	temperature	time
Initial activation step	95 °C	5 min
Loop: (30 - 45)		
Denaturation	94 °C	15 sec
Annealing	Primer specific (50 - 68 °C)	1 min
Extension	72 °C	1 min/kb*
	68 °C	2 min/kb*
Final-Extension	72 °C	10 min
Hold	4 °C	-

* For PCR products <2 kb, an extension time of 1minute per kb DNA was used. For PCR products 2 - 5 kb, an extension time of 2 minutes per kb DNA was used.

2.2.25 Variations in the standard PCR technique

2.2.25.1 Colony-PCR

Colony-PCR was performed to screen a large number of clones. Following bacterial transformation, single colonies were picked using a sterile pipet tip and resuspended in 7 µl of sterile water. As a backup the picked colonies can be smeared on another agar plate. PCR was performed using 7 µl of the resuspended colonies as template DNA and 10 µl of the PCR Master Mix containing the Taq-polymerase buffer, dNTPs, the Taq-polymerase and the specific primer pair. Different primer combinations were used to confirm the presence and size of an insert. The cells were decomposed at 98 °C for 5 minutes in the PCR machine. After cell decomposition, the DNA was exposed and served as a template. In the pause modus of the PCR Machine the temperature was stored at 80 °C and in this time the PCR Master Mix was added. Then the actual PCR reaction was started (see section 2.2.24.1).

Steps of the Colony-PCR:

Steps of the procedure	temperature	time
Cell decomposition	98 °C	5 min
Pause (addition of the Master Mix)	80 °C	variable
Cycle step 1 Denaturation	95 °C	30 sec
Cycle step 2 Annealing	Primer specific	30 sec
Cycle step 3 Extension	72 °C	1 min/kb
End-Extension	72 °C	5 min

2.2.25.2 Touchdown-PCR

Touchdown-PCR is a method for raising the specificity of primers and sensitivity in PCR amplification (Korbie & Mattick 2008). Otherwise, primers can amplify an amount of unspecific bands. The single steps of the Touchdown-PCR reaction were equal to the actual PCR process (see section 2.2.24.1). The initial annealing temperature was set up approximately 10 °C above the calculated melting temperature of the primers. The temperature was high enough that unspecific binding of the primers was inhibited and the primers amplify only the specific sequence. The annealing temperature was decreased about 1 °C in each loop of the Touchdown-PCR. Finally, the temperature reached the primary annealing temperature of the primers.

2.2.25.3 Nested-PCR

Nested polymerase chain reaction (Nested-PCR) was used to increase the sensitivity of the PCR reaction, e.g. when amplifying a cDNA copy of an mRNA that is present in very low quantity. In Nested-PCR, two amplification reactions were performed with two different primer pairs. The first PCR amplification reaction was similar to the conventional PCR reaction (see section 2.2.24.1). The product of the first amplification reaction was used as the template for the second PCR reaction. Thus, the second primer pair (nested primer pair) was within the first PCR product, making the second PCR amplification fragment shorter than the first. By using two primer pairs, a higher number of cycles could be performed, increasing the sensitivity of the PCR.

2.2.26 Phenol-chloroform extraction and ethanol precipitation

2.2.26.1 Phenol-chloroform extraction

The DNA sample was filled up to 200 µl by adding ddH$_2$O. 200 µl (1 volume) of phenol was added to the DNA, the solution was mixed by vortexing and centrifuged at 13,000 rpm for 1 minute. The upper aqueous phase formed after centrifugation was transferred to a second reaction tube (reaction tube 2). 100 µl (0.5 volume) of phenol and 100 µl (0.5 volume) of chloroform were added to the sample in reaction tube 2 and mixed well by vortexing. The sample was centrifuged again at 13,000 rpm for 1 minute. The upper phase was again transferred to a fresh reaction tube (reaction tube 3). 200 µl (1 volume) of chloroform was added to reaction tube 3 and the solution was vortexed and then centrifuged at 13,000 rpm for 1 minute. Finally, the upper phase was removed and transferred to reaction tube 4. Afterwards the DNA was concentrated with an alcohol precipitation.

2.2.26.2 Ethanol precipitation

For purification, the DNA was precipitated from liquid solution by the addition of 0.1 volumes of 3 M natrium acetate (NaAc, pH 5.2) and 0.8 - 1 volumes of isopropanol. The DNA solution was incubated for at least 5 minutes at RT. The DNA sample was pelleted by centrifuging at 13,000 rpm for 15 minutes at RT. The supernatant was discarded. The pellet was washed with 200 µl of 70 % ethanol and re-centrifuged for 15 minutes at 13,000 rpm. The supernatant was discarded again, and the DNA pellets were either air-dried or dried in a SpeedVac (DNA SpeedVac 110, Savant). The dried pellet was resuspended in 30 - 50 µl ddH$_2$O.

2.2.27 Sequencing of DNA

Sequencing of the DNA was performed by LGC Genomics (https://shop.lgcgenomics.com). The DNA was treated and sent to LGC Genomics as the company recommended. Two different services were used: (1) Ready2Run: 10 µl DNA (100 ng/µl) and 4 µl primer (1:10) and (2) FlexiRun (universal primer) 20 µl DNA (100 ng/µl). The DNA to be sequenced was dissolved in ddH_2O.

3. Results

3.1 The dzyN terminus and the alternative translation start

<u>Molecular genetics of the *Drosophila* PDZ-GEF Dzy</u>

Haemocyte migration is the subject of intensive research because the diversity of the components involved alone makes it clear that by no means have all the links in the individual signaling cascades been identified. This is further complicated by the fact that mutations of individual factors such as GEFs, GAPs and GTPases often show no phenotype due to redundancies. In many cases, the function of the individual components can be taken over by factors of the same protein family. Therefore, a mutation often remains phenotypically unnoticed. An alternative way to identify components involved in the process of cell migration is the generation of gain-of-function (gof) mutations. In a gof-screen, the alleles generated by mutagenesis are examined for conspicuous phenotypes. EP-element insertions can be used to generate these gain-of-function mutations (Rørth 1996; Rørth *et al.* 1998). EP-element insertions in a mutagenesis experiment occur at random locations. Prior to this dissertation, Sven Huelsmann and colleagues found a phenotype in the line EP388 carrying the EP-element in close proximity to the gene *dzy* (Huelsmann *et al.* 2006).

Virgins of the *srph>cd2* strain were crossed with males of a genotype from the EP collection (Szeged). In this case, Gal4 was expressed in the haemocytes under the control of the *srp* enhancer (driver). The genes to be tested were under the control of EP-elements that were randomly integrated into the genome of the EP lines. Embryos were collected and stained for CD2 following the methods described in (Hummel *et al.* 1997), embedded in methyl salicylate and examined for macrophage migration and cell shape changes. The EP388 line was chosen because it exhibited a phenotype in the haemocytes. In this work, we aim to investigate the structure and function of the gene *dzy* (Huelsmann *et al.* 2006) in detail and its requirement for proper cell shape and cell migration in the *Drosophila* embryo. For this purpose, alternative splicing of the gene, different protein domains and possible alternative translation initiation sites (altTIS) were analysed.

Role of the dzyN terminus in the regulation of Dzy

In further studies of dzy^{EP}, a full-length cDNA of *dzy* was isolated and thereby an additional exon of *dzy*, termed exon 0, located 5' to the first exon (annotated in Flybase), was mapped (Huelsmann *et al.* 2006). The canonical translation initiation start site (TIS) of *dzy* is located in the central region of exon 1. Accordingly, what is the significance of exon 0 and the 5'-UTR region? Is there a possibility that there are alternative AUGs in this 5' region upstream of the annotated coding sequence (CDS)/main open reading frame (main-ORF)? What if there is an

alternative TIS (altTIS) upstream of the canonical start codon that can initiate the translation of different protein products: either an N-terminal extended isoform of the CDS-encoded protein or an unrelated protein. Do these protein products have regulatory functions?

It is well known that the quantity of genes in eukaryotic genomes does not reflect the biological complexity of the respective organisms. Many genes encode multiple variants of proteins, due to the use of alternative promotors and alternative splicing, which greatly increases the number of proteins produced. These mechanisms have been studied extensively and are usually taken into account when studying gene expression characteristics and coding potential. Alternative translation is another molecular mechanism allowing a single mRNA to produce multiple proteins. The current understanding is that most eukaryotic mRNAs typically contain one translation start site and encode for a single protein product. The possibility of alternative translation is rarely considered. However, the collected experimental data show that dozens of eukaryotic mRNAs generate protein isoforms due to the use of alternative translation initiation sites (Kochetov 2008; Bazykin & Kochetov 2011).

Initiation of translation of eukaryotic mRNAs probably occurs by the "linear scanning" mechanism. According to this scanning model (Kozak 1980), 40S ribosomal subunits are recruited at the 5' terminal cap, scan the mRNA in 5' - to 3' direction and are able to initiate translation at the first AUG that they detect (Kozak 1978). The recognition of an AUG triplet as a translation initiation sites (TIS) depends on its nucleotide context (Kozak 1997). Most 40S ribosomal subunits will recognize the AUG and commence translation, if the context is optimal. However, if the context is suboptimal, some ribosomal subunits will recognize the AUG as a TIS, while others will leave it out, continue scanning in 3' direction and initiate translation at a downstream AUG ("leaky scanning") (Kochetov 2008; Bazykin & Kochetov 2011).

In addition to "linear scanning" and "leaky scanning", it has also been shown that eukaryotic ribosomes can reinitiate translation at a downstream open reading frame (dORF). In this process, the ribosomal subunits remain connected to the mRNA after the termination at an upstream ORF (uORF) stop codon and continue the scanning process. However, the resumption of scanning (reinitiation) only occurs if the first ORF is short. It has been hypothesised that after translation of a rather short uORF, some translation factors stay connected to the ribosome, enabling the reinitiation process (Kochetov 2008).

Types of alternative open reading frames

ORFs originating from alternative start codons may be located at different positions relative to the CDS/main-ORF. Upstream AUGs may serve as start sites of small proteins or peptides that are not associated with the protein product encoded by the main ORF (Fig. 7, uORF A and uORF B (upstream AUG is located out of the CDS frame)). In some cases, an upstream AUG can serve as the start codon of a 5' end extended version of the main-ORF (uORF C (upstream AUG lies in the CDS frame)). If the start codon of the main-ORF is in a suboptimal context, translation at downstream AUGs can be initiated by the leaky scanning mechanism. The "leaky scanning" mechanism can either result in an unrelated small protein (dORF A (downstream AUG is located out-of-frame)) or an isoform of the annotated ORF (CDS) truncated at the N-terminus (dORF B (downstream AUG is located in-frame with CDS)). Thus, an alternative TIS can initiate translation of various protein products: either the N-terminal truncated (dORF B) or the N-terminal extended isoform of the CDS-encoded protein (uORF C) or a rather small, unrelated protein (uORF A, uORF B and dORF A) (Kochetov 2008).
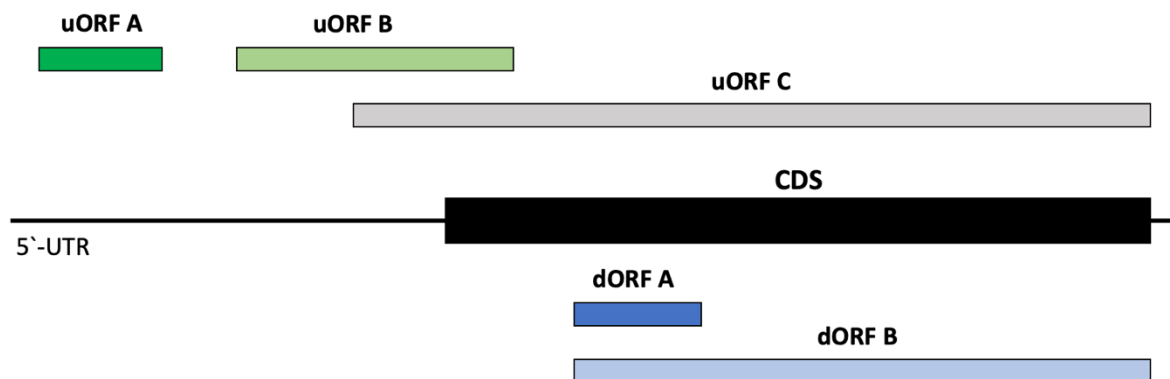
Fig. 7 Alternative TIS and ORFs within eukaryotic mRNA.
uORFs start from AUG codons located in the 5'-UTR and can either be restricted to the 5'-UTR (uORF A, green box), partially overlap with the CDS (uORF B, light green box) or merge with the CDS (uORF C, gray box). dORFs start from AUG codons located downstream of the annotated AUG, which is in a suboptimal context, and can either encode for a small protein (dORF A, blue box) or encode for a protein variant truncated at the N-terminus (dORF B, light blue box). The annotated ORF (CDS) is indicated by a black box.

In this part of the PhD thesis, we wanted to focus on alternative upstream translation initiation sites (altTISs) of the *dzy* transcript. Numerous studies have documented that translation starts not only at the CDS or main-ORF, but also from alternative AUG or even non-AUG start codons in the 5'-UTR of the transcripts. These translation initiation sites are located upstream and represent unrelated upstream open reading frames (uORF type A) and CDS-overlapping uORFs (uORF type B (not in-frame) and uORF type C (in-frame)) that may have critical regulatory functions for gene expression. Among others, for example N-terminal protein extensions may be relevant for the subcellular protein sorting. To investigate the dzyN terminus

and the possibility of an alternative translation initiation start site (altTIS), total RNA was isolated from *Drosophila w⁻* embryos and reverse transcribed into cDNA using a specific primer in exon 2 (PR160). Reverse transcription was performed from 1 µg of total RNA using the Roche Transcriptor First Strand cDNA Synthesis Kit according to the recommendations in the manufacturer's instructions. Subsequently, the 5' and 3' ends of *dzy* cDNA were amplified by PCR using gene-specific primers located in exon 0 (PR 166) and exon 2 (PR 160). As a control for the selected primer combination, the construct *dzyC in pUAST clone 12* was chosen (see Results section 3.3).

Since the identification of new upstream ORFs (uORF A and uORF B) and N-terminal protein extensions (uORF C) was of interest in the first part of the work, a restriction of further analyses to the 5'-UTR and the first two exons (exon 1 and exon 2) of the CDS was chosen. The bands generated by gel electrophoresis (PR160/PR166 = 310 bp) were eluted from the gel and cloned into a TOPO vector. The cloning approach was transformed into chemically competent *DH5α* cells and plated onto Amp-containing media (see Material & Methods). After several repetitions of this procedure, two white colonies were finally picked from the agar plates (see Material & Methods) and grown overnight in LB medium. Plasmid DNA was purified according to the TELT Miniprep protocol (see Material & Methods). To verify that the plasmid DNA had the correct insert size (310 bp), a test PCR analysis of the obtained clones were performed using the primer pair PR166/PR160 in exon 0 and exon 2. Of the two clones, only clone 1 showed the expected 310 bp band. The purified *dzy* construct was sequenced by LGC genomics (LGC Genomics, Berlin, Germany). The sequenced construct was listed as *pCR2.1_166_160rev clone 1*.

Overall, we found two possible alternative AUG start codons in the 5'-UTR of the *dzy* transcript (altTIS1 (uORF1) and altTIS2 (uORF2), Fig. 8). In this study, the focus was on these two uORFs, listed here as uORF1 and uORF2. Initiation at the upstream AUG codon 1 (altTIS1) at position 121 (position related to pCR2.1_166_160rev clone 1) in exon 0 led to the formation of a 12 AS long peptide (Fig. 8B). In contrast, initiation at the upstream AUG codon 2 (altTIS2) at position 167 (position related to pCR2.1_166_160rev clone 1) led to the formation of a 19 AS long peptide (Fig. 8C). These upstream translation initiation sites thus represent upstream open reading frames (uORFs) that are restricted to the 5'-UTR (uORF type A, see Fig. 7) and do not partially overlap with the CDS. No CDS-overlapping uORFs (uORF type B) or N-terminal protein extensions (uORF type C) were found in the pCR2.1_166_160rev clone. These upstream AUGs serve as translation start sites for peptides or small proteins that are not associated with the protein product encoded by the main-ORF.
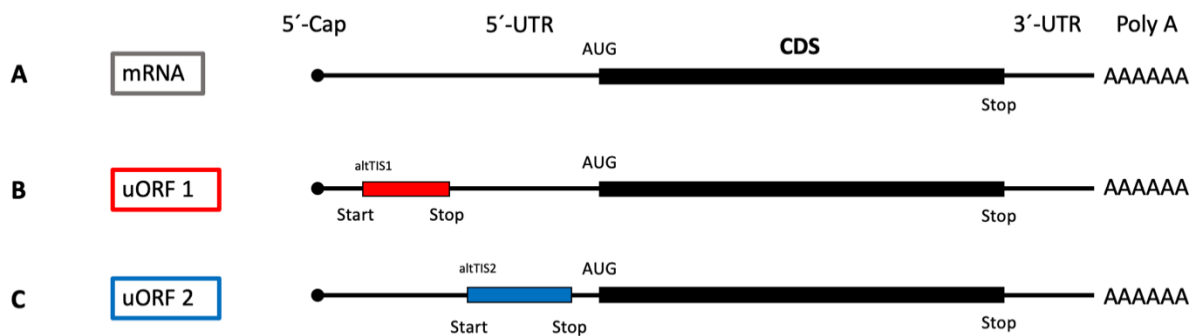
Fig. 8 Schematic representation of the alternative TIS (altTIS1 (uORF1) and altTIS2 (uORF2)) at the dzyN terminus of *pCR2.1_166_160rev*.
(A) Transcript with 5' cap, 5'-UTR, CDS, 3'-UTR and poly(A) is shown in black. The protein coding sequence is drawn as a thick line. The colored boxes show the position of the additional open reading frames. Upstream-located ORFs (B) uORF1 and (C) uORF2 were 5'-UTR-restricted (uORF1, type A, red box and uORF2, type A, blue box). No uORF type B partially overlapping with the CDS or type C with an N-terminal extension of the main-ORF could be found.

For further investigation of the N-terminus, the DNA sequence of the isolated DNA (*pCR2.1_166_160rev clone 1*) was compared with the genomic DNA sequence of *dzy* (*dizzy* map) and the gene construct *dzyC in pUAST* (*dzyC in pUAST clone 12*). When comparing the three DNA sequences (*dizzy* map, *dzyC in pUAST clone 12* and *pCR2.1_166_160rev clone 1*) we discovered a difference in uORF1 (Fig. 9B). In the *dizzy* map and the clone *pCR2.1_166_160rev*, we found a CACACACA sequence segment (fourfold repetition of the two bases cytosine (C) and adenine (A)). Initiation at the upstream AUG codon 1 (altTIS1) at position 5316 (position related to *dizzy* map) and 121 (position related to *pCR2.1_166_160rev clone 1*) in exon 0 resulted in the formation of a 12 AS long peptide. In contrast, the *dzyC in pUAST clone 12* showed only a threefold repeat of the cytosine/adenine sequence segment at position 3469 (position related to *dzyC in pUAST clone 12*) when sequenced. The missing CA in the sequence of *dzyC in pUAST clone 12* led to a shift in the ORF. Initiation at the upstream AUG codon 1 (altTIS1) at position 3445 (position related to *dzyC in pUAST clone 12*) in exon 0 resulted in the formation of an 81 AS long peptide. Thus, the ORF of TIS1 overlapped with the main-ORF (uORF type B, see Fig. 7). However, the AUG codon was not in the same reading frame as the canonical start codon and therefore did not lead to the expression of an N-terminally elongated protein variant (uORF type C). uORF1 was not in-frame with the annotated CDS. In general, uORF1 starting from an alternative AUG codon in the 5'-untranslated region of the *dzy* gene was either restricted to the 5'-UTR (*dizzy* map and *pCR2.1_166_160rev*) or partially overlapped (*dzyC in pUAST*) with the CDS. In contrast, an N-terminal protein extension by uORF1 could not be observed (Fig. 9B).

Upon further examination of the three sequences (*dizzy* map, clone *dzyC in pUAST clone 12* and *pCR2.1_166_160rev clone 1*), we were able to locate another alternative translation

initiation site (altTIS2) in exon 0, slightly downstream of altTIS1. In the sequence of the *dizzy* map and *dzyC in pUAST clone 12*, we were able to identify a guanine residue (G) at the transition from exon 0 to exon 1. The ORF of altTIS2 (uORF2) thus led to the formation of a 66 AS long peptide. In the case of the *dzyC in pUAST clone 12*, altTIS2 was located in the same reading frame as the alternative start codon altTIS1 and thus uORF2 (66 AS) nested within uORF1 (81AS) (Fig. 9C). Like uORF1 (81AS), uORF2 (66AS) was not in-frame with the main-ORF. The presence of the base guanine between the two exons led to a termination of uORF2 at the beginning of exon 2. In contrast to the *dizzy* map and *dzyC in pUAST clone 12*, the *pCR2.1_166_160rev* construct lacked the guanine residue between exon 0 and exon 1. In this case, as already mentioned, the protein would only be 19 AS long and would not overlap with the main-ORF (Fig. 9C). A missing guanine between exon 0 and exon 1 (position 493 in the *pCR2.1_160_166rev clone1* map) resulted in a shift of the ORF and the stop codon terminated translation at the beginning of exon 1.

Thus, we discovered that two different sequence variants of the 5'-UTR of *dzy* exist (A) in exon 0 (CACACACA (4x) or CACACA (3x)) or (B) in the region between exon 0 and exon 1 (G present or G absent). Depending on which variant or variant combination arrives, there is a shift in the ORF and thus new possible stop codons. The length of the proteins to be translated became longer or shorter depending on which variant was present and which stop codon terminated the translation (Tab. 1). It is possible that the regulatory function of each variant differs. In the *dzy* transcript, alternative upstream TIS (altTIS) could start the translation of principally different protein products. At this stage, it is difficult to make a more precise statement about the *dzy* sequence in the exon 0 region. Of the two available constructs, *dzyC in pUAST clone 12* showed a CACACA sequence and a guanine residue between exon 0 and exon 1, while *pCR2.1_160_166rev clone 1* showed a CACACACA sequence and no guanine residue between exon 0 and exon 1. After isolation of further total RNA from flies, a tendency in one direction or a confirmation of both variants might be possible. It would also be interesting to investigate whether the different uORFs have regulatory significance.
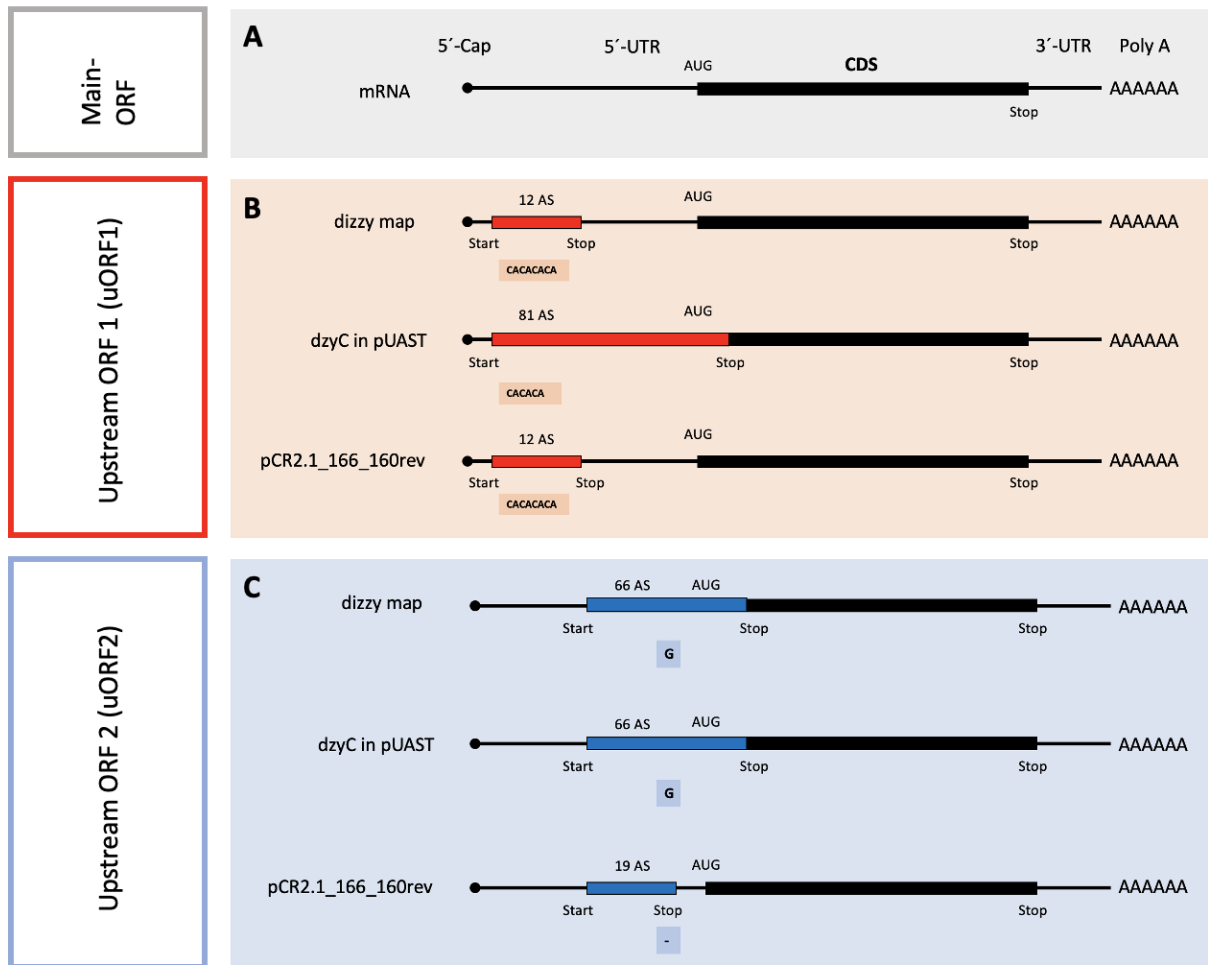
Fig. 9 Analysis of the dzyN terminus.
Comparison of the upstream alternative ORFs (uORF1 and uORF2) in the 5'-UTR of the *dzy* transcript in the three DNA sequences (*dizzy* map, clone *dzyC in pUAST* and clone *pCR2.1_166_160rev*). (A) Main-ORF (B) uORF1, originating from an alternative AUG codon in the 5'-untranslated region of the *dzy* gene was either restricted to the 5'-UTR (*dizzy* map and *pCR2.1_166_160rev,* uORF type A) or partially overlapped (*dzyC in pUAST*, uORF type B) with the CDS/main-ORF (A). (C) uORF2 was located slightly downstream of uORF1 and was either unrelated to the CDS (*pCR2.1_166_160rev,* uORF type A) or partially overlapped with the main-ORF (*dizzy* map and *dzyC in pUAST,* uORF type B).

Tab. 1 Investigation of the dzyN terminus.
Comparison of the upstream alternative ORFs (uORF1 and uORF2) in the 5'-UTR of the *dzy* transcript in the three DNA sequences (*dizzy* map, *dzyC in pUAST* and *pCR2.1_166_160rev*).

	dizzy map	dzyC in pUAST (dzyC in pUAST clone 12)	pCR2.1_166_160rev (pCR2.1_166_160rev clone 1)
uORF1 **altTIS1** **Location: Exon 0**	CACACACA (4x) Length: 12AS	CACACA (3x) Length: 81AS Note • Overlap with CDS • Not in-frame with CDS	CACACACA (4x) Length: 12AS
uORF2 **altTIS2** **Location: Exon 0**	Guanine (exon 0 - exon 1) present Length: 66AS Note • Overlap with CDS • Not in-frame with CDS	Guanine (exon 0 - exon 1) present Length: 66AS Note • Overlap with CDS • Not in-frame with CDS • In-frame with uORF1	Guanine (exon 0 - exon 1) absent Length: 19AS

3.2 The different isoforms of *dzy*

As mentioned in the introduction, Dzy is an essential component in macrophage migration and adhesion. In this part of the work, we focused on the detailed analysis of the structure of the *dzy* transcript. The *dzy* genomic locus comprises nine exons. All PDZ-GEF conserved domains reside in exon 3. Based on ESTs (expressed sequence Tags), *dzy* gives rise to three different mRNA splice variants *dzyA*, *dzyB* and *dzyC*. All of these splice forms show a common structure from exon 0 to exon 4 (see Introduction Fig. 6). Exon 5 is either included entirely (splice form *dzyA*), truncated (named exon 5S) (*dzyB*) or spliced out (*dzyC*). Three proline rich domains, which are usually responsible for protein-protein interactions, are encoded by parts of exon 4, 5S and 5. Accordingly, the different splice forms *dzyA* and *dzyB* feature all three, while splice form *dzyC* features only one proline-rich domain. The loss of exon 5 in the *dzyC* form leads to the connection of exon 4 with exon 6L. The mRNA sequence of the different variants can be continued with either exon 6 and 7 (*dzyA*), or exon 6L (a longer version of exon 6) and exon 7L (exon 7* - exon 7) (*dzyB and dzyC*). These sets are combined and result in the following three forms: *dzyA*, *dzyB* and *dzyC*.
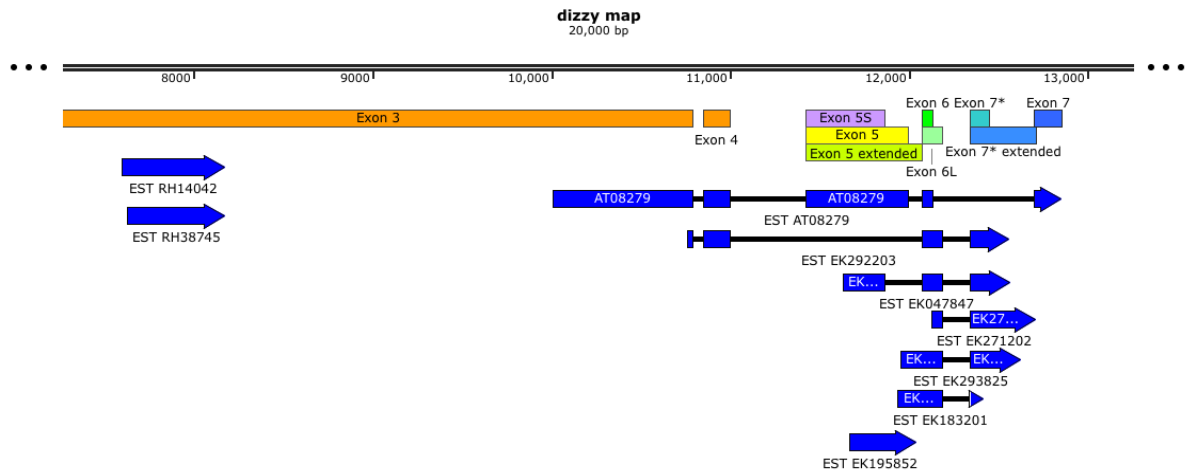
Fig. 10 Schematic representation of the ESTs.
Representation of the different ESTs known for the region exon 5 to exon 7 of the *dzy* locus.

Tab. 2 Summary of the ESTs schematically shown in Fig. 10.
Overview of the ESTs with the corresponding exons and introns as well as the associated *dzy* splice forms. The *dzy* region covered by the ESTs is shown in blue.

EST							
AT08279	Exon 5	-	Exon 6	-	-	Exon 7	*dzyA*
EK292203	-	-	Exon 6L	Exon 7*	Intron 7*-7		*dzyC*
EK047874	Exon 5S	-	Exon 6L	Exon 7*	Intron 7*-7		*dzyB*
EK271202			Exon 6L	Exon 7*	Intron 7*-7	Exon 7	*dzyB, dzyC*
EK293825	Exon 5	Intron 5-6	Exon 6	Exon 7*	Intron 7*-7		*dzyA**
EK183201	Exon 5	Intron 5-6	Exon 6	Exon 7*			*dzyA**
EK195852	Exon 5	Intron 5-6					*dzyA**

In addition to the three isoforms, *dzyA*, *dzyB* and *dzyC*, the three ESTs EK292203, EK183201 and EK195852 (Fig. 10, Tab. 2) provide evidence for an alternative variant (*dzyA** form) of the *dzyA* form. Compared to the *dzyA* splice form, the *dzyA** variant contains exon 5, which is characteristic for the *dzyA* form, but retains the intron between exon 5 and exon 6. Another difference is seen in the C-terminus; like the *dzyB* and the *dzyC* form, the *dzyA** form is extended after exon 6L by exon 7* and the intron between 7* and 7. The *dzyA** form is mentioned here for completeness, but it will not be discussed further in this work. The focus is on the three forms *dzyA*, *dzyB* and *dzyC*.

Consequently, what are the structural differences of the three Dzy proteins? All conserved domains that are typical for PDZ-GEF proteins reside in exon 3, such that all splice forms contain these domains. In addition, the splice forms share a proline-rich motif (PRM1) encoded by exon 4 (Fig. 11). However, they are distinguished by their specific C-termini and the presence or absence of two additional PRMs (PRM2 and PRM3) encoded by exon 5/5S. The DzyA protein contains a C-terminal area of 26 amino acids which is encoded by the 3' part of
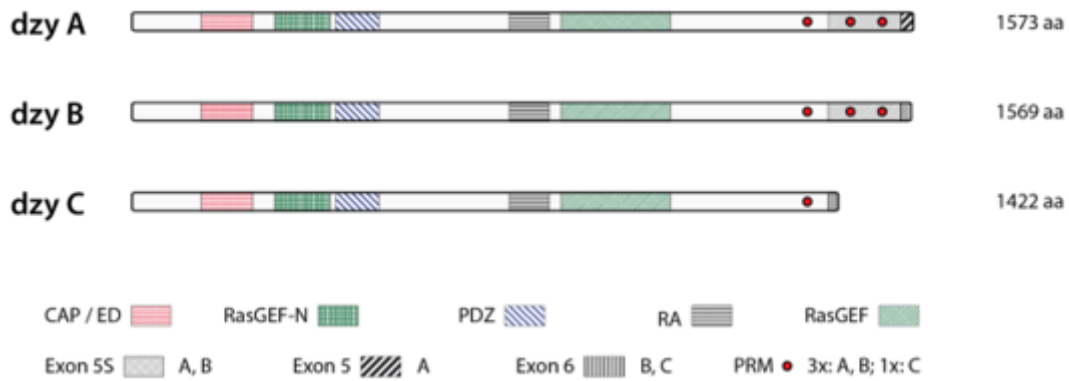
Fig. 11 Scheme of the three Dzy proteins.
The proteins are distinguished by their C-termini. DzyA differs by the C-terminus encoded by the 3' region of exon 5, which is not present in exon 5S. *dzyB* and *dzyC* encoded proteins do not show a unique C-terminus. The C-terminus of the B- and the C-isoform is encoded by exon 6L. Another distinguishing feature of the different Dzy isoforms is the presence or absence of two proline-rich motifs (PRM2 and 3) encoded by exons 5/5S. They are present only in the DzyA and DzyB form, while the third PRM1, encoded by exon 4 is constitutively present in all forms. The alternative splicing leads to the formation of three different theoretical proteins: DzyA, DzyB and DzyC. The predicted proteins of the mRNA are 1573 amino acids (DzyA), 1569 amino acids (DzyB) and 1422 amino acids (DzyC) long.

exon 5, which is not included in exon 5S. The DzyB and DzyC form do not contain a unique protein sequence at the C-terminal area. The two proteins differ solely by the presence or absence of exon 5S. Concerning PRM2 and 3, the splice forms *dzyA* and *dzyB* contain exon 5 or 5S respectively and therefore include all three P-rich motifs. Only the *dzyC* form lacks this pair of PRMs, as exon 4 is spliced directly to exon 6L. Two relevant stop codons are present in the *dzy* locus (see asterices in Introduction Fig. 6). One stop codon in exon 5 terminates translation for splice form *dzyA*. The second stop codon is located in exon 6L and arrests the translation of the *dzyB* form and *dzyC* form since their mRNA do not contain the stop within exon 5. So, the open reading frame of *dzyB* and *dzyC* end in exon 6L.

Comparison with other species

The *dzy* gene encodes for three isoforms of dPDZ-GEF, which differ in their C-terminal ends. The proteins DzyA, DzyB and DzyC contain six conserved domains and binding motifs (from N- to C-terminal): the cNMP binding motif (also CAP/ED), the N-terminal GEF domain (GEFN) and the PDZ domain are located at the N-terminus of the protein, the RA domain and the GEF domain are located in the central part, and the proline-rich motifs (PRMs) are located at the C-terminus. All domains and their arrangements have been reported from known PDZ-GEFs except of the C-terminal proline-rich regions, which are not common to all PDZ-GEFs (Fig. 12). The composition and spacing of the cMNP (CAP/ED), GEFN, and the PDZ domains on one side and the RA and GEF domains on the other side are particularly characteristic for GEFs for Ras-like small GTPases. Nevertheless, some variation occurs at the termini of PDZ-GEFs:

At the N-terminus some PDZ-GEFs have one cNMP domain similar to human PDZ-GEF1 (RAPGEF2), others have two cNMP domains like human PDZ-GEF2 (RAPGEF6) (Kuiperij *et al.* 2003). The occurrence of the proline-rich region and the PBM (PDZ binding motif) at the C-terminus varies within PDZ-GEFs and within different isoforms of one protein. For instance, human PDZ-GEF2A have both domains, the proline-rich region and the PBM, whereas the two domains are absent in the hPDZ-GEF2B isoform (Kuiperij *et al.* 2003). The ortholog of PDZ-GEF in *C.elegans* PXF-1A lacks a proline-rich motif but has a PBM at its C-terminus (Fig. 12). All three Dzy isoforms have one cNMP domain at their N-terminus similar to human PDZ-GEF1. At the C-terminus two isoforms have three proline rich motifs but lack the PBM (DzyA and DzyB), whereas the short DzyC lacks two proline-rich motifs and the PBM. The Dzy orthologue proteins of *Drosophila pseudoobscura* and *Drosophila ananassae* have a similar structure with a single N-terminal cNMP domain and the proline-rich regions at the C-terminus (Fig. 12).

Fig. 12 Comparison with other species.
Comparison of the protein domains of the three Dzy isoforms A, B and C of *D. melanogaster* with the PDZ-GEF proteins of *D. pseudoobscura* and *D. ananassae*, as well as the three human isoforms PDZ-GEF1, PDZ-GEF2A and PDZ-GEF2B and the *C.elegans* ortholog PXF-1. The GEF domain and the corresponding GEFN are shaded green and light green, respectively; the PDZ domain is blue and the RA domain is grey. cNMP is shown in red; hPDZ-GEF2 and PXF-1A have two cNMP domains at the N-terminus. The proline-rich regions are shown with red bars, the C-terminal PBMs with purple bars. The numbers indicate the length of the different proteins. Graph and data have been modified, originally from Department of Animal Genetics, Huelsmann).

3.2.1 Two isoforms of dzy mRNA were found in the *Drosophila* embryo

To identify the different isoforms, cDNA was synthesized from total RNA isolated from *Drosophila* embryos. For this purpose, a specific primer for exon 7 (PR189 or PR296), exon 7* (PR190 or PR297), intron 7 - 7* (PR298) or an oligo-(dT) primer attached to the poly(A) tail of the RNA served as the starting point for the first strand cDNA synthesis. A primer located in exon 3 was used to prime the second-strand synthesis using either a Taq-polymerase or

HotStar HighFidelity polymerase. The obtained cDNA was used as the template for further PCR analysis. In order to systematically search for alternatively spliced *dzy* mRNA, we performed PCR with two primer pairs, one pair for exon 3 and exon 7 (PR231/PR189), the other for exon 3 and exon 7* (PR231/PR190). These two primer combinations were used to detect all possible splice variants (Fig. 13, Fig. 14).

In an initial preliminary experiment to identify the individual splice forms, total RNA was isolated from *w⁻* embryos of *Drosophila* and reverse-transcribed into cDNA. The reverse primer was either located in exon 7* or exon 7 to generate the various splice variants *dzyA, dzyB* and *dzyC*. The 3' ends of *dzy* cDNA were amplified by PCR using the primer pair exon 3 - exon7* or exon 3 - exon 7. While the primer combination exon 3 - exon 7* showed a double band on the gel, no signal could be detected with the primer combination exon 3 - exon 7. The bands generated by agarose gel electrophoresis were eluted from the gel, cloned into a TOPO TA vector and sequenced by LGC Genomics (Fig. 13).

In the *Drosophila* embryo, two of the three splice forms, the dzyB form and the *dzyC* form, could be detected. The PCR product based on the cDNA exon 3 - exon 7 indicates the existence of splice forms containing both exon 7* and 7, even though PCR with the primer pair PR189/PR231 did not yield a result. However, the detailed C-terminal structure of the *dzyB* and *dzyC* forms is not yet fully known. Additional isoforms consisting only of 7* cannot be ruled out, so far. It is still unclear why the *dzyA* form cannot be detected although a corresponding EST exists.
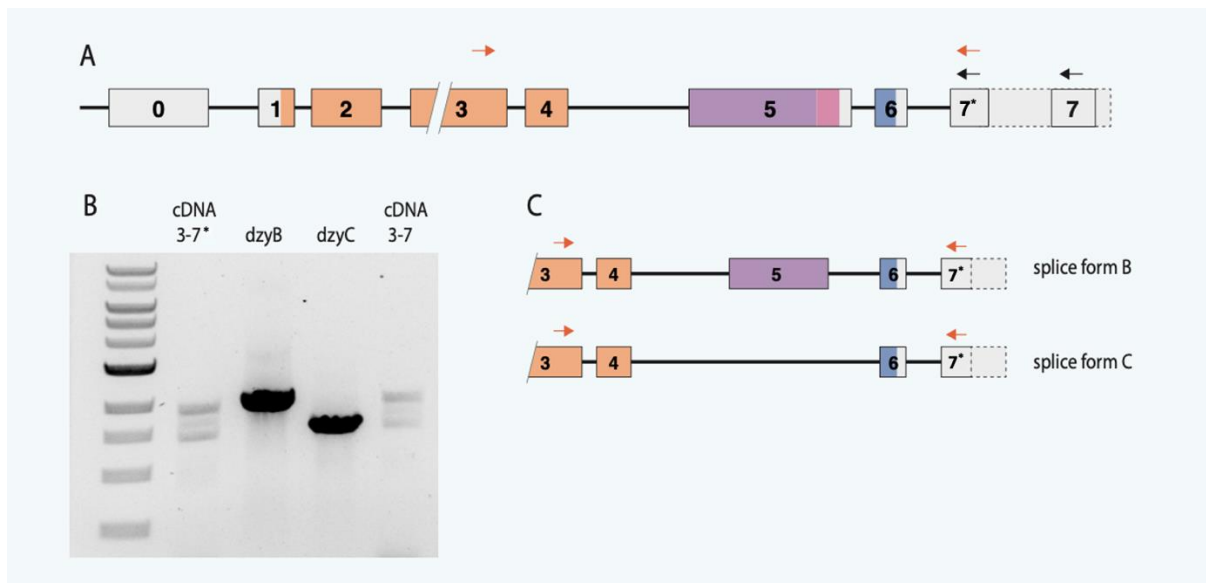
Fig. 13 Embryonic expression of the *dzy* splice forms.
(A) Schematic representation of the *dzy* locus. (B) Total RNA was isolated from *w⁻* embryos of *Drosophila* and reverse-transcribed to cDNA. The reverse primer was either located in exon 7* or exon 7 (black arrows) to produce the different splice variants. Then, the 3`ends of *dzy* cDNA were amplified by PCR (exon 3 – exon 7*, red arrows) and subcloned in TOPO TA. (C) In the *Drosophila* embryo, two of the three splice forms, the *dzyB* form and the *dzyC* form were detected. The PCR product based on the cDNA exon 3 - 7 indicates the existence of splice forms containing both exon 7* and 7. However, the detailed C-terminal structure of the *dzyB* and *dzyC* form is not fully understood, yet. Additional isoforms comprising only 7* cannot be excluded, so far. It is still unclear why the *dzyA* form cannot be detected, although a respective EST does exist.

In further experiments, specific primers for exon 7 (PR296), exon 7* (PR297) or intron 7 - 7* (PR298) served as the starting point for the synthesis of the first cDNA strand. A primer located in exon 3 was used to prime the second strand synthesis. The obtained cDNA was used as a template for further PCR analysis. To systematically search for alternatively spliced *dzy* mRNA, we performed PCR with two primer pairs, one pair for exon 3 and exon 7 (PR231/PR189), the other for exon 3 and exon 7* (PR231/PR190). With these two primer combinations, all possible splice variants could be detected (Fig. 13). Half of the PCR preparation was applied to the gel, while the remaining 50 % was used for sequencing and further cloning into the TOPO TA vector. Cloning approaches 3 (PR231/PR189) and 4 (PR231/190) were transformed into chemically competent *DH5α* cells and plated onto Amp-containing media (see Material & Methods). Individual colonies were picked from the plates and grown overnight. Plasmid DNA was purified using peqGold Plasmid Miniprep Kit or TELT Prep (see Material & Methods). Test PCR analyses of the obtained clones were performed using the primer pairs exon 3 - exon 7* (PR231/PR190) and exon 3 - exon 7 (PR231/189) (Fig. 14). To identify the different *dzy* splice forms, the sequence was then analysed via sequencing (LGC Genomics).
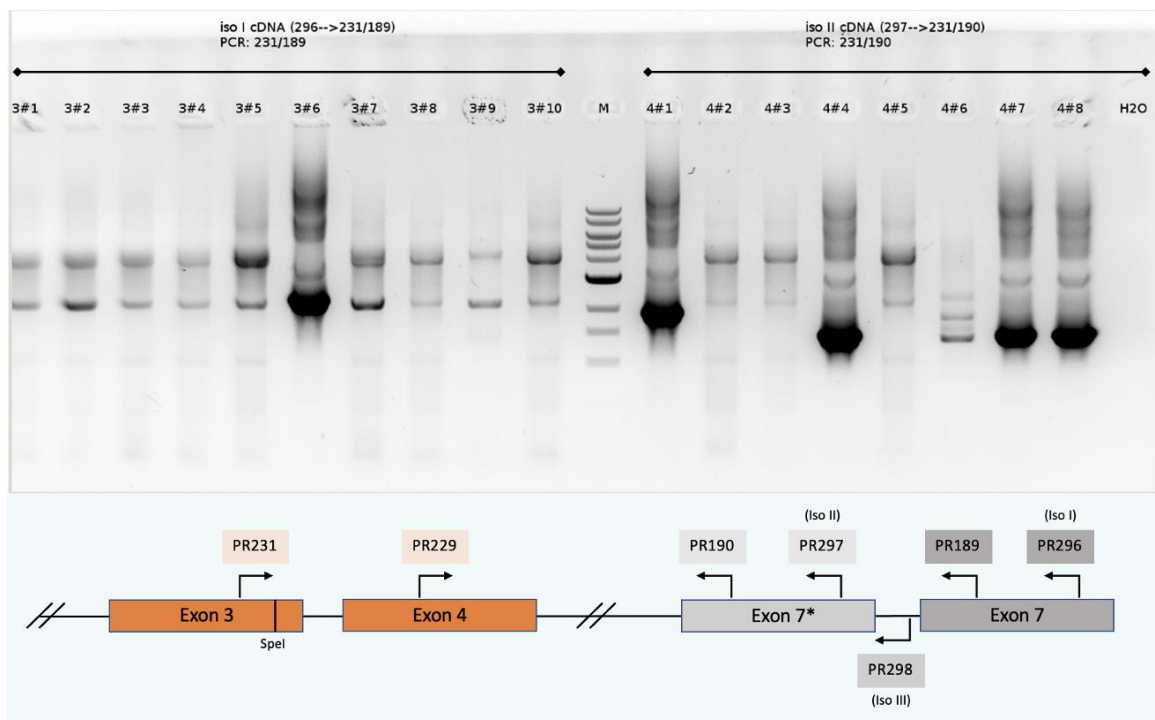
Fig. 14 Results of the PCR analysis (*dzyB* and *dzyC*).
10 mg of adult *Drosophilia w* flies were used for total RNA isolation (RNeasy Plus Mini Kit, Qiagen). RNA (1 μg) was transcribed into cDNA (Transcriptor First Strand cDNA Synthesis Kit, Roche) using specific primers: PR296 (IsoI in exon 7) and PR297 (IsoII in exon 7*). PCR was performed with two primer pairs, exon 3/exon 7 (PR231/PR189) and exon 3/exon 7* (PR231/PR190). These two primer pairs are able to detect all three splice variants of *dzy*. In addition, a primer was designed that binds between the two exons 7* and 7 (PR 298) and thus recognizes the splice forms with the exon 7L variant. As a control, 50 % of the amplicon was applied to the agarose gel and the remainder used for cloning into a TOPO TA vector. The resulting clones were analysed by PCR analysis using the two primer pairs PR231/PR190 and PR231/PR189. The resulting TOPO TA clones *3#6, 4#1, 4#4, 4#7* and *4#8* were selected for futher investigation.

Sequence analysis of a larger number of clones showed that there are definitely two different mRNA types of *dzy* that could be found in the *Drosophila* embryo using the PCR method described. Alternative splicing at one position in the primary transcript resulted in the two splice forms *dzyB* and *dzyC*. Of the three originally expected splice forms, only two could be detected using this approach. The splice form *dzyA*, based on EST AT08279, was not found. A more detailed analysis of these two sequenced forms revealed that no variability was observed concerning the 5' part of these cDNAs between exon 0 and exon 4. First, we distinguished the two different splicing forms for exon 5 (Fig. 15). Based on ESTs, this exon is either entirely included in the mRNA (*dzyA*), spliced as a shorter exon 5S due to an alternative splice site at its 3' end (*dzyB*) or spliced out (*dzyC*) (cf. Fig. 6). As expected, *dzyB* (Clone *3#6* and *4#1*), showed the exon 5S, while exon 5 was completely absent in the *dzyC* form (Clone *4#4, 4#7* and *4#8*) (Fig. 15, Tab. 3). A vector map of the different clone constructs *3#6, 4#1, 4#4, 4#7 and 4#8* can be found in Appendix Fig. S1.
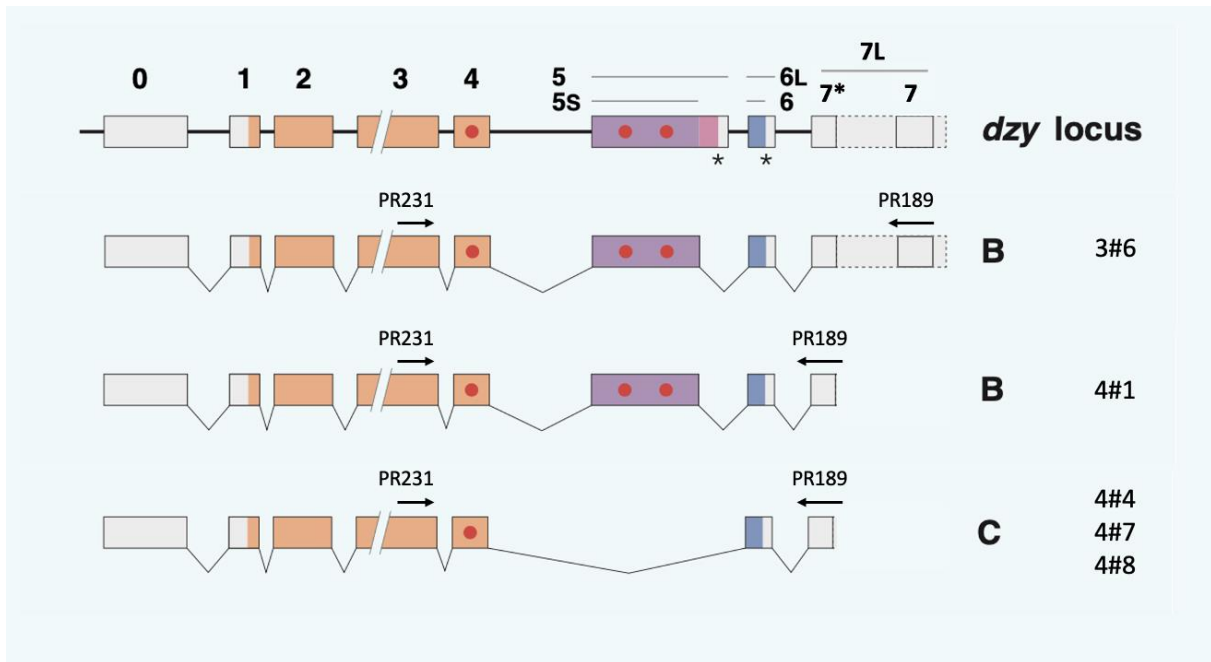
Splice variants found so far:

Fig. 15 Schematic representation of the identified *dzyB* und *dzyC* forms.
In the *Drosophila* embryo, two of the three splice forms, the *dzyB* form and the *dzyC* form were detected. *dzyB* (Clone *3#6* and *4#1*), showed exon 5S, while exon 5 was completely absent in the *dzyC* form (Clone *4#4, 4#7* and *4#8*). *dzyB* clone *3#6* contained the extended exon 7L, consisting of exon 7*, exon 7 and the intervening intron part. Since the primer pair exon 3/exon 7* (PR231/PR190) had a significantly higher cloning success rate than the primer pair exon 3/exon 7 (PR231/PR189), the majority of cDNA segments found by PCR contained only exon 7*. Isoforms comprising only 7* cannot be excluded, thus far.

Tab. 3 Overview of the dzy splice forms.
Summary of *dzy* splice forms, schematically shown in Fig. 15 with the corresponding exons and introns, ESTs and primer combinations. The *dzy* region covered by the different ESTs is shown in blue.

PR231/PR189	Exon 3/Exon 7	3#6	*dzyB*	Exon 7L (Exon 7* and Exon 7)
PR231/PR190	Exon 3/Exon 7*	4#1	*dzyB*	Exon 7*
PR231/PR190	Exon 3/Exon 7*	4#4	*dzyC*	Exon 7*
PR231/PR190	Exon 3/Exon 7*	4#7	*dzyC*	Exon 7*
PR231/PR190	Exon 3/Exon 7*	4#8	*dzyC*	Exon 7*

EST							
AT08279	Exon 5	Exon 6	-	-	Exon 7	*dzyA*	Not found
EK292203	-	Exon 6L	Exon 7*	Intron 7*-7		*dzyC*	Partially found
EK047874	Exon 5S	Exon 6L	Exon 7*	Intron 7*-7		*dzyB*	Found
EK271202		Exon 6L	Exon 7*	Intron 7*-7	Exon 7	*dzyB, dzyC*	Found (dzyB)
EK293825	Exon 5	Exon 6	Exon 7*	Intron 7*-7		*dzyA**	Not found
EK183201	Exon 5	Exon 6	Exon 7*			*dzyA**	Not found
EK195852	Exon 5					*dzyA**	Not found

Second, we examined the 3' end of the mRNA. The *dzyB* and *dzyC* splice forms contained exon 6L, a longer version of exon 6 due to an alternative splice site at its 3' end. We found that all cDNAs (PR231/PR190) of the *dzyB* and *dzyC* forms continued after exon 6L with exon 7*, which is located between exon 6L and exon 7 in the genome (Fig. 15). Since the primer pair exon 3/exon 7* (PR231/PR190) had a significantly higher cloning success rate than the primer pair exon 3/exon 7 (PR231/PR189), the majority of cDNA segments found by PCR contained only exon 7*. However, *dzyB* clone *3#6* provides circumstantial evidence that both splice forms *dzyB* and *dzyC* contain the extended exon 7L, consisting of exon 7*, exon 7 and the intervening intron part, as already suspected. In summary, it can be assumed that the *dzyB* and the *dzyC* splice forms contain exon 6L and 7L (exon7* - exon7). EST EK292203 already gave an indication of the possibility of this specific 3' end. Due to the small number of samples (cDNA PR231/PR189), we cannot completely exclude the existence of single forms containing only exon 7* so far. Other combinations were not detected in this work.
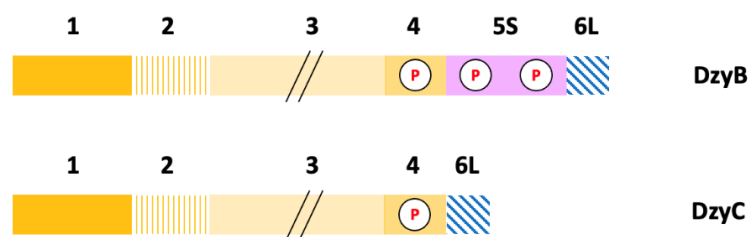

Fig. 16 Scheme of the two natural Dzy spliceforms.
The two proteins are not distinguished by their C-termini. *dzyB* and *dzyC* encoded proteins do not show a unique C-terminus. The C-terminus of the DzyB and the DzyC isoform is encoded by exon 6L. The only feature to distinguish the two isoforms is the presence or absence of two proline-rich motifs (PRM2 and 3) encoded by exons 5/5S. They are present only in the DzyB form, while the third PRM1, encoded by exon 4, is constitutively present in both forms. The predicted proteins of the mRNA are 1569 amino acids (DzyB) and 1422 amino acids (DzyC) long.

Thus, we found two differentially spliced RNA forms that differ in the presence of exon 5 and their number of PRMs, but not in their C-terminal ends. As expected, proline-rich motifs (PRMs) were present in exons 4 and 5, so that the DzyB protein showed three P-rich motifs (exon 4 PRM1 and exon 5S PRM2 und PRM3) and the DzyC protein only one (exon 4 PRM1). So, the alternative splicing leads to the formation of two different proteins: in the DzyB form and the DzyC form in fact, a stop codon is located in exon 6L and terminates the translation. The proteins of the identified mRNA are 1569 aa (DzyB) and 1422 aa (DzyC) long (Fig. 11, Fig. 16).

<u>Unlike the *dzyB* and *dzyC* isoform, the *dzyA* splice form could not be detected in the *Drosophila* embryo</u>

It is important to briefly mention here that based on ESTs and other references in the literature, there should be three different splice forms *dzyA*, *dzyB* and *dzyC*, but only two splice forms were found in this series of experiments. There are several indications for the existence of the *dzyA* form. First, EST AT08279 was obtained from the testis of adult *Drosophila* flies and shows a sequence with exons 5, 6 and 7 (Fig. 10, Tab. 2). Furthermore, EST EK183201 also gives an indication of *dzyA*. This is a slightly modified variant of *dzyA*, with exon 5, intron 5-6, 6L and 7* (here titled as *dzyA** form, Tab. 2). Secondly, there is evidence in the literature for the existence of the *dzyA* splice form (Wang *et al.* 2006). Wang et al. investigated the expression of the Gef26 protein in the testis of *Drosophila*. They used an anti-Gef26 polyclonal antibody to detect the Gef26 protein. Wild-type testes were immunostained with anti-Gef26. A peptide corresponding to the peptides 1548 - 1567 (amino acid sequence: GKTTGPQERWFPDCRRPTTKQ) of Gef26 was used to produce antibodies in rabbits. According to NCBI, this sequence belongs to a PDZ domain-containing guanine nucleotide exchange factor, the isoform *dzyA*. The antiserum was purified using the peptides as affinity reagents. In wild-type testes, Gef26 was highly concentrated at the hubGSC interface and between the hub cells (Wang et al. 2006). In summary, Wang and colleagues produced an antibody specifically against the *dzyA* isoform and detected the protein in the *Drosophila* testes. This gives clear evidence that a *dzyA* form exists. Since the *dzyA* form, unlike the other two isoforms *dzyB* and *dzyC*, could not be detected in this way using the method described above, a number of further detection experiments were performed. On the one hand, we tried to detect the *dzyA* form using a *dzyA*-specific primer or increasing the transcript amount with a Nested-PCR approach. On the other hand, we tried to detect the missing isoform by explicitly focusing on the original location of *dzyA*, the testis of adult *Drosophila* flies.

PCR analysis with a *dzyA*-specific primer (PR183)

The *dzyA* isoform contains a 26 aa long sequence region, that is only present in the *dzyA* variant. This specific region in exon 5 is missing in both the *dzyB* and *dzyC* form. Total embryonic RNA was isolated and transcribed into cDNA using specific *dzy* primers (PR190, PR189, PR296, PR297) or an anchored oligo-(dT) primer. The PCR was performed with the *dzyA* specific primer PR183, located in the 26 aa long region unique for the A-variant. Several primers located in exon 3 and exon 4 respectively (PR181 (exon 3), PR231 (exon 3) and PR229 (exon 4)) served as second primers. However, despite the use of a specific *dzyA* primer that binds to the part in exon 5 specific for the *dzyA* form, no signal was visible after PCR and gel electrophoresis. The clone *dzyA in pUAST 4* (see Results section 3.3) was used as positive control. The clone *dzyC in pUAST 12* served as negative control since the primer PR183 cannot bind here due to the absence of exon 5.

Nested polymerase chain reaction (Nested-PCR)

Since no *dzyA* variant could be detected with the *dzyA*-specific primer, we suggested that the lack of detection might be perhaps due to a low concentration of the *dzyA* splice form in the *Drosophila* embryo. Therefore, a Nested-PCR was performed to increase the sensitivity and specificity of the previous PCR. Nested-PCR is an efficient method to amplify a cDNA copy of mRNA that is present in very low quantities. In this PCR variant, two sequential amplification reactions are usually performed, each using a different primer pair. The product of the first amplification reaction is used as a template for the second PCR, which is primed by oligonucleotides placed further inward from the first primer pair. By using two primer pairs, a higher number of cycles can be performed, increasing the sensitivity of the PCR. The improved specificity of the reaction results from the binding of two separate primer sets to the same target template. For this experiment, total RNA was isolated from the *Drosophila* embryo and transcribed into cDNA using specific primers located in exon 7 (PR297), exon 7* (PR296) or with an oligo-(dT) primer. The synthesis of the second strand was performed with the primer pairs exon 3/exon 7 (PR231/PR296) and exon 3/exon 7* (PR231/PR297). The second PCR reaction was performed with specific primers placed internally to the first primer pair. In our case, the primer pairs exon 3/exon 7 (PR231/PR189) and exon 3/exon 7* (PR231/PR190) were used. After the *dzyA* form was still not found, the primer in exon 3 (PR231) was replaced by an alternative more internal primer in exon 4 (PR219), also without result. *dzyA* could not be detected even with Nested-PCR. Other primer combinations with the *dzyA*-specific primer PR183 (PR181/PR183, PR231/PR183, PR219/PR183) also failed to detect a *dzyA* splice form. *dzyA in pUAST* served as a positive control.

<u>The *dzyA* form in adult flies</u>

Since the *dzyA* form was originally found in the adult fly (EST AT08279), the next approach was to investigate whether the *dzyA* form is only undetectable in the embryo. Is there a *dzyA* form in the adult fly? For this approach, RNA had to be obtained from adult flies. It turned out that the isolation of RNA from adult flies presented us with a new challenge. With the RNeasy® Plus Mini Kit originally used for embryonic RNA isolation, no RNA could be obtained from adult flies. So, various RNA isolation kits, including the NucleoSpin® RNA Plus Kit from Macherey Nagel, and different homogenisation methods were tested. RNA isolation from adult flies was finally achieved using the peqGold RNAPure™ Kit and the miRNAeasy Micro Kit. The adult flies were placed in liquid nitrogen and stored at -80 ºC for a short period of time. The frozen flies were then homogenised with QIAzol® Lysis Reagent. This procedure gave the best results and was used from this point on for further experiments (see Material & Methods). The isolated RNA was then transcribed into cDNA using specific primers in exon 7, exon 7* and an anchored oligo-(dT) primer (Transcriptor First Strand cDNA Synthesis Kit, Roche). For better comparability, embryonic RNA was also isolated using this new procedure and the new kit, and it was carried along in parallel in each step. The PCR was carried out with the primer pairs, exon 3/exon 7 (PR231/PR190) and exon 3/exon 7* (PR231/PR189), as well as exon 4/exon 7 (PR219/PR190) and exon 4/exon 7*(PR219/PR190). In addition, the presence of the *dzyA* form was examined using the *dzyA*-specific primer (PR183): exon 3/exon 5 (PR231/PR183) and exon 4/exon 5 (PR219/PR183). The constructs *dzyA in pUAST* and *dzyC in pUAST* were used as positive controls. ddH$_2$O served as a negative control (Fig. 17).

After gel electrophoresis, the different *dzy* splice forms were identified based upon the presence of PCR products that differ in size. The two primer pairs PR189/PR231 and PR190/PR231 were used to detect the three splice forms in adult fly cDNA, as was done for embryonic cDNA. The primer pair in exon 3/exon 7 (PR189/PR231) identified the splice form *dzyA* and the primer pair exon 3/exon 7*, PR190 and PR231 identified the splice forms *dzyB* and *dzyC*. With the mentioned primer pairs, *dzyA* results in a 1927 bp band, *dzyB* in an 1825 bp band and *dzyC* produces a 1385 bp band. At this point, it should be mentioned that the two primer pairs PR231/PR189 and PR231/PR190 were used to detect all *dzy* splice forms. However, at this point it is still unclear what the C-terminus of the *dzyA* form looks like in detail. It is therefore quite possible that *dzyA*, like the forms dzyB and dzyC, has an exon 7L (exon 7 and exon 7*) and would therefore also be detectable with the primer pair PR190/PR321. The PCR assay using the primer pair in exon 3/exon 7* resulted in two bands, an 1825 bp *dzyB* and a 1385 bp *dzyC* band, while with the primer pair in exon 3/exon 7 (PR189/PR231) and the primer pair in exon 3/exon 5 (PR231/PR183) no signal could be detected. Interestingly, PCR
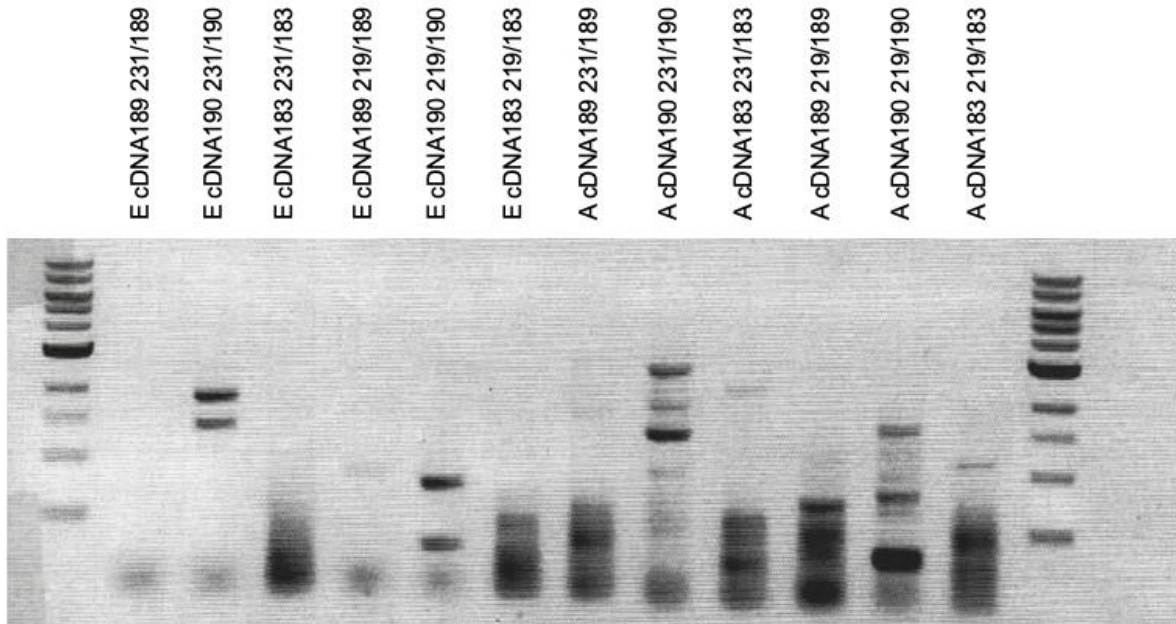
Fig. 17 Results of the PCR analysis (*dzyA*).
The isolated RNA was transcribed into cDNA (embryo cDNA (E) and adult cDNA (A)) using specific primers in exon 7 (PR189), exon 7* (PR190) and exon 5 (PR183). PCR with the primer pair in exon 3/exon 7* (PR231/PR190) yielded an 1825 bp *dzyB* and a 1385 bp *dzyC* band, while the primer pair in exon 3/exon 7 (PR189/PR231) and the primer pair in exon 3/exon 5 (PR231/PR183) yielded no bands. Adult (A) cDNA PR231/PR190 showed an additional PCR product compared to E cDNA. The two bands, *dzyB* and *dzyC*, were directly under a third PCR product. The results could be confirmed with an alternative primer in exon 4 (E cDNA PR219/PR189, E cDNA PR219/PR190, E cDNA PR219/PR183 and A cDNA PR219/PR189, A cDNA PR219/PR190, A cDNA PR219/PR183).

with the *w* genomic sequence (E cDNA and A cDNA) using the primer pair PR231/PR189 did not yield a PCR product. Although it could already be proven that the splice forms *dzyB* and possibly *dzyC* have a terminal exon 7L (exon 7 and 7*). Fig. 17 shows the results of the PCR amplification test.

Compared to the E cDNA, the PCR assay performed on a subset of adult *Drosophila* resulted in three PCR products using the primers PR190 and PR231. Two conspicuous bands of about 1.9 kb and 1.4 kb were present in the PCR test. These two PCR fragments were the two splice forms *dzyB* and *dzyC*. As expected, *dzyB* yielded a band of 1825 bp and *dzyC* a band of 1385 bp. These two splice forms could already be detected in the embryo. *dzyB* and *dzyC* are therefore expressed both in the *Drosophila* embryo and in the adult fly. The two bands, *dzyB* and *dzyC*, were directly under a third PCR product of approximately 2.5 kb. As mentioned earlier, the *dzyA* form should appear as a band of 2.0 kb. Thus, the third band found could indeed be the *dzyA* form with an exon 7L terminus, the *dzyA** form or even a new splice form. Furthermore, no bands other than the three PCR products were detected with this PCR approach. To identify the 2.5 kb band, the PCR product (A cDNA190 with PR231/PR190 or PR219/PR190 and A cDNA183 with PR231/PR183 or PR219/PR183) was cloned in TOPO TA, transformed into chemically competent *DH5α* cells and plated onto media containing Amp.

Several white colonies were selected from the agar plate for further investigation (see Material & Methods). Plasmid DNA was purified using peqGold Plasmid Miniprep Kit or TELT Prep. PCR was used to identify the clones with the highest of the three bands (Fig. 18), these clones were then sequenced (LGC Genomics). The sequencing data showed that the PCR product under investigation was unspliced pre-mRNA. The introns were all completely present, so it was not the *dzyA* variant. We found that depending on the type and method of RNA isolation, the pre-mRNA can also be detected.
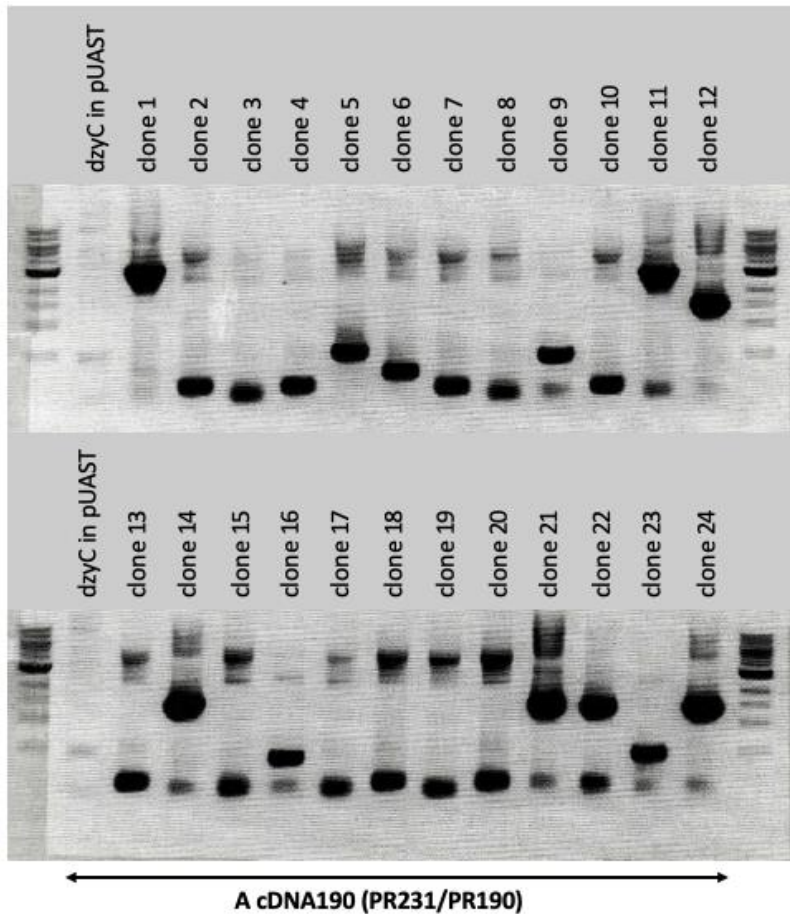
Fig. 18 Results of the A cDNA190 (PR231/PR190) PCR analysis.
PCR product (A cDNA190 with PR231/PR190) was cloned in TOPO TA, transformed into chemically competent *DH5α* cells and plated onto media containing Amp. Several white colonies were selected from the agar plate for further investigation. Plasmid DNA was purified using peqGold Plasmid Miniprep Kit or TELT Prep. PCR analysis was performed with the primer pair exon 3/exon 7* (PR231/PR190) to identify the different clones. Clone 1 and 11 were selected for further investigation and sequenced by LGC Genomics.

A repeat of the experiment with newly isolated RNA and newly prepared cDNA also showed a band of three on the gel (PR231/PR190). An approach with alternative primer pairs: exon 4/exon 7 (PR229/PR189), exon 4/exon 7* (PR229/PR190), exon 4/exon 5 (PR229/PR183) and exon 3/exon 5 (PR231/PR183) was also investigated. Unfortunately, no *dzyA* clone could be found with this approach either. Again, the longest of the three PCR products was the unspliced pre-mRNA. In addition to detect the *dzyA* form, this approach (total RNA isolation) was also used to test for the presence of the *dzyB* and *dzyC* forms in the adult fly. Are the two splice forms also expressed at this later stage of development or is their presence restricted to the embryonic stage? It could be shown by sequencing the PCR products that the two remaining

bands (height: 1825 bp and 1385 bp, A cDNA190 PR231/PR190) are the two splice forms *dzyB* and *dzyC*. *dzyB* and *dzyC* are therefore not only expressed in the embryo but also in the adult fly. There is still no trace of the third form, *dzyA*.

Detection of the *dzyA*-form in the adult testis of *Drosophila*

In a final attempt to detect the missing *dzyA* variant, RNA was isolated from the testes of adult male *Drosophila* flies. The theoretical sequence for the *dzyA* splice form is based on EST AT08279. The abbreviation AT in this case stands for adult testis and served as the basic idea for this approach. Furthermore, as mentioned in the section above, Wang and colleagues were also able to detect a *dzyA* variant in *Drosophila* testes using a specific *dzyA* antibody (Wang *et al.* 2006).

To isolate the testes from adult *w⁻* flies, the flies were placed on a slide in a drop of ice-cold 1x PBS and the testes were removed with a needle (see www.jova.com for procedure). For better comparability, RNA from embryos (E) and adult flies (A) was isolated alongside with the RNA from the adult testes (AT). Total RNA was isolated using the miRNeasy Micro Kit and QIAzol® Lysis Reagent as previously described. The cDNA synthesis was performed using different primers in exon 7 (PR189), exon 7* (PR190) and exon 5 (PR183). Subsequent PCR was then performed with the following primer combinations: PR231/PR189, PR219/PR189, PR231/PR190, PR219/PR190, PR231/PR183 and PR219/PR183 (Fig. 19). cDNA produced with the primer in exon 7 (PR189) or the primer in exon 5 specific for the *dzyA* form (PR183) showed no result. No bands were visible on the gel. In comparison, using the primer combination PR231/PR190, the two isoforms *dzyB* and *dzyC* could be detected. In the embryo (E) and in the adult fly (A and AT), *dzyC* was slightly more strongly expressed than *dzyB*; a strong C band and a weaker B band were seen on the gel. The result for the adult testis (AT) showed a strong *dzyC* band and an extremely weak *dzyB* band. The two dzy forms could thus be detected in the embryo, in the adult fly and in the testis of *Drosophila*. It should be mentioned here that in the RNA isolation from adult flies (A) and adult testis (AT), a very weak third band appeared. This PCR product was tested and it turned out that it was again not the *dzyA* form but the pre-mRNA. Despite several and different approaches, including Nested-PCR (Nested-PCR on A cDNA190 PR231/190 with the primer pairs PR181/PR188 and PR181/PR183), only the *dzyB* and *dzyC* slice form could be detected. The *dzyA* form could not be detected by this method either. Since the construct *dzyA* had already been cloned in parallel in pUAST at this point (*dzyA in pUAST 4*) and, as mentioned above, there are also other sources for the existence of this splice form, the *dzyA* form was included in the further experiments for the sake of completeness.
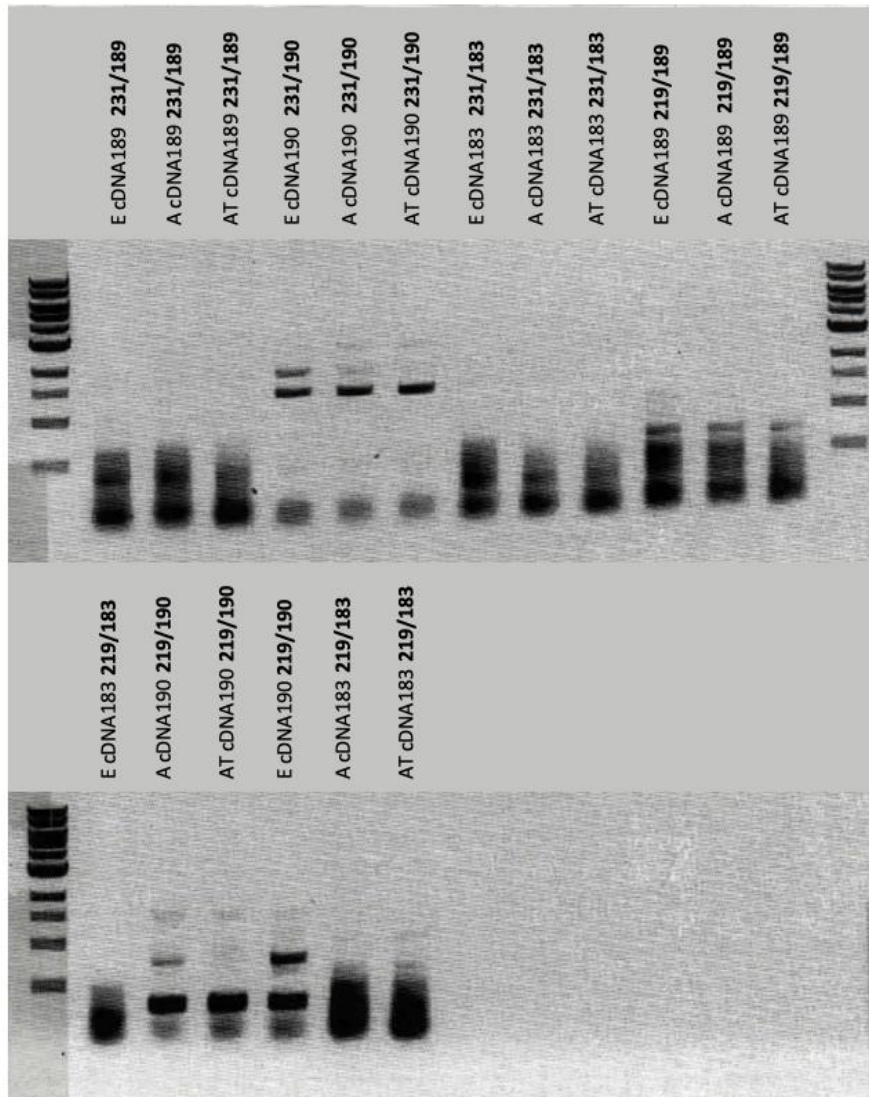
Fig. 19 PCR analysis of embryo (E), adult (A) and adult testis (AT) cDNA.
PCR analysis of E cDNA, A cDNA and AT cDNA was performed with the following primer combinations: PR231/PR189, PR219/PR189, PR231/PR190, PR219/PR190, PR231/PR183 and PR219/PR183. cDNA produced with the primer in exon 7 (PR189) or the primer in exon 5 specific for the *dzyA* form (PR183) showed no result. No bands were visible on the gel. In comparison, using the primer combination PR231/PR190, the two isoforms *dzyB* and *dzyC* could be detected. With *dzyC* showing a stronger signal than *dzyB*.

3.2.2 Alternative splicing of *dzy* might be developmentally regulated

Above, we showed that the two splice forms *dzyB* and *dzyC* are expressed in the *Drosophila* embryo and the adult fly. We wondered how the splice forms, originally isolated from embryonic RNA, are expressed during the life cycle of the animal. So, we wanted to know if the expression of the splice forms is differentially regulated during the *Drosophila* life cycle. To analyze this question, we performed a PCR experiment with total RNA from embryos (E), larva (L), pupae (P) and adult flies (A). RNA isolation and cDNA synthesis were performed as described before. RNA isolation was performed with the Quick Start Protocol using QIAzol® Lysis Reagent or Direct-zol™ RNA Miniprep Plus (Zymo Research). Embryos deposited overnight were

bleached, collected and transferred to an eppendorf tube. Larvae, pupae and anaesthetised adult *w⁻* flies were removed from fly tubes and also collected in Eppendorf tubes. Collected samples were immersed in liquid nitrogen for 5 minutes prior to RNA isolation. The cDNA was prepared using the Roche Transcriptor First Strand cDNA Synthesis Kit (oligo-(dT) primer) or the LunaScript RT SuperMix Kit.

The specific primer for exon 7* (PR190) was selected for the PCR reaction, as it had shown the best results so far and is present in all detected splice variants. This primer was combined with a second primer in exon 3 (PR231). PCR of *Drosophila* total RNA at different developmental stages was thus performed with the primer pair exon 3/exon 7* (PR231/PR190). All approaches showed PCR products that matched the splice variants *dzyB* (1825 bp) and *dzyC* (1385 bp) in terms of length (Fig. 20). The results showed that the two splice forms *dzyB* and *dzyC* were expressed at all developmental stages. In embryos (E) and adult flies (A), both splice forms were expressed at approximately equal levels. In comparison, the *dzyB* form was significantly more strongly expressed in larvae (L) and pupae (P). As this is not a quantitative PCR, no definitive conclusions can be drawn; the results merely indicate an expression pattern.
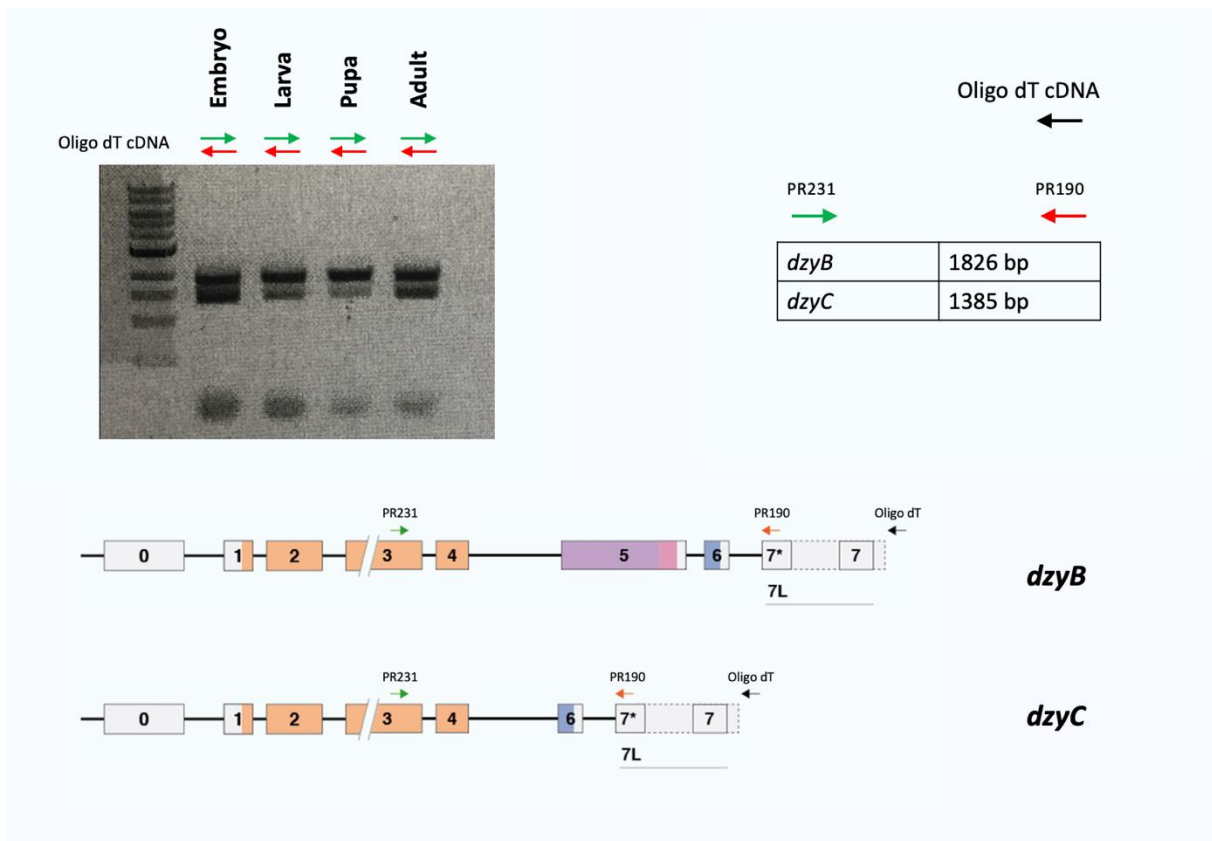
Fig. 20 The two *dzy* splice forms are differentially expressed during the life cycle.
PCR of *Drosophila* total RNA at different developmental stages was performed using the primer pair exon 3/exon 7* (PR231/PR190). All lanes showed PCR products specific for the splice variants *dzyB* and *dzyC*, so that the two splice forms were expressed at all developmental stages. In embryos and in adult flies, both splice forms were expressed at approximately equal levels. In larvae and pupae, however, dzyB showed a significantly stronger expression. Since this is not a quantitative PCR, no definitive conclusions can be drawn; the results merely suggest an expression pattern.

In addition to the primer pair already described (PR231/PR190), many PCR primer combinations (including PR229/PR189, PR231/PR296, PR231/PR189 and PR229/PR298) were tested. The primer PR189 in exon 7 in combination with a primer in exon 4 (PR229) produced the same band pattern as PR231/PR190. Again, the splice variants *dzyB* (1010 bp) and *dzyC* (569 bp) were shown to be expressed at all stages of development. In the embryo and in the adult fly, the *dzyC* form appears to be expressed either more strongly than (E) or about as strongly as (A) the *dzyB* form in this experiment. In larvae (L) and pupae (P), however, dzyB showed significantly stronger expression (Fig. 21).
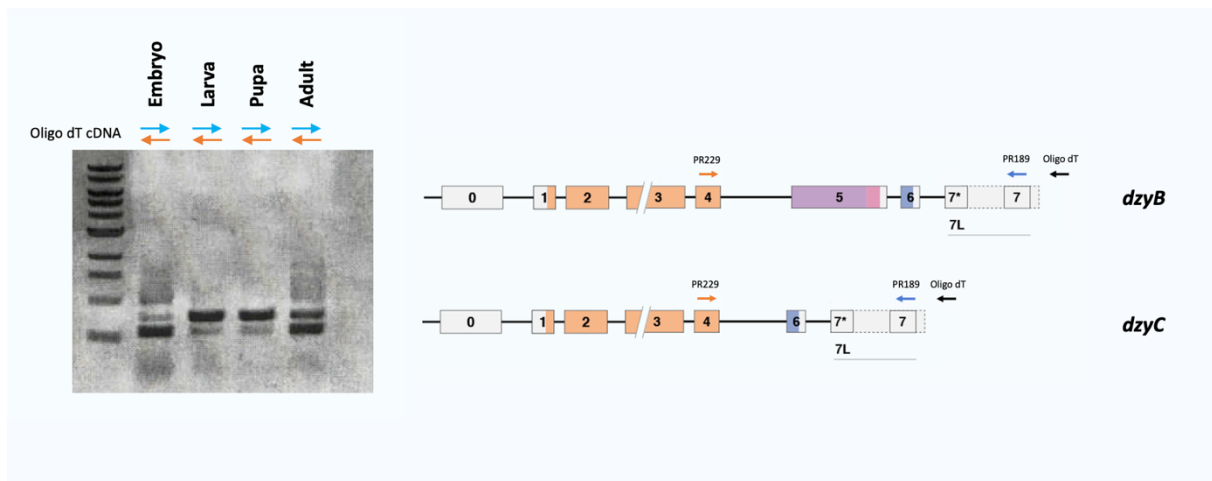
Fig. 21 The two *dzy* isoforms show developmentally regulated expression.
PCR of *Drosophila* total RNA at different developmental stages was performed with additional primer combinations besides the primer pair exon 3/exon 7* (PR231/PR190). One of these alternative primer pairs was exon 4/exon 7 (PR229/PR189). The resulting PCR products were again specific for the splice variants *dzyB* and *dzyC*, showing that the two splice forms were expressed at all stages of development. While in the adult fly both splice forms were expressed at approximately the same level, a stronger expression of the dzyC form was observed in the embryo. In larvae and pupae, however, *dzyB* was significantly more strongly expressed. As this is not a quantitative PCR, no definitive conclusions can be drawn; at best, the results indicate a pattern of expression.

To verify the splice forms found, the PCR approach L cDNA oligo-(dT) PR229/PR189 was cloned in TOPO TA, transformed into chemically competent *DH5α* cells and plated out onto Amp-containing media. 12 white colonies were selected from the agar plate for further analysis. Plasmid DNA was purified using TELT Prep. PCR (PR229/PR189) was used to identify the clones (Fig. 22). One clone with a higher band (L cDNA oligo-(dT) PR229/PR189 clone 2 (2L2)) and one clone with a lower band (L cDNA oligo-(dT) PR229/PR189 clone 11 (2L11)) on the agarose gel were subsequently sequenced (LGC Genomics). The sequencing data showed the *dzyB* and *dzyC* forms, respectively. Thus, only the *dzyB* and *dzyC* form were found in the larva. There was no evidence for the presence of the *dzyA* variant or another unknown isoform.
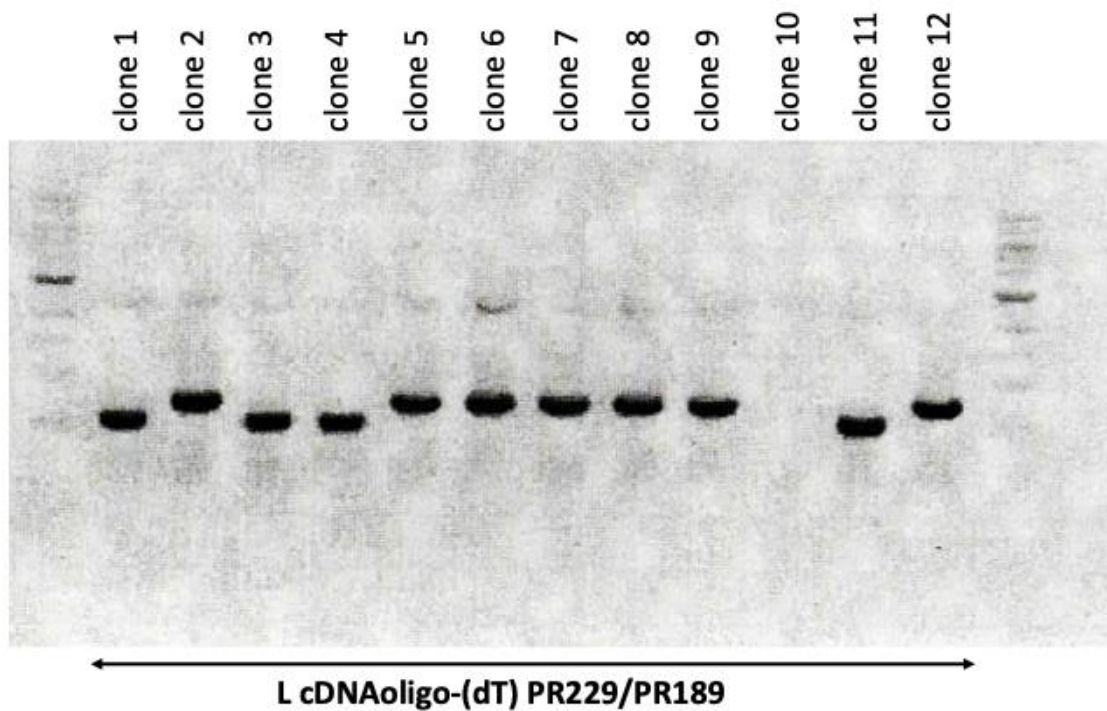
Fig. 22 Results of the L cDNA oligo-(dT) PR229/PR189 PCR analysis.
PCR product (L cDNA oligo-(dT) with PR229/PR189) was cloned in TOPO TA, transformed into chemically competent *DH5α* cells and plated onto media containing Amp. 12 white colonies were selected from the agar plate for further investigation. Plasmid DNA was purified using peqGold Plasmid Miniprep Kit or TELT Prep. PCR analysis was performed with the primer pair exon 4/exon 7 (PR229/PR189) to identify the different clones. Clones 2 and 11 were selected for further analysis and sequenced by LGC Genomics.

Although our data only allows a relatively rough quantification of mRNA abundance, they can provide information about the existence of the two *dzy* splice forms in the different developmental stages. Thus, we concluded that the two identified splice variants, *dzyB* and *dzyC*, were expressed in all developmental stages. In the embryo and in the adult fly, both splice forms were expressed at approximately the same level. In some previous experiments, the *dzyC* band was observed to be significantly stronger than the *dzyB* band in A cDNA (see Fig. 17 and Fig. 19). Thus, in the embryo and in the adult fly, the *dzyC* form appears to be either equally or more strongly expressed than the *dzyB* form. Whereas, *dzyB* showed significantly stronger expression in larva and pupa compared to the *dzyC* form.

3.3 The *dzyC* splice form expressed in migrating macrophages is able to induce cell shape changes

We have previously shown that *dzy* is required in embryonic macrophages for proper cell shape and motility. In mutant embryos, macrophages have significantly smaller cellular protrusions and migrate less efficiently along the ventral nervous system. Complementary to the loss-of-function phenotype, macrophage-specific overexpression from an EP-element in the *dzy* locus (*dzy^{EP}*) leads to a massive enlargement of the cellular protrusions (Huelsmann *et al.* 2006). Since the *dzy^{EP}* line express the entire *dzy* locus, we wondered whether all splice forms *dzyA*, *dzyB* and *dzyC* or only one of them could be responsible for the cell shape change phenotype observed in the *dzy^{EP}* lines. We wondered whether the structural differences of the various Dzy splice forms were related to the different functions of the proteins in regulating haemocyte cell shape and motility.

The UAS-Gal4 system (Brand & Perrimon 1993) was used for the gain-of-function experiments. In these experiments, tissue-specific drivers were used to overexpress the genes of interest. The haemocytes of the *Drosophila* embryo originate from the head mesoderm, where their precursors become specified during early embryogenesis. The GATA factor *serpent (srp)* is expressed early in these precursors and is required for their specification, as *srp* mutant embryos lack haemocytes (Rehorn *et al.* 1996). To study the cell shape and motility of macrophages in the *Drosophila* embryo, we used a *srph-Gal4* line (Fly strain collection stock 580), which allows expression of the different *UAS-dzy_{splice form}* constructs in macrophages. For the examination of migrating macrophages in fixed embryos, this line was used to express the heterologous cell membrane marker CD2 (Dunin-Borkowski & Brown 1995). Therefore, we generated transgenic animals for the *UAS-dzy_{splice form}* constructs and expressed the different *UAS-dzy* constructs in macrophages by crossing these animals with a fly strain carrying the macrophage-specific driver (*srph-Gal4*) coupled with *UAS-cd2*, allowing detection of cell shape and position via antibody staining directed against CD2 (Huelsmann *et al.* 2006).

Assembly of the *UAS-dzy* constructs

In general, cDNAs of the three isoforms were used to generate the *UAS-dzy_{splice form}* constructs (*UAS-dzyA*, *UAS-dzyB* and *UAS-dzyC*). The specific ORF coding regions of the different *dzy*-transgene constructs were amplified by PCR, digested via restriction enzymes and ligated into the *pUAST Drosophila* transformation vector (Brand & Perrimon 1993). The pre-existing *dzyC in the pUAST* construct (originally *dzyCII in pUAST*; source Department of Animal Genetics, renamed in the context of this work in *dzyC in pUAST*) served as a template for the generation of the other two *pUAST-cDNA* constructs *dzyA in pUAST* and *dzyB in pUAST*. A vector map of the construct *dzyC in pUAST clone 12* can be found in Appendix Fig. S2.

dzyA in pUAST

Although the *dzyA* isoform could not be detected with the methods available, there is strong circumstantial evidence for its existence. The existence of the *dzyA* isoform has been demonstrated by Wang and colleagues, and EST AT08279 also provided strong evidence as mentioned in the section above. For completeness, the *dzyA* isoform was also cloned and analysed alongside the other two forms, *dzyB* and *dzyC*. The construct *dzyC in pUAST* and the EST AT08279 served as modules for the resulting *dzyA* construct. In several intermediate steps, the two modules were combined to form the construct *dzyA in pUAST*. The construct *dzyC in pUAST* served as the vector and 5' region of the *dzyA* insert, including exon 0 to exon 4 (*dzyA fragment_1*), of the later *dzyA* isoform. Still, the *dzyC* isoform in *pUAST* contains exon 0 - 4 and the *pUAST* vector, it does not encode for exon 5, including the proline-rich motifs (PRM) 2 and 3, and the C-terminal exon 7. For this reason, the construct EST AT08279 in pOTB7 was introduced into this cloning process. Thus, the EST construct *AT08279 in pOTB7* served as the 3' region of the *dzyA* fragment (*dzyA fragment_2*), and encoded for exons 5, 6 and 7. The assembly of the two parts, yielding the final construct, took place in many intermediate steps, as many of the restriction sites required for cloning were not unique but were present in multiple copies.

The cloning strategy for generating the *dzyA* isoform construct was divided into three distinct sections, which are shown in Fig. 23. In the first step, the 3' part of the *dzyA* fragment was cloned into a pBluescript (pBS) cloning vector. A short sequence of 1363 bp (*dzyA fragment_1*) was excised from the construct *dzyC in pUAST* using restriction enzymes (EcoRI/SpeI) and ligated into a pBS cloning vector (resulting in the construct *dzyC_Spe in pBS SK*). Furthermore, the digested *dzyA fragment_2* containing the region exon 5, 6 and 7 was cloned downstream of the *dzyA fragment_1* cDNA into the BamHI/NotI site of the construct *dzyC_Spe in pBS SK*, resulting in the intermediate construct *dzyA_Spe in pBS SK*. In the final step, the full-length *dzyA* DNA fragment was cut out from the pBS vector and transferred into a *Drosophila* transformation vector pUAST to generate the final construct *dzyA in pUAST*.

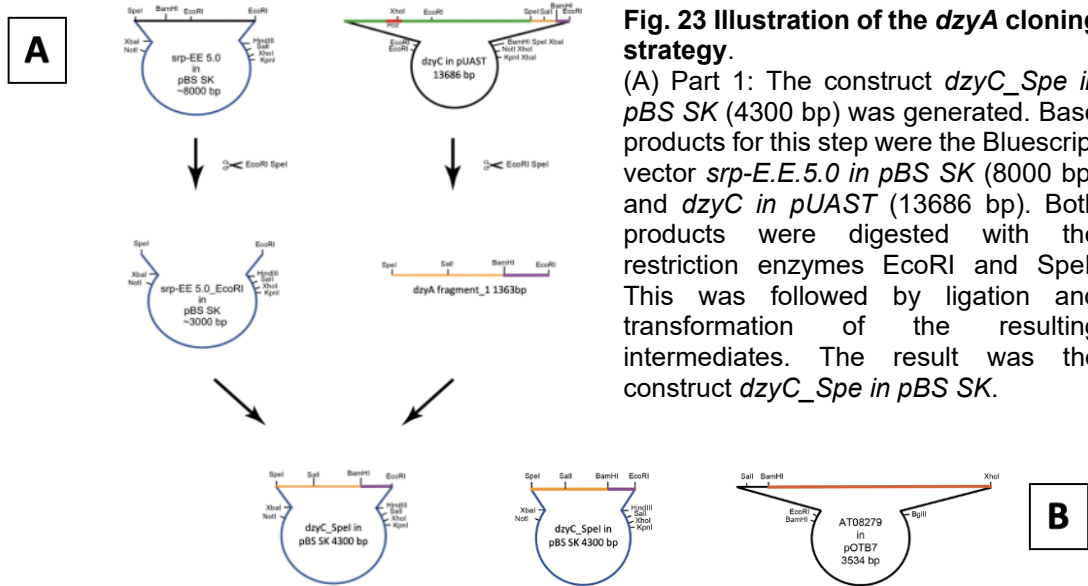**Fig. 23 Illustration of the *dzyA* cloning strategy**.

(A) Part 1: The construct *dzyC_Spe in pBS SK* (4300 bp) was generated. Base products for this step were the Bluescript vector *srp-E.E.5.0 in pBS SK* (8000 bp) and *dzyC in pUAST* (13686 bp). Both products were digested with the restriction enzymes EcoRI and SpeI. This was followed by ligation and transformation of the resulting intermediates. The result was the construct *dzyC_Spe in pBS SK*.

(B) Part 2: The construct *dzyA_SpeI in pBS SK* (4881 bp) was generaed. Basic products for this step were *dzyC_SpeI in pBS SK* (4300 bp), cloned in part 1 and *AT08279 in pOTB7* (3534 bp). The products were digested with the restriction enzymes BamHI and XhoI, ligated and analysed via Touchdown-Colony-PCR. The result was the construct *dzyA_SpeI in pBS SK* (4881 bp).
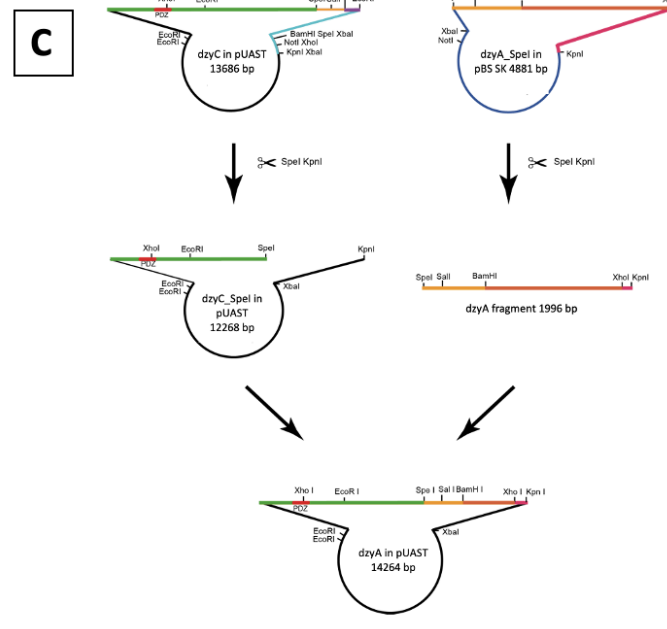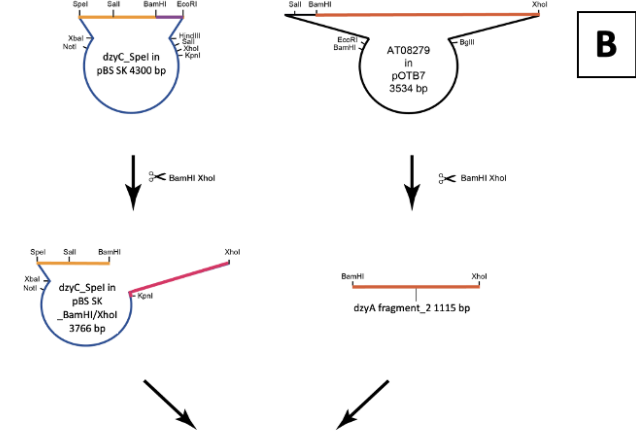
(C) Part 3: In the last part of the cloning strategy, the *dzyA* DNA fragment was cut from the vector pBS SK and inserted into the transformation vector pUAST. Basic products for this step were the construct *dzyA_SpeI in pBS SK* (4881 bp), containing the *dzyA fragment* (1996 bp), and the vector *dzyC in pUAST* (13686 bp). Both products were digested with the restriction enzymes KpnI and SpeI. Restriction digestion was followed by ligation and transformation of the ligation mixture into *DH5α* cells. The *dzyA in pUAST* (14264 bp) construct was generated.

<u>Part1: Cloning of the construct *dzyC_Spe in pBS*</u>

The primary goal of this first part of the cloning strategy was to clone the *dzyA fragment_1* into the *pBluescript* vector and generate the construct *dzyC_SpeI in pBS SK* (4300 bp). The construct *dzyC in pUAST* (13686 bp) was cut with the restriction enzymes EcoRI and SpeI (Fig. 23A). This separated the 1363 bp *dzyA fragment_1* from the *pUAST* vector backbone. The *srp-EE5.0 in pBS KS* vector (8000 bp) was cut with EcoRI and SpeI for 1.5 hours. The EcoRI/SpeI digested DNA components were separated on a 0.8 % agarose gel containing EtBr (see Material & Methods) to complete purification of the inserts and vectors and also to confirm that the size of the inserts and vectors was correct. The bands were visualized using a Gel Documentation Imaging System. This 1363 bp *dzyA fragment_1*, and the linearized *pBS* vector on 3000 bp were cut out from the gel and purified using the Macherey Nagel Nucleospin® Gel and PCR Clean-up Kit (see Material & Methods). The purified *dzyA fragment_1* was then ligated into the purified *srp-EE5.0_EcoRI in pBS KS* (3000 bp) vector. A vector concentration of 50 ng and an insert:vector ratio of 3:1 was used for the ligation process (see Material & Methods). The ligation reaction was transformed into competent *E.coli DH5α* cells as described in Material & Methods and plated onto LB media with Amp.

Amp-resistant colonies were picked from the plates for screening. Colonies were randomly selected using sterile eppendorf tips and submerged into labelled microfuge tubes containing 100 µl of sterile distilled water to be used as templates for amplification by PCR. The eppendorf tips were subsequently streaked onto fresh LB Amp plates to produce replicates. The Colony-PCR primer pair for the identification of *dzyC_SpeI in pBS SK* led to an amplification product of known size (324 bp). Plasmid DNA of the selected colonies (positive Colony-PCR) was miniprepped from overnight bacterial cell cultures using PeqGold Plasmid Miniprep Kit, before being tested via control PCR (PR229/PR248). Purified *dzy* constructs were sent to LGC Genomics for sequencing. The result was the construct *dzyC_SpeI in pBS KS* (4300 bp).

<u>Part 2 Cloning of the construct *dzyA_Spe in pBS SK*</u>

The next step was to combine the two *dzyA* fragments (*dzyA fragment_1* and *dzyA fragment_2*) to obtain full-length *dzyA* sequence. While the A splice form of *dzy* contains the entire exon 5, in the *dzyC* splice form, the entire exon 5 is spliced out. Thus, the sequenced construct *dzyC_SpeI in pBS SK* (4300 bp) contains only one of the three PRMs (PRM1 in exon 4), but not PRM2 and PRM3 in exon 5. For this reason, *EST AT08279 in pOTB7* was inserted into the cloning strategy. The EST *AT08279* in *pOTB7* (3534 bp) encoded for the exons 5, 6 and 7 and served as the 3' region of the *dzyA* fragment (*dzyA fragment part_2*).

The two constructs *dzyC_SpeI in pBS SK* (4300 bp) and *AT08279* in *pOTB7* (3534 bp) served as base products for the *dzyA_SpeI in pBS KS* (4881 bp) construct. *The dzyC_SpeI in pBS*

SK (4300 bp) construct was cut with BamHI and XhoI, and the *dzyA fragment_2* was cut out from the *AT08279 in pOTB7* vector (3534 bp) with BamHI and XhoI (Fig. 23B). This separated the 1115 bp *dzyA fragment_2* fragment from the *AT08279 in pOTB7* vector backbone (3534 bp). The digested components were separated by agarose gel electrophoresis and purified using the Macherey Nagel Nucleospin® Gel and PCR Clean-up Kit. The isolated insert *dzyA fragment_2* (1115 bp) was then ligated into the vector source *dzyC_SpeI in pBS SK_BamHI/XhoI* (3766 bp). A vector concentration of 50 ng and an insert:vector ratio of 3:1 was used for this ligation process. The ligation products were transformed in chemically competent cells and grown on agar plates. For the identification of the *dzyA_SpeI in pBS SK* construct, different primer combinations were used for Touchdown-Colony-PCR (see Material & Methods). The identification of the *dzyC_SpeI in pBS SK* (4300 bp) and the *dzyA_SpeI in pBS SK* (4881 bp) construct resulted from the difference in size of the PCR products. The colonies were analyzed using three different primer combinations: M13fw/PR181 (*dzyA* (967 bp)/*dzyC* (386 bp)), M13fw/M13rev (*dzyA* (2153 bp)/*dzyC* (1572 bp)) and M13rev/PR188 (*dzyA* (1909 bp)/*dzyC* (1336 bp)). Thus, the *dzyA* fragment (*dzyA_SpeI in pBS SK*) produced a 580 bp longer PCR product than the *dzyC* fragment (*dzyC_SpeI in pBS SK*). Constructs of the desired length were sequenced by LGC Genomics.

Part 3 Cloning of the construct *dzyA in pUAST*

Provided that the subcloning into *pBluescript* was successful, the *dzyA* fragment can be further cloned into the *pUAST* vector by cutting both constructs, *dzyA_SpeI in pBS SK* (*dzyA* fragment) and *dzyC in pUAST* (*pUAST* vector) with KpnI and SpeI. The *dzyA_SpeI in pBS SK* construct (4881 bp) generated in part 2 was digested with KpnI and SpeI, and the *dzyA* fragment was cut out from the *pBS* vector and cloned into the *pUAST* transformation vector to generate the *dzyA in pUAST* construct (Fig. 23C). When separated on a 0.8 % agarose gel, two different band sizes were seen: the upper band contained the *pBS* vector (2885 bp) and the lower band indicated the *dzyA_fragment* (1996 bp).

The DNA fragment *dzyA_fragment* (1996 bp) was then ligated into the *pUAST* transformation vector. *dzyC in pUAST* (13686 bp) served as the source for the *pUAST* vector. The *dzyC in pUAST* construct was digested with the same restriction enzymes (SpeI/KpnI) as the *dzyA_SpeI in pBS SK* construct. The two fragments were separated and purified with the Nucleospin® Gel and PCR Clean-up Kit. For the ligation process, a vector concentration of 50 ng and different insert:vector ratios (3:1, 2:1 or 5:1) were used. Multiple ligation reactions were performed to increase the number of correct ligation products. The usual ligation procedure was used and different amounts and concentrations of plasmid vector and DNA insert were prepared in a total volume of 20 µl. Furthermore, an overnight ligation reaction was set up and the ligation mixtures were transformed into chemically competent cells. Single colonies were

picked from the plate and grown overnight in LB medium. To detect the *dzyA in pUAST* construct, purified plasmid DNA was screened via PCR using the primer pair PR229 and PR230 (Fig. 24). Bands of approximately 1245 bp (*dzyA in pUAST*), or 668 bp (initial construct *dzyC in pUAST*) were expected. Purified dzy constructs were sequenced by LGC Genomics using the two primers M13rev (PR248) and M13fw (PR247). The sequenced data represented the *dzyA in pUAST* construct (*dzyA in pUAST clone 4*, 14296 bp). A vector map of the construct *dzyA in pUAST clone 4* can be found in Appendix Fig. S2.
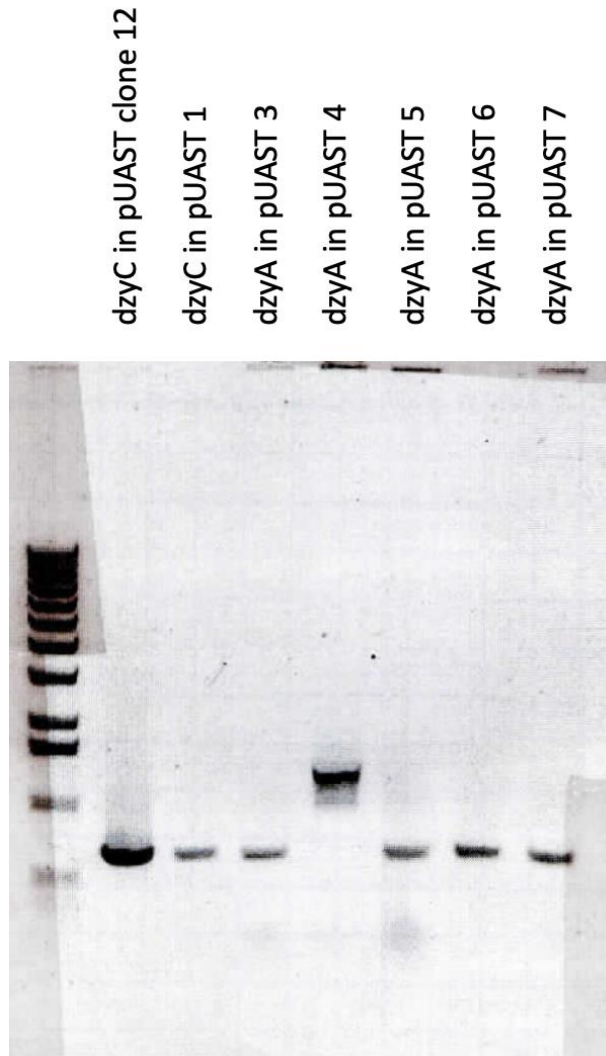
Fig. 24 Agarose gel electrophoresis of the *dzyA in pUAST* assembled construct.
Test PCR of the colonies was performed with the primer pair PR230 and PR 229. A 0.8 % agarose gel was used to screen for the expected plasmid size: *dzyA in pUAST* 1245 bp, *dzyC in pUAST* 668 bp. *dzyC in pUAST* (668 bp) served as a control for the PCR reaction. The DNA *dzyA in pUAST clone 4* appeared to be the correct size on the gel. *dzyA in pUAST clone 4* was sent for sequencing to confirm that the cloned plasmid received the correct insertion sequence.

dzyB in pUAST

Unlike the *dzyA* form, the *dzyB in pUAST* construct was not generated based on an EST sequence. The strategy used for cloning *dzyB* was to amplify the *dzyB190 PCR fragment*, containing exon 3 to exon 7*, via PCR and clone it into the *pCR2.1 TOPO* vector (Fig. 25B). Different primer combinations were used to generate longer parts of *dzyB* in a single PCR reaction. Total RNA from *Drosophila* embryos was used as template. For the *dzyB* form, single-stranded cDNA (Roche Transcriptor First Strand cDNA Synthesis Kit) was synthesised from

Drosophila total RNA (Qiagen RNeasy® Plus Mini Kit) using PR190. Double-stranded cDNA was amplified by PCR with a primer pair in exon 3 (PR231) and exon 7* (PR190) using HotStar HighFidelity DNA Polymerase to avoid errors in the DNA sequence (cDNA #8 190 cDNA (PR231/PR190)).

The resulting PCR product served as the 3' region of the further *dzyB* fragment (*dzyB190 PCR fragment*). The 5' region of the *dzyB* splice form was again represented by the *dzyC in pUAST* construct, providing the missing exons (exon 0 – exon 3a) and the *pUAST* vector source. To see if the *dzyB190* fragment was successfully amplified using this method, the PCR products were separated on an agarose gel. The *dzyB190 PCR fragment* amplified by HotStar HighFidelity DNA Polymerase was cloned directly into the TOPO vector (*pCR®2.1*). The insert-vector mixture was transformed into chemically competent *E.coli DH5α* cells and afterwards plated onto agar plates containing Kanamycin (Kan). Blue-white screening (see Material & Methods) was performed to identify colonies containing the *pCR2.1_dzyB190* construct. The specification of the *pCR®2.1 TOPO TA* vector allowed a colour selection in which clones with integrated foreign DNA appear light blue to white, while vectors without foreign DNA lead to a strong blue coloration of the bacterial colony. Therefore, only white (light blue) clones were used for further analyses. Clones obtained from the TOPO cloning were characterised by sequencing. Depending on the way the *dzyB190* fragment was inserted into the TOPO TA vector, *pCR2.1_dzyB190rev* and *dzypCR2.1_B190fw* clones were found. We chose the construct *pCR2.1_dzyB190rev* for further cloning steps.
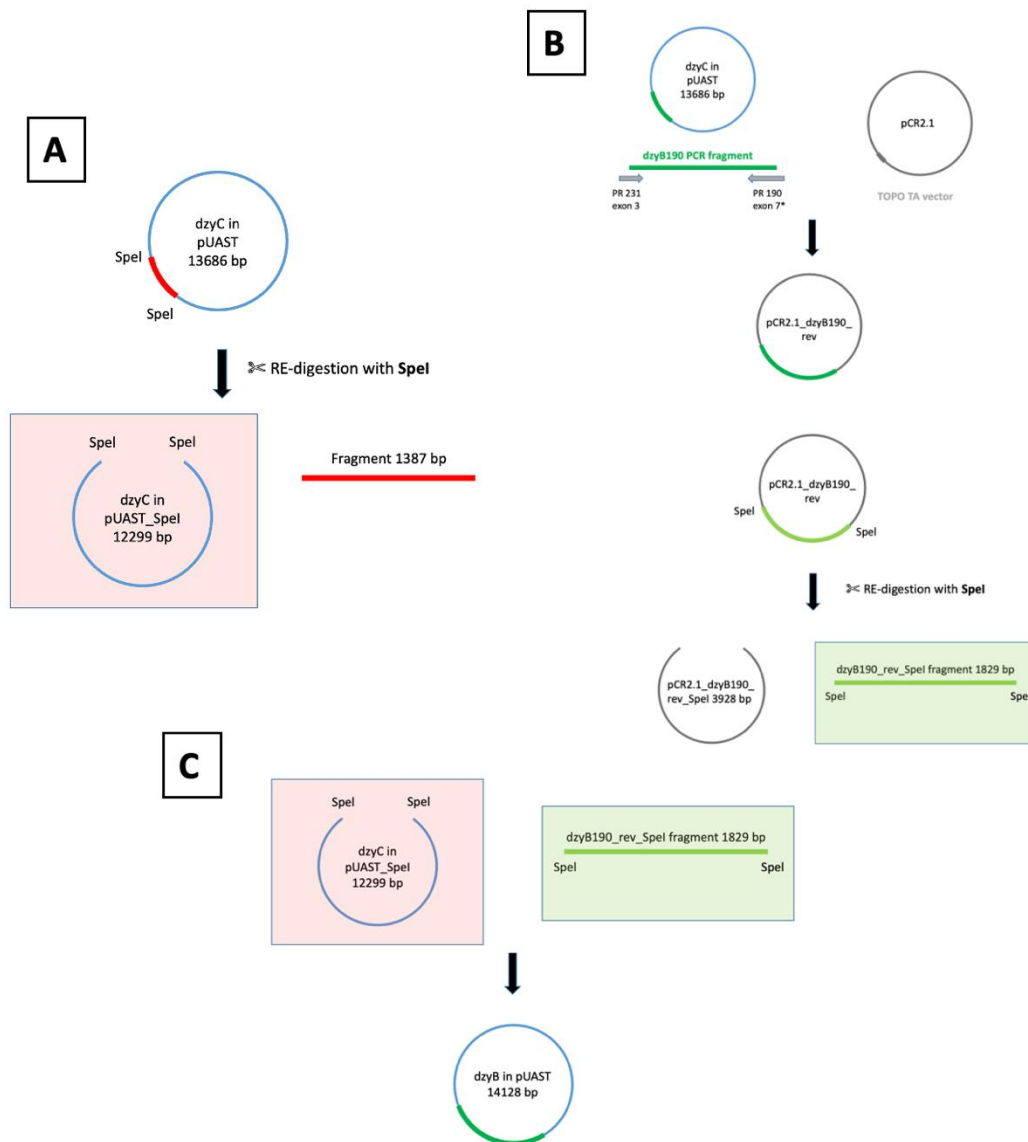
Fig. 25 Cloning of the *dzyB in pUAST* construct using PCR and restriction enzyme digestion.
The *dzyB190 PCR* fragment was amplified by PCR and cloned into the *pCR2.1 TOPO TA* vector
(*pCR2.1_dzyB190rev*). Total RNA from embryos was used as template. The generated
pCR2.1_dzyB190rev (B) and the *dzyC in pUAST* (A) construct were digested with the restriction enzyme
SpeI. Digestion of the two constructs yielded two fragments: *dzyB190rev_SpeI fragment* (1829 bp) and
dzyC in pUAST_SpeI (12299 bp). (C) The isolated insert *dzyB190rev_SpeI fragment* was ligated into
the vector backbone *dzyC in pUAST_Spe*. The result was the construct *dzyB in pUAST*.

To assemble the 3' region (exon 3b - exon 7*) *dzyB190* fragment (*pCR2.1_dzyB190rev*) with
the 5' region of the *dzyB* fragment (exon 0 - exon 3a) and the *pUAST* vector source (*dzyC in
pUAST*), both constructs were digested with the restriction enzyme SpeI (Fig. 25A and B). The
digestion of the two constructs resulted in two fragments: *dzyB190rev_SpeI fragment*
(1829 bp) and *dzyC in pUAST_SpeI* (12299 bp). The digested components were separated by
agarose gel electrophoresis and purified with the Nucleospin® Gel and PCR Clean-up Kit
(Macherey Nagel). The isolated insert *dzyB190rev_SpeI fragment* was ligated into the vector
backbone *dzyC in pUAST_SpeI* (Fig. 25C). Since gel purification of the vector involved loss of

DNA, an alternative method was used in parallel to this approach. The *dzyC in pUAST* vector was cut with SpeI for 30 minutes at 37 ºC before the vector was treated with SAP (rAPid Alkaline Phosphatase) (see Material & Methods) to prevent relegation of the vector in the ligation reaction. The gel purified *dzyB190rev_SpeI fragment* was then ligated into the SAP-treated expression vector *dzyC in pUAST_SpeI* (Fig. 25C). A vector concentration of 50 ng and an insert:vector ratio of 5:1 was used for the overnight ligation process. The ligation reaction of the two approaches (1) gel-purified and (2) SAP-treated *dzyC in pUAST_SpeI* was transformed into chemically competent *E.coli DH5α* cells and plated onto media containing Amp. The correct assembly of the construct was checked by Colony-PCR and sequencing. To identify the final *dzyB in pUAST* (14128 bp) construct, a primer in exon 3 (PR231) and a primer in exon 6 (PR188) were used for the PCR reaction. The construct *dzyB in pUAST* showed a 1705 bp band with the selected primer combination. For an undigested *dzyC in pUAST* construct, a 1264 bp band appeared on the gel (Fig. 26).

The determination of the constructs thus resulted from the difference in size of the PCR products. The *dzyB* isoform containing exon 5S was about 440 bp longer than the *dzyC* form in *pUAST*. Plasmid DNA of the Colony-PCR-positive colonies was miniprepped from overnight bacterial cell cultures using PeqGold Plasmid Miniprep Kit, before tested via control PCR using PR231 and PR188. Purified *dzy* constructs were sent to LGC Genomics for sequencing. The result was the construct *dzyB in pUAST* (*dzyB in pUAST clone 3*, 14128 bp). A vector map of the construct *dzyB in pUAST clone 3* can be found in Appendix Fig. S2.
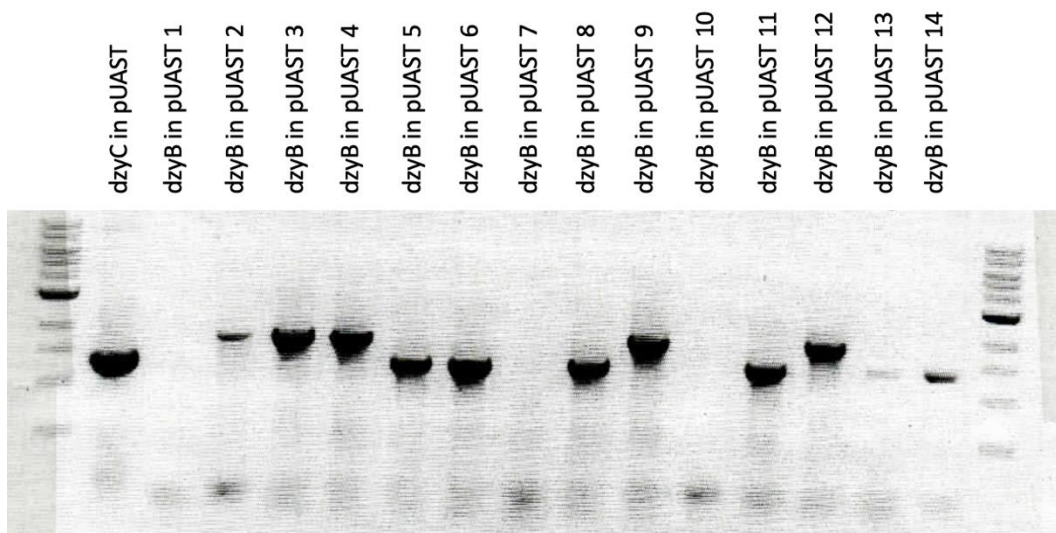

Fig. 26 Agarose gel electrophoresis of the *dzyB in pUAST* assembled construct.
Colony-PCR of the colonies was performed with the primer pair PR231 (*dzy* exon 3) und PR188 (*dzy* exon 6). A 0.8 % agarose gel was used to determine the expected plasmid size: *dzyB in pUAST* 1705 bp. *dzyC in pUAST* (1264 bp) served as a control for the PCR reaction. DNA *dzyB in pUAST clone 3, 4, 9* and *12* appeared at the correct size on the gel. *dzyB in pUAST clone 3* was sent for sequencing to confirm that the cloned plasmids had the correct insertion sequence and direction.

Generation of transgenes

The specific expression in the macrophages of the entire *dzy* locus in the *dzy*^{EP} lines resulted in a characteristic phenotype in which macrophage protrusions appear elongated and connect to form a network of cells (Huelsmann *et al.* 2006). Since the *dzy*^{EP} lines express the entire *dzy* locus in the macrophages, we wondered whether all or only one of the three different splice forms (*dzyA*, *dzyB* or *dzyC*) could be responsible for the cell shape change phenotype observed in the *dzy*^{EP} lines. One of the aims of this work was to investigate the differences in cell shape between the *dzy* isoforms. Thus, we generated transgenic animals for the *UAS-dzy*_{*splice form*} constructs.

The *dzy in pUAST* constructs (*dzyA in pUAST*, *dzyB in pUAST* and *dzyC in pUAST*) were used to generate transgenic flies by means of P-element-mediated germline transformation, as described (Rubin & Spradling 1982). The different constructs were purified with the Macherey Nagel® NucleoBond® Xtra Midi Kit and injected into dechorionated embryos following standard procedures for P-element mediated germline transformation (see Material & Methods).

The three strains examined in this work (*UAS-dzyA*, *UAS-dzyB* and *UAS-dzyC*) each originated from a different source. The *UAS-dzyA* strain was commissioned externally from a *Drosophila* embryo injection service. The *UAS-dzyB* strain was produced by injection (see Material & Methods) in the lab by the author and her colleagues as part of the laboratory work for this study. The *UAS-dzyC* strain was previously generated in the same laboratory (Department of Animal Genetics) by the author's predecessor and made available for use in this study.

UAS-dzyA transgenic flies

The purified plasmid *dzyA in pUAST* was subsequently used to generate *UAS-dzyA* transgenic flies via P-element-mediated germline transformation. The *dzyA in pUAST* construct was not injected by our department. For embryo injection, we used the high-quality *Drosophila* transgene service of the *Drosophila* microinjection service Fly Facility (France). Purified plasmid DNA was sent to the Injection company. After several attempts, no transgenic fly strains could be generated. Even after re-injection of another 200 embryos, no transformants were obtained. Another attempt to successfully inject the *dzyA* DNA was carried out with the *Drosophila* embryo injection service BestGene (http://www.thebestgene.com, US). BestGene performed injections with our purified plasmid construct and the P-element helper plasmid. For *Drosophila* P-element transformation, a transposon-based construct was injected with the *white* marker. For *UAS-dzyA*, one line was screened positive for *white*⁺ phenotype (*UAS-dzyA* line 1 (named *UAS-dzyA 1*), see Appendix Tab. S1). *UAS-dzyA* transgenic flies were shipped

as larvae. When these animals reached adulthood, transposable element mapping was performed for the P-element line. *Drosophila* has four pairs of chromosomes, the first, the sex chromosomes (X or Y), the 2nd, 3rd, and 4th pairs. Transposon-mediated integration relies on the ability to insert a foreign piece of DNA at any position in the fly genome. Therefore, chromosome mapping (see Material & Methods) was performed to determine the position of the insertion site. In the *UAS-dzyA 1* line, the transgene is located on the 2nd chromosome. A table of the transgenic *UAS-dzy* lines can be found in the Appendix (see Tab. S1).

<u>*UAS-dzyB* transgenic flies</u>

To generate transgenic *UAS-dzyB* flies, the plasmid *dzyB in pUAST* containing the desired coding sequence for *dzyB* was used for microinjection into 30-min-old dechorionated *w⁻ Drosophila* embryos following a standard procedure for P-element-mediated germline transformation (see Material & Methods). Briefly, embryos of white-eyed flies (*w⁻*) were injected with two types of plasmids: Plasmids containing a P-element transposon with a desired transgene linked to a marker gene that produces red eye pigments, and a plasmid containing the P-transposase enzyme. The injection was made at the site of the embryo where the germline cells arise. Once both constructs were injected, the transposase enzyme is produced, which excises the entire transposon construction from the other plasmid and inserts it into the germ cell genome at a random location. When the successfully injected embryos reached adulthood, they produced a number of offspring containing the modified transgene containing chromosomes. The adult flies were mated, and if their offspring contained the transgene, they had red eyes due to the expression of the marker gene. So, to clearly determine whether the transgene was successfully integrated, we screened for an easily observable red eye phenotype.

We found that five different lines passed the transgene to the next generation (named *UAS-dzyB* line 1-5). A table of the *UAS-dzyB* transgenic lines generated by injection is in the Appendix (see Tab. S1). Thus, we generated transgenic animals for the *UAS-dzyB* splice form construct by injecting the DNA into *w⁻ Drosophila* embryos. Once the transgenic lines for the *dzyB in pUAST* construct were established, the insertion was mapped to determine which chromosome the insertion was located on (see Appendix Tab. S1). The *UAS-dzyB 3* and *UAS-dzyB 4* strains were selected for further experiments. The transgenes are located on the 2nd (*UAS-dzyB 3)* and 3rd (*UAS-dzyB 4*) chromosome in these lines.

<u>*UAS-dzyC* transgenic flies</u>

The strain *UAS-dzyC* had already been produced several years ago by members of the Department of Animal Genetics. At the time of this work, two fly strains exist for the *UAS-dzyC* construct (Fly strain collection stock 1303 and stock 1307). The insert was located on the 3rd

chromosome. The two transgenic *UAS-dzyC* lines are listed in the Appendix, together with the *UAS-dzyA* line and the *UAS-dzyB* lines (see Appendix Tab. S1).

Before the transgenic lines were used for further experiments, the lines were verified by DNA isolation from single flies using the "quick n dirty" protocol (see Material & Methods) and subsequent PCR analysis. Single flies of the strains *UAS-dzyA* (*UAS-dzyA 1*), *UAS-dzyB* (*UAS-dzyB 3*), *UAS-dzyC* (*UAS-dzyC 1* and 2, Fly strain collection stocks 1303 and 1307), and UAS-dzyCΔPDZ (*UAS-dzyCΔPDZ 7*) (see Results section 3.4) were crushed with SQ buffer, heated to 85 °C and then centrifuged. PCR with the isolated DNA was performed with the primer combination PR101 (vector *pUAST*) and PR159 (*dzy* exon 2). In the presence of a *UAS-dzy* construct, a 432 bp band appeared on the gel (Fig. 27). All lanes except lane 4 (*UAS-dzyC 2*) showed the expected length of 432 bp. The PCR for the line *UAS-dzyC 2* was repeated and the result was reproduced. The line *UAS-dzyC 2* was then excluded for all further experiments. In addition to the verification of the individual splice forms, a viability assay was performed to determine the lethality of ubiquitous *dzy* overexpression (see Results section 3.5). It was shown that the ubiquitous expression of the different *dzy* splice forms is neither lethal nor leads to sterility of the progeny.
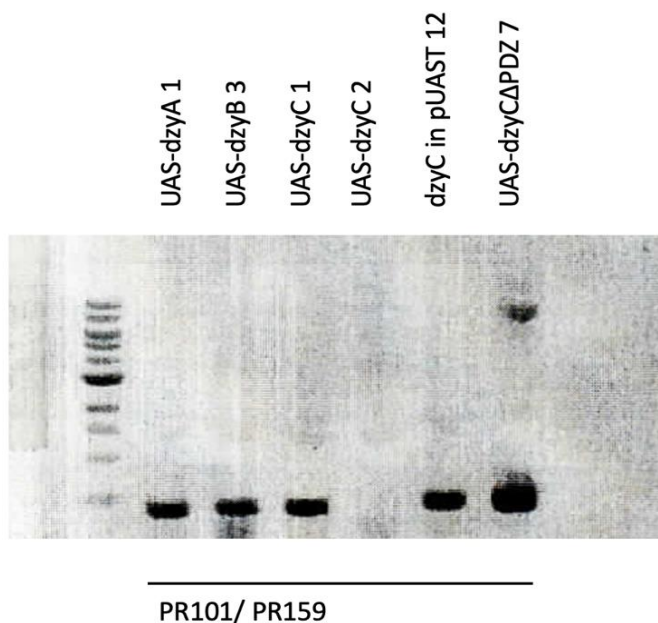

Fig. 27 Analysis of the fly strains *UAS-dzyA*, *UAS-dzyB* and *UAS-dzyC* by "quick n dirty" DNA isolation, PCR and agarose gel electrophoresis.
DNA was isolated from single flies of the strains to be tested. After PCR with the primers PR101 (vector *pUAST*) and PR159 (*dzy* exon 2), DNA was run for 20 min at 100 V on a 0.8 % agarose gel. DNA bands were imaged under a gel doc (gel documentation system). The first lane shows single fly DNA isolated from the UAS-*dzyA* line, the second lane from the UAS-*dzyB line* and the third and fourth lane from the two different UAS-*dzyC lines*. The fifth lane contains the PCR product from the *UAS-dzyCΔPDZ* line (see Results section 3.4). All lanes, excepting lane 4 (*UAS-dzyC 2*), show the expected length of 432 bp. With the exception of the *UAS-dzyC 2* line, all *UAS-dzy* fly strains could be verified.

The different Dzy isoforms are functionally distinct in the *Drosophila* embryo

Complementary to the loss-of-function phenotype, macrophages-specific overexpression from an EP-element in the *dzy* locus (*dzy^EP^*) results in a considerable enlargement of the cellular protrusions. In different regions of the embryo, these long cellular protrusions touch each other and thus form a network, due to stabilization of their cellular tails (Huelsmann *et al.* 2006). We wondered whether the structural differences between the different Dzy splice forms are related to different functions of the proteins in regulating changes in cell shape. Gal4-induced expression of *dzy* in macrophages from the *dzy^EP^* allele leads to the expression of all three isoforms. Thus, there is no evidence for specific involvement of a particular isoform. To test whether such a specific function exists, we expressed the single splice forms under the control of the macrophage-specific *srph-Gal4* driver (Fig. 28). As a control for these experiments, we used the *dzy^EP^* transgene, which allows simultaneous overexpression of all *dzy* splice forms in the same genetic background. So, in this part of this work, we expressed all *UAS-dzy* constructs (*UAS-dzyA*, *UAS-dzyB* and *UAS-dzyC*) in macrophages and analyzed the shape of these cells. By crossing animals carrying the *UAS-dzy*~splice forms~ with animals carrying the macrophage-specific *srph-Gal4* driver coupled with *UAS-cd2*, we were able to characterize the shape and position of macrophages in the different fly strains using CD2-specific antibody staining.
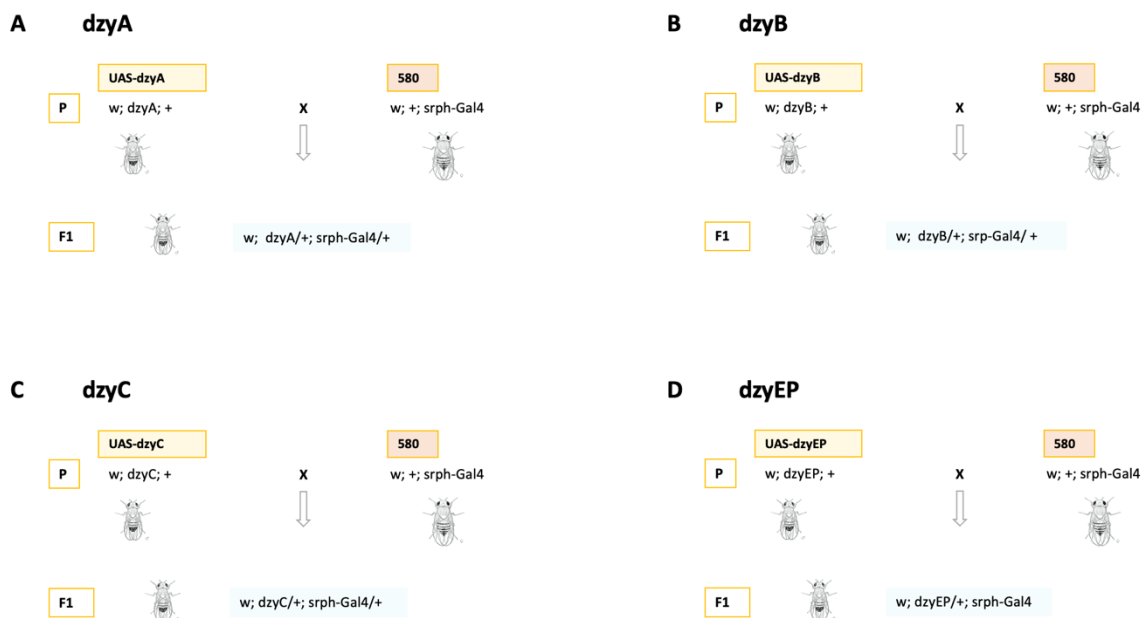

Fig. 28 Crossing scheme for the combination of the *UAS-dzy* and the *srph-Gal4* lines.
The crossing scheme shown was used to obtain transgenic flies expressing the different *dzy*~splice forms~ in macrophages. Virgin females of the *srph-Gal4* line were mated with males of the different *UAS-dzy* lines (*UAS-dzyA* (A), *UAS-dzyB* (B), *UAS-dzyC* (C) *or UAS-dzy^EP^* (D)). Embryos of the F1 generation (*srph-Gal4/UAS-dzy*) were collected, fixed, stained and examined for the different cell shape phenotypes.

The CD2-specific primary antibody was detected by either a fluorescent or chromogenic reaction. Fluorescent detection works via a fluorophore that emits light when excited by a light source. The chromogenic method, on the other hand, uses chromogens that undergo a chemical reaction. With this method, a more intensive and sensitive signal is obtained than with fluorescence detection.

<u>Avidin Biotin Complex (ABC)-based detection of macrophages</u>

The chromogenic detection method is based on enzymes bound to secondary antibodies, which in turn bind to primary antibodies against the protein of interest. A commonly used enzyme is horseradish peroxidase (HRP), which converts the chromogen 3,3'-diaminobenzidine (DAB) into a brownish precipitate by oxidation after the addition of hydrogen peroxidase (H_2O_2). The coloured product is visible under the light microscope. The chromogenic detection method was performed with an Avidin Biotin complex (ABC) (VECTASTAIN Elite ABC Kit). The ABC method (see Material & Methods) is based on biotinylated secondary antibodies and an Avidin-biotinylated peroxidase complex. The protein Avidin binds many molecules of the vitamin Biotin. This results in a formation of a large complex, which is then attached to a biotinylated secondary antibody. By labeling the detection enzyme HRP with biotin, and a secondary antibody with biotin as well, these two compounds can then be irreversibly linked with Avidin. Since there are always some Biotin binding sites available on an ABC, more enzymes can be located at the antigen sites, resulting in increased sensitivity.

The stained embryos were embedded in methyl salicylate or araldite-acetone and subsequently examined under the light microscope. At the time of bright-field imaging, the cloning process of the *dzyB in pUAST* construct (Fig. 29) was not yet fully completed. Therefore, there was no *UAS-dzyB* line yet. Accordingly, only the *UAS-dzyA* and *UAS-dzyC* fly strains were used for this ABC detection approach. Macrophage-specific expression of the *dzyA* form had no effect on the shape of macrophages: the macrophages appear rounded and with short protrusions as in the wild-type (Fig. 29B). In contrast, expression of the *dzyC* splice form induced cellular protrusions of more than approximately 2-3 times larger than those of wild-type macrophages (Fig. 29C), a phenotype that was as strong as when *dzy^{EP}* was expressed (Fig. 29A). Overexpression of the *UAS-dzyC* construct was able to induce the formation of long cellular protrusions, leading to the formation of the same characteristic cell network phenotype that we have shown in the *dzy^{EP}* line. The *dzyC* form was singularly sufficient to cause a dramatic change in cell shape. Thus, the Dzy splice form C is sufficient to induce a change in cell shape when specifically expressed in macrophages, whereas the DzyA

form is unable to affect macrophage morphology under the same conditions, demonstrating a differential functionality of the two splice forms in the embryo.
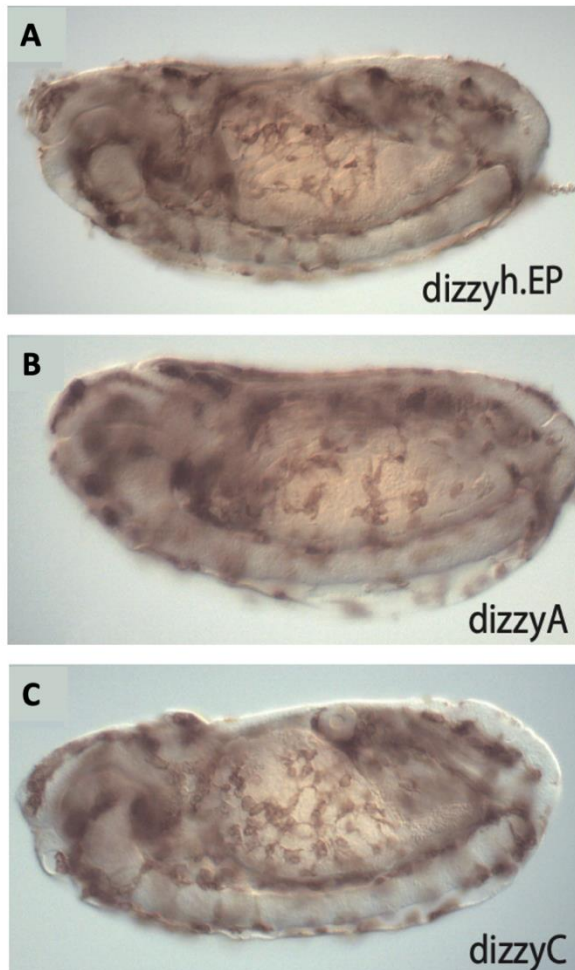

Fig. 29 Overexpression of the *dzy* splice forms in macrophages.
The *UAS-dzy* constructs *UAS-dzyA*, *UAS-dzyC* and *UAS-dzy^{EP}* were introduced into the *Drosophila* genome. Macrophage-specific Gal4 expression (*srph-Gal4*) drives overexpression of the UAS-related *dizzy* constructs. Bright-field microscope images represent an overlay of a sagittal optical section and the lateral view. Expression of *dizzy$^{h.EP}$* (*dzy^{EP}*) results in cell shape changes. Cells form a network in which they connect with each other, and the cellular protrusions are significantly longer (A). Analogous effects were observed when the *dizzyC* (*dzyC*) construct (C) was expressed. Macrophages do not appear to be significantly affected by the overexpression of the *dizzyA* (*dzyA*) form (B). Only the *dzyC* isoform can induce cell shape changes in macrophages. Cloning of the *dzyB* construct and generation of transgenic flies was currently in progress at the time of this imaging.

Fluorescence-based detection of macrophages

In order to obtain a better representation of the migrating cells and their protrusions, fluorescence images were taken under a confocal microscope in addition to the bright-field images. Here it was possible to illuminate the different layers of the embryo and thus also the different layers of the macrophages. Due to the lack of background, the cell protrusions could be visualised in more detail. As before, the *UAS-dzy* constructs were expressed in macrophages. The generated transgenic animals for the *UAS-dzy*$_{splice forms}$ (*UAS-dzyA* line 1, *UAS-dzyB* line 3 and *UAS-dzyC* line 1) were crossed with animals carrying the macrophage-specific driver (*srph-Gal4*) and the *UAS-cd2* construct. Thus, both *dzy* and *cd2* were expressed in the macrophages of the *Drosophila* embryo. The shape and the position of macrophages in the different fly strains were characterised using CD2-specific antibody staining under a confocal microscope. For detection, fluorescent dyes were used. Fluorescent dyes cannot be genetically introduced into cells and are therefore commonly used in combination with labeled

antibodies. In general, fluorophores absorb light at a high energy level and emit the absorbed light at a lower energy and longer wavelength, which must be measured by colour-specific detectors. Antibody staining was performed using the primary mouse anti-CD2 antibody (1:4000). Embryos were incubated with the primary antibody and the corresponding secondary antibodies conjugated with different fluorescent dyes. The secondary antibodies we used for this experiment were labelled with Cy3 (goat anti mouse GAM Cy3) and were used at a concentration of 1:250. The images were taken with a confocal laser scanning microscope.

The resulting confocal microscope images confirmed the results already seen in the bright-field images. Macrophage-specific expression of the *dzyA* form (Fig. 30A) had no influence on the cell shape of the macrophages. The macrophages appear roundish and with short protrusions. Expression of the *dzyB* splice form (Fig. 30B) in macrophages was also examined here and showed the same phenotype as the *dzyA* splice form. The cells overexpressing *dzyB* resembled the wild-type cells (Fig. 30E) by their round shape and small protrusions. In contrast to both the *dzyA* and *dzyB* forms, overexpression of the *UAS-dzyC* construct (Fig. 30C) showed the formation of long cellular protrusions, resulting in the formation of the same characteristic cell network phenotype that we have already shown in the *dzy*^{EP} line (Fig. 30D). Thus, the *dzy* splice form C alone is sufficient to induce a change in cell shape when specifically expressed in the macrophages, whereas the other splice forms, *dzyA* and *dzyB*, are not able to influence macrophage morphology under the same conditions.
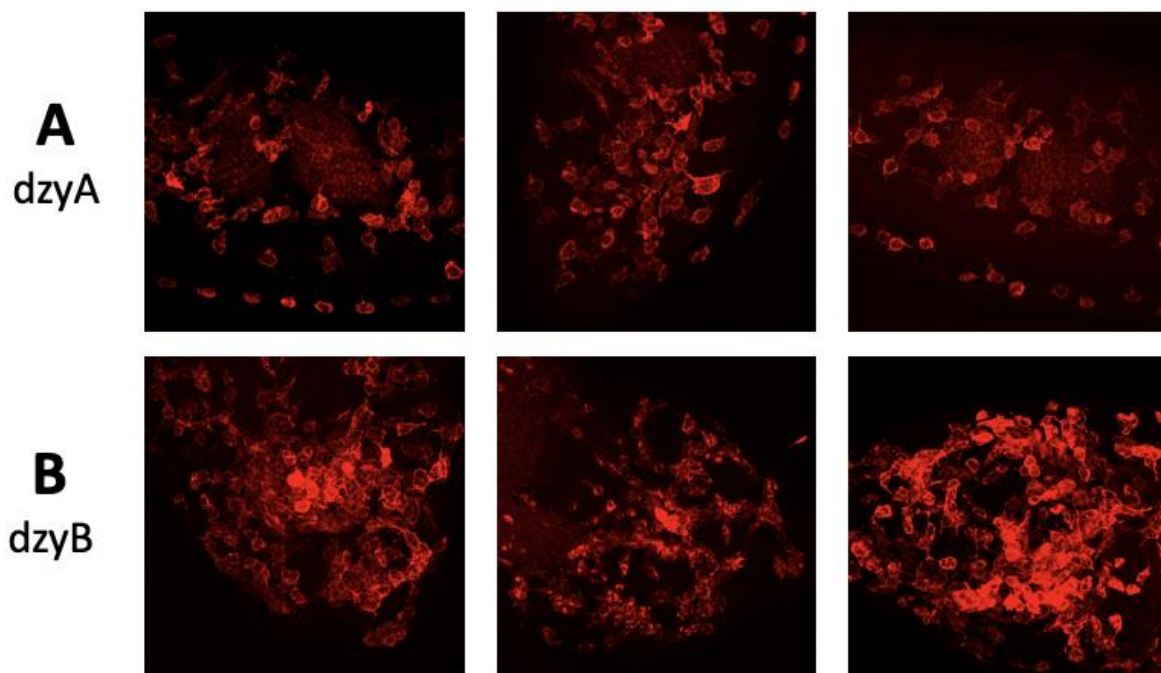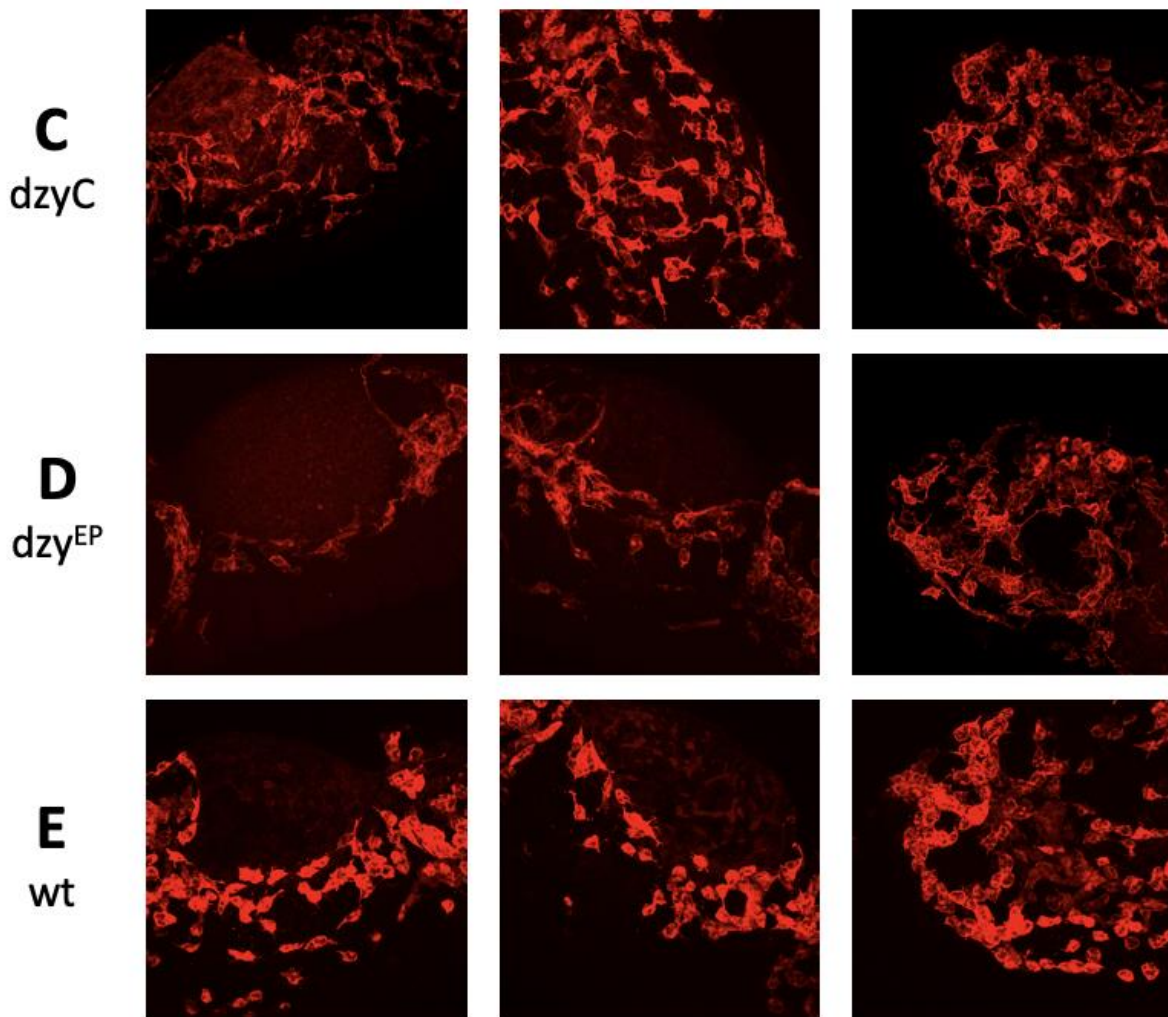
Fig. 30 Only the *dzyC* isoform can induce cell shape changes in macrophages.
Confocal images show macrophages in various areas of *Drosophila* embryos. Macrophages were detected by the expression of CD2. (A) In the *UAS-dzyA* embryos, the cell bodies of the macrophages are rounded, form small protrusions and rarely touch each other. (B) Expression of the *dzyB* isoform has no significant effect on the length of the protrusions. (A-B) Macrophages are not affected by the expression of either the *dzyA* or the *dzyB* isoform and are indistinguishable from cells of wild-type embryos (E). (C) In contrast, expression of the *dzyC* isoform results in a change in cell shape, an elongation of the protrusions, which is essentially the same as observed in *dzy^EP* (D). (D) Expression of *dzy^EP* leads to a dramatic change in cell shape. Cells form a network in which they connect to each other, and the cellular protrusions are significantly longer.

In summary, both the *dzy^EP* and *dzyC* form are individually sufficient to cause a dramatic cell shape change. The overexpression of the *dzyC* construct is sufficient to induce the formation of long protrusions leading to the formation of the same characteristic cell network observed in the *dzy^EP* line. In contrast, the macrophage expression of the *dzyA* and the *dzyB* construct showed no effect. The macrophages appeared roundish and with short protrusions as in the wild-type controls.

<u>Determination of the expression level of the different isoforms using *in situ* hybridization of *Drosophila* embryos</u>

Macrophage-specific expression of the individual Dzy splice forms had a very specific effect on cell morphology (see Fig. 29 and Fig. 30). Since the Dzy splice form DNAs were randomly inserted into the fly genome upon injection, it was important to clarify the question of whether the position of the insert influenced the respective expression level. The so-called position effect refers to the variation in expression of identical transgenes that are randomly inserted into different regions of the genome. In this case, the difference in expression is often due to enhancers that regulate neighboring genes. These local enhancers can also influence the expression level of the transgene. Therefore, the question arose whether the level of experimental RNA expression was comparable between the different forms. Does a higher expression level of the dzyC splice form lead to the phenotype of elongated protrusions? Would dzyA and dzyB also form longer protrusions if their expression levels were higher? In order to exclude a phenotype that is solely due to the position of the P-element and thus the expression level of the splice form, in situ hybridization was carried out. In situ hybridization (ISH) is a semi-quantitative method for identifying and comparing mRNA levels of a gene in fixed tissue across multiple samples (Wunderlich et al. 2014). For this method, a digoxigenin (DIG)-labeled RNA probe was prepared that binds to the central region of the dzy mRNA (see Material & Methods) and can thus detect all three splice forms. An anti-DIG antibody conjugated to AP was used to detect the probe. Embryos were placed in a staining buffer to initiate a colour reaction in the presence of anti-DIG-AP. This procedure allows the detection of target molecules in the whole embryo.

Thus, to rule out that the observed cell shape phenotype was due to different expression levels, we overexpressed the different splice forms (UAS-dzyA, UAS-dzyC and UAS-dzyEP) in macrophages (srph-Gal4) and visualized gene expression in the Drosophila embryo. At the time of in situ hybridization, the cloning process of the dzyB in pUAST construct was not yet fully completed. Accordingly, only the UAS-dzyA and UAS-dzyC fly strains were used to confirm the expression level. RNA expression of dzy was analyzed during various developmental stages for dzyA (Fig. 31A), dzyC (Fig. 31B), dzyEP (Fig. 31C) and dzyGFP (Fig. 31D) via in situ hybridization. For further experiments (see Results section 3.5 and 3.6), the dzyGFP form was carried along in addition to the dzyEP form and examined for its expression.

After analysis of the stained embryos under the bright-field microscope, the existence of the individual splice forms could be concluded. Macrophage-specific expression of dzy was observed in the different UAS-dzy embryos. No expression or light blue background staining was detected in the negative control (Fig 31E). However, it was very difficult to make a precise

statement comparing the different expression levels. Compared to the dzyA form, the individual macrophages could be accurately detected in the dzyC form. dzyA and dzyEP showed bluish staining at the expected locations, but individual macrophages could not be detected in either form. In general, dzyC showed a stronger signal with the dzy probe (Fig. 31B). Nevertheless, at this stage of the work it was assumed that the concentrations of the experimental RNA were comparable and essentially not very different from each other. dzyGFP showed a significantly stronger expression with clearly recognizable individually demarcated macrophages than the other dzy forms. UAS-dzyGFP was used as a positive control for the "adult rescue experiment" in Results section 3.5 of this work.
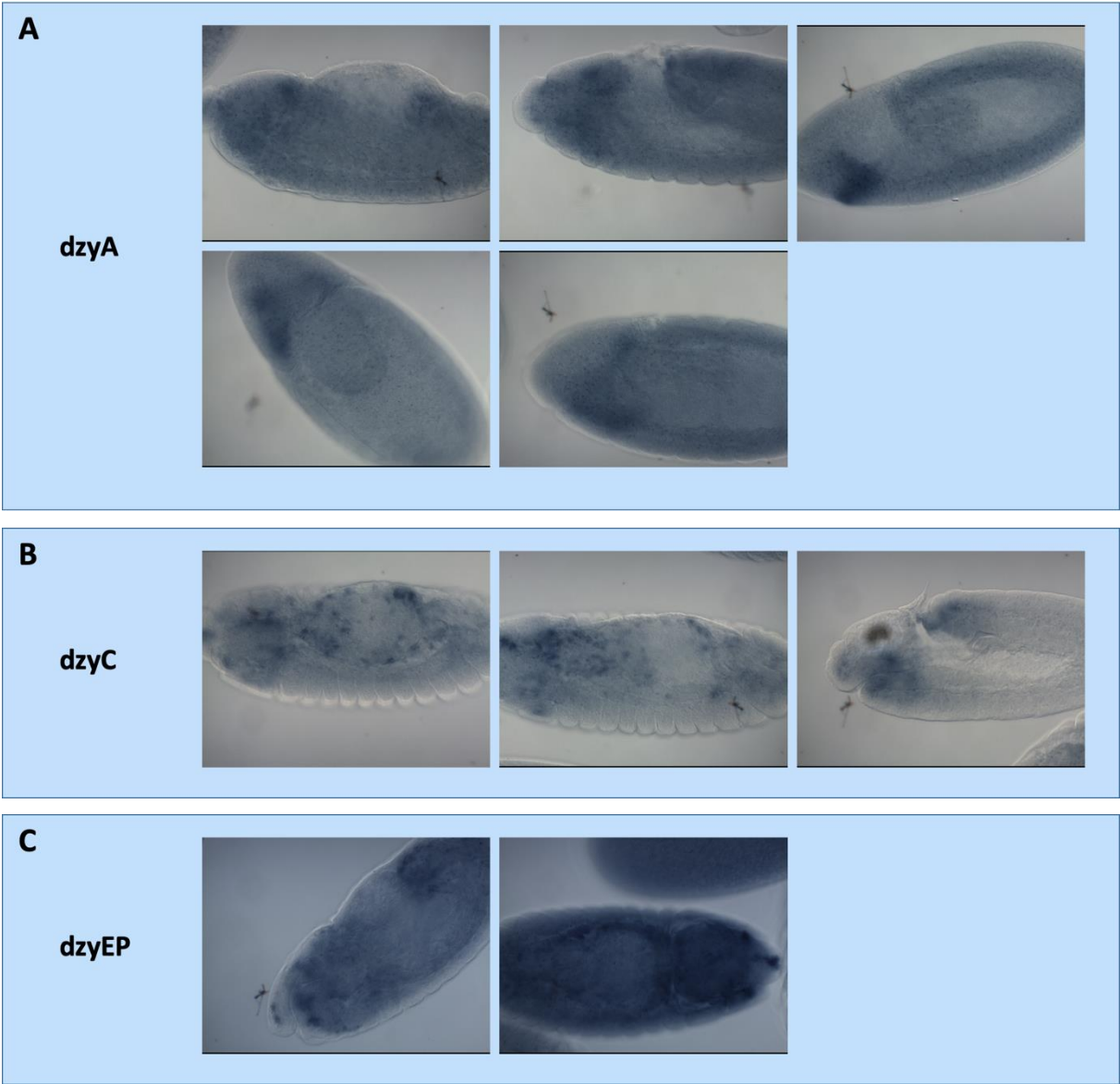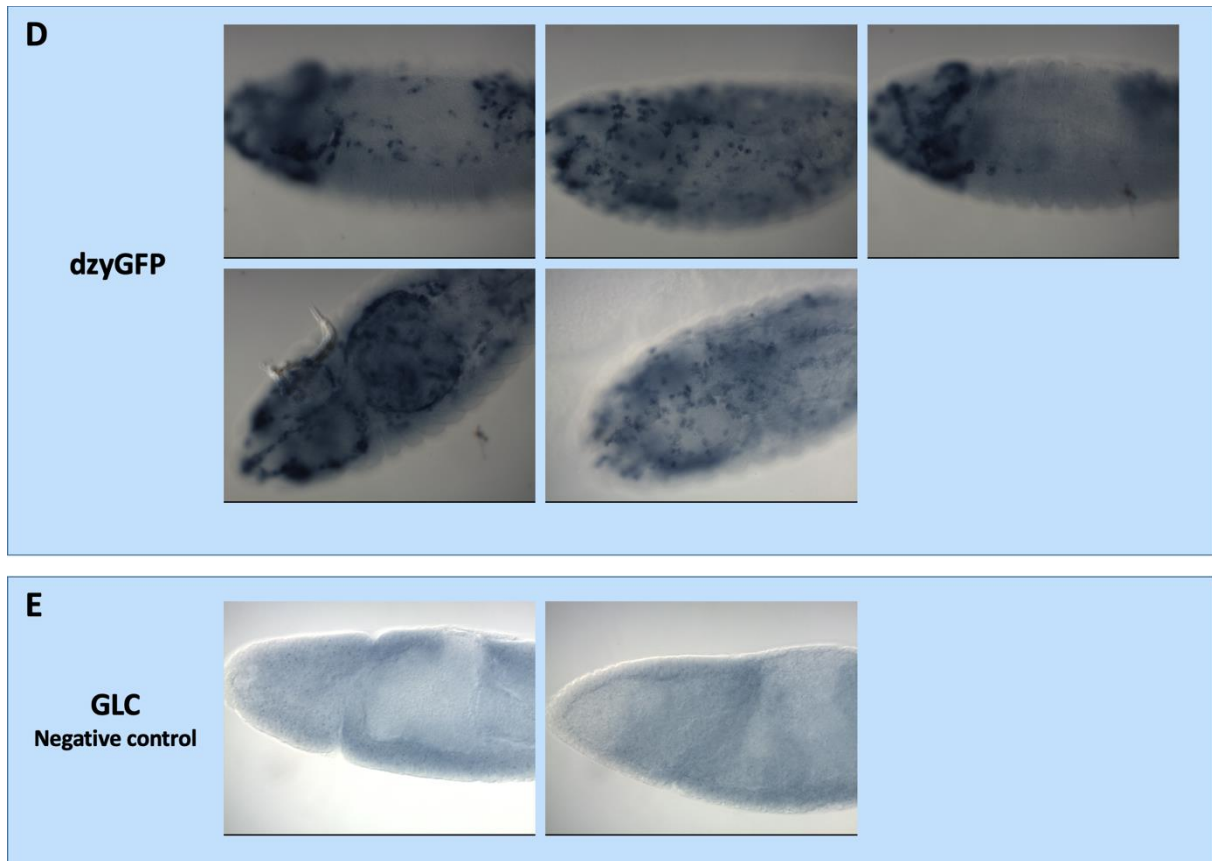
Fig. 31 Visualisation of *dzy* mRNA inside the *srph-Gal4/UAS-dzy Drosophila* embryos by *in situ* hybridization. (A-E) Embryos at different stages were hybridized with the *dzy* probe.
Representative images of RNA *in situ* hybridization show *dzy*-specific mRNA accumulation in macrophages of *srph-Gal4/UAS-dzyA* (A)*, srph-Gal4/UAS-dzyC* (B), *srph-Gal4/UAS-dzy^{EP}* (C) and *srph-Gal4/UAS-dzyGFP* (D) embryos. No hybridization was detected in the negative control (E). In these images, blue staining is present along invariant migration pathways of the macrophages. *srph-Gal4/UAS-dzyC* (B) and *srph-Gal4/UAS-dzyGFP* (D) embryos clearly show the contours of the individual cells.

3.4 The function of the PDZ domain and the proline-rich motifs of Dzy in the *Drosophila* embryo

The various *dzy* splice forms display distinct functions in the *Drosophila* embryo. In particular, the *dzyC* isoform is the only one that is sufficient to effect cell shape change. What could be the structural basis for this particular property? There is no protein sequence in DzyC that is not found in the other Dzy forms. The main difference between *dzyC* and the other *dzy* splice forms is the absence of exon 5/5S, suggesting that the domain encoded by this exon exerts an inhibitory effect in the DzyA and DzyB forms. Within the C-terminus of the splice forms *dzyA* and *dzyB*, there is a section encoded by exon 5/5S where we identified two PRMs (PRM2 and PRM3) as potentially relevant structural features. We wondered whether these two PRMs encoded by exon 5/5S act as an inhibitory element, either by mediating an intermolecular Dzy protein dimerization or by interacting intramolecularly with other parts of the protein and

changing its conformation. Preliminary experiments by predecessors of this working group already provided initial evidence that this is an intramolecular interaction and that the N-terminal PDZ domain could be a component required for this interaction. Another indication for the PDZ domain as an interaction partner for the C-terminal PRMs in exon 5/5S is the fact that the conserved PDZ domain, characteristic for all PDZ-GEFs, is a protein interaction module that often recognizes short amino acid motifs at the C-termini of proteins (Lee & Zheng 2010). We hypothesized that an interaction occurs between the C-terminal PRMs encoded by exon 5/5S and the N-terminal PDZ domain within exon 3. We would expect the possible intramolecular interaction to result in reduced accessibility of the PDZ domain and the exon 5-derived motifs to their respective partners in other protein molecules. Therefore, in the A and B splice forms of Dzy, but not in the DzyC form, there is a intramolecular interaction between the PDZ domain of exon 3 and the PRMs in exon 5/5S. This interaction leads to a conformational change and makes the two domains within the DzyA and the DzyB form inaccessible. It was assumed that the PDZ domain and the PRMs interact with each other and thus have an influence on the functionality of the Dzy protein. To confirm this model and to investigate the function of the PDZ domain, the PRMs and their interaction, the domains of interest were completely removed from the DNA sequence. To investigate whether these domains are critical for the function of *dzy*, deletion constructs containing protein deletions of the PDZ (ΔPDZ) and the PRMs (ΔPRMs) were tested for their ability to change cell shape in macrophages. Functional analysis of the different domains of the PDZ-GEF will allow us to understand how Dzy mediates its function and potentially lead to the identification of new components that interact with Dzy.

Assembly of the *UAS-dzy* deletion constructs

In general, cDNA of the *dzyA* isoform and the *dzyC* isoform were used to generate the deletion constructs for *UAS-dzy* (*UAS-dzyAΔPRM2*, *UAS-dzyAΔPRM3* and *UAS-dzyCΔPDZ*). The various *dzy*-transgene constructs' specific ORF coding regions were amplified via PCR with specific primers, digested with restriction enzymes and ligated into the *pUAST Drosophila* transformation vector (Brand & Perrimon 1993). This part of the work focused on the function of the domain interactions, particularly the PDZ domain and the PRMs of the Dzy protein. The interaction of these regions is thought to affect the functionality of the Dzy protein. To investigate this, different Dzy isoforms with non-functional regions (*dzyCΔPDZ*, *dzyAΔPRM2* and *dzyAΔPRM3*) were generated, allowing testing for which functions of Dzy, during haemocyte migration for example, are dependent on the PDZ domain or the proline-rich motifs PRM2 and PRM3.

<u>The deletion of the Dzy PDZ domain: *dzyCΔPDZ in pUAST*</u>

To investigate the function of the PDZ domain, a Dzy isoform with an inoperative PDZ domain was generated. This form allowed us to investigate which functions of Dzy, for instance in relation to cell shape change or haemocyte migration, are dependent on the PDZ domain. To construct the non-functional PDZ domain, significant parts of the PDZ domain were deleted as a necessity. One method used to achieve this deletion of the PDZ domain was to assemble the regions upstream (*dzyCΔPDZ fragment_1*) and downstream (*dzyCΔPDZ fragment_2*) of the PDZ domain without the domain itself. The PDZ domain contains a restriction site for the restriction enzyme XhoI in the 3' region of the domain. To delete the PDZ domain, the insertion of a second XhoI restriction site into the 5' region of the domain was required. A second XhoI restriction site was inserted into the sequence via PCR with specifically designed primers. As a result, the PDZ domain was rendered non-functional due to its being indirectly excised from the sequence. The cloning process for the construct *dzyCΔPDZ in pUAST* had already been started by predecessors in the Department of Animal Genetics, was continued during the author's Master's thesis and completed within the scope of this work. For the sake of completeness and better understanding, the complete and revised cloning process is presented below.

<u>Part 1</u>

To generate a construct with a deleted PDZ domain (*dzyCΔPDZ* construct), a cloning strategy with four distinct parts, shown in Fig. 32, is used. First, the 5' part of the *dzyCΔPDZ* fragment (*dzyCΔPDZ fragment_1*), upstream from the PDZ domain was amplified and cloned into a *TOPO TA* cloning vector. To generate the fragment *dzyCΔPDZ fragment_1,* a forward and a reverse primer were designed through varying the base sequence and inserting specific restriction sites (PR222 XhoI down PDZ/PR221 BglII up PDZ) for further cloning steps. Located upstream from the 5' region of the PDZ domain itself, the forward primer inserted a restriction site for the enzyme BglII in the sequence of the PCR product (Fig. 32A). The reverse primer was located in the 5' region of the PDZ domain itself and contained an XhoI restriction site. These two primers were used in a PCR reaction which resulted in an insert containing both restriction sites and only a short segment of the primary PDZ domain. The *pUAST-dzyCII* (14515 bp) construct served as a template for the designed primer pair. The resulting PCR product was amplified by PCR and purified using agarose gel electrophoresis. Subsequently, the isolated insert (*dzyCΔPDZ fragment_1*, 1484 bp) was ligated into the *TOPO TA* cloning vector which resulted in the construct *pCR2.1_dzyCΔPDZ_1*. The PCR primer pair (M13fw/M13rev) used for the purpose of identifying *pCR2.1_dzyCΔPDZ_1* resulted in an amplification product of known size (1636 bp). The purified *dzy* constructs were sent to LGC

Genomics for sequencing. The data confirmed that the construct was indeed *pCR2.1_dzyCΔPDZ_1* (5417 bp).

Part 2

To generate the 3' region downstream of the PDZ domain (*dzyCΔPDZ fragment_2*), the construct *pUAST-dzyCII* (14515 bp) was first digested with the restriction enzyme XbaI to remove the excess XbaI restriction site for the next cloning step. The intermediate construct *pUAST-dzyCII_XbaI* (14487 bp) was then digested with the enzymes XhoI and XbaI to receive the *dzyCΔPDZ fragment_2* (2973 bp) (Fig. 32B). Due to the XhoI restriction site in the 3' region of the PDZ domain, only a short region of the PDZ domain was captured. After digestion, the insert *dzyCΔPDZ fragment_2* (2973 bp) was gel-purified and isolated.

Part 3

The next step was to combine the two *dzyCΔPDZ* fragments (*dzyCΔPDZ fragment_1* and *dzyCΔPDZ fragment_2*) to obtain the full-length *dzyCΔPDZ* sequence. To clone the insert *dzyCΔPDZ fragment_2* (2973 bp) into the *pCR2.1_dzyCΔPDZ_1* (5417 bp) construct, both segments had to be treated with the same restriction enzymes to create compatible ends (Fig. 32C). Therefore, the TOPO TA vector source *pCR2.1_dzyCΔPDZ_1* containing the 5' upstream part (*dzyCΔPDZ fragment_1*) was also treated with the restriction enzymes XhoI and XbaI. The digested component was separated by agarose gel electrophoresis and purified using the Nucleospin® Gel and PCR Clean-up Kit (Macherey Nagel). In the next step, the two modules were ligated to create the construct *pCR2.1_dzyCΔPDZ* (8333 bp), which contains the upstream and downstream segments with a non-functional PDZ domain. The isolated insert *dzyCΔPDZ fragment_2* (2973 bp) was ligated into the vector source *pCR2.1_dzyCΔPDZ_1_XbaI/XhoI*. The ligation products were transformed into chemically competent cells and grown on agar plates with Ampicillin (Amp). To identify the *pCR2.1_dzyCΔPDZ* (8333 bp) construct, colonies were analysed using the primer combination PR164 and PR169. The *pCR2.1_dzyCΔPDZ* produced a 500 bp PCR product.
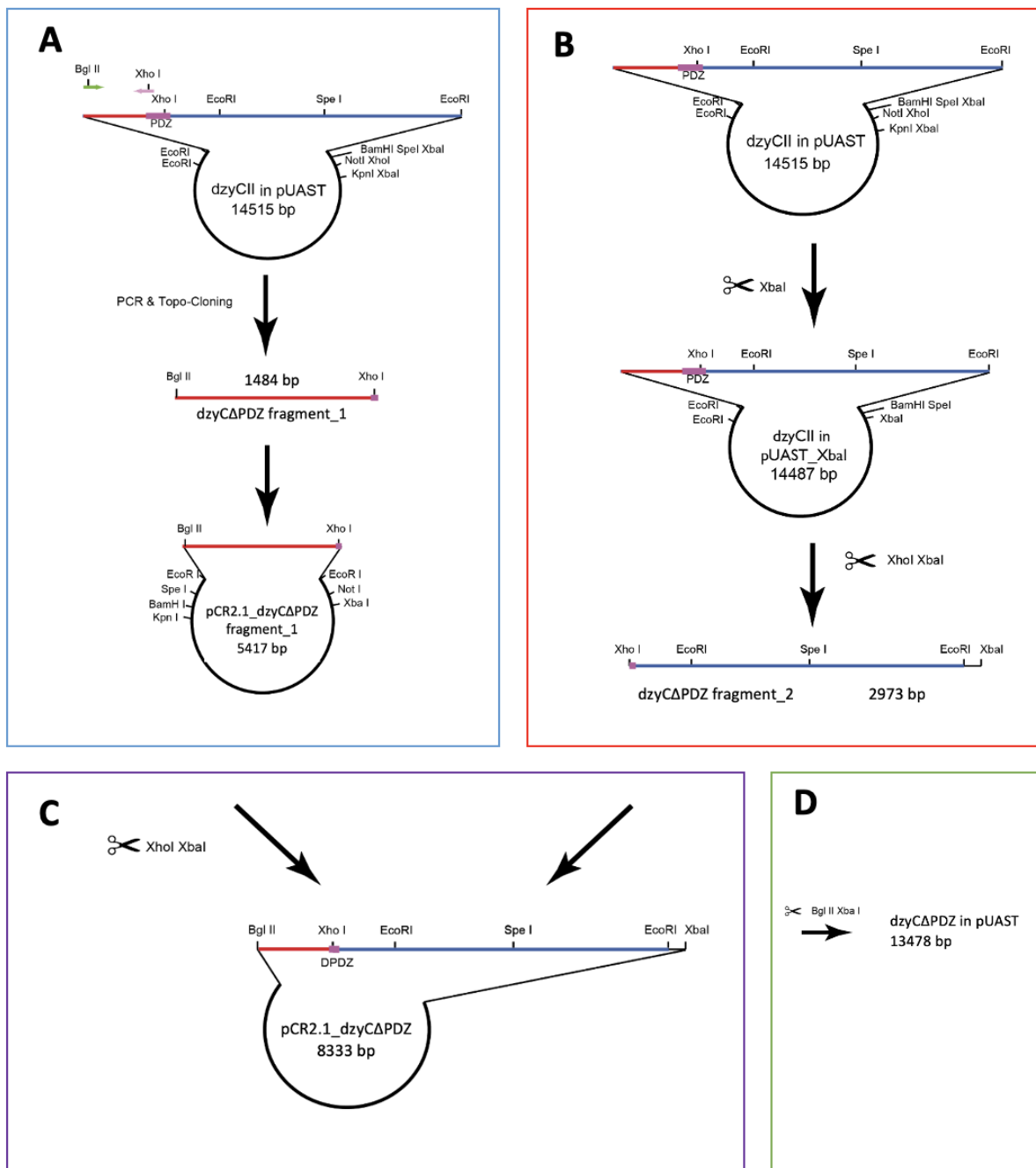
Fig. 32 Overview of the *dzyCΔPDZ* cloning strategy.
The construct *dzyCΔPDZ in pUAST* (13478 bp), which carries an inoperative PDZ domain, was generated by several intermediate steps. (A) Part 1: Generation of the *dzyCΔPDZ fragment_1* by PCR with specific primers inserting restriction sites. One restriction site (XhoI) was inserted in the PDZ domain itself and another restriction site (BglII) was inserted upstream of the PDZ domain. The PCR product of the two primers contain both restriction sites and a short region of the PDZ domain. The construct *pUAST-dzyCII* (14515 bp) served as the template for the modified primers. The insert *dzyCΔPDZ fragment_1* (1484 bp) was ligated into the TOPO TA vector. The construct *pCR2.1_dzyCΔPDZ_1* (5417 bp) was generated. (B) Part 2: Construction of the 3' region downstream of the PDZ domain. The construct *pUAST-dzyCII* (14515 bp) was digested with the restriction enzyme XbaI to eliminate the excess XbaI restriction site. The construct *pUAST-dzyCII_XbaI* (14487 bp) was then digested with XhoI and XbaI to yield the *dzyCΔPDZ fragment_2* (2973bp). (C) Part 3: To combine the two *dzyCΔPDZ* fragments, *dzyCΔPDZ fragment_1* and *dzyCΔPDZ fragment_2*, and obtain the full-length *dzyCΔPDZ* sequence, the *dzyCΔPDZ fragment_2* (2973 bp) was ligated into *pCR2.1_dzyΔPDZ_1* (5417 bp). *pCR2.1_dzyCΔPDZ_1* containing the *dzyCΔPDZ fragment_1* was treated with the restriction enzymes XhoI and XbaI. The isolated insert *dzyCΔPDZ fragment_2* (2973 bp) from (B) was then ligated into the

vector source *pCR2.1-dzyΔCPDZ_1_XbaI/XhoI*. The result was the construct *pCR2.1_dzyCΔPDZ* (8333 bp). (D) Part 4: In the final part of the cloning strategy, the full-length *dzyCΔPDZ* DNA fragment (4457 bp) was cut from the construct *pCR2.1_dzyCΔPDZ* (8333 bp) and inserted into the transformation vector *pUAST*. Both the construct *pCR2.1_dzyCΔPDZ* (8333 bp) and the *pUAST* vector were digested with the restriction enzymes BglII and XbaI. The isolated insert *dzyCΔPDZ fragment_BglII/XbaI* was then ligated into the vector *pUAST_BglII/XhoI*. The *dzyCΔPDZ in pUAST* (13478 bp) construct was generated.

<u>Part 4</u>

The final step during this cloning process was to ligate the full-length *dzyCΔPDZ* fragment (*dzyCΔPDZ fragment_1* and *dzyCΔPDZ fragment_2*) into the *pUAST* transformation vector (approximately 9100 bp), to generate the final construct *dzyCΔPDZ in pUAST* (13478 bp). To clone the *dzyCΔPDZ fragment* into the *pUAST* vector, both the construct *pCR2.1-dzyCΔPDZ* (8333 bp) and the *pUAST* vector were digested with the two restriction enzymes BglII and XbaI (Fig. 32D). The components were separated by agarose gel electrophoresis. The desired DNA bands were excised from the gel and purified using the Nucleospin® Gel and PCR Clean-up Kit (Macherey Nagel). The isolated insert *dzyCΔPDZ fragment_BglII/XbaI* (4457 bp) was then ligated into the vector *pUAST_BglII/XhoI*. A vector concentration of 50 ng and an insert:vector ratio of 3:1 was used for this ligation process. The ligation products were transformed in chemically competent cells and grown on agar plates with Ampicillin (Amp). To detect clones carrying the *dzyCΔPDZ in pUAST* construct (13478 bp), plasmid DNA was analysed via Colony-PCR using primer pair PR229/PR100 (Fig. 33). Bands of about 620 bp (*dzyCΔPDZ in pUAST*) were expected. The purified *dzy* constructs were sequenced by LGC Genomics. The sequenced data showed the *dzyCΔPDZ in pUAST* construct (*dzyCΔPDZ in pUAST clone 1*).
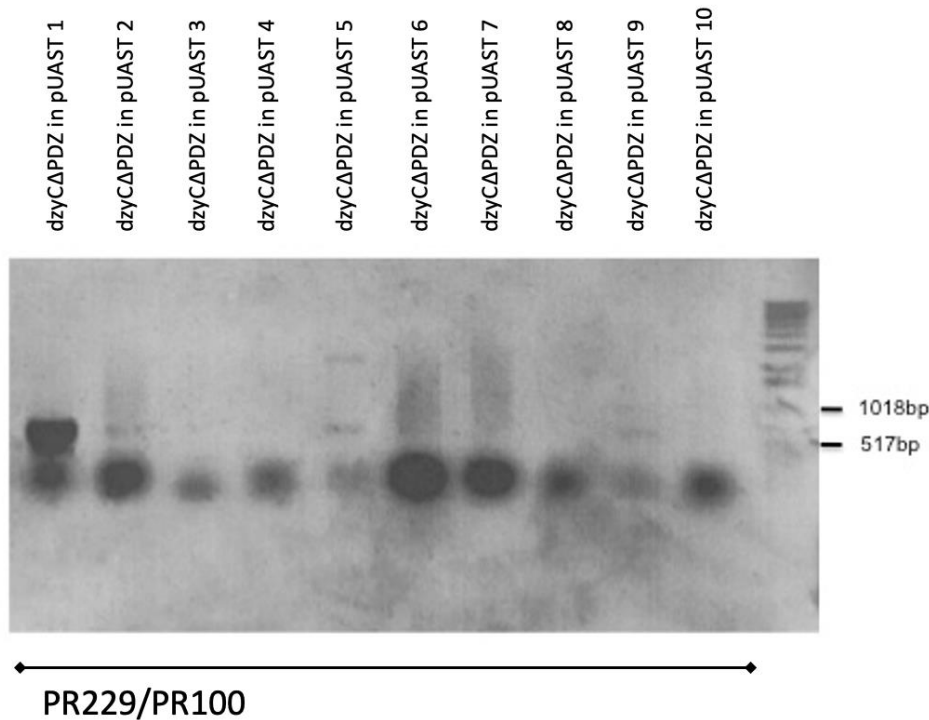
Fig. 33 Identification of the assembled construct *dzyCΔPDZ in pUAST* by Colony-PCR.
Colony-PCR of the different clones (1-10) was performed with the primer pair PR229/PR100. A 0.8 %
agarose gel was used to screen for the expected plasmid size: *dzyCΔPDZ in pUAST* 620 bp. The DNA
dzyCΔPDZ in pUAST clone 1 appeared to be the correct size on the gel. *dzyCΔPDZ in pUAST clone 1*
was sent for sequencing to confirm that the cloned plasmid had received the correct insertion sequence.

The deletion of the Dzy PRMs: *dzyAΔPRM2 in pUAST* and *dzyAΔPRM3 in pUAST*

As mentioned earlier, the main difference between the *dzyA*, *dzyB* and *dzyC* form is the
presence or absence of the region encoded by exon 5/5S. Within the exon 5/5S of the splice
forms *dzyA* and *dzyB*, we identified two proline-rich motifs (PRM2 and PRM3) as potentially
relevant structural features for the interaction with the N-terminal PDZ domain. We wondered
what might happen in terms of cell shape changes if either one or both of these PRMs were
mutated and their prolines replaced with a sequence of alternative amino acids. How do the
mutated domains affect the cell shape of macrophages? Is it possible that the interaction with
the PDZ domain is disrupted, leading to a phenotype comparable to DzyC? Are both PRMs,
PRM2 and PRM3, of exon 5/5S required for this interaction?

Changes in cell shape and cell migration can be caused by different numbers of PRMs. To
study the role of the proline-rich motifs in macrophage migration, we generated Dzy isoforms
with non-functional PRM-domains (ΔPRM2 and ΔPRM3). The *dzyA* splice form served as
template for the mutation of the different PRMs and further investigation of the domain
interactions. Using these forms, we were able to investigate which functions of Dzy, for
instance in relation to cell shape change or haemocyte migration, are dependent on the
different PRMs. Mutation of the various PRMs could result in an insufficient connection

between the PDZ domain and the PRMs. The loss of these connection could influence the function of the Dzy protein. The two constructs, *UAS-dzyAΔPRM2* and *UAS-dzyAΔPRM3*, were produced via several PCR and digestion steps. The construction of the two non-functional PRM domains (ΔPRM2 and ΔPRM3) depended on the deletion of the significant part of the proline-rich motifs. As with the deletion of the PDZ domain, ΔPRM constructs were generated by assembling the regions upstream (*dzyAΔPRM_PCR_L*) and downstream (*dzyAΔPRM_PCR_R*) of the PRMs without the domain itself. The PRMs are very short regions and do not contain any restriction site for restriction enzymes. Deletion of the PRMs therefore requires the insertion of restriction sites in the 5' region and the 3' region of the domain. These restriction sites were inserted into the sequence by PCR with specifically designed primers. Thus, for the generation of the ΔPRM constructs, four specific primers were designed for the deletion of the PRM regions: two primers for the region upstream of the PRMs and two primers for the region downstream of the PRMs. Since there were only a limited number of possibilities to insert two restriction sites within the proline-rich motif due to the low number of bp, an ORF shift was introduced in addition to the 5' RE site to ensure that as little of the original proline as possible was present. This ORF shift was cancelled by the primer in the 3' region of the PRMs. So, for the complete deletion of the PRMs, a open reading frame shift was introduced in addition to the RE sites. There were no more prolines and the function of the domain was thus completely switched off. Consequently, the PRMs (PRM2 and PRM3), like the PDZ domain, were non-functional as they were indirectly excised from the sequence. The cloning of a *UAS-dzyA* construct, in which both PRMs were knocked out simultaneously, proved to be more difficult than expected and was still in the early stages, which is why it was not elaborated further in this work.

The deletion of the Dzy PRM2: *dzyAΔPRM2 in pUAST*

Part1

The cloning strategy to generate a construct with a deleted PRM2 (*dzyAΔPRM2*) was divided into three distinct parts, which are shown in Fig. 34. In the first step, the 5' part of the *dzyAΔPRM2* fragment (*dzyAΔPRM2L*) upstream of the PRM2 domain and the 3' part of the *dzyAΔPRM2* fragment (*dzyAΔPRM2R*) downstream of the PRM2 were amplified and cloned into TOPO TA cloning vector. Four primers, two forward primers (PR231 (PRM2L)/PR226 (PRM2R)) and two reverse primers (PR225 (PRM2L)/PR224 (PRM2R)) were designed to generate the *dzyAΔPRM2L* and *dzyAΔPRM2R* fragments by varying the base sequence and inserting specific restriction sites (PR225, BglII and PR226, BamHI) for further cloning steps. The reverse primer for the *dzyAΔPRM2L* fragment (PR225) was located in the 5' direction of the PRM2 domain and inserted a restriction site for the enzyme BglII into the sequence of the

PCR product (Fig. 34A). The forward primer for the *dzyAΔPRM2R* fragment (PR226) contained an BamHI restriction site and was located within the 3' region of the PRM2 domain. The primer pair PR231/PR225 was used to amplify the fragment *dzyAΔPRM2L* (1431 bp; BglII), and the primers PR226 and PR224 generated the fragment *dzyAΔPRM2R* (627 bp; BamHI). The use of the two primer pairs in a PCR reaction resulted in two inserts containing the respective restriction site and only a short region of the primary PRM2 domain. The construct *dzyA in pUAST* (14296 bp) served as template for the designed primers. The PCR product was amplified by PCR and seperated by agarose gel electrophoresis. Isolation of the two PCR fragments from the gel was done using Nucleospin® Gel and PCR Clean-up Kit (Macherey Nagel). Subsequently, the isolated inserts *dzyAΔPRM2L* (1431 bp) and *dzyAΔPRM2R* (637 bp) were ligated into the TOPO TA cloning vector, resulting in the constructs *pCR2.1_dzyAΔPRM2L* (5362 bp) and *pCR4_dzyAΔPRM2R* (4583 bp) (Fig. 34A). The insert-vector mixture was transformed into chemically competent *E.coli DH5α* cells and then plated onto Amp-containing agar plates. Clones obtained from the TOPO cloning were characterised via sequencing. The PCR primer pair M13fw/M13rev used to identify *pCR2.1_dzyAΔPRM2L* and *pCR4_dzyAΔPRM2R* resulted in an amplification product of known size (PRM2L: 1637 bp; PRM2R: 829 bp). The production of the construct *pCR2.1_dzyAΔPRM2L* required several attempts, where the insert had to be amplified and cloned several times. Finally, purified *pCR2.1_dzyAΔPRM2L* clone 1 and 3 and *pCR4_dzyAΔPRM2R* clone 1 and 5 were sent to LGC Genomics for sequencing. The sequencing data confirmed that the constructs were *pCR2.1_dzyAΔPRM2L* (5362 bp) and *pCR4_dzyAΔPRM2R* (4583 bp).

Part2

In the second part of the cloning process, both constructs (*pCR2.1_dzyAΔPRM2L* and *pCR4_dzyAΔPRM2R*) were digested. The construct *pCR2.1_dzyAΔPRM2L* (5362 bp) was digested with the enzymes SpeI and BglII to receive the *pCR2.1_dzyAΔPRM2L_SpeI/BglII* fragment (1397 bp). The next step was to combine the two *dzyAΔPRM2* fragments (*dzyAΔPRM2L* and *dzyAΔPRM2R*) to obtain the full-length *dzyAΔPRM2* sequence. To clone the insert *dzyAΔPRM2L_SpeI/BglII* (1397 bp) into the *pCR4_dzyAΔPRM2R* (4583 bp) construct, both fragments had to be treated with restriction enzymes to create compatible ends (Fig. 34B). BamHI generates compatible ends to BglII. Therefore, the TOPO TA vector source *pCR4_dzyAΔPRM2R* containing the 3' downstream part (*dzyAΔPRM2R*) was treated with the restriction enzymes SpeI and BamHI. The digested components (*dzyAΔPRM2L_SpeI/BglII* (1397 bp) and *pCR4_ dzyAΔPRM2R_SpeI/BamHI* (4546 bp) were separated by agarose gel electrophoresis and purified with Nucleospin® Gel and PCR Clean-up Kit (Macherey Nagel). These two components were ligated to create the construct *pCR4_dzyAΔPRM2* (5943 bp),

which contains the upstream and downstream segments with a non-functional PRM2 region. The isolated insert *dzyAΔPRM2L_SpeI/BglII* (1397 bp) was ligated into the vector source *pCR4_ dzyAΔPRM2R_SpeI/BamHI*. Ligation was performed with 50 ng of vector and 5 times the amount of insert. The ligation product was transformed into chemically competent cells and grown on agar plates with Ampicillin (Amp). For analysis of the clones, colonies were picked from the plates and cultured overnight in LB medium. Subsequently, the plasmid DNA was purified using a Miniprep Kit. To identify the *pCR4_dzyAΔPRM2* construct (5943 bp), colonies were analysed using the primer combination PR181 and PR188. *pCR4_dzyAΔPRM2* produced a PCR product with a length of 708 bp. *pCR4_dzyAΔPRM2* clone 1 was sent for sequencing and was confirmed to be the construct *pCR4_dzyAΔPRM2*.

Part3

The final step during this cloning process was to ligate the full-length *dzyAΔPRM2* fragment (*dzyAΔPRM2L* and *dzyAΔPRM2R*) into the *pUAST* transformation vector to generate the final construct *dzyAΔPRM2 in pUAST* (14367 bp). The complete insert *ΔPRM2* was cut from the TOPO vector (*pCR4*) and transferred into the *pUAST* transformation vector. To clone the *dzyAΔPRM2* fragment into the *pUAST* vector, the two constructs *pCR4_dzyAΔPRM2* (5943 bp) and the *pUAST* vector were digested with the two restriction enzymes SpeI and NotI (Fig. 34C). Digestion of the two constructs yielded the following fragments: *pCR4_dzyAΔPRM2_SpeI/NotI* 2065 bp and 3910 bp and *dzyC in pUAST_SpeI/NotI* 1400 bp and 12286 bp.The digested components were separated by agarose gel electrophoresis. The desired DNA bands (2065 bp (insert) and 12286 bp (vector)) were excised from the gel and purified using the Nucleospin® Gel and PCR Clean-up Kit (Macherey Nagel). The isolated insert *dzyAΔPRM2_Spe/Not* (2065 bp) was then ligated into the vector source *dzyC in pUAST_ Spe/NotI* (12286 bp). The *dzyC in pUAST* vector, cutted with SpeI and NotI, was either gel purified or alternatively treated with SAP (rAPid Alkaline Phosphatase) (see Material & Methods) to prevent relegation of the vector in the ligation reaction. The gel purified *dzyAΔPRM2_Spe/Not* fragment was then ligated into the gel-purified or SAP-treated expression vector *dzyC in pUAST_SpeI/NotI*. A vector concentration of 50 ng and an insert:vector ratio of 5:1 was used for the 3-h ligation process. The ligation products of the two approaches (1) gel-purified and (2) SAP-treated *dzyC in pUAST_SpeI/NotI* were transformed into chemically competent *E.coli DH5α* cells and grown on agar plates with Ampicillin (Amp). To detect colonies carrying the *dzyAΔPRM2 in pUAST* construct (14367 bp), plasmid DNA was analysed by Colony-PCR using the primer pair PR181/PR188 (Fig. 35). Bands of about 708 bp (*dzyAΔPRM2 in pUAST*) were expected. For an undigested *dzyC in pUAST* construct, a 150 bp band appeared on the gel. To obtain the desired bands and thus the correct construct, several repetitions of the cloning process, the preparation of the components and the ligation

step, were necessary. Plasmid DNA of the Colony-PCR-positive colonies (Fig. 35) was mini-prepped from overnight bacterial cell cultures using TELT Prep. The purified *dzy* constructs *dzyAΔPRM2 in pUAST* clone 3 and clone 10 were sequenced by LGC Genomics. The sequenced data showed the *dzyAΔPRM2 in pUAST* construct.
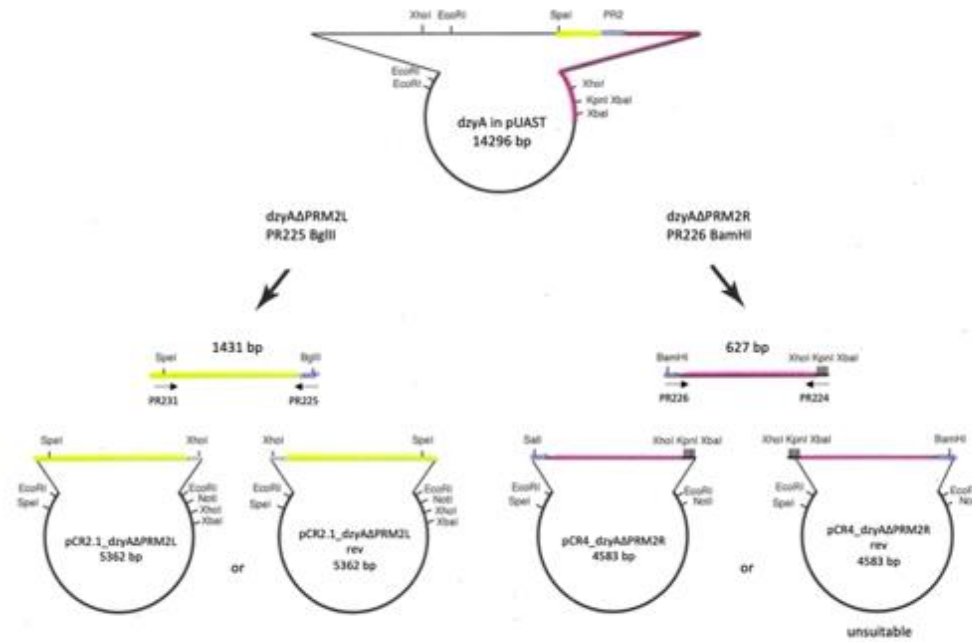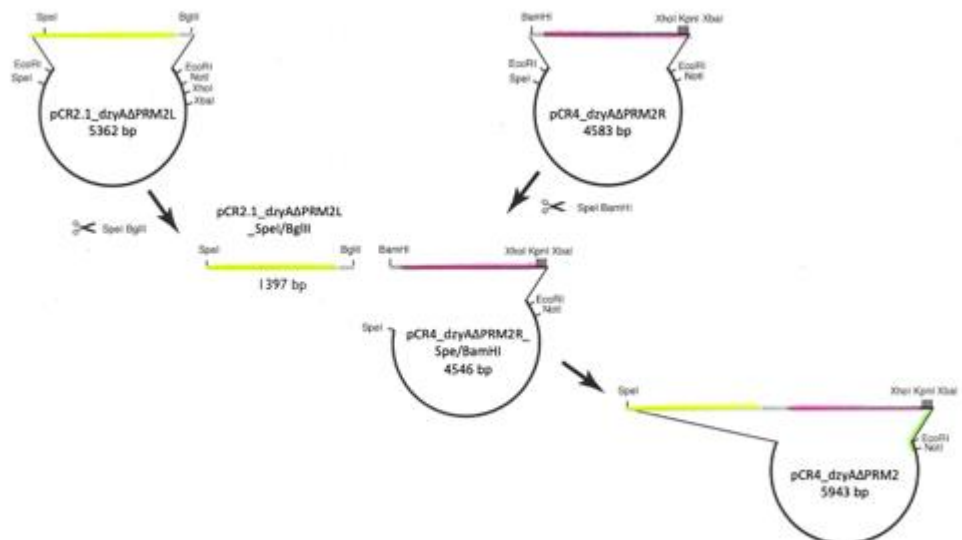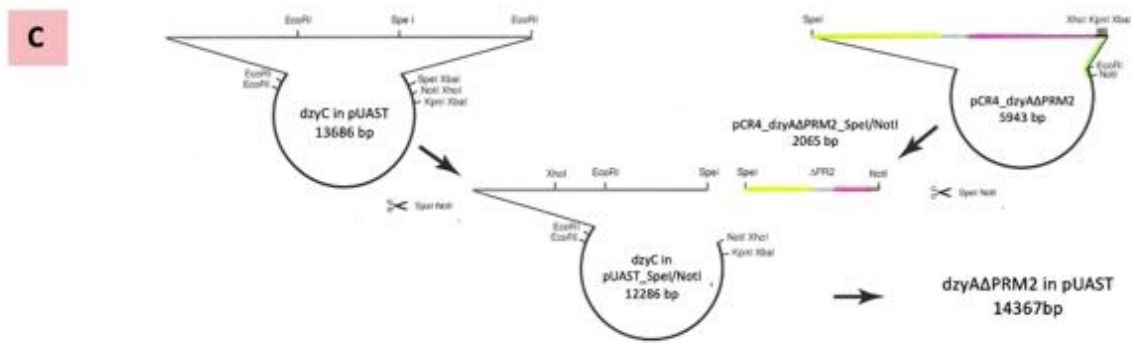
Fig. 34 Cloning strategy for the *dzyAΔPRM2 in pUAST* construct.
The *dzyAΔPRM2 in pUAST* construct (14367 bp), carrying an inoperative PRM2 domain, was generated by several intermediate steps. (A) Part 1: Generation of the two fragments *dzyAΔPRM2L* and *dzyAΔPRM2R* by PCR with specific primers inserting restriction sites. One restriction site (BglII, PR225) was inserted in the 5' region of the PRM2 domain and another restriction site (BamHI, PR226) was inserted in the 3' region of the PRM2 domain. The PCR product *dzyAΔPRM2L* was generated with the primer pair PR231/PR225 (1431 bp) and contained the BglII restriction site. The PCR product *dzyAΔPRM2R* (627 bp) was amplified with the primer pair PR226/PR224 and contained the BamHI restriction site. The construct *dzyA in pUAST* (14296 bp) served as a template for the modified primers. The inserts *dzyAΔPRM2L* and *dzyAΔPRM2R* were ligated into the TOPO TA vector. The constructs *pCR2.1_dzyAΔPRM2L* (5362 bp) and *pCR4_dzyAΔPRM2R* (627 bp) were generated. (B) Part 2: To combine the two *dzyAΔPRM2* fragments, *dzyAΔPRM2L* and *dzyAΔPRM2R*, and obtain the full-length *dzyAΔPRM2* sequence, the *pCR2.1_dzyAΔPRM2L* construct was digested with the restriction enzymes SpeI and BglII and the resulting fragment *dzyAΔPRM2L_SpeI/BglII* (1397 bp) was ligated into *pCR4_dzyAΔPRM2R* (4583 bp). The construct *pCR4-dzyAΔPRM2R* containing the *dzyAΔPRM2R* fragment, was treated with the restriction enzymes SpeI und BamHI. The isolated insert *dzyAΔPRM2L_SpeI/BglII* (1397 bp) was then ligated into the vector source *pCR4-dzyAΔPRM2R_SpeI/BglII* (4546 bp). The result was the construct *pCR4_dzyAΔPRM2* (5943 bp). (C) Part 3: In the final part of the cloning strategy, the full-length *dzyAΔPRM2* DNA fragment (2065 bp) was cut from the construct *pCR4_dzyAΔPRM2* (5943 bp) and inserted into the transformation vector *pUAST*. Both the construct *pCR4_dzyAΔPRM2* and the *pUAST* vector were digested with the restriction enzymes SpeI and NotI. The isolated insert *dzyAΔPRM2_SpeI/NotI* was then ligated into the vector *dzyC in pUAST_SpeI/NotI* (12286 bp). The construct *dzyAΔPRM2 in pUAST* (14367 bp) was generated.
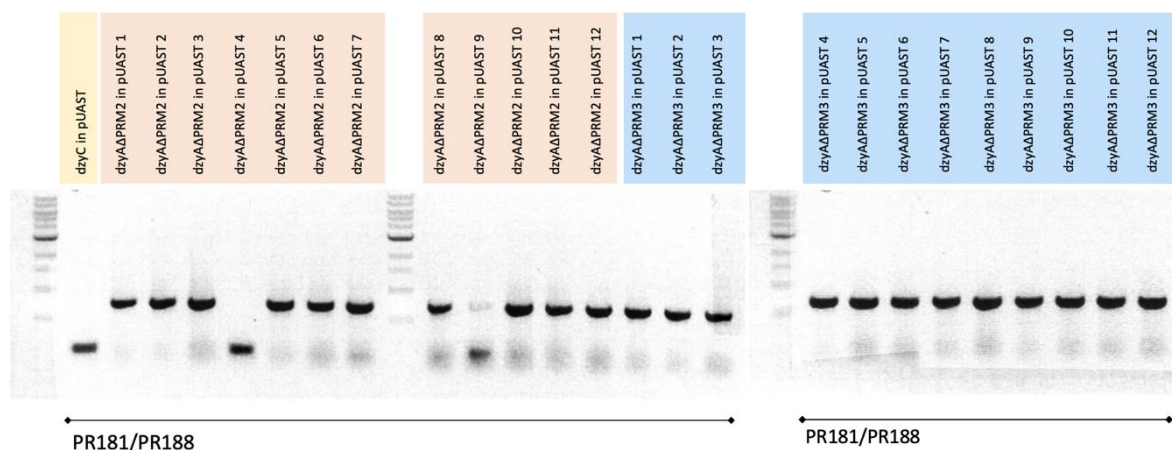

Fig. 35 Agarose gel electrophoresis of the deletion constructs *dzyAΔPRM2 in pUAST* and *dzyAΔPRM3 in pUAST*.
Colony-PCR of the ΔPRM2 and ΔPRM3 colonies was performed with the primer pair PR181 (insert exon 4) and PR188 (insert exon 6). A 0.8 % agarose gel was used to determine the expected plasmid size: *dzyAΔPRM2 in pUAST* and *dzyAΔPRM3 in pUAST* both around 700 bp. *dzyC in pUAST* (expected

plasmid size 150 bp) served as a control for the PCR reaction. *dzyAΔPRM2 in pUAST* clone 1, 2, 3, 5, 6, 7, 8, 10, 11 and 12 appeared at the correct size on the gel. *dzyAΔPRM2 in pUAST* clone 3 and 10 were sent for sequencing. For the construct *dzyAΔPRM3 in pUAST*, all clones (clones 1 - 12) appeared in the correct size on the gel. *dzyAΔPRM3 in pUAST* clone 4 and 8 were sent for sequencing to confirm that the cloned plasmids had the correct insertion sequence and direction.

The deletion of the Dzy PRM3: *dzyAΔPRM3 in pUAST*

Part1

The structure of the cloning strategy of the *dzyAΔPRM3 in pUAST* construct is generally similar to the cloning strategy of ΔPRM2 and is therefore only briefly explained. The regions before and after PRM3 were assembled without the domain itself. Two primer pairs were designed to generate the two fragments, *dzyAΔPRM3R* and *dzyAΔPRM3L*: PR231/PR227 amplified the fragment upstream of the PRM3 domain (*dzyAΔPRM3L*, 1569 bp), and PR228/PR224 amplified the fragment downstream of the PRM3 domain (*dzyAΔPRM3R*, 483 bp).

The two primers PR227 and PR228, within PRM3, introduced the restriction sites XhoI and SalI, respectively. In addition to the restriction sites, the two primers were designed so that PR227, which was located in the 5' direction of the PRM3 domain, inserted a shift in the open reading frame that was reversed by PR228, which was in the 3' region of the PRM3 domain. This ensured that the original prolines in the amino acid sequence were completely deleted.

The construct *dzyA in pUAST* (14296 bp) served as a template for the designed primers. The PCR products *dzyAΔPRM3L* (1569 bp) and *dzyAΔPRM3R* (483 bp) were amplified by PCR, purified via agarose gel electrophoresis, isolated and ligated into a TOPO TA cloning vector, leading to the constructs *pCR2.1_dzyAΔPRM3L* (5500 bp) and *pCR2.1_dzyAΔPRM3R* (4445 bp) (Fig. 36A). The clones obtained from TOPO cloning were characterised by Touchdown-PCR (see Material & Methods) with the primer pair PR51/M13rev. The construct *pCR2.1_dzyAΔPRM3L* resulted in an amplification product of 1771 bp and *pCR4_dzyAΔPRM3R* gave an amplification product of 684 bp. While *pCR4_dzyAΔPRM3R* was relatively easy to clone, the construct *pCR2.1_dzyAΔPRM3L* required several attempts to obtain the desired bands and thus the correct construct. *pCR2.1_dzyAΔPRM3L* clone 3 and *pCR2.1_dzyAΔPRM3R* clone 3 were sent to LGC Genomics for sequencing. The sequencing data confirmed that the constructs were *pCR2.1_dzyAΔPRM3L* (5500 bp) and *pCR2.1_dzyAΔPRM3R* (4445 bp).

Part2

In the following step, the two fragments *dzyAΔPRM3L* and *dzyAΔPRM3R* were combined to obtain the full-length *dzyAΔPRM3* sequence. To do this, the construct *pCR2.1_dzyAΔPRM3L* (5500 bp), which contains the 5' upstream part of ΔPRM3, was digested with the enzymes SpeI and XhoI to receive the fragment *pCR2.1_dzyAΔPRM3L_SpeI/BglII* (1535 bp). To clone

the insert *dzyAΔPRM3L_SpeI/BglII* (1535 bp) into the construct *pCR2.1_dzyAΔPRM3R* (4407 bp), which contains the 3' downstream part (*dzyAΔPRM3R*) of *dzyAΔPRM3*, the TOPO TA vector source *pCR2.1_dzyAΔPRM3R* was treated with the restriction enzymes SpeI and SalI to generate compatible ends (Fig. 36B). The digested components *dzyAΔPRM3L_SpeI/XhoI* (1535 bp) and *pCR2.1_ dzyAΔPRM3R_SpeI/SalI* (4407 bp) were separated by agarose gel electrophoresis, purified using Nucleospin® Gel and PCR Clean-up Kit and subsequently ligated to yield the construct *pCR2.1_dzyAΔPRM3* (5942 bp). To identify the *pCR2.1_dzyAΔPRM3* construct, colonies were harvested and analysed via PCR using the primer combination PR181 and PR188. *pCR2.1_dzyAΔPRM3* generated a 708 bp long PCR product. *pCR2.1_dzyAΔPRM3* clone 1 was sent for sequencing, and confirmed as the construct *pCR4_dzyAΔPRM3*.

<u>Part3</u>

In the final part of the cloning process, the full-length *dzyAΔPRM3* fragment was cut from the TOPO TA vector (*pCR2.1*) and transferred into the *pUAST* transformation vector to obtain the final construct *dzyAΔPRM3 in pUAST* (14367 bp) (Fig. 36C). For ligation of the *dzyAΔPRM3* fragment with the *pUAST* vector, the construct *pCR2.1_dzyAΔPRM3* (5942 bp) was digested with the restriction enzymes SpeI and NotI. The digested component was separated by agarose gel electrophoresis (2081 bp and 3861 bp) and the lower band was cut from the gel. The isolated insert *pCR2.1_dzyAΔPRM3_Spe/Not* (2081 bp) was subsequently ligated into the vector *dzyC in pUAST_SpeI/NotI* (12286 bp). To detect the *dzyAΔPRM3 in pUAST* construct (14367 bp), the plasmid DNA was analysed by Colony-PCR using the primer pair PR181/PR188 (Fig. 35). Bands of about 708 bp (*dzyAΔPRM3 in pUAST*) were expected. *dzyAΔPRM3 in pUAST* clone 4 and clone 8 were sequenced by LGC Genomics. The sequenced data showed the *dzyAΔPRM3 in pUAST* construct.
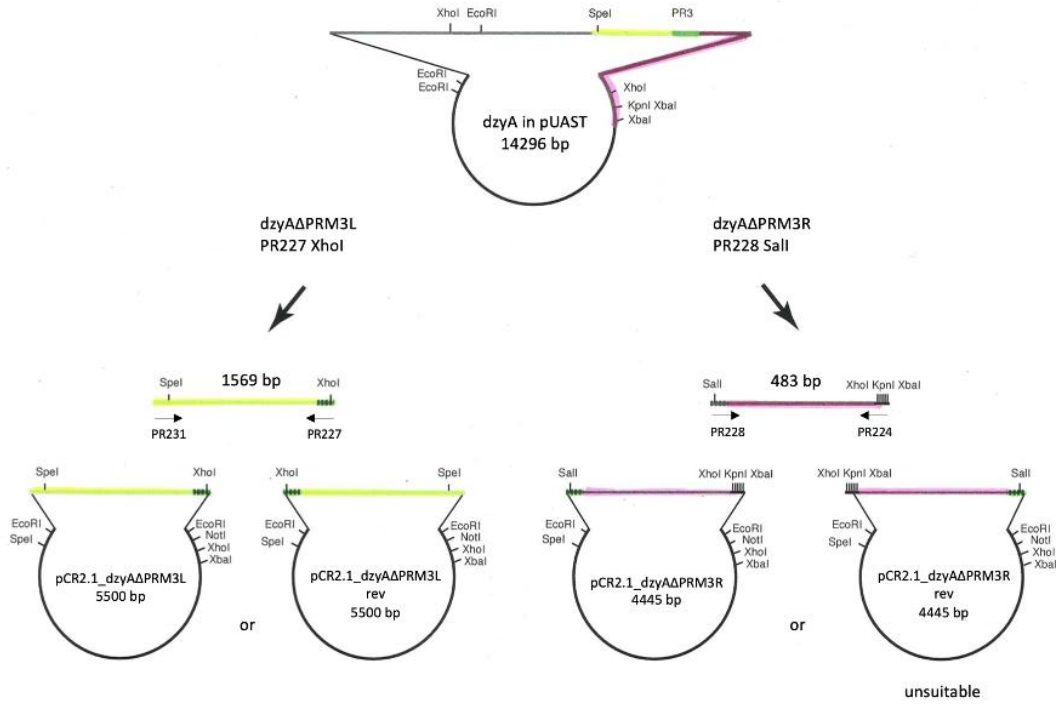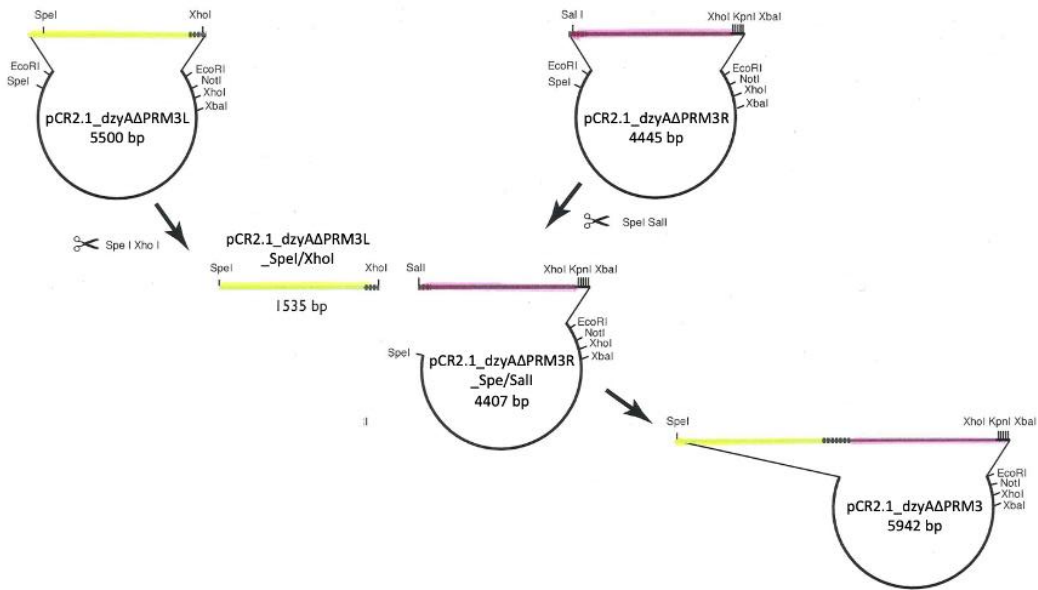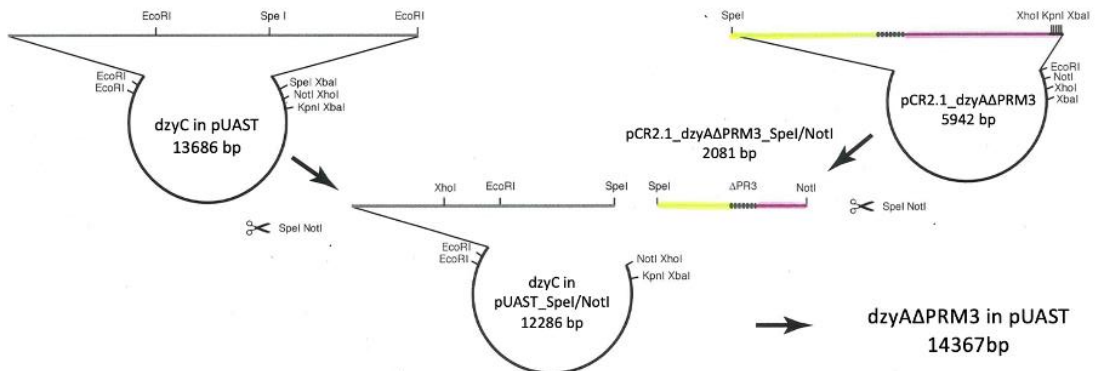
Fig. 36 Cloning of the *dzyAΔPRM3 in pUAST* construct by PCR and restriction enzyme digestion. The cloning strategy for the *dzyAΔPRM3 in pUAST* construct (14367 bp) carrying a non-functional PRM3 domain was divided into three distinct parts. (A) Part 1: Amplification of the upstream and downstream *dzyAΔPRM3* fragments by PCR with specific primer pairs: PR231/PR227 and PR228/PR224 were used to produce the PCR products *dzyAΔPRM3L* (1569 bp) and *dzyAΔPRM3R* (483 bp), respectively. Primer PR227 inserted a XhoI restriction site into the 5' region of the PRM3 domain and PR228 inserted a SalI restriction site into the 3' region of the PRM3 domain. The two fragments *dzyAΔPRM3L* and *dzyAΔPRM3R* were cloned into the *pCR2.1* TOPO TA vector to generate the constructs *pCR2.1_dzyAΔPRM3L* (5500 bp) and *pCR2.1_dzyAΔPRM3L* (4445 bp). (B) Part 2: To combine the two *dzyAΔPRM3* fragments (*dzyAΔPRM3L* and *dzyAΔPRM3R*) and obtain the full-length *dzyAΔPRM3* sequence, the *pCR2.1_dzyAΔPRM3L* construct was digested with the restriction enzymes SpeI and XhoI, and the resulting fragment *pCR2.1_dzyAΔPRM3L_SpeI/XhoI* (1535 bp) was ligated into the vector source *pCR2.1_dzyAΔPRM3R_SpeI/SalI* (4407 bp). The result was the construct *pCR2.1_dzyAΔPRM3* (5942 bp). (C) Part 3: In the final part of the cloning strategy, the full-length *dzyAΔPRM3* DNA fragment was transformed from the construct *pCR2.1_dzyAΔPRM3* (5942 bp) into the transformation vector pUAST. The constructs *pCR2.1_dzyAΔPRM3* and *dzyC in pUAST* were digested with the restriction enzymes SpeI and NotI. The isolated insert *pCR2.1_dzyAΔPRM3_SpeI/NotI* (2081 bp) was then ligated into the vector backbone *dzyC in pUAST_SpeI/NotI* (12286 bp). The final construct *dzyAΔPRM3 in pUAST* (14367 bp) was generated.

Generation of transgenes

Injection of the cloned DNA constructs and the resulting transgenic flies yielded information on the existence of differences in the cell shape and the role of the PDZ domain, the PRMs and their interaction during macrophage migration. Transgenic animals for the UAS *dzy*-domain deletion constructs were generated by injection of cloned DNA into *w⁻ Drosophila* embryos. The injection was performed either by the injection company Fly Facility or in our laboratory.

UAS-*dzyCΔPDZ* transgenic flies

Specific expression of the *dzy* locus in the macrophages in the the *dzyC* line resulted in a characteristic phenotype in which macrophage protrusions were elongated and connected to form a network of cells (see Results Section 3.3). We wondered whether the *dzyC* form with a deleted PDZ domain could produce the cell shape change phenotype observed in the *dzyC* line. Therefore, we generated transgenic animals for the *UAS-dzyCΔPDZ* deletion construct. The purified plasmid *dzyCΔPDZ in pUAST* was subsequently used to generate *UAS-dzyCΔPDZ* transgenic flies by P-element-mediated germline transformation. The *dzyCΔPDZ in pUAST clone 1* construct was not injected by our department. Instead, the injection was contracted externally from the *Drosophila* Embryo Injection Service Fly Facility (France). For *UAS-dzyCΔPDZ*, nine lines were tested positive for the *white⁺* phenotype (*UAS-dzyCΔPDZ line 1-9*, see Appendix Tab. S2). The transgenic *UAS-dzyCΔPDZ* flies were sent to us at the larval stage. In the hatched flies, transposable element mapping was performed for each of the nine P-element lines to determine the position of the insertion site. It was found that the transgene in *UAS-dzyCΔPDZ* line 1, 3 and 9 was located on the second chromosome, while in *UAS-dzyCΔPDZ* line 2, 4, 6, 7 and 8 the transgene was located on the third chromosome.

In *UAS-dzyCΔPDZ* line 5, the transgene was mapped on the X chromosome. A table of the transgenic *UAS-dzyCΔPDZ* lines can be found in the Appendix (see Tab. S2).

<u>*UAS-dzyAΔPRM2* and *UAS-dzyAΔPRM3* transgenic flies</u>

The *dzyC* isoform is the only one that is sufficient to effect cell shape changes. The difference between *dzyC* and both *dzyA* and *dzyB* is the absence of the two PRMs in exon 5/5S. To investigate if the changes in cell shape and cell migration are caused by the different numbers of PRMs and study the role of the proline-rich motifs in macrophage migration, we attempted to generate transgenic flies for the *UAS-dzyAΔPRM2 and UAS-dzyAΔPRM3* deletion constructs.

To generate transgenic *UAS-dzyAΔPRM2 and UAS-dzyAΔPRM3* flies, the purified plasmids *dzyAΔPRM2 in pUAST* clone 3 *and dzyAΔPRM3 in pUAST* clone 4 were used together with a helper plasmid Δ2-3 for microinjection into 30-min-old dechorionated *w⁻ Drosophila* embryos following standard procedure for P-element-mediated germline transformation (see Material and Methods). Despite several injection approaches, no transgenic ΔPRM flies could be generated. A total of 763 embryos were injected with the construct *dzyAΔPRM2 in pUAST*, 137 larvae were collected and 76 hatched adults were crossed with *w⁻* flies. To clearly determine whether the transgene was successfully integrated, we screened for an easily observable red-eyed phenotype. Also with the construct ΔPRM3, despite several approaches and the injection of 522 embryos, 90 collected larvae and 53 adults, no red-eyed flies could be observed. For *UAS-dzyAΔPRM2* and *UAS-dzyAΔPRM3*, no flies tested positive for the *white+* phenotype and thus no *UAS-dzyAΔPRM* lines could be generated. While the injection of the *UAS-dzyCΔPDZ* construct into the flies was successfully performed by the Fly Facility, the two constructs *UAS-dzyAΔPRM2* and *UAS-dzyAΔPRM3* could not be successfully introduced into the flies. Despite multiple injection attempts, no red-eyed flies could be identified. The following experiments were therefore only carried out with the *UAS-dzyCΔPDZ* strains.

Before the transgenic *UAS-dzyCΔPDZ* lines were used for further experiments, the lines were verified by DNA isolation from single flies using the "quick n dirty" protocol (see Material & Methods) and subsequent PCR analysis. DNA from individual flies, e.g. from the strain *UAS-dzyCΔPDZ* line 7, was isolated and analysed by PCR using the primer combination PR101 (vector *pUAST*) and PR159 (*dzy* exon 2). In the presence of the *UAS-dzyCΔPDZ* construct, a 432 bp band appeared on the gel (see Results section 3.3). The lane with the *dzyCΔPDZ* DNA showed the expected length of 432 bp. Therefore, the *UAS-dzyCΔPDZ* line 7 was used for further experiments.

The PDZ domain is sufficient for the shape change phenotype

Similar to *dzy*[EP], macrophages-specific overexpression from the *dzyC* construct resulted in a marked enlargement of cellular protrusions. In various regions of the embryo, the long cellular protrusions touch each other and form a network (see Results section 3.3). We therefore wondered whether the PDZ domain conserved in the different Dzy splice forms is important for regulating changes in cell shape. To test whether such a specific function of the PDZ domain exists, we expressed the *dzyCΔPDZ* form under the control of the macrophage-specific *srph-Gal4* driver. Thus, in this part of this work, we expressed a *UAS-dzyC* construct with a deleted PDZ domain in macrophages and analyzed the shape of these cells.

By crossing the *UAS-dzyCΔPDZ* line with flies carrying the macrophage-specific *srph-Gal4* driver coupled with *UAS-cd2* (Fig. 37), we were able to study the changes in cell shape in the *Drosophila* embryo using CD2-specific antibody staining. We analysed the shape and position of the macrophages under the bright-field microscope (antibody detection: chromogenic reaction) and the confocal microscope (antibody detection: fluorescent reaction) and compared them with the *dzyC* splice form. *dzyC* and *dzyCΔPDZ* differ exclusively in the presence of a functional PDZ domain.
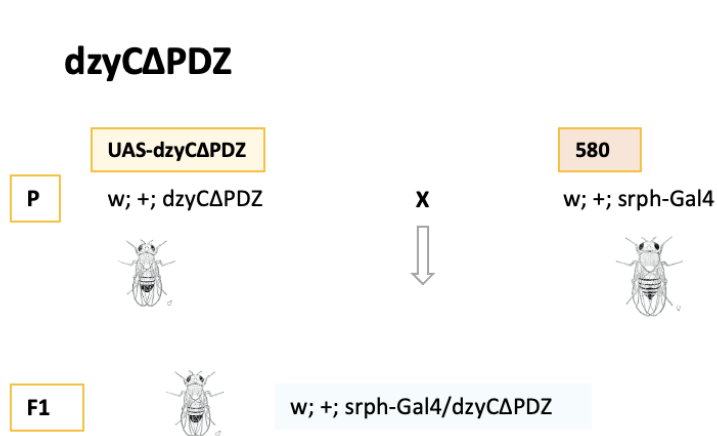

Fig. 37 Crossing scheme for the combination of the *UAS-dzyCΔPDZ* line and the *srph-Gal4* line.
The crossing scheme shown was used to obtain transgenic flies expressing the *dzyCΔPDZ* form under the control of the *srph-Gal4* driver in macrophages. Virgins of the *srph-Gal4* line were mated with males of the *UAS-dzyCΔPDZ* line. Embryos of the F1 generation (*srph-Gal4/UAS-dzyCΔPDZ*) were collected, fixed, stained, and examined for the cell shape phenotypes.

Bright-field imaging and ABC-based detection of macrophages

As described in Results section 3.3, the chromogenic detection method for the CD2 antibody was performed using an Avidin Biotin Complex (ABC) (VECTASTAIN Elite ABC Kit). The ABC method (see Materials & Methods) is a three-step detection method: the CD2 primary antibody binds to the antigen in the tissue, which in turn is recognised by the biotinylated secondary antibody; complexes of Avidin and biotinylated enzyme (ABC) can then attach to the latter. By labelling the detection enzyme HRP with biotin and the secondary antibody with Biotin, these

two compounds can be irreversibly linked to Avidin. The stained embryos were embedded (methyl salicylate or araldite-acetone) and then examined under the light microscope. While the expression of *dzyC* led to a pronounced elongation of the cell extensions (Fig. 38B), this influence on the shape of the macrophages could not be observed with the *dzyCΔPDZ* form. The macrophage-specific expression of the *dzyCΔPDZ* form led to short processes and rather round-looking macrophages (Fig. 38A). DzyCΔPDZ thus resembles the wild-type form more than the DzyC form.

Thus, overexpression of the *UAS-dzyCΔPDZ* construct was not able to induce the formation of the long cellular protrusions or the characteristic cell network (cf. *UAS-dzyC* construct). The two constructs *UAS-dzyC* and *UAS-dzyCΔPDZ* differ only in the presence of the PDZ domain. For this reason, *UAS-dzyC* was used for comparison and to identify the function of the PDZ domain. The *dzyC* form, but not the *dzyCΔPDZ* form, was sufficient to cause a dramatic change in cell shape, demonstrating a functional role for the PDZ domain. It is likely that the PDZ domain has an influence on this process. Thus, the PDZ domain of the Dzy splice form C is necessary to induce a change in cell shape. How the influence of the PDZ domain in this process looks still needs to be investigated in more detail. Is there possibly an interaction of the PDZ domain with the PRMs? Is the difference in the protrusion lengths due to the interaction of the two regions? The investigation of ΔPRM2 and ΔPRM3 could provide the answer to this question.
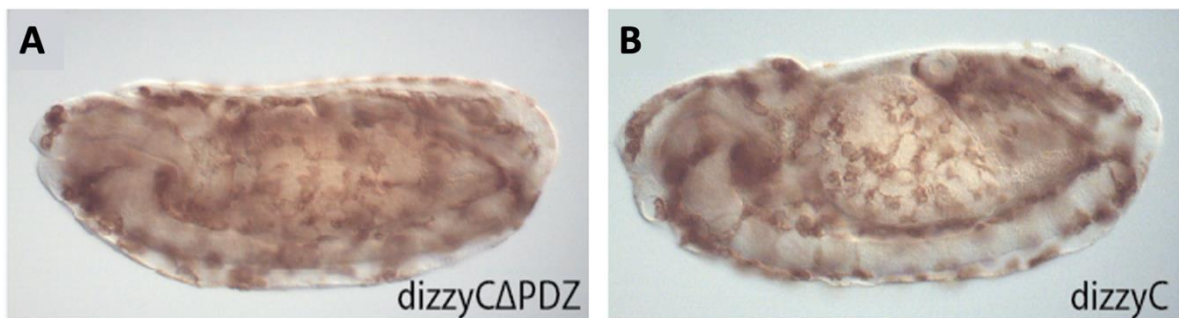

Fig. 38 Overexpression of the *dzyCΔPDZ* splice form in macrophages.
The construct *dizzyCΔPDZ (dzyCΔPDZ in pUAST)* was introduced into the *Drosophila* genome by injection. Overexpression of the *UAS-dzyCΔPDZ* construct in macrophages was driven by the macrophage-specific *srph-Gal4* driver coupled with *UAS-cd2*. Cell shape changes and the position of the macrophages in the *Drosophila* embryo were visualized using CD2-specific antibody staining. Bright-field microscope images show an overlay of a sagittal optical section and the lateral view. Expression of *dizzyC* (*dzyC*) with an intact PDZ domain led to a change in cell shape (see Results section 3.3). The cells form distinctly longer protrusions and a network in which they connect to each other (B). In contrast, macrophages did not appear to be significantly affected by the overexpression of the *dzyCΔPDZ* form (A). Only the *dzyC* isoform can induce cell shape changes in macrophages, demonstrating the important role of the PDZ domain in this specific phenotype.

<u>Fluorescence-based detection of the CD2 antibody in macrophages</u>

To obtain further visualisation of the migrating cells and their protrusions, fluorescence images were acquired in addition to bright-field images, as previously described in Results section 3.3. To express the *UAS-dzyCΔPDZ* construct in macrophages, the generated transgenic animals (*UAS-dzyCΔPDZ* line 7) were crossed with a fly strain carrying the macrophage-specific driver (*srph-Gal4*) and the *UAS-cd2* construct. Thus, both *dzy* and *cd2* were expressed in the macrophages of the *Drosophila* embryo.

In this approach the shape of the macrophages were characterised using CD2-specific antibody staining under a confocal microscope. Antibody staining was performed with the primary mouse anti-CD2 antibody (1:4000). Embryos were incubated with the CD2 antibody and then treated with the corresponding secondary antibodies conjugated to the fluorescent dye Cy3 (goat anti mouse GAM Cy3, 1:250). Images were taken with a confocal laser scanning microscope. The resulting confocal microscope images confirmed the results already seen in the bright-field images. Macrophage-specific expression of the *dzyCΔPDZ* form (Fig. 39A) had no effect on the cell shape of the macrophages. The macrophages appeared roundish and with short protrusions. Compared to *dzyCΔPDZ*, overexpression of the *UAS-dzyC* construct (Fig. 39B) showed the formation of long cellular protrusions, resulting in the formation of the characteristic cell network phenotype. The data showed that *dzy* splice form C with a functional PDZ domain (*UAS-dzyC*) is sufficient to cause a change in cell shape when specifically expressed in macrophages, whereas *dzy* splice form C with an inactive PDZ (*UAS-dzyCΔPDZ*) is unable to affect macrophage morphology under the same conditions.

In summary, overexpression of the *dzyC* construct is sufficient to cause a dramatic change in cell shape and induce the formation of long protrusions leading to the formation of the same characteristic cell network. In contrast, macrophage expression of the *dzyCΔPDZ* construct showed no effect on macrophage shape. The macrophages appeared roundish and with short protrusions as in the wild-type controls. Since the two constructs *UAS-dzyC* and *UAS-dzyCΔPDZ* differ only in the presence of the PDZ domain, we were thus able to show that the PDZ domain plays an important role in this process.
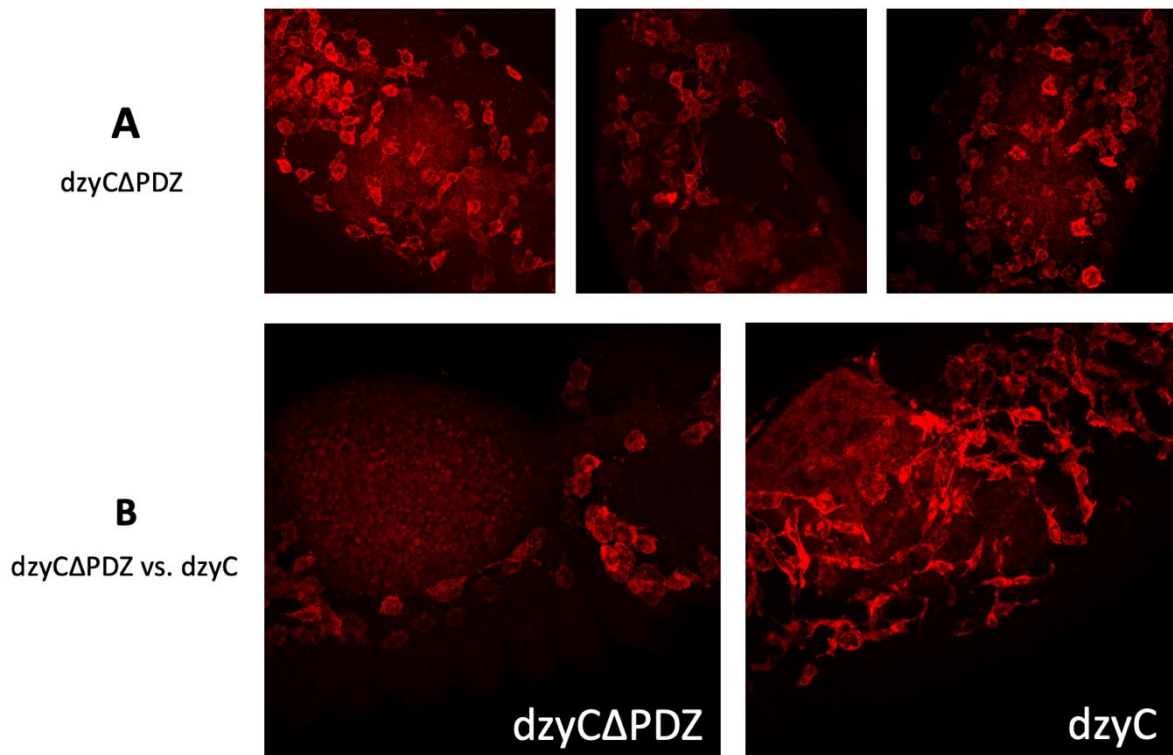
Fig. 39 The *dzyC* isoform, but not the *dzyCΔPDZ* isoform, can induce cell shape changes in macrophages.
Confocal images show macrophages in various areas of the *Drosophila* embryos. Macrophages were detected by the expression of CD2. (A) In the *UAS-dzyCΔPDZ* embryos, the cell bodies of the macrophages are rounded, form small protrusions and rarely touch each other. (B) In contrast, expression of the *dzyC* isoform leads to a change in cell shape, elongation of the protrusions and formation of the characteristic networks.

3.5 The different Dzy isoforms play distinct roles in adult morphogenesis

Lethality of ubiquitous *dzy* overexpression (viability assay)

In *Drosophila melanogaster*, viability assays are used to determine the fitness of a specific genetic background. Allelic variations can lead to partial or complete loss of viability at different developmental stages (Rockwell *et al.* 2019). To investigate whether ubiquitous expression of the Dzy protein leads to animal death, the different *UAS-dzy* constructs (*UAS-dzyA*, *UAS-dzyC* and *UAS-dzyCΔPDZ*) were crossed with the *tub-Gal4* driver (Fly strain collection stock 746). The *tub-Gal4* line allowed expression of the *UAS-dzy* target gene in all tissues of the fly; however, this often leads to lethality as the target gene is expressed in tissues or cells where it is otherwise absent or present only at low levels. To assess the viability of the different *UAS-dzy* strains (*UAS-dzyA (UAS-dzyA line 1)*, *UAS-dzyC* (Fly strain collection stock 1307) and *UAS-dzyCΔPDZ (UAS-dzyCΔPDZ line 1*)), the total number of adult *Drosophila* was counted until 9 days after the first adults were observed (Fig. 40A). To control the functionality of this

approach, the *UAS-srp* line (Fly strain collection stock 260) was used and also crossed with the *tub-Gal4* strain (Fig. 40B). As already established in previous studies, ubiquitous overexpression of *UAS-srp* leads to lethality.
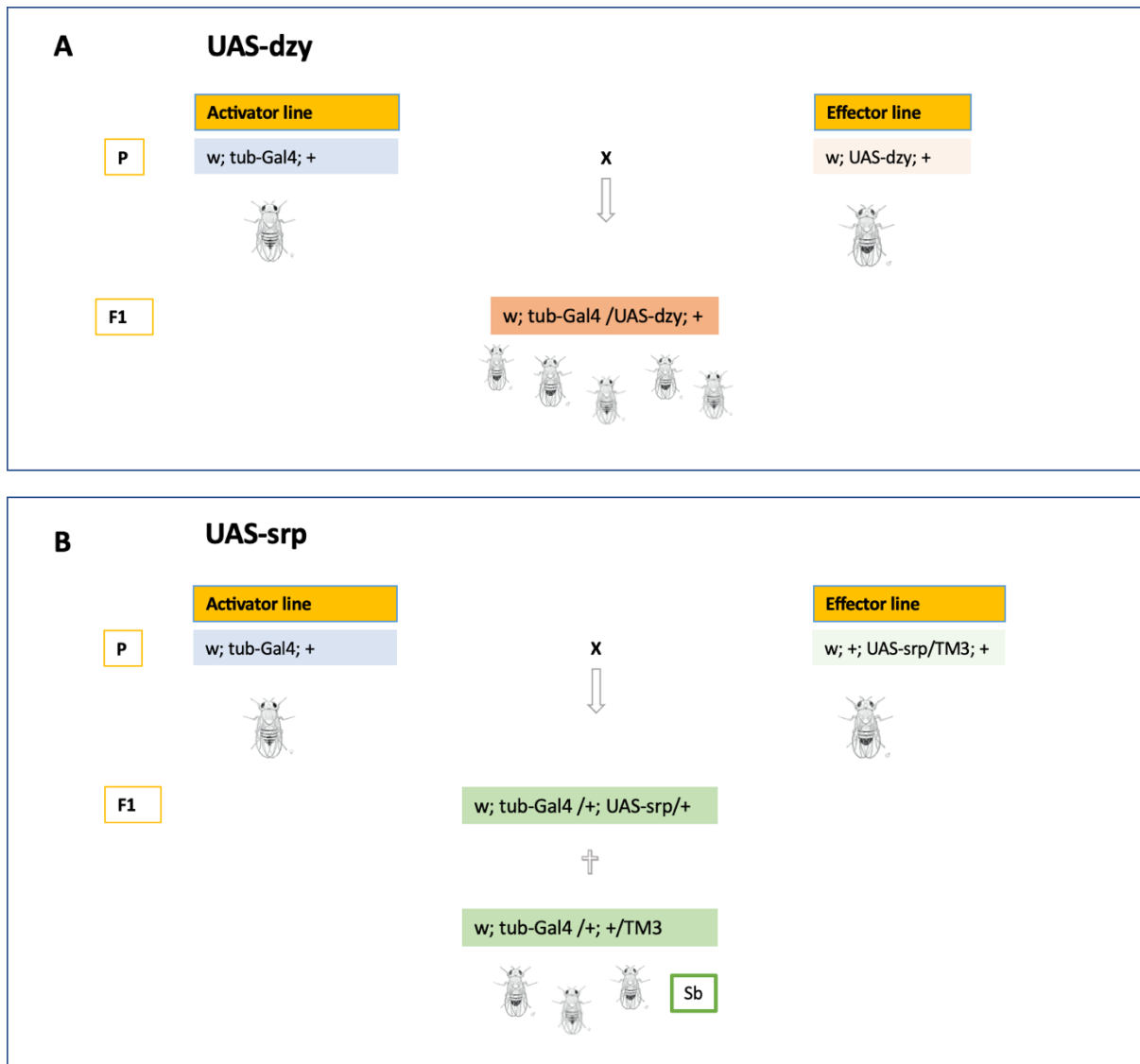

Fig. 40 Crossing schemes for the viability assay.
(A) Crossing scheme for the ubiquitous expression of *UAS-dzy*: the *UAS-dzy* parental strain (P) was homozygous for *UAS-dzy* and thus does not carry a balancer chromosome. In contrast to *UAS-srp* (B), all progeny should therefore possess both the *UAS-dzy* construct and the *tub-Gal4* driver. (B) Crossing scheme for the ubiquitous expression of *UAS-srp*: The *UAS-srp* parental strain carries the balancer chromosome TM3. The Sb marker contained on TM3 leads to shortened bristles on the fly's dorsum compared to wt, so that the progeny possessing both the *UAS-srp* construct and the driver *tub-Gal4* can be recognised by their wild-type phenotype for this marker (long bristles).

In contrast to the *UAS-dzy* strains (*w; UAS-dzy; +), UAS-srp* flies (*w; +; UAS-srp/TM3*) were heterozygous for the *third*-chromosome balancer. The progeny carrying the balancer chromosome were easily sorted out: *tub-Gal4/TM3 flies* were identified by the presence of the TM3 balancer chromosome and the shortened bristles on the fly's dorsum. *tub-Gal4/UAS-srp* flies possessing both the *UAS-srp* construct and the driver *tub-Gal4* can be recognised by their

wild-type phenotype for this marker (long bristles). As expected, we were not able to find *tub-Gal4/UAS-srp* flies in the progeny. Only animals carrying the dominant stubble (Sb) marker could be found in this cross (Fig. 40B). Compared to the lethal overexpression of *srp*, we detected many progeny when crossing *UAS-dzy* animals with flies carrying the *srph-Gal4* driver (*tub-Gal4/UAS-srp)* (Fig. 40A). Thus, ubiquitous expression of the different *dzy* splice forms does not appear to be lethal. To rule out male sterility as well, single *tub-Gal4/UAS-dzy* males were crossed with *w⁻* virgin flies. Many embryos, larvae, pupae and subsequently adult flies could be observed. The ubiquitous expression of the different *dzy* splice forms is thus neither lethal nor does it lead to sterility of the offspring. The necessary expression for the following adult rescue experiments was thus ensured under the control of the *dzy* promoter and the *heat shock* (*hs)-Gal4* driver. The latter seems feasible, as the ubiquitous expression of the different *dzy* forms does not appear to be lethal and no spatial restriction of *dzy* expression has been observed so far.

The *dzyC* splice form have a function in the adult morphogenesis

In this work, we have provided the first detailed description of *dzy* splicing and we have shown that one of the three splice forms, the *dzyC* form, plays an important role in the migration of embryonic macrophages. The other two forms, *dzyA* and *dzyB*, were not sufficient in the macrophages to induce a change in cell shape and cell migration. Since *dzyC* was the only isoform able to induce a cellular phenotype in the *Drosophila* embryo, the question arose whether the other two forms, *dzyA* and *dzyB*, might play a role at later stages of development. Indeed, *dzy* is known to play a role in adult morphogenesis. Wang and colleagues demonstrated in previous studies that homozygosity of *dzy* is lethal, but that there is a small fraction of adult "escaper" flies. These *dzy* homozygous escapers display a characteristic phenotype with bent downward wings, a rough eye phenotype, male sterility and distorted genitalia (Lee *et al.* 2002; Wang *et al.* 2006). To answer the question whether the two isoforms *dzyA* and *dzyB* play a role during the adult fly morphogenesis, a rescue experiment with adult flies was conducted. In this experiment, we asked ourselves the question: Is the expression of a single splice form in a mutant background sufficient to rescue the adult mutant phenotype? Or is a single splice form sufficient to rescue all or at least one part of the adult mutant phenotype?

dzy mutant background (*dzyΔ8/ Df ED380*)

To test the functional relevance of the single splice forms in adult morphogenesis, we carried out "adult rescue experiments" and expressed the different *dzy* isoforms into a *dzy* mutant background. So, the first step of these adult rescue experiments was the construction of a *dzy* mutant background with the mutant allele *dzy^{Δ8}* in *trans* with the *dzy* deficiency *Df(2L)ED380*.

Mutations can result in mutant alleles that no longer produce the same level of active product as the wild-type allele. Alleles with a complete loss-of-function are referred to as amorphic or null alleles. $dzy^{\Delta 8}$ is an allele with a deleted transcription start site, so it lacks endogenous dzy RNA expression in the embryo and therefore appears to be a null allele (Huelsmann et al. 2006). *Df(2L)ED380* (Ryder *et al.* 2007) is a deficiency from the DroDel Deletion collection, a genome-wide chromosomal deficiency resource for *Drosophila*. *Df(2L)ED380* is a chromosomal deletion in which chromosome segments 26C1 to 26D7 have been removed. We established that animals hemizygous for the $dzy^{\Delta 8}$ allele and the deficiency *Df(2L)ED380* ($dzy^{\Delta 8}$*/Df(2L)ED380*) almost all die as embryos or sporadically in early larval stages (1st instar larvae). Nevertheless, a small fraction, the so-called escapers, emerge as adults. Such escapers had defects, did not live very long and showed the characteristic escaper phenotype: the eyes were rough and reduced in size, the wings were bent downwards and the male genitalia were deformed, probably contributing to infertility. To verify this hypothesis, a small number of escapers were tested for fertility and we found that hemizygous males and females ($dzy^{\Delta 8}$*/Df(2L)ED380*) of the severe dzy allele Δ8 were not fertile.

hs-Gal4 driver

To express the different dzy spliceforms into the mutant background ($dzy^{\Delta 8}$*/Df(2L)ED380*), we used the UAS-Gal4 binary system, in which the transcription factor Gal4 binds to the *UAS* to activate the downstream gene expression (Brand & Perrimon 1993). For ubiquitous expression of transgenic Dzy in dzy null mutants, we used a *hs-Gal4* driver in which Gal4 expression was controlled by a heat-inducible *hsp70* promotor (*hs-Gal4*, Flybase). The use of the heat shock expression system (*hs-Gal4*) offers precise temporal control of transgene expression in a ubiquitous distribution throughout the whole fly. For the adult rescue experiment, the UAS-Gal4 system was activated at 36 °C at several defined time points. Various preliminary experiments were carried out to find the best time setting for the *hs-Gal4* driver. A transgenic fly strain with a *dzyGFP* construct (*UAS-dzyGFP*) was used as positive control for the adult rescue experiments (Boettner & van Aelst 2007, *UAS-dPDZ-GEF^{EGFP}*). This construct showed the complete genomic dzy locus (from start codon AUG exon 1) and is fused to a GFP sequence. The strain *w; +; UAS-dzyGFP*, already present in the lab group, was tested for functionality using an *elav-Gal4* driver before crossing the strain with the *Df(2L)ED380* line and generating the *Df(2L)ED380/UAS-dzyGFP* transgenic flies. To examine the ability of *UAS-dzyGFP* to rescue the adult mutant phenotype, these *Df(2L)ED380/UAS-dzyGFP* flies were crossed with flies carrying a *hs-Gal4* driver ($dzy^{\Delta 8}$*/hs-Gal4*, Fig. 42) which drives target gene expression in the whole embryo.
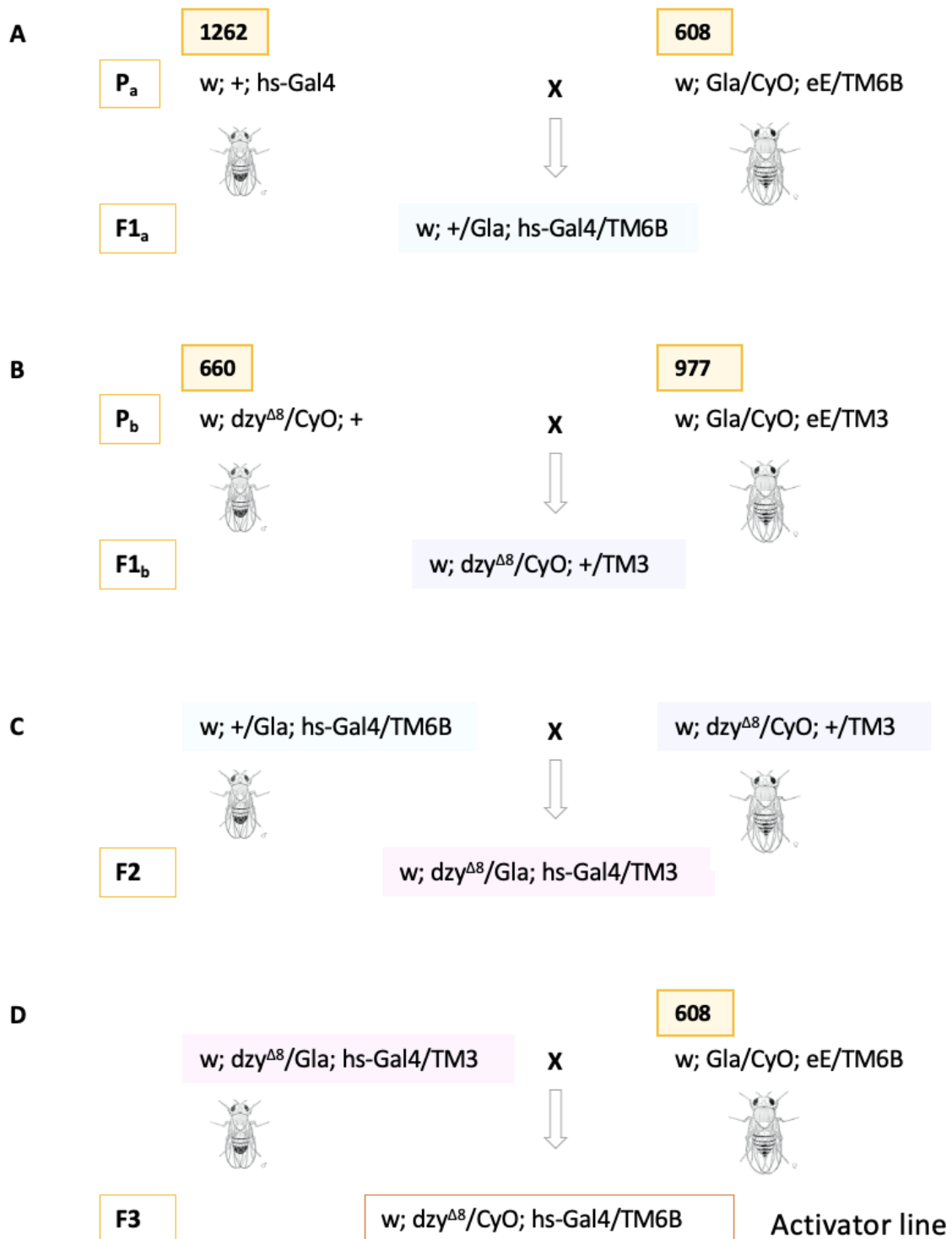
Fig. 41 Crossing scheme for the generation of the *dzy^Δ8/hs-Gal4* activator line.
(A) and (B) 5 males of the strains carrying *hs-Gal4* or the *dzy^Δ8* allele were mated with 20 virgin females of the multibalancer stocks 608 and 977. (C) Combination of *dzy^Δ8* and *hs-Gal4* to generate the *dzy^Δ8/hs-Gal4* activator line. (D) F2 generation males that carrying *dzy^Δ8* on chromosome 2 balanced over Gla and *hs-Gal4* on chromosome 3 balanced over TM3 were crossed with virgin females from the balancer stock 608 to obtain the desired chromosomal markers for further rescue experiments. Males and females of the F3 generation were then crossed to produce the *dzy^Δ8/hs-Gal4* activator line.

119

Crosses were made between activator (*hs-Gal4*) and *UAS-dzyGFP* effector flies (Fig. 43), and the progeny were subjected to a heat shock (HS) at 36 °C for 20 minutes (2x, with a 30-min rest), 30 minutes (1x or 2x, with a 30-min rest) and 1 hour (1x). Flies reared at 25 °C were treated with a heat shock to induce *hs-Gal4* expression of *UAS-dzyGFP*. It was found that 36 °C for 1h induced a strong and reproducible activator response without causing abnormalities in control embryos (*Δ*, without *UAS* effector). Interestingly, the positive control (*dzyGFP*) did not show complete rescue at any heat shock time point, but partial rescue of the wings and genitalia. The effects of the partial rescue were strongly dependent on the timing of the heat shock. Flies were crossed and allowed to lay their eggs for two days before the parent generation was collected and transferred to a new vial. When flies were placed in the water bath at 36 °C at an early time point, 2 - 4 days after egg deposition, the number of hatched flies was greatly reduced and the adult flies did not show partial rescue. The effects of partial rescue that we saw in the positive control were only evident when the flies received a one-hour heat shock at 36 °C 5 days after egg laying (AEL, d5) and maintained at 25 °C. Therefore, we used this temperature and time setting for all adult rescue experiments.
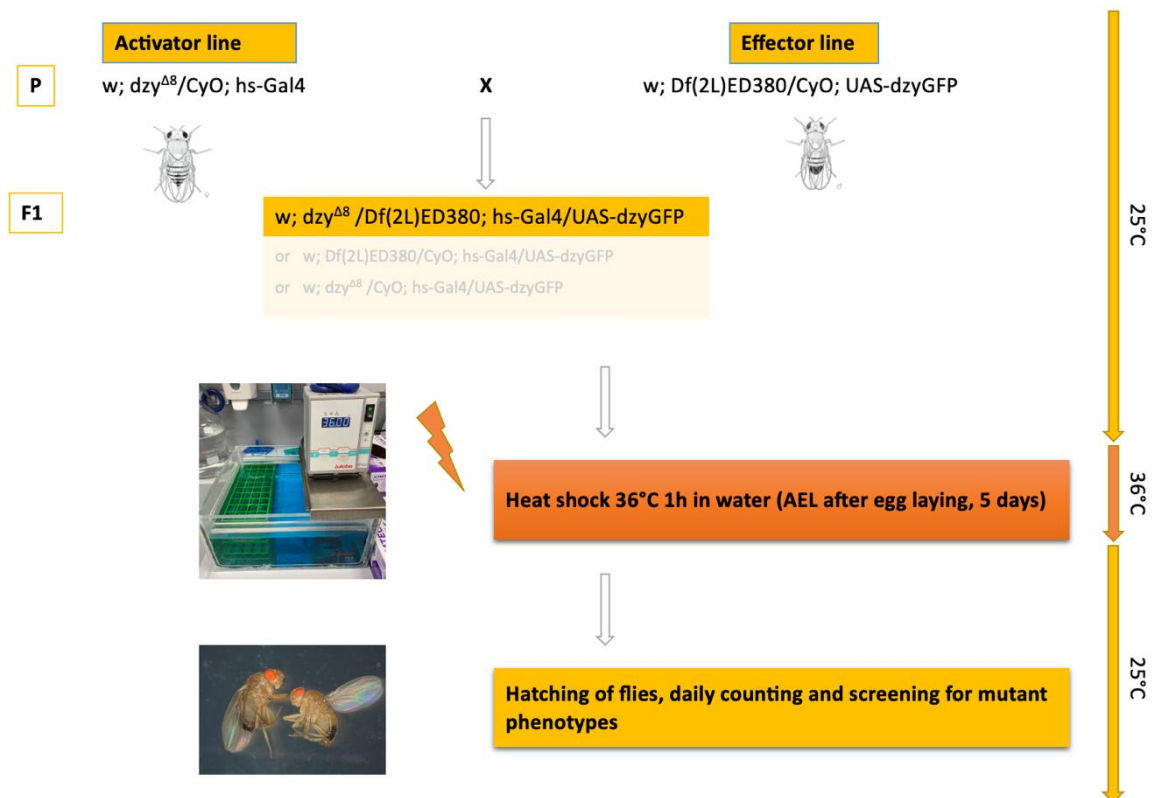
Fig. 42 Schematic representation of the heat shock (HS) incubation protocol.
Crosses for the rescue experiment: the effector line *Df(2L)ED380/UAS-dzyGFP* was crossed with the *dzy^{Δ8}/hs-Gal4* activator line, and their F1 progeny were maintained at 25 °C. 5 days after egg laying (AEL, 5 days), the progeny carrying the heat shock-inducible *hs-Gal4* driver received a one-hour HS at 36 °C in a water bath. The flies were reared at 25 °C until hatching and the flies were counted daily and screened for defects.

For heat shock induction 5 days after egg laying (AEL, d5), the vials were, after an acclimation phase of 1 hour, submerged in a 36 °C water bath, until the bottom of the foam stopper (inside the vials) was below the water surface, thereby ensuring that the larva could not escape the heat shock. After the vials remained submerged for 1 hour, they were transferred to a climate chamber (25 °C). The flies were analyzed every day. The progeny of the cross were screened for the different mutant phenotypes. The flies were analysed every day. Hemizygous mutant escapers were identified in the progeny of heterozygotes by the absence of a balancer chromosomes and the dominant marker Cy (Fig. 42).

<u>Dzy splice forms in the adult morphogenesis</u>

To examine the ability of the different splice forms to rescue the characteristic adult mutant phenotype, the individual splice forms were thus expressed with the *hs-Gal4* driver in a *dzy* mutant background. For the rescue experiment, the mutant allele *dzy$^{\Delta 8}$* was recombined with the *hs-Gal4* driver (Fig. 41). These stocks were then further crossed with another strain carrying *Df(2L)ED380* and the different *UAS-dzy$_{splice\ form}$* transgenes. The crossing schemes used to generate each *Df(2L)ED380/UAS-dzy* strain: *Df(2L)ED380/UAS-dzyGFP* (*w; Df(2L)ED380/TM3; UAS-dzyGFP*), *Df(2L)ED380/UAS-dzyA* (*w; Df(2L)ED380 UAS-dzyA/CyO; +*), *Df(2L)ED380/UAS-dzyB* (*w; Df(2L)ED380/CyO; UAS-dzyB*) and *Df(2L)ED380/UAS-dzyCΔPDZ* (*w; Df(2L)ED380/CyO; UAS-dzyCΔPDZ/TM3*), are shown in the Appendix Fig. S3-S6. The strain *Df(2L)ED380/UAS-dzyC* (*w; Df(2L)ED380/CyO; UAS-dzyC*) did not need to be generated as it was already present in the laboratory (Fly strain collection stock 1263). The *Df(2L)ED380/UAS-dzy* flies were crossed with flies carrying the *hs-Gal4* (*dzy$^{\Delta 8}$/hs-Gal4*) transgene, which controls the *dzy* gene expression throughout the embryo (Fig. 43). *Df(2L)ED380/UAS-dzyGFP* flies served as a positive control and *Df(2L)ED380* flies without a *UAS* construct (*Δ, w; Df(2L)ED380/CyO; +,* Fly strain collection stock 1228) as a negative control. The progeny of the different crosses were heat shocked for 1 hour at day 5 AEL and screened for the different mutant phenotypes. The rescue experiment in the adult fly was performed for each *UAS-dzy$_{splice\ form}$* construct to test whether one splice form was sufficient to rescue the different aspects of the adult mutant phenotype.

A   dzyA

Activator line		Effector line
P	w; dzy^Δ8/CyO; hs-Gal4 X	w; Df(2L)ED380 UAS-dzyA/SM1; +
F1	w; dzy^Δ8 /Df(2L)ED380 UAS-dzyA; hs-Gal4/+	
	w; dzy^Δ8 /SM1; hs-Gal4/+	
	w; Df(2L)ED380 UAS-dzyA/CyO; hs-Gal4/+	

B   dzyB

Activator line		Effector line
P	w; dzy^Δ8/CyO; hs-Gal4 X	w; Df(2L)ED380/CyO; UAS-dzyB
F1	w; dzy^Δ8 /Df(2L)ED380; hs-Gal4/UAS-dzyB	
	w; dzy^Δ8 /CyO; hs-Gal4/UAS-dzyB	
	w; Df(2L)ED380/CyO; hs-Gal4/UAS-dzyB	

C   dzyC

Activator line		Effector line
P	w; dzy^Δ8/CyO; hs-Gal4 X	w; Df(2L)ED380/CyO; UAS-dzyC
F1	w; dzy^Δ8 /Df(2L)ED380; hs-Gal4/UAS-dzyC	
	w; dzy^Δ8 /CyO; hs-Gal4/UAS-dzyC	
	w; Df(2L)ED380/CyO; hs-Gal4/UAS-dzyC	

D   dzyCΔPDZ

Activator line		Effector line
P	w; dzy^Δ8/CyO; hs-Gal4 X	w; Df(2L)ED380/CyO; UAS-dzyCΔPDZ/TM3
F1	w; dzy^Δ8 /Df(2L)ED380; hs-Gal4/UAS-dzyΔPDZ	
	w; dzy^Δ8 /Df(2L)ED380; hs-Gal4/TM3	
	w; dzy^Δ8 /CyO; hs-Gal4/UAS-dzyΔPDZ	
	w; dzy^Δ8 /CyO; hs-Gal4/TM3	
	w; Df(2L)ED380/CyO; hs-Gal4/UAS-dzyΔPDZ	
	w; Df(2L)ED380/CyO; hs-Gal4/TM3	

E   dzyGFP

Activator line		Effector line
P	w; dzy^Δ8/CyO; hs-Gal4 X	w; Df(2L)ED380/CyO; UAS-dzyGFP
F1	w; dzy^Δ8 /Df(2L)ED380; hs-Gal4/ UAS-dzyGFP	
	w; dzy^Δ8 /CyO; hs-Gal4/UAS-dzyGFP	
	w; Df(2L)ED380 /CyO; hs-Gal4/UAS-dzyGFP	

F   Δ

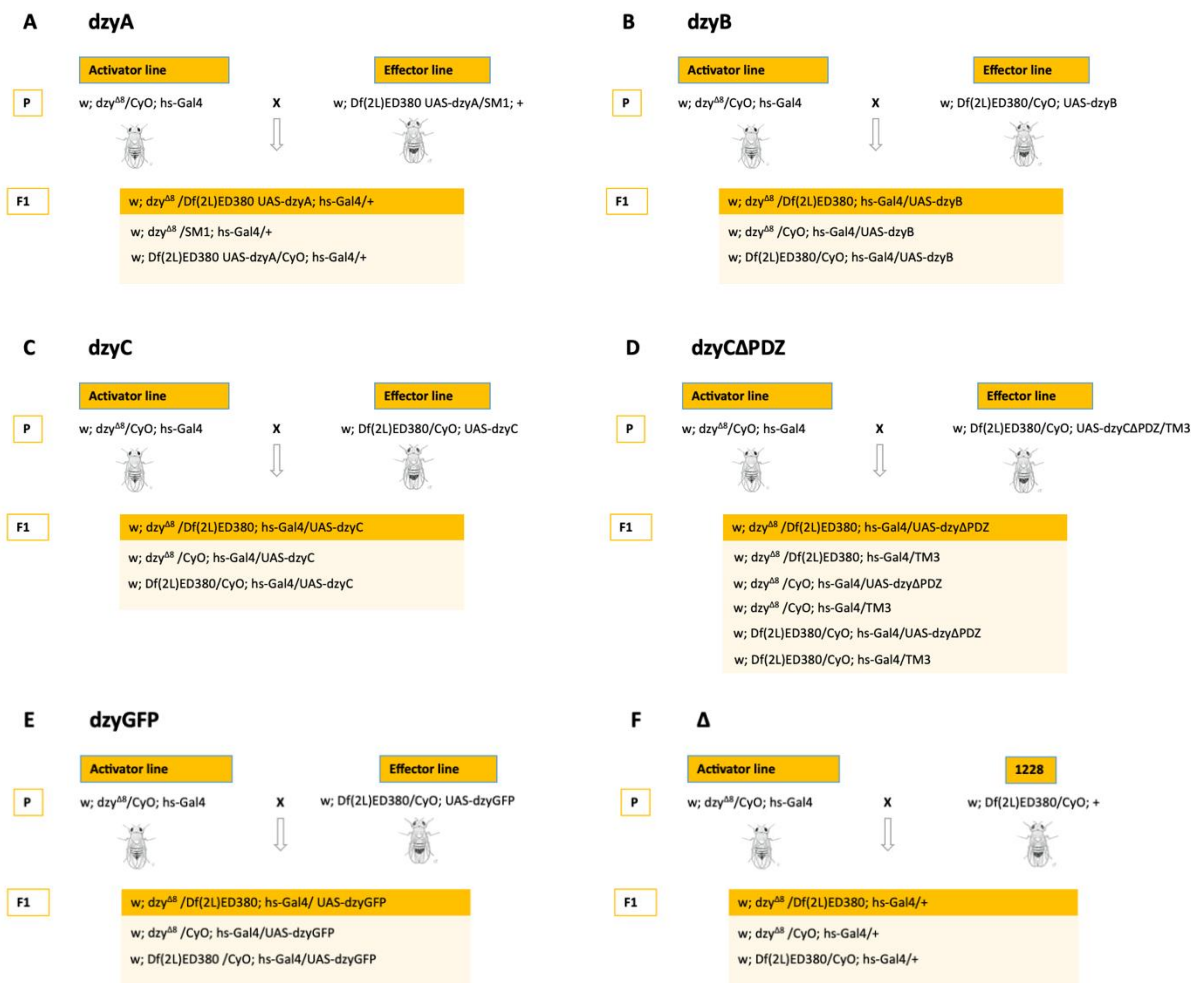| Activator line		1228
P	w; dzy^Δ8/CyO; hs-Gal4 X	w; Df(2L)ED380/CyO; +
F1	w; dzy^Δ8 /Df(2L)ED380; hs-Gal4/+	
	w; dzy^Δ8 /CyO; hs-Gal4/+	
	w; Df(2L)ED380/CyO; hs-Gal4/+	

Fig. 43 Crossing scheme for combining the activator and effector lines.
The depicted crossing scheme was used to obtain transgenic flies expressing the different *dzy* splice forms in a *dzy* mutant background (*dzy^Δ8/Df(2L)ED380*). 20 virgin females of the activator line (*dzy^Δ8/hs-Gal4*) were mated with 5 males of the effector line (*Df(2L)ED380/UAS-dzyA* (A), *Df(2L)ED380/UAS-dzyB* (B), *Df(2L)ED380/UAS-dzyC* (C), *Df(2L)ED380/UAS-dzyCΔPDZ* (D) or *Df(2L)ED380/UAS-dzyGFP* (E)). A *Df(2L)ED380* line without UAS transgene (*Δ*) was used as negative control (F). The F1 generation was screened for the different phenotypes. Flies carrying the dominant marker Cy (*dzy^Δ8*/CyO and *Df(2L)ED380*/CyO) were counted and discarded. Flies carrying *dzy^Δ8* and *Df(2L)ED380* on the 2nd chromosome and thus not showing curved wings were collected and examined for the possible phenotypes: wing⁻, eye⁻ and wing⁺, eye⁻ escaper.

Indeed, we were able to obtain the escapers of the lethal phenotype of *dzy* hemizygous through large scale cultures of the flies. We were able to find more than 896 escapers (wing⁻,eye⁻) at a frequency of 17.3 % between the *dzy/CyO* and *dzy/TM3* parents, distinguished by the Cy and the Sb dominant marker. These *dzy* hemizygous mutants displayed conspicuous features. The wing edges were rolled downwards (Fig. 44B; compared with Fig. 44A), and the eyes became small and rough (Fig. 44B'), compared to those of *wt* flies (Fly strain collection stock 580, *w; +; srph-Gal4*) (Fig. 44A'). Similar to the expression of *dzy* splice forms in embryonic macrophages, the expression of a single splice form, *dzyC*, into the mutant background under the control of the *hs-Gal4* driver was sufficient to at least partially rescue the mutant phenotype.

The escapers of this cross no longer showed the typical bent downward wings (Fig. 44C). Instead, the flies showed straight wings (wing⁺, eye⁻), like the wings of the wild-type flies. These results were consistent with the positive control *dzyGFP*, *dzyC* and *dzyGFP*, which both showed a partial rescue of the mutant phenotype. Interestingly, besides the wing phenotype, male sterility was also affected in these flies.

The genitalia of the male flies with straight wings were examined in more detail and we found that they were similar in appearance to those of wt flies (Fig. 44E + E'). Compared to the escaper flies, they no longer showed destroyed, modified genitalia. Thus, partial rescue could also be achieved in this area of the adult phenotype. To check whether the rescue of the genital phenotype was only visual or whether the sterility of the flies had also changed, the partially rescued *dzyGFP* and *dzyC* male flies with straight, "wild-type" wings and "wild-type" looking genitalia were crossed with *w⁻* virgins. The result of this cross was numerous offspring that no longer exhibited any phenotype. The males were thus demonstrably no longer sterile. The *dzyC* form reached the same rescue level as the genomic *dzyGFP* and was thus able to rescue the wing and genital phenotype. However, compared to *dzyGFP* (8.2 %), the total number of partially rescued escapers (wing⁺, eye⁻) was slightly reduced in *dzyC* (6.0 %) (Fig. 45). However, despite the partial rescue of wings and genitalia, the rough eye phenotype remained unchanged (Fig. 44C').

Interestingly, in contrast to *dzyC*, expression of *dzyCΔPDZ* into the mutant background under the control of the *hs-Gal4* driver was not sufficient to partially rescue the mutant phenotype. The total number of escapers of this cross was slightly increased (18 %) compared to the control (*Δ*, 1-hour HS 14.0 % or *Δ*, ∅ HS 9.2 %), but the escapers all showed the characteristic mutant phenotype (Fig. 45). Since *dzyC* and *dzyCΔPDZ* differ only in the presence of the PDZ domain, it appears that the PDZ domain plays an important role not only in the process of cell shape change and cell migration in *Drosophila* embryos, but also in this context.
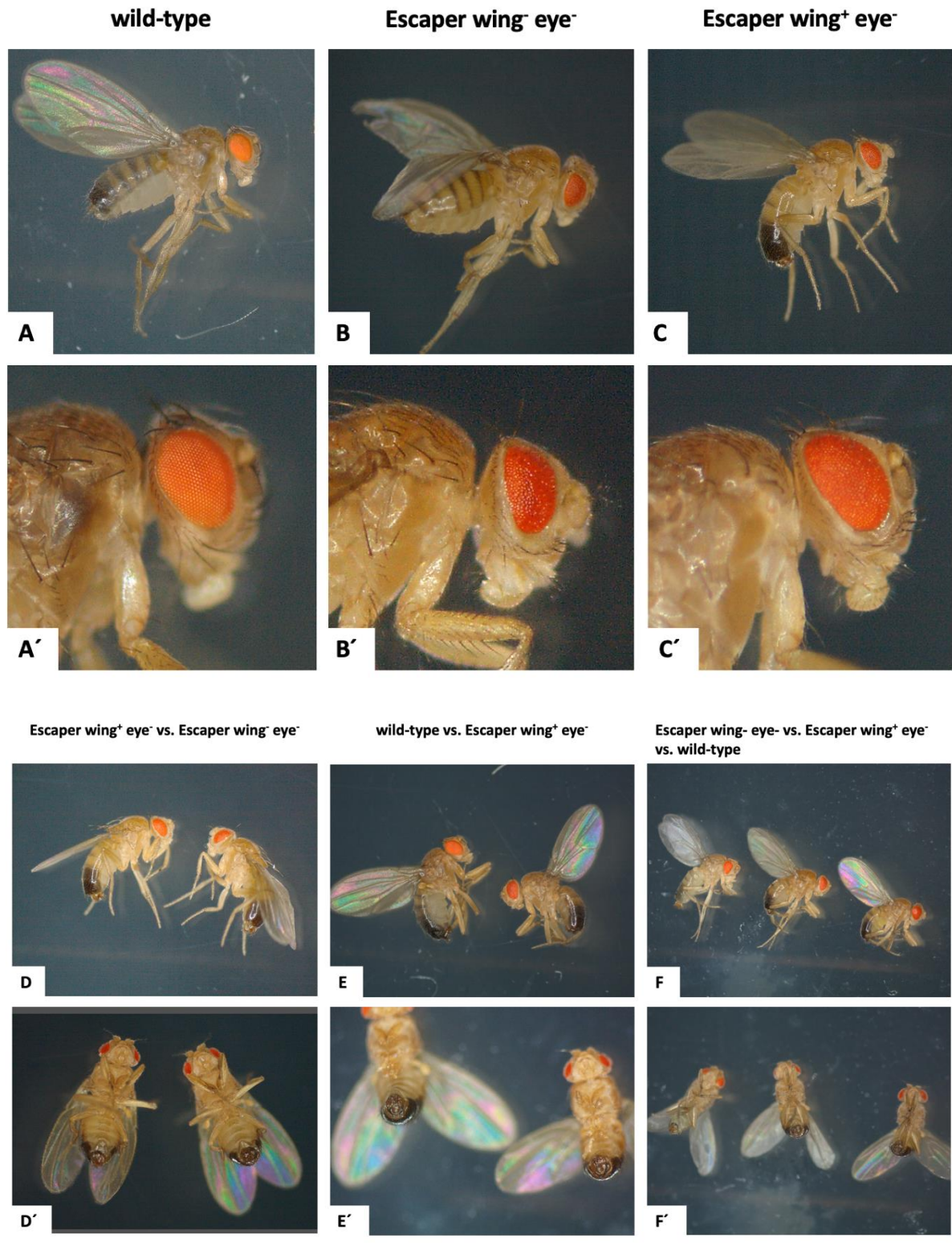
Fig. 44 The phenotypes of *dzy* hemizygous escapers.
Bent downward wing blades were visible in the lateral view of *dzy* hemizygous mutants (B), but were not observed in wild-type flies (*w; +; srph-Gal4,* Fly strain collection stock 580) (A). The *dzy* hemizygous escaper flies showed the characteristic rough eye phenotype: surface images of the adult *Drosophila* eyes from wild-type (A') and *dzy^Δ8/Df(2L)ED380* flies (B'). Expression of *dzyC* into the *dzy* mutant background (C) was sufficient to rescue the bent downward wings, but not the rough eye phenotype (C'), both characteristic defects of hemizygous escaper flies. Interestingly, in addition to the wing phenotype, the genitalia of escapers with these straight "normal" wings (wing⁺, eye⁻) were similar to those of wt flies (E, E'). Compared to the escaper flies (wing⁻, eye⁻) they no longer showed destroyed,

modified genitalia (D, D'). In (F) and (F') a direct comparison of the wings, eyes and genitalia of the three genotypes escaper wing⁻, eye⁻, escaper wing⁺, eye⁻ and Oregon (Bloomington *Drosophila* stock centre wild-type lines) is shown.

While the positive control *dzyGFP* and the *dzyC* splice form resulted in the rescue of several aspects of the mutant phenotype, such as wings, genitalia and sterility, *dzyA* and *dzyB* were unable to rescue the different defects. The rescue experiment clearly showed a different function of the different isoforms in adult morphogenesis. For the *dzyA* form, we did not see a rescue of the different aspects of the mutant phenotype, but we did detect a significant increase in escaper number (24.1 %) compared to the negative control in which no *UAS* construct was expressed (Fig. 45). Thus, the *dzyA* form may decrease the *dzy⁻* lethality rates. Expression of the *dzyB* form failed to rescue hemizygous *dzy⁻* flies; we observed neither a partial rescue nor an increased number of escapers. We did not see any individuals with "normal" eyes, "normal" wings or genitalia, nor did we see individuals in which only one of these aspects was rescued. Since the *dzyB* form is presumably increased in expression in the *Drosophila* larva and pupa (see Results section 3.2) this isoform seems to play an important role at these stages of development.
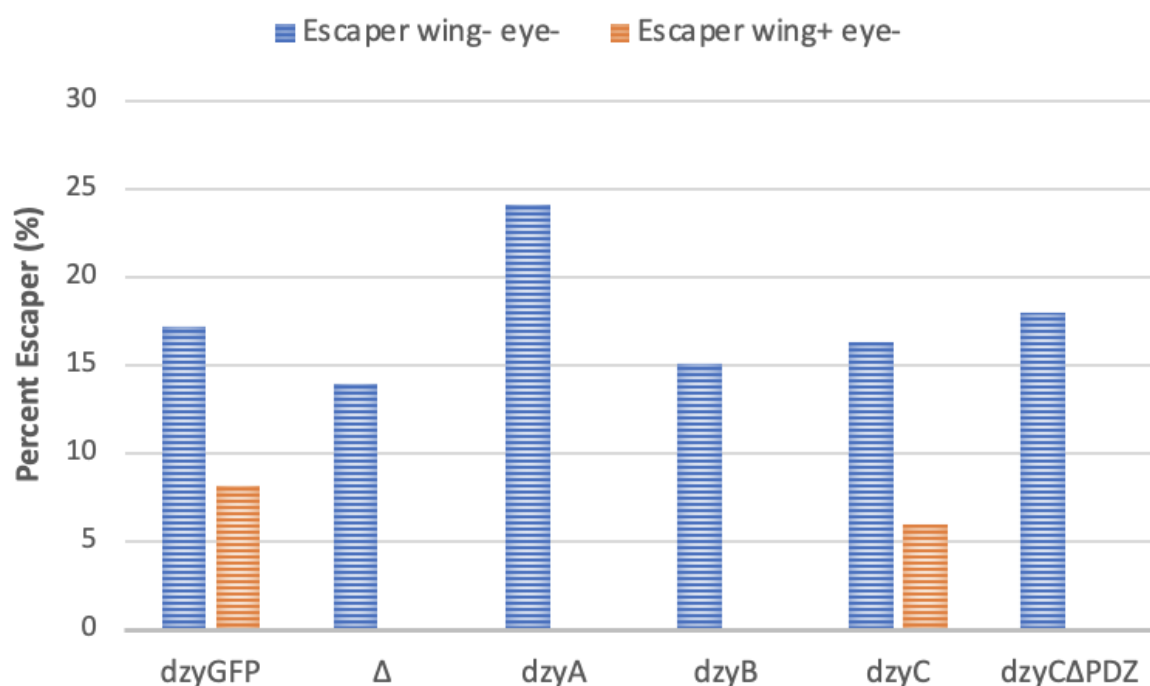

Fig. 45 The *dzyC* splice form is sufficient to rescue the wing and genitalia phenotype, but not the eye mutant phenotype.
The number of *dzy⁻* hemizygotes is indicated as a proportion of all hatched flies of the respective crosses. In the progeny of *dzy⁻,* hemizygous escapers showed the characteristic phenotype with bent downward wings (wing⁻) and small rough eyes (eye⁻). When in the same genetic mutant background *dzy* is expressed from the *dzyGFP* or the *dzyC* transgene under the control of the *hs-Gal4* promoter, about one-third of all hatched flies are *dzy* hemizygotes. About 8.2 % (*dzyGFP*) and 6.0 % (*dzyC*) of these showed a partial phenotypic rescue with "normal" wings (wing⁺, eye⁻). A rescue of the eye phenotype was not observed. In contrast, expression of the *dzyA* isoform led to a significant increase in the number of escapers, but all of the flies were affected in eye and wing morphogenesis (wing⁻, eye⁻). The expression of the *dzyB* isoforms had no detectable rescue activity for eclosing adults.

In this part of the work, we have shown that the *dzy* splice forms have different functions in adult *Drosophila* flies, as only the *dzyC* form is sufficient to rescue the *dzy* mutant wing and genital phenotype. The *dzyC* form, which is capable of causing a cell shape change in migrating macrophages, was also relevant for at least partial rescue in adults, suggesting that this isoform may not be specifically linked to embryogenesis in terms of cell migration or cell adhesion.

No rescue of the eye phenotype was achieved with the *gmr-* and *eyeless-Gal4*

We wondered why the expression of *dzyC* and *dzyGFP* under the control of the *hs-Gal4* was sufficient to rescue the wing and genital phenotype of the *dzy* mutant, but not the eye phenotype. The partially rescued escapers continued to exhibit the small rough eye phenotype. To explicitly rescue the rough eye phenotype of the *dzy* mutant background flies, an *eyeless-* and a *gmr-Gal4* driver were used. The different transgenic *Df(2L)ED380/UAS-dzy* lines were crossed with a strong *gmr-Gal4* (2nd) and an *eyeless-Gal4* (2nd) driver to overexpress *dzy* exclusively in the *Drosophila* eye. The two Gal4 driver strains (*w; gmr-Gal4; +* and *w; ey-Gal4/CyO; +*) were paired with the *dzy^{Δ8}* allele (*w; gmr-Gal4 dzy^{Δ8}/SM1; +* and *w; ey-Gal4 dzy^{Δ8}/SM1; +*) and crossed with the different *Df(2L)ED380/UAS-dzy* strains. The respective crossing schemes can be found in the Appendix (see Fig. S7 - S10). As observed in the *hs-Gal4* rescue experiments, none of the splice forms showed a rescue of the rough eye phenotype. The *Df(2L)ED380/UAS-dzyGFP* strain was used as a positive control; again, no rescue of the eye mutant phenotype was observed.

dzy promotor (*pdzy*) and alternative Gal4 drivers

In numerous preliminary experiments, other Gal4 drivers were tested in parallel to the *hs-Gal4* driver for their functionality and suitability for the adult rescue experiment. While *daughterless-Gal4* and *tubulin-Gal4*, among others, were not considered in the subsequent experiments, we decided to perform the adult rescue experiment with a *pdzy* promotor-*Gal4*. The *dzy* promotor and the *hs-Gal4* driver seemed to be the most appropriate for this type of experiment. The *hs-Gal4* driver gave the strongest and clearest result in the preliminary experiments and provided the advantage of temporal regulation of expression. In comparison, the *dzy* promotor allowed expression of the gene at a level closest to the natural expression level of *dzy*. The possibility of distorting the results due to a very strong overexpression was thus prevented.

Using a phylogenetic footprint approach, previous work in this lab group identified an upstream region spanning about 1.2 kb as a possible *dzy* promotor candidate. To characterize the minimal promotor, this 1.2 kb upstream region was taken and three 5' truncation constructs of this element were generated: 1 kb (*pdzy-1*), the others were 0.4 kb (*pdzy-2*), 0.3 kb (*pdzy-3*), 0.15 kb (*pdzy-4*), respectively (Fig. 46).
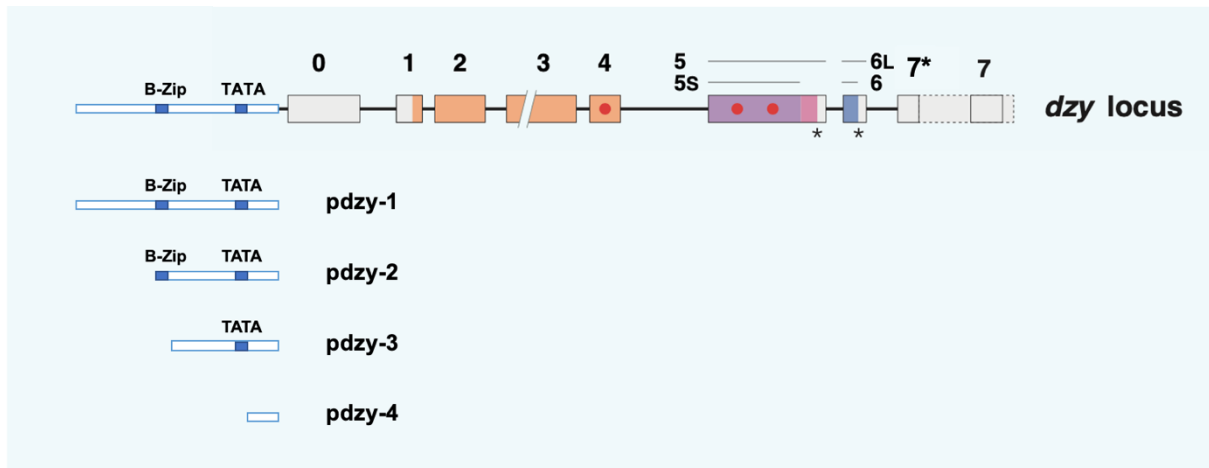
Fig. 46 *dzy* promotor deletion study for promotor analysis.
Here, the *dzy* transgene is shown. The other fragments refer to the promotor truncation to produce the different *pdzy-Gal4* drivers. In the 1.2 kb fragment a B-Zip binding domain and a TATA box have been found, shown as blue boxes.

At the time of this work, fly lines with two, *pdzy-1 (w; Pdzy(1)-Gal4 dzy(Δ8) FRT2L/SM1; +,* Fly strain collection stock 1241) and *pdzy-3 (w; Pdzy(3)-Gal4 dzy(Δ8) b pr FRT/CyO; +,* Fly strain collection stock 1229), of the four different truncation products were available for further investigation. In order to test these fly strains for promotor functionality, the *UAS-Stinger* transgene was expressed under the control of *pdzy-1-Gal4* and *pdzy-3-Gal4* drivers. The *pdzy-3* promotor led to an illumination of the nuclei and thus to a positive signal in the larvae. Since *pdzy-1* has no effect, the following adult rescue experiments were carried out exclusively with the *pdzy-3* promotor. To investigate the functional relevance of the splice forms in the adult morphogenesis, we expressed the *UAS-dzy*_{splice forms} and the *UAS-dzyGFP* construct in *dzy⁻* flies (*dzy^Δ8/Df(2L)ED380*) under the control of the *pdzy-3-Gal4* driver. The respective crossing schemes for the different *UAS-dzy* fly strains can be found in the Appendix Fig. S11. We observed no fully rescued "normal", or partially rescued mutant flies in which only the wings or the eyes were rescued. No rescue of any aspect of the mutant phenotype was observed in either *UAS-dzyGFP* or any of the splice forms. Also, the number of escapers did not change significantly compared to the negative control without the *UAS* construct. Thus, the same experimental set up performed with the strong *hs-Gal4* driver showed no usable results when performed with the weaker *pdzy-Gal4* driver. Presumably, the expression level of the *dzy* promoter was too low to achieve a visible effect.

3.6 Embryonal rescue experiment: Investigation of the ability of the single splice forms to rescue the macrophage migration phenotype of *dzy* mutants.

In wild-type embryos, macrophages from the anterior and the posterior part of the embryo migrate towards each other along the midline of the ventral nerve cord (VNC). At stage 13 and 14, macrophages span the entire midline of the VNC completely. In contrast, macrophages of homozygous *dzy* mutant embryos show a marked delay in macrophage migration, especially in the migration along the ventral nerve cord (VNC). In *dzy* mutant embryos, there is a gap of a few neuromeres in the posterior region of the VNC (Huelsmann *et al.* 2006). In some embryos, this ventral gap is visible until later stages, while in others the defect disappears (Huelsmann *et al.* 2006). Thus, in *dzy* mutant embryos, macrophages are not evenly distributed and there are fewer macrophages in the posterior-ventral part of the embryo than in the corresponding area of a wild-type embryo. The activity of *dzy* is thus required within the macrophages for proper cell motility. So, mutations in *dzy* impair macrophage migration.

Furthermore, we have shown that the expression of the individual *dzy* splice forms in macrophages has very specific influence on cell morphology. Overexpression of the *dzyC* form alone was sufficient to cause a change in cell shape and the formation of the cell network phenotype (see Results section 3.3). Therefore, we wondered whether any of the dzy splice forms were specifically required for macrophage migration. However, due to the combinatorial nature of *dzy* mRNA splicing, there is no straight-forward way to generate a splice form-specific knockout of *dzy*, for example by RNA silencing, and test such a requirement directly. Therefore, we chose an alternative path and asked whether one of the single splice forms would be sufficient to rescue the macrophage migration phenotype of dzy mutants in the *Drosophila* embryo. To answer this question, an "embryonal rescue experiment" was performed with *Drosophila* embryos. In these rescue experiments we focused on macrophage migration along the VNC midline at stage 13 to 14, as migration along this substrate is most impaired in *dzy* mutants. In comparison, other migrations, such as migration along the dorsal epidermis, are not impaired to the same extent in *dzy* mutants (Huelsmann *et al.* 2006). To quantify the rescue effects of the described "cell gap", we defined three different phenotypic classes in advance of the experiments according to the number of neuromeres of the VNC without macrophages. The following classes were defined: class 1, missing gap; class 2, gap of 1 - 2 neuromeres and class 3, gap of 3 - 5 or more neuromeres. This subdivision should serve to also identify partial rescues of the *dzy* mutant phenotype. To examine the ability of the various splice forms to rescue the migration defect and close the "cell gap", we expressed *UAS-dzyGFP* and the individual *UAS-dzy* isoforms (*dzyA*, *dzyB*, *dzyC* and *dzyCΔPDZ*) into the *dzy* mutant background $dzy^{Δ8}/Df(2L)ED380$ (see Results section 3.5). Since the expression of the different

isoforms in *Drosophila* embryo macrophages was to be investigated, the expression was performed under the control of the *srph-Gal4* driver.

In a first step, the mutant allele *dzy^Δ8* was recombined with the *srph-Gal4* driver (*dzy^Δ8/srph-Gal4*, Fig. 47). This strain was then further crossed with another strain carrying *Df(2L)ED380* and the different *UAS-dzy_splice form* transgenes. The different *Df(2L)ED380/UAS-dzy* strains (*Df(2L)ED380/UAS-dzyGFP, Df(2L)ED380/UAS-dzyA, Df(2L)ED380/UAS-dzyB, Df(2L)ED380/UAS-dzyC and Df(2L)ED380/UAS-dzyCΔPDZ*), generated for the adult rescue experiment in the Result section 3.5 of this work, were used for this approach. The crossing schemes used to generate each *Df(2L)ED380/UAS-dzy* strain are shown in the Appendix Fig. S3-S6. *Df(2L)ED380* flies without a UAS construct (*Δ*, Fly strain collection stock 1228) served as negative control.
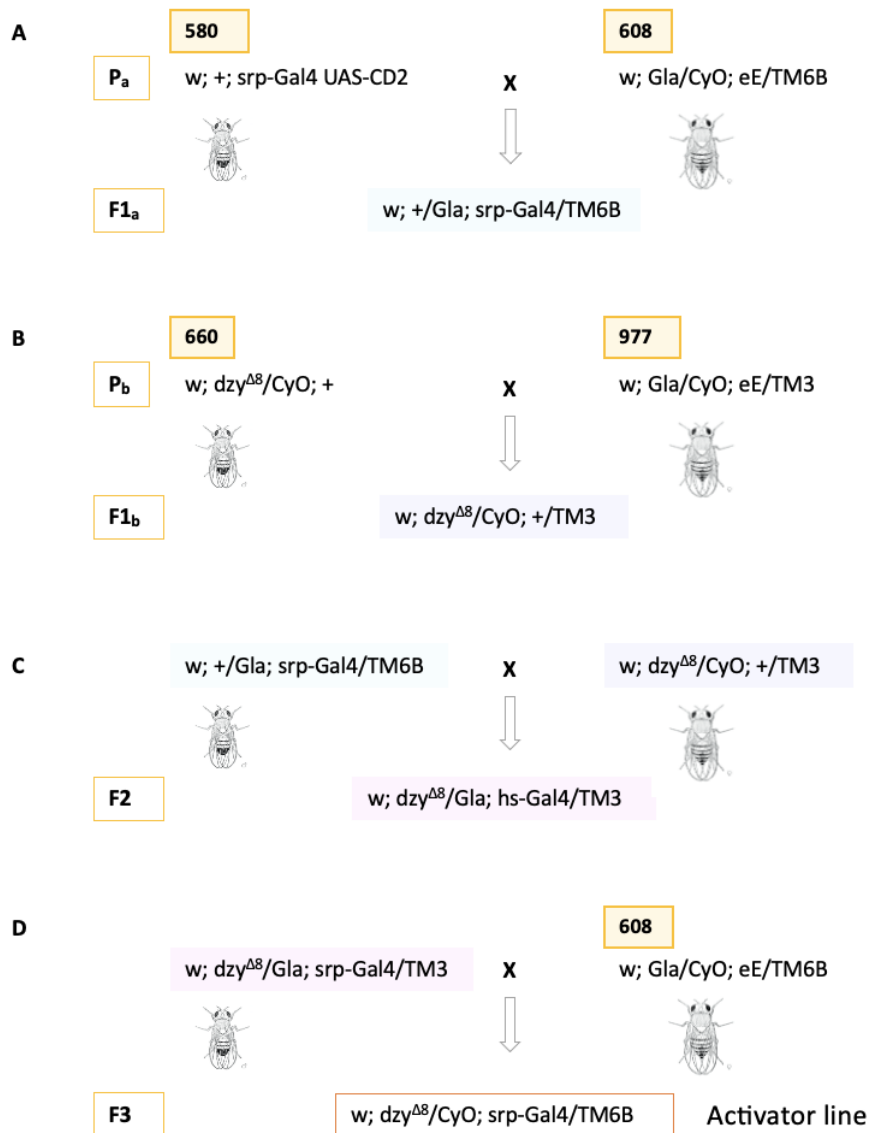
Fig. 47 Crossing scheme for the generation of the *dzy^Δ8/srph-Gal4* activator line.
Males of the strains carrying (A) the *srph-Gal4* (Fly strain collection stock 580) or (B) the *dzy^Δ8* allele (Fly strain collection stock 660) were mated with virgins of the multibalancer stocks 608 and 977. (C) Combination of *dzy^Δ8* and *srph-Gal4* to generate the *dzy^Δ8/srhp-Gal4* activator line. (D) Males of the F1 generation carrying *dzy^Δ8* on chromosome 2 balanced over Gla and *srph-Gal4* on chromosome 3 balanced over TM3 were crossed with the balancer strain 977 to obtain the desired chromosomal markers for the embryonal rescue experiments.

Initial experiments were conducted to test the functionality of this experimental approach. Here, *Df(2L)ED380/UAS-dzyGFP* transgenic flies served as controls for the embryonal rescue experiment. Thus, we expressed *UAS-dzyGFP* in a mutant background with the *dzy^Δ8* allele and the *dzy*-deficient *Df(2L)ED380*. Balancer chromosomes were used to identify homozygous mutant progeny. In a balanced cross, mutants can be selected by the absence of the markers on the balancer chromosomes. Originally, balancers had markers with adult phenotypes, but there are also several balancers that express the green fluorescent protein (GFP). GFP fluorescence in these "green balancers" can be measured in embryos in addition to larvae and adults (Casso *et al.* 1999). To identify the *dzy^Δ8/Df(2L)ED380* embryos in the progeny and distinguish them from the heterozygous embryos (*dzy^Δ8/CyO,GFP* and *Df(2L)ED380/CyO,GFP*), we used modified CyO balancer chromosomes (CyO, GFP) (Fig. 48). Green fluorescent embryos carrying the balancer (*dzy^Δ8/CyO,GFP* and *Df(2L)ED380/CyO,GFP* whereas non-fluorescent embryos lacking this balancer (*dzy^Δ8/Df(2L)ED380*).
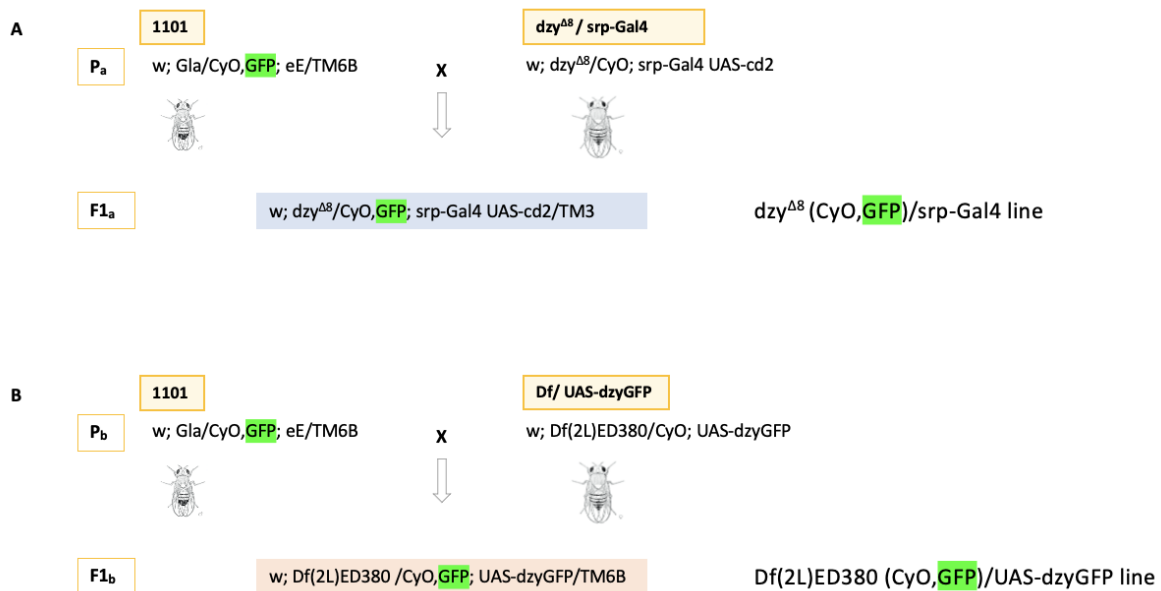

Fig. 48 Crossing scheme for the generation of the fly strains *dzy^Δ8(CyO,GFP)/srph-Gal4* and *Df(2L)ED380(CyO,GFP)/UAS-dzyGFP*.
Virgin flies from the strains (A) *dzy^Δ8/srph-Gal4* and (B) *Df(2L)ED380/UAS-dzyGFP* were crossed with the balancer chromosome strain 1101 (*w; Gla/CyO,GFP; eE/TM3*). To obtain the strains

dzy^Δ8(CyO,GFP)/srph-Gal4 and *Df(2L)ED380(CyO,GFP)/UAS-dzyGFP*, male and female flies (Cy and Sb) were collected from the progeny.

Crosses were made between activator (*dzy^Δ8(CyO,GFP)/srph-Gal4*) and *Df(2L)ED380(CyO,GFP)/UAS-dzyGFP* effector flies (Fig. 49). The flies were placed together in a cage and the plates collected after 24 hours of overnight egg deposition. Embryos of different stages were collected, dechorionated, fixed, stained for CD2 and then examined under the fluorescence microscope. Before screening for the embryonic mutant macrophage migration phenotype ("cell gap") and quantifying the rescue effect, embryos were genotyped by balancer GFP expression. Non-fluorescent embryos with a mutant background (*dzy^Δ8/Df(2L)ED380)* could be identified in the progeny of heterozygotes (*dzy^Δ8/CyO,GFP* and *Df(2L)ED380/CyO,GFP*) by the absence of the balancer chromosome CyO,GFP. Green-fluorescent embryos are thus excluded from further investigations.

When crossing the transgenic *Df(2L)ED380(CyO,GFP)/UAS-dzyGFP* animals with flies carrying *dzy^Δ8(CyO,GFP)* and the macrophage-specific *srph-Gal4* driver coupled with *UAS-cd2*, we were unable to detect any fluorescence signal. A differentiation of homozygous and heterozygous embryos was therefore not possible. It could not be shown which embryos express *dzy* in the mutant background and thus no statement could be made about a possible rescue. This first approach of the embryonal rescue experiment could not show whether *dzyGFP* or another splice form is able to rescue the migration phenotype of the *dzy* mutant. Further experiments are therefore necessary to be able to give an accurate answer to this question.
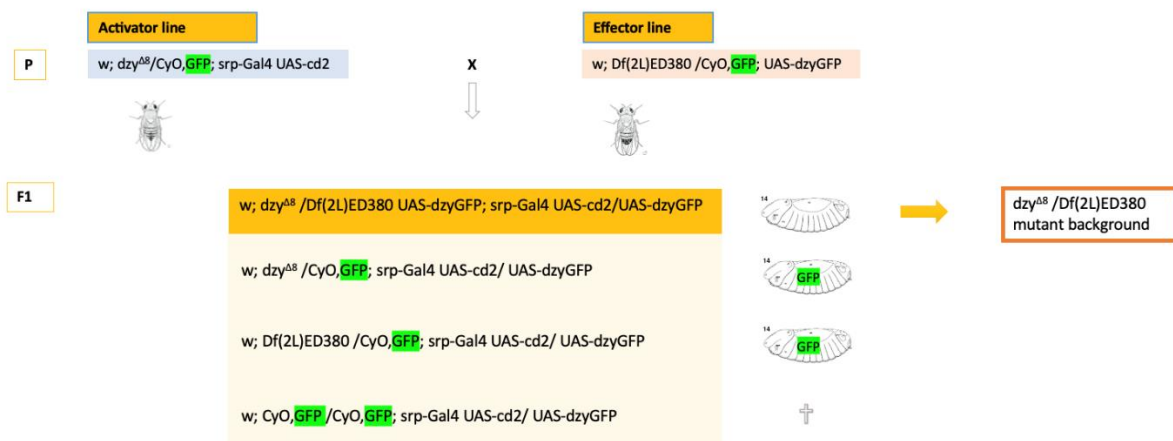

Fig. 49 Crossing scheme for the combination of the activator and effector lines for the embryonal rescue experiment.
The crossing scheme shown was used to obtain transgenic flies expressing *dzyGFP* in a *dzy* mutant background (*dzy^Δ8/Df(2L)ED380*). Virgins of the activator line (*dzy^Δ8(CyO,GFP)/srph-Gal4*) were mated with males of the effector line (*Df(2L)ED380(CyO,GFP)/UAS-dzyGFP*). The F1 generation was screened for fluorescent and non-fluorescent embryos. Flies carrying the "green balancer" CyO,GFP (*dzy^Δ8/CyO,GFP* and *Df(2L)ED380/CyO,GFP*) are counted and discarded. Non-fluorescent embryos

carrying *dzy^{Δ8}* and *Df(2L)ED380* on the 2nd chromosome are examined for the *dzy* mutant macrophage migtration phenotypes. Graphic of stage 14 embryo from Atlas of *Drosophila* development, Hartenstein.

3.7 Cloning of docking site *dzy* splice form constructs using RE-digestion and the NEBuilder HiFi DNA Assembly Kit

Expression of the individual *dzy* splice forms in macrophages had very specific influence on cell morphology. Overexpression of the *dzyC* form alone was sufficient to cause a change in cell shape and the formation of the cell network phenotype. The random integration and genomic position of the different dzy splice forms at various locations in the genome may affect transgene expression. Expression level analysis was performed using in situ hybridization and a dzy probe (see Results sectiont 3.3). Generally, the dzyC splice form in particular, which affected cell shape and migration, showed a slightly stronger signal with the dzy probe. However, it was difficult to make a precise statement about the comparison of the different expression levels of the splice forms. Since the dzy splice form constructs were randomly integrated into the genome and in situ hybridization analysis could not provide an accurate statement about the indication and comparison of the expression levels, we wanted to take an alternative approach to better compare the different splice forms and thus exclude a position effect.

One characteristic feature of P-elements is their random integration behaviour. Although this randomness is advantageous and useful for the generation of deletion and mutation studies, it is generally not ideal for transgene analysis. Random integration of P-elements requires considerable effort in mapping insertions. Genomic position effects can strongly influence gene expression, complicating transgene analysis and make precise structure-function analysis almost impossible. It is therefore desirable to be able to insert the genes of interest at the same chromosomal location. Strategies have been developed to circumvent the problem of randomness by using targeted integration systems in *Drosophila*. One of these integration methods is based on the site-specific PhiC31 integrase (Bischof *et al.* 2007). The bacteriophage PhiC31 encodes a serine integrase that mediates sequence-directed recombination between a bacterial attachment site (attB) and a phage attachment site (attP). This method of PhiC31 integration allows the insertion of any desired transgene into specific landing sites at the same genetic locus in the fly genome. Purified DNA is injected into early embryos and can be inserted into the attP target site of the fly genome. A plasmid containing the gene or cDNA of interest, an attB site and a phenotypic marker, is injected into an attP-containing fly strain with a source of the PhiC31 integrase. The integrase then facilitates recombination of these sites inserting the gene of interest into the *Drosophila* genome (Bischof *et al.* 2007).

The plan moving forward was to generate *Drosophila* transgenic for *dzy_GFP* using the site-specific pUASTattB/PhiC31 integrase system. First, *dzy_GFP in pUASTattB* plasmids were planned, containing an attB site, the white+ selectable marker gene, one of the different *dzy_GFP* fragments and a single loxP site. The corresponding landing site for the attB-containing plasmid was located in fly strain *yw, C31; +; 86 FB* (Fly strain collection Sven Huelsmann) on the third chromosome. This landing site strain with endogenous PhiC31 activity (X-chromosome) contained the attP site and a DsRFP marker gene driven by a 3xP3 promoter. This RFP reporter gene led to a pink eye color in the adult flies. The 3xP3-RFP marker cassette was flanked by loxP sites. PhiC31 integrase mediated recombination between the attB site in the plasmid and the attP site in the fly line genome, resulting in the integration of *pUASTattB-dzy_GFP* into the landing site. Integration of the *pUASTattB* plasmid into the attP landing site resulted in attR and attL hybrid sites that were refractory to PhiC31 integrase. The result was irreversible integration of *dzy_GFP in pUASTattB* into the fly genome (Fig. 50). The adults obtained after injection of the plasmid into *yw, C31; +; 86 FB* embryos were individually crossed with *w−* animals, and their progeny were screened for white+ expression. The pink eye colour (3xP3-RFP), however, was clearly distinct from the colour resulting from expression of *white*.
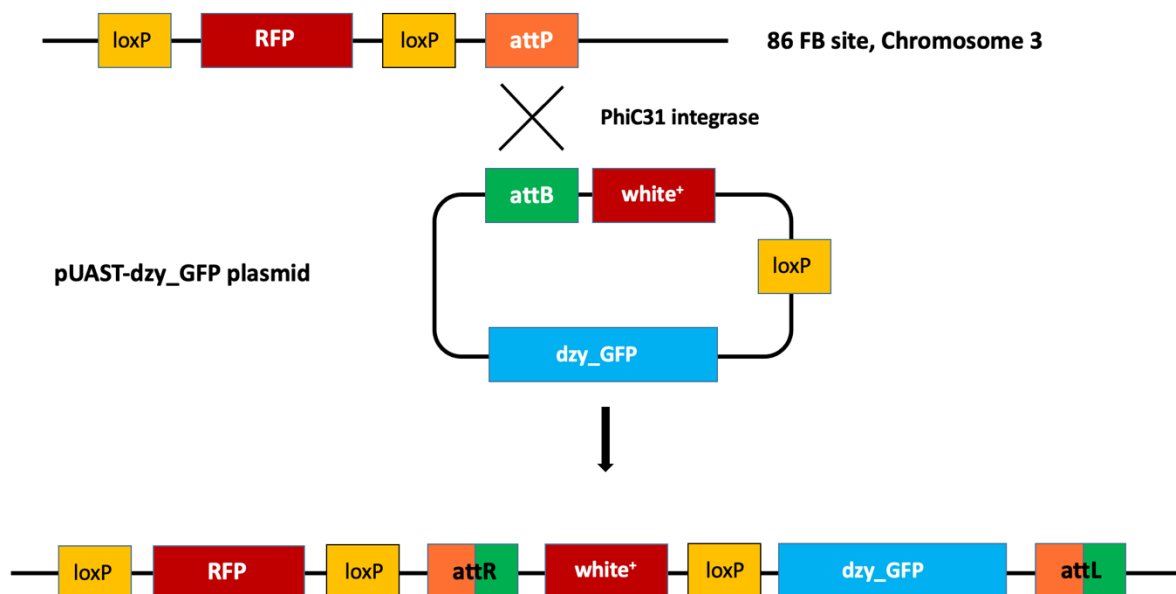

Fig. 50 PhiC31/pUASTattB-mediated site-specific transgenesis in *Drosophila*.
The *dzy_GFP in pUASTattB* plasmids contained an attB fragment, the white+ marker gene and the *dzy_GFP* transgene. During PhiC31 integrase-mediated integration, the unique attP site in the *yw, C31; +; 86 FB* (Sven Huelsmann) fly line genome recombined with the pUASTattB site in the *pUASTattB-dzy_GFP* vector, forming attR and attL hybrid sites in the generated transgenic lines (Bischof et al. 2007). This results in the integration of the *pUASTattB-dzy_GFP* splice forms into the fly genome. The loxP sites enabled the elimination of the red fluorescence protein (RFP) and w+ marker genes after PhiC31 mediated transgenesis.

3.7.1 Cloning of the *dzy_GFP in pUASTattB* constructs via RE-digestion

The *dzy_GFP in pUASTattB* expression vectors were generated using restriction enzyme digestion. To generate *dzy_GFP in pUASTattB* constructs (Fig. 51), the ORFs encoding the three different *dzy* splice forms were amplified via PCR from the constructs *dzyA in pUAST*, *dzyB in pUAST* and *dzyC in pUAST*. The PCR products were then cut with the appropriate restriction enzymes (*dzy* fragment: XbaI/NotI) and ligated into the digested *pUASTattB Drosophila* transformation vector (*pUASTattB* vector: KpnI/XbaI). Additionally, a *GFP* fragment was fused to *dzy* to track subcellular localisation of the Dzy protein and to facilitate macrophage visualisation. The PCR product of the *GFP* cDNA was digested (*GFP* fragment: NotI/KpnI) and cloned upstream of the different *dzy* splice form DNA sequences into the *Drosophila* transformation vector *pUASTattB*, to generate *dzyA_GFP in pUASTattB*, *dzyB_GFP in pUASTattB* and *dzyC_GFP in pUASTattB*. The expected resulting plasmids were to be sequenced and subsequently used to generate transgenic flies. The constructs were then to be injected into embryos containing the desired attP landing site (*yw C31; +; 86 FB*; integration on the third chromosome). So, in contrast to the *dzy in pUAST* constructs, the new constructs were thus introduced directionally into the genome and additionally fused with GFP (Appendix Fig. S12).
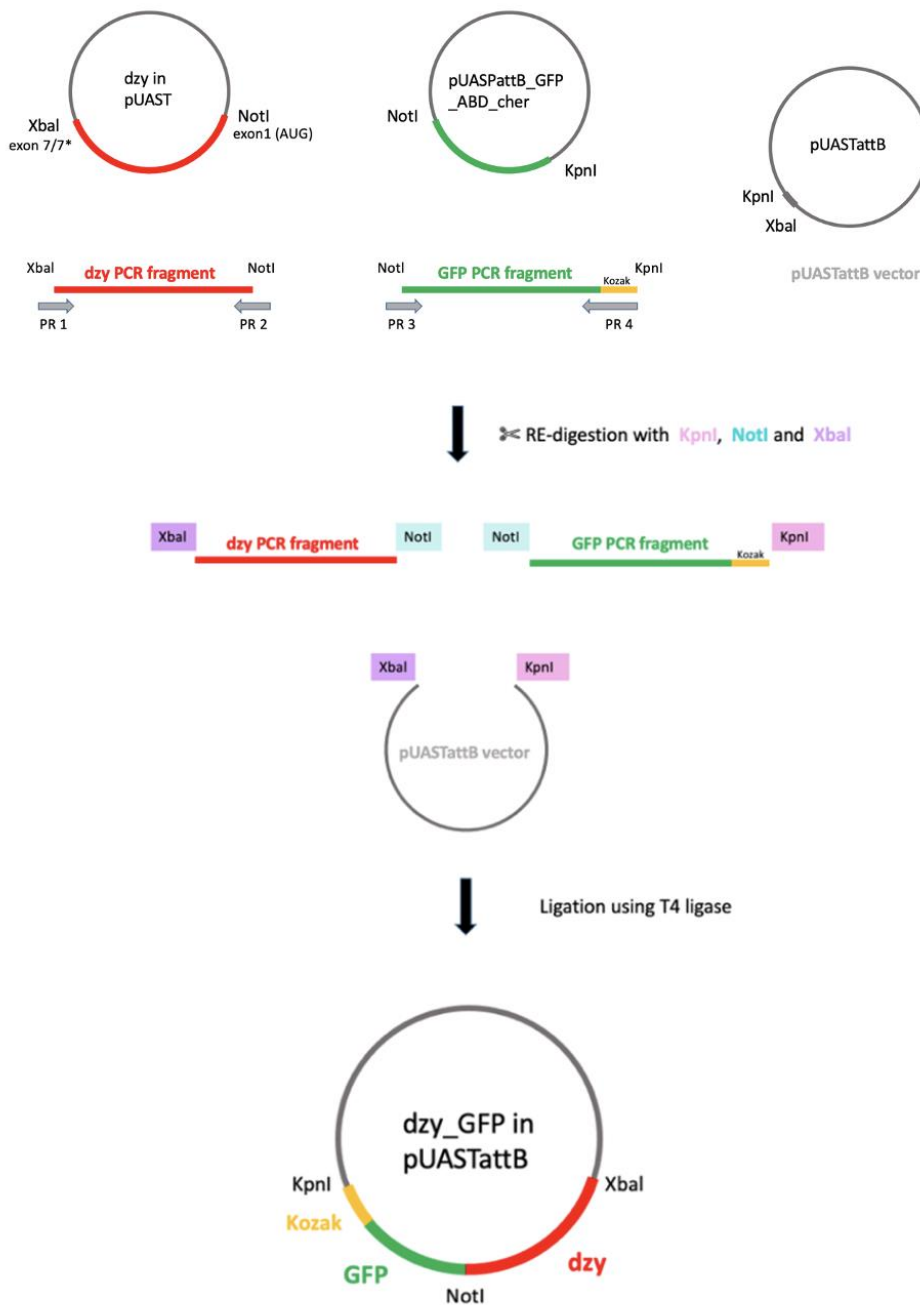
Fig. 51 Cloning of the *dzy_GFP in pUASTattB* constructs using restriction enzyme digestion.
The different *dzy* fragments and the *GFP* fragment were amplified by PCR from the *dzy in pUAST* constructs and the *pUASPattB-GFP_ABD_cher* plasmid. Forward and reverse primers inserted the appropriate restriction sites. The PCR products were then cut with the appropriate restriction enzymes (*dzy* fragment: XbaI/NotI, *GFP* fragment: NotI/KpnI) and ligated into the linearised pUASTattB *Drosophila* transformation vector (*pUASTattB* vector: KpnI/XbaI). DNA fragments and the digested vector backbone were assembled using T4 DNA ligase, generating the *dzy_GFP in pUASTattB* constructs.

<u>*dzy* fragments</u>

Primers containing appropriate restriction enzyme sites were generated (PR2 Top ABC, PR1a Bottom dzyA and PR1b Bottom dzyBC) and used for PCR to amplify the A, B and C fragments of *dzy*. The primer combinations were used to generate larger parts of *dzy* in a single PCR reaction. Phusion® High-Fidelity Polymerase or HotStar HiFidelity Polymerase was used for all PCR reactions. PCR amplification of fragments requires a forward (fw, Top) and reverse (rev, Bottom) primer for each fragment. The different *dzy* isoforms were amplified by PCR from the respective *dzy in pUAST* constructs (*dzyA in pUAST*, *dzyB in pUAST* and *dzyC in pUAST*) using PR2 Top ABC and PR1a Bott A (*dzyA*) or PR2 TopABC and PR1b Bott BC (*dzyB* and *dzyC*). PR1 came in two variants (PR1a and PR1b) because, unlike *dzyB* and *dzyC*, *dzyA* ends with exon 7 instead of exon 7* and therefore required a different primer sequence for the C-terminal part. The PCR-generated *dzy* fragments thus started with the AUG start codon in exon 1 and ended with exon 7/7* (cf. Boettner & van Aelst 2007). PR2 Top ABC was located just before the actual translation start in exon 1 and contains the NotI restriction site (Fig. 52). Compared to the *dzy in pUAST* constructs, the *dzy_GFP in pUASTattB* constructs should follow the *dzyGFP* form (Boettner & van Aelst 2007) and start with exon 1 instead of exon 0. The second primer (PR1) was located in exon 7 (*dzyA*) Bott A or exon 7* (*dzyB* and *dzyC*) Bott BC. A restriction site for the restriction enzyme XbaI was inserted into this primer. To see which of the fragments had successfully been amplified, the PCR products were separated on agarose gel for 30 minutes. The results of the test PCR reaction shown in Fig. 54 indicated that the *dzyA* fragment, the *dzyB* fragment and the *dzyC* fragment were successfully amplified using this method (Expected bands: *dzyA* 5017 bp, *dzyB* 4840 bp and *dzyC* 4399 bp). Bands around 5000 bp were cut from the gel and the DNA was then purified. Gel purification was performed with column elution from the gel using the Macherey Nagel Nucleospin® Gel and PCR Clean-up Kit, the NEB Monarch® DNA Gel Extraction Kit or the OMEGA E.Z.N.A® Gel Extraction Kit.
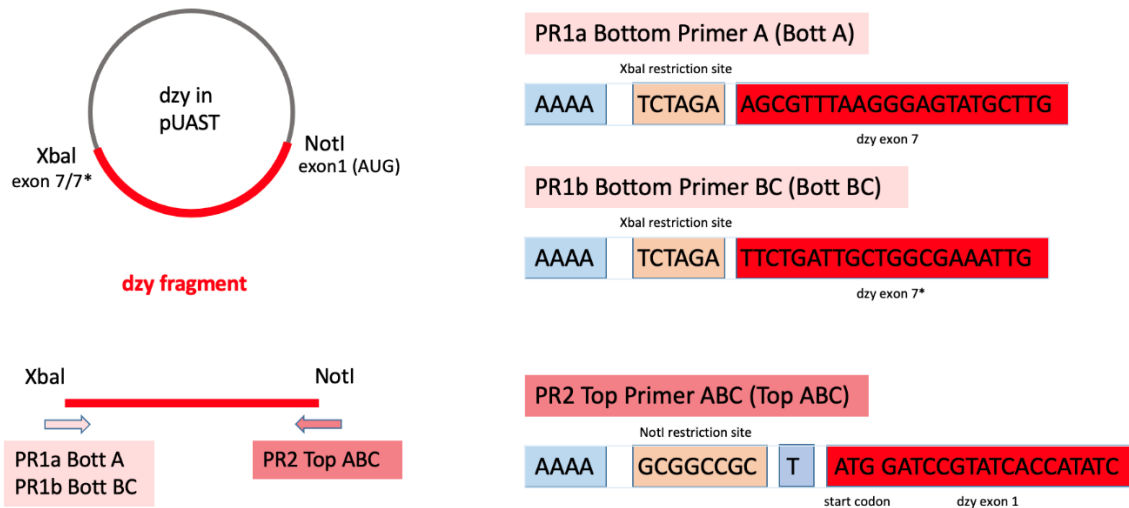
Fig. 52 Primers for the amplification of the *dzy* fragments.
Primers containing appropriate restriction enzyme sites and a gene-specific sequence were generated (PR2 Top ABC, PR1a Bottom *dzyA* and PR1b Bottom *dzyBC*) and used for PCR to amplify the A, B and C fragments of *dzy*. PR1 was located in exon 7 (*dzyA*) PR1a Bott A or exon 7* (*dzyB* and *dzyC*) PR1b Bott BC. A restriction site for the restriction enzyme Xbal was inserted into this primer. PR2 Top ABC was located in exon 1 before the translation start and contained the NotI restriction site.

GFP fragment

For the amplification of the *GFP* fragment, we had designed a forward primer PR4 (Top GFP) and a reverse primer PR3 (Bott GFP). Primer 4 (PR4) Top GFP and primer 3 (PR3) Bott GFP flank the complete *GFP* fragment. As with the *dzy* fragments, restriction sites were introduced into the GFP sequence. The two primers thus contained the priming sequence of GFP and inserted two restriction sites (Fig. 53).
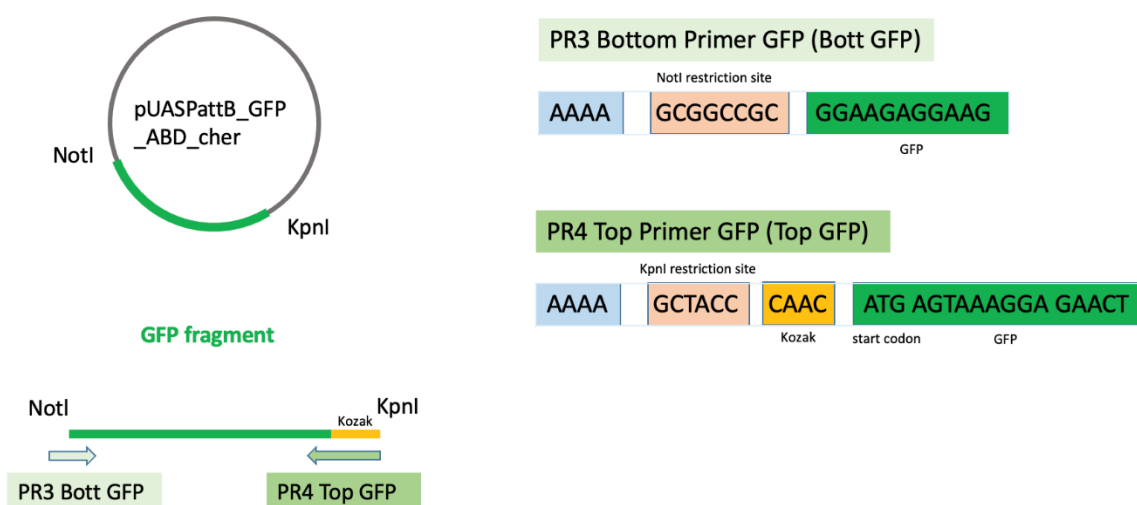
Fig. 53 Primers for the amplification of the *GFP* fragment.
A forward and a reverse primer containing appropriate restriction enzyme sites and a gene-specific sequence were generated (PR 4 Top GFP and PR 3 Bottom GFP) and used for PCR to amplify the *GFP* fragment. PR4 Top GFP and PR3 Bott GFP flank the complete *GFP* fragment. PR4 Top GFP introduced the Kozak sequence and a KpnI restriction site into the PCR product. PR3 Bott GFP inserted the required NotI restriction site. The construct *pUASPattB-GFP_ABD_cher* was used as a template to amplify the *GFP* cDNA.

For the GFP forward primer PR4, we further incorporated a Kozak sequence of CAAC (Cavener 1987) to facilitate subsequent transcription. The Kozak sequence was located right at the beginning of the GFP sequence (Fig. 53). Primer 4 introduced the Kozak sequence and the KpnI cleavage site into the later PCR product. Primer 3 at the 5' end of the *GFP* fragment inserted the required NotI restriction site as described in the cloning scheme (Fig. 51). The construct *pUASPattB-GFP_ABD_cher* (10948 bp) was used as a template to amplify the *GFP* cDNA. The PCR product was separated on agarose gel and the *GFP* fragment, amplified from the *pUASPattB-GFP_ABD_cher,* showed up at the expected 752 bp length (Fig. 54). The DNA was isolated from the gel and purified using the gel extraction kits described above (see <u>dzy fragments</u>).
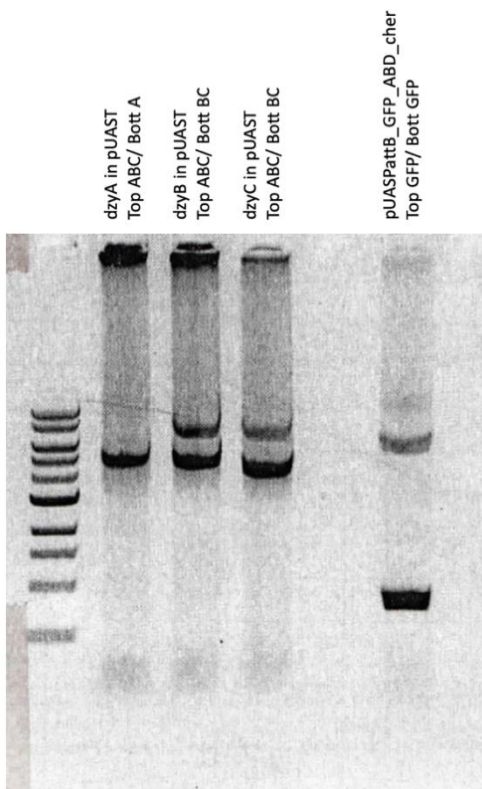

Fig. 54 Analysis of the PCR products *dzyA*, *dzyB*, *dzyC* and *GFP* by agarose gel electrophoresis. After PCR with the PCR primers Top GFP, Bott GFP, Top ABC, Bott A and Bott BC, DNA was run for 20 min at 100 V on a 0.8 % agarose gel. DNA bands were imaged under a gel doc (gel documentation system). The first lane showed the *dzyA* fragment (5017 bp), the second lane the *dzyB* fragment (4840 bp) and the third lane the *dzyC* fragment (4399 bp). The fourth lane contained the *GFP* gene, which was amplified from the *pUASPattB-GFP_ABD_cher* and had the expected 752 bp length. GeneRuler DNA ladder mix was used for size determination. The DNA bands corresponding to the different fragments were extracted from the gel using Macherey Nagel, NEB or Omega Gel Extraction Kit.

Before the three *dzy* fragments and the *GFP* fragment could be cloned into the *pUASTattB* vector, they had to be digested and gel purified. The individual fragments were cut with the respective restriction enzymes (*dzy* fragment with NotI-HF/XbaI; *GFP* fragment with NotI-HF/KpnI-HF), separated on a 0.8 % agarose gel and purified from the gel. Three alternative strategies were considered: Macherey Nagel Nucleospin® Gel and PCR Clean-up Kit, NEB

Monarch® DNA Gel Extraction Kit or the Omega E.Z.N.A® Gel Extraction Kit.

pUASTattB vector

The digested PCR fragments *GFP* and *dzyA*, *dzyB* and *dzyC* were to be assembled into the vector *pUASTattB*. Bacteria stocks containing the *pUASTattB* plasmid (8489 bp) were grown in LB medium with appropriate antibiotics, and DNA Midipreps were prepared as described in Material & Methods. The *pUASTattB* plasmid was digested with the restriction enzymes KpnI-HF and XbaI, for 1.5 to 3 hours at 37 °C before the vector was treated with rAPid Alkaline Phosphatase for 30 minutes at 37 °C to prevent relegation of the vector in the ligation reaction. DNA was separated on a 0.8 % agarose gel for about 30 minutes. The linearised vector on 8485 bp was excised from the gel and purified using NEB and Omega Gel Extraction Kits. As an alternative to the purification kits used, alcohol precipitation (see Materia & Methods) was also performed to purify the DNA.

Ligation und transformation

The digested gel-purified PCR products, the *dzy* fragments and the *GFP* fragment were then ligated into the linearised vector *pUASTattB*. The concentration and purification of the digested PCR products and the linearised vector were determined using Nanodrop 2000. DNA fragments and the digested vector backbone were assembled using T4 DNA ligase (see Material & Methods). For the ligation reaction with the three subunits (*GFP*, *dzy* and *pUASTattB*), we used 50 ng of the linearised vector and three times the amount of inserts (molar ratio 1:3 vector:insert). The ligation reaction was performed with a digested vector concentration of 50 ng. The calculation performed to determine the amount of fragment (ng) to be used with the corresponding amount of backbone was done using the T4 ligase formula (see Material & Methods). The mixture was incubated at room temperature overnight or at 37 °C for 2 hours. After inactivation of the ligase for 15 minutes at 65 °C, the ligation reaction was transformed into chemically competent *E. coli DH5α* cells and plated onto media containing Amp (see Material & Methods). Single colonies were picked from the plates and were grown overnight. Plasmid DNA was purified using peqGold Plasmid Miniprep Kit. To check for plasmid DNA with correct inserts, purified DNA was tested via PCR and RE-digestion.

For the test PCR reaction with Taq-polymerase, one primer was chosen in *dzy* exon 3 (PR231) and a second primer in *dzy* exon 6 (PR188). Depending on whether the *GFP* fragment was located between the two parts, the size of the PCR product obtained changed. The different *dzy in pUAST* constructs (*dzyA in pUAST*, *dzyB in pUAST* and *dzyC in pUAST*) were used as controls. The resulting DNA fragments were separated, a 0.8 % agarose gel was used to confirm that the cloning of *dzy* and *GFP* in *pUASTattB* was successful. In parallel with the

PCR, a test digest reaction of the DNA was also performed. For the digest reaction, the purified DNA was digested with XhoI and the resulting DNA fragments were separated on a 0.8 % agarose gel. After digestion with the restriction enzyme, two bands should be seen, one band at approximately 2600 bp and one band at approximately 12000 bp. The different *dzy in pUAST* constructs were used as controls. Despite multiple repetitions, a change in ligation time and quantity ratios between the individual components, no correct clones could be found. Cloning such a large fragment and vector turned out to be complex. Therefore, the cloning strategy was adapted: parallel to the direct cloning into the *pUASTattB* vector, an approach with an intermediate cloning step was performed. The *dzy* fragments and the *GFP* fragment were first to be cloned into a *pBluescript* vector (*pBS KS+*) and then transferred into the *pUASTattB* vector. The *dzy* fragment and the *GFP* fragment were cloned into a NotI/KpnI (*GFP*) and a NotI/XbaI (*dzy*) digested *pBluScript* (*pBS KS+*) vector. Intermediate cloning of the inserts into *pBS KS+* also ensured that all fragments involved in the final cloning step (*dzy_GFP pUASTattB*) had the required restriction sites. Despite an alternative approach and multiple repetitions, no correct clones were found here either.

3.7.2 Cloning of the *dzy_GFP in pUASTattB* constructs using the NEBuilder HiFi DNA Assembly

Overall, the assembly with two fragments inserted into the *pUASTattB* vector via various restriction enzymes in the previously used way (Fig. 51) did not produce a final construct after several attempts, so we switched to a new method, the NEBuilder HiFi DNA Assembly. NEBuilder HiFi DNA Assembly Master Mix is used to improve the efficiency and accuracy of DNA assembly. This method allows seamless assembly of multiple DNA fragments, regardless of fragment length or end compatibility. The NEBuilder Master Mix enables restriction-free assembly of one or more DNA fragments in a one-step isothermal reaction in less than one hour, without the need for unique restriction sites. The *in vitro* overlap-based cloning method was used as previously described (see Materials & Methods). Briefly, DNA fragments (*dzyA*, *dzyB*, *dzyC* and *GFP*) with 15 to 20 bp long homology regions were prepared by PCR and assembled with linearised and dephosphorylated plasmids. The NEBuilder Assembly Master Mix reaction contains different enzymes working together in the same reaction mixture (Fig. 55): the exonuclease created single-stranded 3' overhangs that facilitate the annealing of the overlap regions, the polymerase fills in the gaps within the annealing fragment, and the DNA ligase seals the nicks in the assembled DNA. The end result is a double-stranded, fully sealed DNA molecule that serves as a template for a variety of other molecular biology applications, including direct transformation of *E. coli*. The transformation was performed according to the NEB high efficiency protocol (see Material & Methods). The correctness of the DNA assembly was verified by sequence analysis (PCR and sequencing (LGC Genomics)).
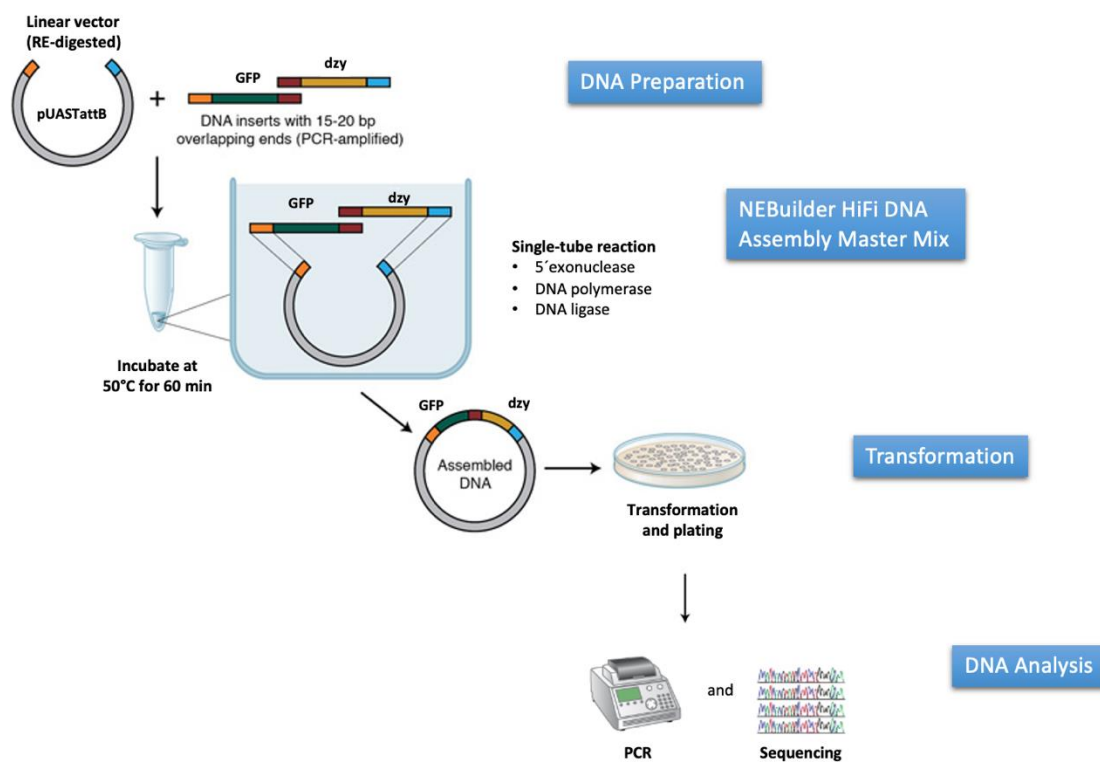
Fig. 55 Illustration of the workflow of the NEBuilder HiFi DNA Assembly method.
Primers were designed to amplify fragments with appropriate overlaps using a high-fidelity DNA polymerase. Linearised vector was prepared by restriction enzyme digestion using the restriction enzyme EcoRI. The two PCR fragments (*dzy* and *GFP*) and the linearised vector (*pUASTattB*) were added to NEBuilder HiFI DNA Assembly Master Mix containing the three enzymes exonuclease, polymerase and DNA ligase and incubated at 50 °C for one hour. The reaction mix was then transformed into *DH5-alpha* competent *E. coli*. DNA analysis was performed by PCR and sequencing (LGC Genomics).

Design and PCR of fragments for DNA Assembly

The overarching strategy for the cloning process began with the amplification of the inserts with primers that had 15 - 25 nt overlap with their respective neighbouring fragments (Fig. 55). Furthermore, the backbone vector was prepared via digestion with the restriction enzyme required for the respective vector. These components were then ligated together using the NEBuilder HiFI DNA Cloning Kit. The NEBuilder HiFI DNA Assembly Master Mix was used to assemble the *pUASTattB* vector backbone and the *dzy* and *GFP* insert fragments to obtain the constructs *dzyA_GFP in pUASTattB*, *dzyB_GFP in pUASTattB* and *dzyC_GFP in pUASTattB*. The NEBuilder Assembly Tool, available at nebuilder.neb.com, was used to design PCR primers with overlapping sequences between adjacent DNA fragments and for their assembly into a cloning vector (Appendix Fig. S13). The structure of the overlapping PCR primers for use in HiFi DNA assembly consisted of two sequence components: an overlapping sequence required for correct annealing of adjacent fragments and a gene-specific sequence required

for template priming during PCR. In general, the non-priming overlap sequence was added at the 5' end of the primer. This sequence is homologous to the 5' terminal sequence of the adjacent fragment to be assembled. The priming gene-specific sequence was added at the 3' end of the primer after the overlap sequence. Using the NEB tool, we designed different primers with nucleotide overhangs for the assembly of the two PCR fragments (*dzyA*, *dzyB* or *dzyC* and *GFP*) into the cloning vector *pUASTattB* (Fig. 56).
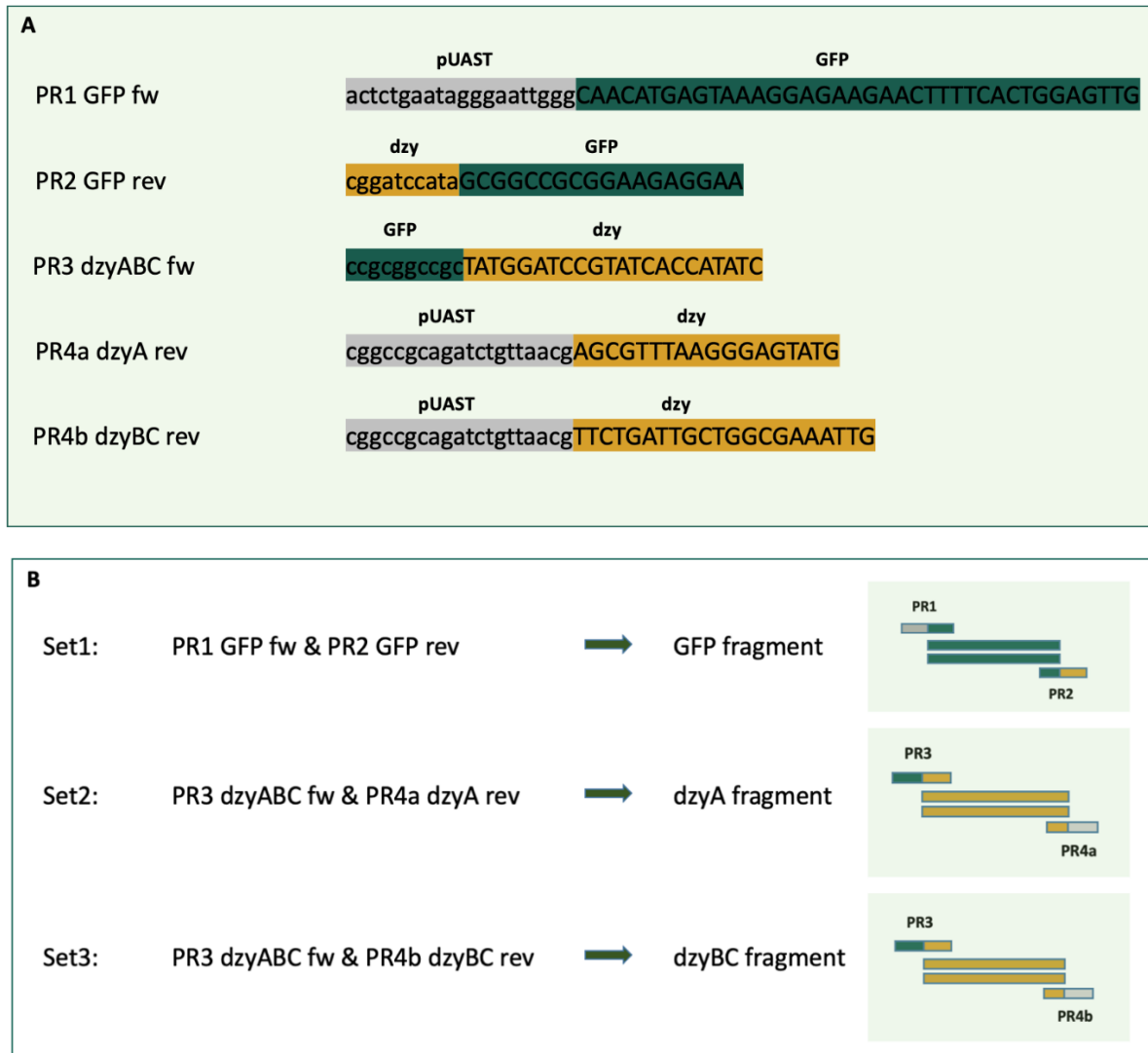

Fig. 56 Primers for NEBuilder HiFi DNA Assembly.
The NEBuilder Assembly Tool was used to design PCR primers with overlapping sequences between adjacent DNA fragments. (A) The structure of the PCR primers consisted of two components: an overlapping sequence required for correct annealing of adjacent fragments and a gene-specific sequence required for template priming during PCR. PR1 (GFP fw) and PR2 (GFP rev) were designed for amplification of the *GFP* fragment and PR3 (dzyABC fw) and PR4a (dzyA rev) or PR4b (dzyBC rev) for the amplification of the three *dzy* isoforms. (B) There were three different primer pairs: set 1, *GFP* (PR1 and PR2); set 2, *dzyA* (PR3 and PR4a) and set 3, *dzyB* and *dzyC* (PR3 and PR4b).

PCR amplification of fragments requires a forward (fw) and reverse (rev) primer for each fragment. So, we designed PR1 (GFP fw) and PR2 (GFP rev) for the amplification of the *GFP*

fragment and PR3 (dzyABC fw) and PR4 (dzyA rev and dzyBC rev) to amplify the three *dzy* isoforms. PR4 came in two variants because *dzyA*, unlike *dzyB* and *dzyC*, ended with exon 7 instead of 7* and thus required a different primer sequence for the C-terminal part. In general, we generated three primer pairs containing a forward and a reverse primer for the amplification of both fragments: set 1, *GFP* (PR1 and PR2); set 2, *dzyA* (PR3 and PR4a) and set 3, *dzyB* and *dzyC* (PR3 and PR4b). To clone the two inserts *GFP* and *dzy* into the expression vector *pUASTattB*, terminal regions of linearised *pUASTattB* sequence were added to the 5' ends of the two primers PR1 GFP fw and PR4 dzyA rev/dzyBC rev. So, these primers contain the priming sequence of *GFP* and *dzy* and were homologous to the 3' and 5' regions of the vector (Fig. 56). Specifically, the primers PR1 (GFP fw) and PR4a (dzyA rev)/ PR4b (dzyBC rev) carried a structure, where the first component of the primer matched the vector *pUASTattB* at a side that recognized a restriction enzyme cut site, followed by the priming sequence of *GFP* or *dzy*. For the GFP forward primer PR1, we further incorporated a Kozak sequence of CAAC (Cavener 1987) to aid with later transcription. The Kozak sequence was located directly at the beginning of the GFP sequence (Fig. 56). To generate the *GFP* fragment and the three different *dzy* fragments, the constructs *pUASPattB-GFP_ABD_cher*, *UAS-dzyA*, *UAS-dzyB* and *UAS-dzyC* were used. The upstream *GFP* fragment was PCR amplified from the Cheerio GFP construct *pUASPattB-GFP_ABD_cher* (Sven Huelsmann) using PR1 and PR2 (set 1), while the downstream *dzy* subunits were amplified by PCR from the different *dzy in pUAST* constructs using PR3 and PR4a (*dzyA*, set 2) or PR3 and PR4b (*dzyB* and *dzyC*, set 3). *dzyA in pUAST* served as the template for the *dzyA* fragment, *dzyB in pUAST* for the *dzyB* fragment and *dzyC in pUAST* for the *dzyC* fragment. The *dzy* fragments started with the AUG start codon in exon 1 and ended with exon 7/7* (cf. (Boettner & van Aelst 2007).
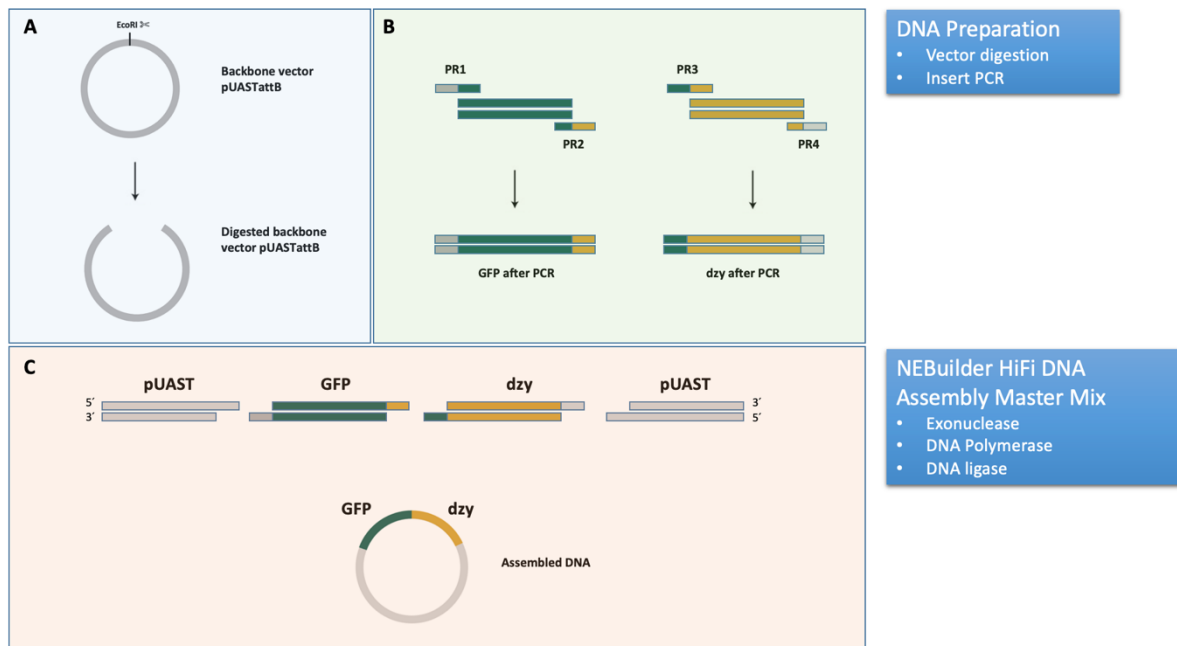
Fig. 57 Schematic assembly of pUASTattB plasmid with *GFP* and *dzy* subunits using NEBuilder HiFi DNA Assembly.
(A) Plasmid backbone *pUASTattB* was digested with the restriction enzyme EcoRI. (B) PCR was performed with the specific primers (designed using NEBuilding Assembly Tool: Primer Design) and generated the different overhang-containing fragments. (C) Ligation reaction was performed using undigested, gel-purified PCR products with the digested vector backbone. Complementary sequences then annealed, creating the *dzy_GFP in pUASTattB* construct. Grey coloured: linearised vector, cut with EcoRI. Green coloured: *GFP* upstream fragment amplified with the primer set 1 (PR1 and PR2). Yellow coloured: *dzyA* subunit amplified with the primer set 2 (PR3 and PR4a), *dzyB* and *dzyC* subunit amplified with the primer set 3 (PR3 and PR4b).

Performing PCR with Phusion® High-Fidelity Polymerase and the specific primers (designed using NEBuilding Assembly Tool: Primer Design), the different overhang containing fragments, *GFP* (768 bp) and *dzyA* (5025 bp), *dzyB* (4846 bp) and *dzyC* (4407 bp), were generated and subsequently purified. PCR products were verified by separation on 0.8 % agarose gels (Fig. 58). GeneRuler DNA ladder mix was used for size determination. DNA was purified using either the NEB Monarch® DNA Gel Extraction Kit, the Omega E.Z.N.A® Gel Extraction Kit and the Zymo Research Zymoclean Gel DNA Recovery Kit.according to the suppliers' respective protocols. Purity and concentration of DNA inserts were checked using the NanoDrop 2000 spectrophotometer. The resulting *dzy* and *GFP* gene sequences contained 15 to 40 nucleotide overlap regions with complementarity to the adjacent fragment and the *pUASTattB* vector (Fig. 56).

Fig. 58 Analysis of the subunits *dzyA*, *dzyB*, *dzyC* and *GFP* by agarose gel electrophoresis.
After PCR with the overlapping primers, DNA was run for 20 min at 100 V on a 0.8 % agarose gel. DNA bands were imaged under a gel doc (gel documentation system). The first lane shows the *dzyA* fragment, the second lane *dzyB* and the third lane the *dzyC* fragment. The fourth lane contains the *GFP* fragment amplified from the *pUASPattB-GFP_ABD_cher* showing up at the expected 757 bp length. GeneRuler DNA ladder mix was used for size determination. The DNA bands corresponding to the different fragments (*dzyA* = 5025 bp, *dzyB* = 4846 bp, *dzyC* = 4407 bp and *GFP* = 768 bp) were extracted from the gel using NEB Monarch® DNA Gel Extraction Kit, the Omega E.Z.N.A® Gel Extraction Kit or the Zymo Research Zymoclean Gel DNA Recovery Kit.
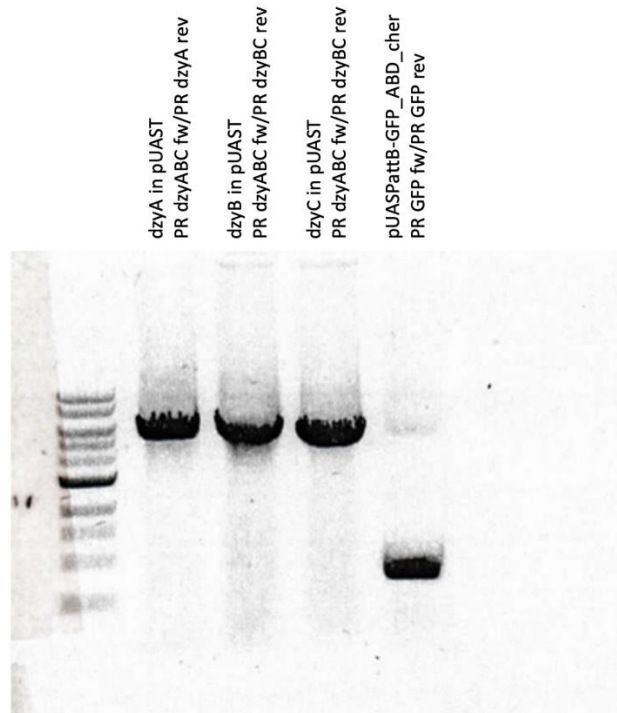
Preparation of the vector with RE-digestion

After generating the fragments using PCR, we prepared our backbone vector via digestion with the incisive single cutting restriction enzyme for the specific vector. In general, the cloning vector can be linearised by any restriction endonuclease displaying one or more unique site(s) at the desired locations within the vector sequence. We digested the plasmid backbone *pUASTattB* with the restriction enzyme EcoRI (NEB) for 90 minutes at 37 °C. To avoid religation of the vector, digested *pUASTattB* was treated with shrimp Alkaline Phosphatase and incubated at 37 °C for 30 minutes. Purification of restriction endonuclease-digested vector was not necessary. The restriction endonuclease EcoRI was heat inactivated at 65 °C for 20 minutes. Without further purification of the linearised *pUASTattB* vector, assembly was run with the confirmed PCR products using the NEBuilder HiFi DNA Assembly Master Mix according to the manufacturer's instructions (Fig. 57).

Ligation Reaction using NEBuilder HiFi DNA Assembly Master Mix

The ligation reaction was performed using undigested, gel-purified PCR products with digested vector backbone. The concentration and purification of the different PCR products and the digested vector were determined using Nanodrop 2000. DNA fragments with 15 - 25 bp overlapping regions and the digested vector backbone were assembled using NEBuilder HiFi DNA assembly protocol as described by the manufacturer. For the assembly of 2 - 3 fragments, the NEBuilder HiFi Assembly manual recommends using 50 - 100 ng of the linearised vector

and twice the amount of inserts. Briefly, the two fragments (*dzy* and *GFP*) were incubated together with the vector at a 1:2 vector:insert molar ratio, in a maximum volume of 10 µl and a maximum molarity of 0.2 pmol. For the NEBuilder reaction, we tried both 50 ng and 100 ng for the vector amount. The calculation performed to determine the amount of fragment (ng) to be used with its corresponding vector amount was done according to the manufacturer's formula (see Material & Methods) or the NEB Ligation Calculator. Each *pUASTattB-dzy_GFP* plasmid Assembly Mix was then filled up to 10 µl with deionised water and 10 µl NEBuilder HiFi DNA Master Mix was added. The mixture was incubated at 50 °C for 1 hour. During the one-hour incubation, the three enzymes of the Master Mix (exonuclease, DNA polymerase and DNA ligase) set to work on the fragments. First, the exonuclease component of the NEBuilder DNA HiFi Assembly Master Mix chewed back the 5' end to create the single-stranded 3' overhangs to facilitate assembly of the overlapping regions. These complementary sequences then annealed, creating the double-stranded DNA of interest. Subsequently, a high-fidelity DNA polymerase elongated the 3' ends, filling the gaps that form between the assembled fragments, and a DNA ligase finally sealed the remaining nicks. The end result was a fully-sealed, double-stranded DNA molecule that could be used as a template for a variety of molecular biology applications, including direct transformation of chemically competent *E. coli*.

Transcription and DNA Analysis (PCR and Sequencing)

We used NEBuilder DNA HiFi Assembly Master Mix to facilitate the ligation reaction and then transformed this cloning product into chemically competent bacterial cells. After 1 hour, 2 µl of the NEBuilder ligation mixture were used for the transformation of competent *DH5α* cells. A transformation volume of 100 µl out of 500 µl total volume was plated on LB agar plates containing Amp. After 16 hours, many colonies grew on the agar plates and 8 single colonies were isolated from different agar dishes with different molarity ratios (undiluted and 2:6 dilution). Individual colonies picked from the plates were grown in 5 ml LB medium with added Amp, and plasmid DNA was extracted from the broth and purified using peqGold Plasmid Miniprep Kit or TELT Miniprep. Test PCR of the colonies was performed with the primer pair PR101 (*pUAST*) und PR160 (*dzy* exon 2). A 0.8 % agarose gel was used to screen for the expected plasmid size: *dzyB_GFP in pUASTattB* (Fig. 59) and *dzyC_GFP in pUASTattB* (Fig. 60), both measured at 938 bp. *dzyC in pUAST* (436 bp) served as a control for the PCR reaction. The DNAs that appeared in the correct size on the gel were sent for sequencing to confirm that the cloned plasmids had the correct insertion sequence and direction. The sequencing results confirmed that *dzyB* clone 10 and *dzyC* clone 5 were the two constructs *dzyB_GFP in pUASTattB* and *dzyC_GFP in pUASTattB*. Cloning of the *dzyA_GFP in pUASTattB* construct was not previously possible. By means of PCR and subsequent sequencing, it could be shown that the *dzyA* fragment was correctly incorporated into the

vector. The *GFP* fragment, on the other hand, was missing; instead, an undefinable mini-fragment was inserted between the *dzyA* fragment and the *pUASTattB* vector.
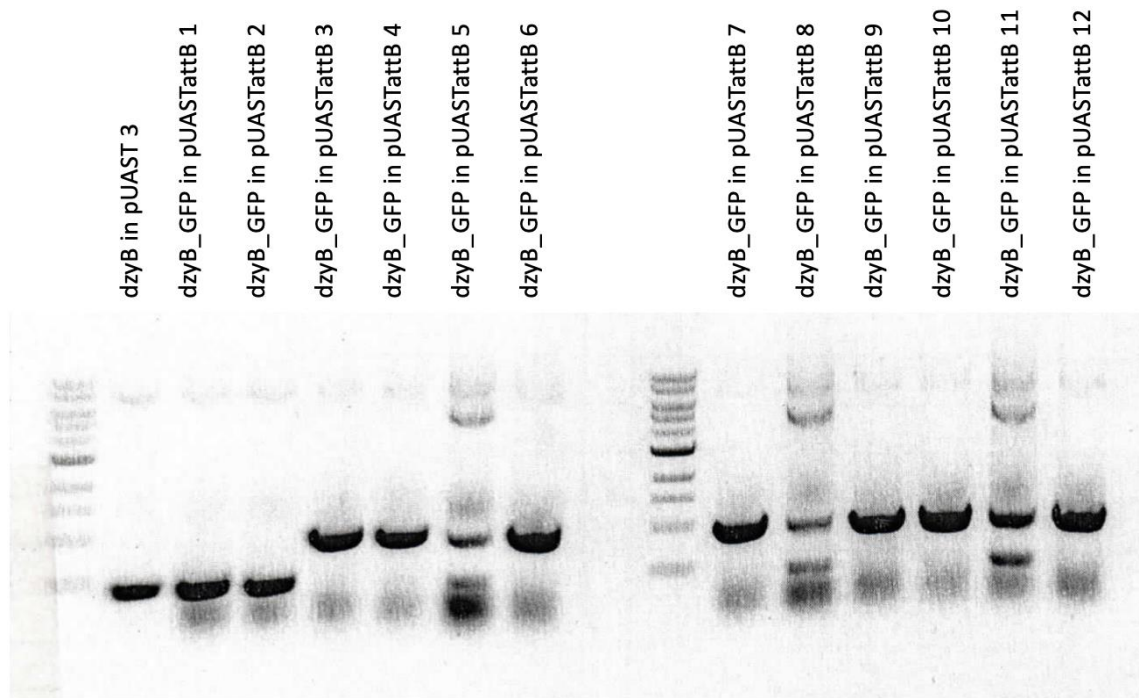

Fig. 59 Agarose gel electrophoresis of the *dzyB_GFP in pUASTattB* assembled construct.
Test PCR of the colonies was performed with the primer pair PR101 (*pUAST*) und PR160 (*dzy* exon 2). A 0.8 % agarose gel was used to screen for the expected plasmid size: *dzyB_GFP in pUASTattB*, 938 bp. *dzyB in pUAST* (436 bp) served as a control for the PCR reaction. DNA *dzyB in pUASTattB* clone 4, 5, 7, 9, 10 and 11 appeared at the correct size on the gel. *dzyB in pUASTattB* clone 10 was sent for sequencing to confirm that the cloned plasmids had the correct insertion sequence and direction.
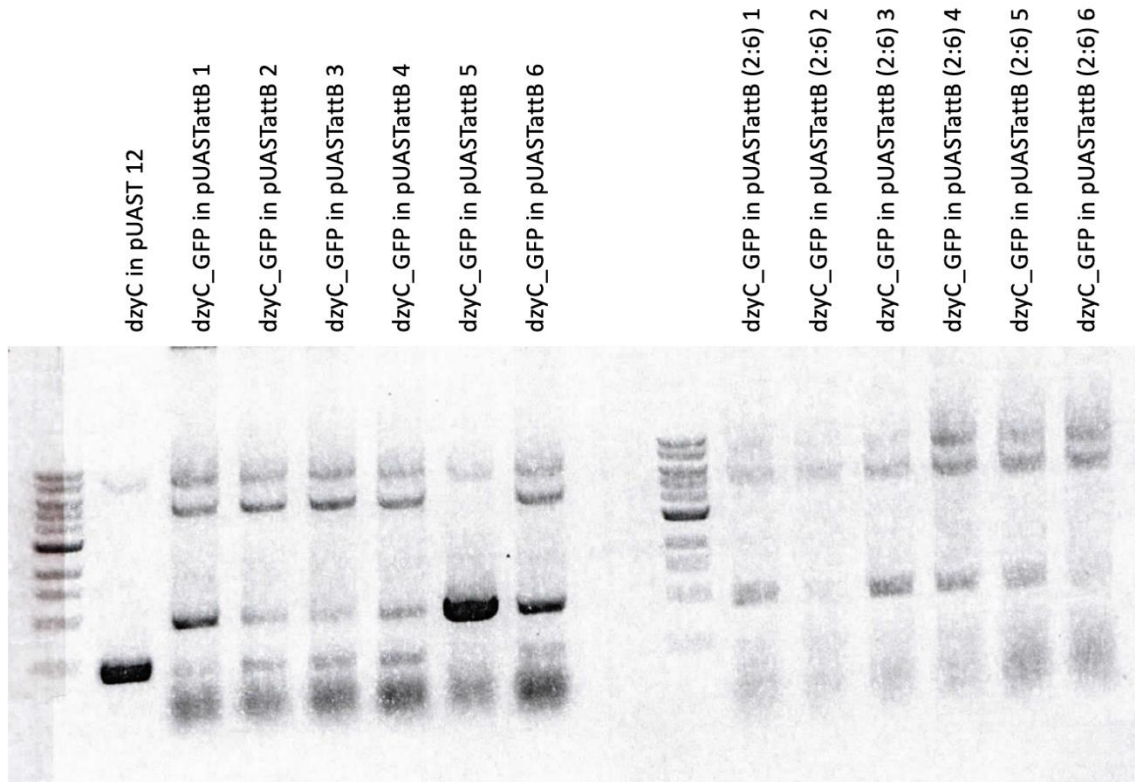
Fig. 60 Agarose gel electrophoresis of the *dzyC_GFP in pUASTattB* assembled construct.
Test PCR of the colonies (transformation with undiluted or 2:6 diluted ligation mix) was performed with the primer pair PR101 (*pUAST*) und PR160 (*dzy* exon 2). A 0.8 % agarose gel was used to screen for the expected plasmid size: *dzyC_GFP in pUASTattB,* 938 bp. *dzyC in pUAST* (436 bp) served as a control for the PCR reaction. DNA *dzyC in pUASTattB* clone 1, 5 and 6 appeared at the correct size on the gel. *dzyC in pUASTattB* clone 5 was sent for sequencing to confirm that the cloned plasmids had the correct insertion sequence and direction.

Injection und crossing with *srph-Gal4* flies

The verified clones *dzyB_GFP in pUASTattB* and *dzyC_GFP in pUASTattB* were purified using the Macherey Nagel® NucleoBond® Xtra Midi Kit and then injected into 30-min-old dechorionated embryos. The two constructs were injected into the attP-containing fly strain *yw C31; +; 86 FB* (see Material & Methods). Offspring with red eyes were tested for the presence of *dzy_GFP in pUASTattB* construct using DNA preparation of single flies and the primer pair PR100 (*pUAST*) and PR181 (*dzy* exon 4). The two primers could only amplify a fragment if both the vector and the *dzy* sequence were present. All DNAs from each fly strain (see Appendix Tab. S3; *UAS-dzyB_GFP* and *UAS-dzyC_GFP* transgenic lines) appeared in the right size on the gel. *dzyB_GFP in pUASTattB* and *dzyC_GFP in pUASTattB* showed the expected signal. *w⁻* flies served as negative controls. To investigate the expression of the different GFP-coupled splice forms in macrophages, the newly generated *dzy_GFP* strains were crossed with *srph-Gal4/UAS-cd2* flies (Fly strain collection stock 580). The flies were placed together in a cage and the plates gathered the next day. Embryos of different stages were collected, dechorionated, fixed and then examined under the fluorescence microscope.

148

All embryos should have both *srph-Gal4* and *UAS-dzy_GFP* and thus show fluorescent macrophages. When crossing the transgenic animals carrying the constructs *dzyB_GFP in pUASTattB* or *dzyC_GFP in pUASTattB* with animals carrying a macrophage-specific *srph-Gal4* driver coupled with *UAS-cd2*, we were unable to detect fluorescent macrophages. Instead of fluorescent macrophages, a luminescent peripheral nervous system (PNS) could be observed in most of the embryos.

For further investigations, test crosses with different Gal4 drivers and UAS strains were carried out:

	Effector line		Activator line	Results
A	UAS-dzyC_GFP 4	x	srp-Gal4	Fluorescent peripheral nervous system (PNS). No macrophages were visible.
B	UAS-dzyB_GFP 1	x	srp-Gal4	Fluorescent PNS; no macrophages were visible.
C	UAS-dzyGFP (Boettner, 2007)	x	srp-Gal4	Strong autofluorescence: intestine, yolk, salivary glands. Macrophages were particularly visible in early embryos.
D	UAS-dzyC_GFP 1	x	prd-Gal4	prd-Gal4 pattern was detected in early embryos, later fluorescent PNS.
E	UAS-dzyC_GFP 8			Fluorescent PNS was observed.
F	UAS-dzyB_GFP 6			Fluorescent PNS was observed.
G	Injection line (yw, C31; +; 86 FB)			Fluorescent PNS was observed.
H	R24 (w; +; TM3/TM6B)			No fluorescent PNS was found.

dzyGFP (Fly strain collection stock 1235, (Boettner & van Aelst 2007)) was crossed with virgins (Fly strain collection stock 580) to verify the functionality of the *srph-Gal4* strain. Embryos of this cross showed strong autofluorescence, but macrophages were visible mainly in early embryos. To test the functionality of the newly generated *UAS-dzy_GFP* strains, *prd-Gal4* was

149

used as Gal4 driver instead of *srph-Gal4*. The typical *prd-Gal4* pattern was visible in early embryos, but later the PNS was also clearly visible. Then, deposits of the injection line and the *UAS-dzy_GFP* strains were examined under the fluorescence microscope. In both strains, embryos showed a bright, luminescent PNS. The fluorescent PNS was therefore already found in the injection strain. To investigate whether the presence of PhiC31 integrase leads to the fluorescent PNS phenotype, *UAS-dzy_GFP* strains were generated without PhiC31 integrase (ØPhiC31) on the X-chromosome (Fig. 61).
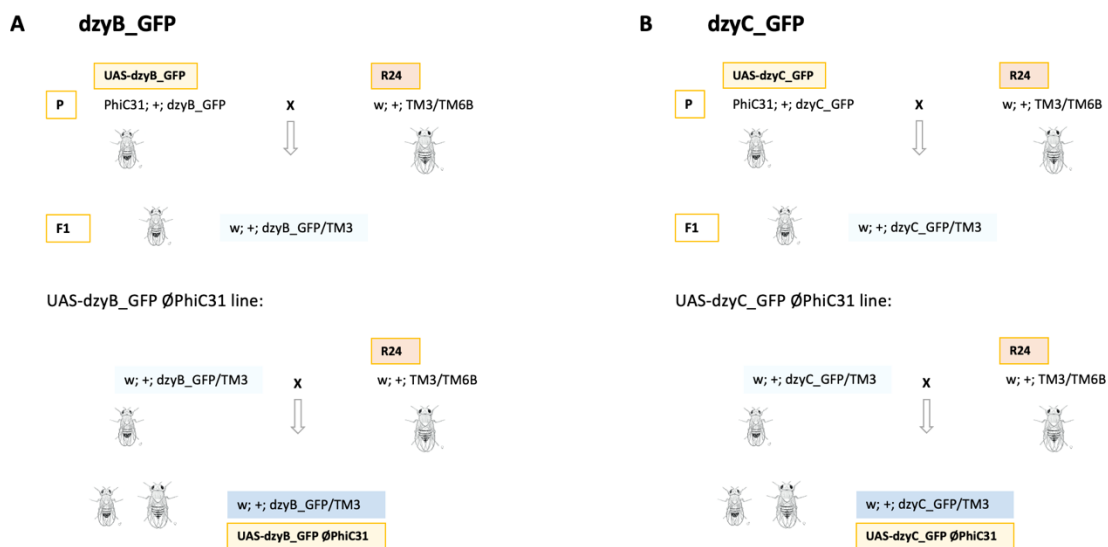
Fig. 61 Crossing scheme for the generation of the fly strains (A) *UAS-dzyB_GFP ØPhiC31* and (B) *UAS-dzyC_GFP ØPhiC31*.
UAS-dzy_GFP males were crossed to the balancer chromosome strain R24. TM3 male flies were collected from the progeny. For maintenance of the strains, the TM3 males were again crossed with the balancer chromosome strain R24.

The transgenic fly strains: *UAS-dzyB_GFP 1 ØPhiC31* (dzyB_GFP 3 No 3), *UAS-dzyB_GFP 6 ØPhiC31* (dzyB_GFP #5), *UAS-dzyC_GFP 1 ØPhiC31* and *UAS-dzyC_GFP 9 ØPhiC31* were crossed with animals carrying the macrophage-specific *srph-Gal4* driver coupled with *UAS-cd2* and the progeny were examined under the fluorescence microscope. Although any fluorescent nervous system was no longer observable, we still could not detect macrophages.

	Effector line		Activator line	Results
A	UAS-dzyB_GFP 2 ØPhiC31	X	srp-Gal4	No macrophages detected; autofluorescence salivary glands, gastrointestinal tract
B	UAS-dzyB_GFP 6 ØPhiC31	X	srp-Gal4	No macrophages detected; autofluorescence salivary glands, gastrointestinal tract
C	UAS-dzyC_GFP 1 ØPhiC31	X	srp-Gal4	No macrophages detected; autofluorescence salivary glands, gastrointestinal tract
D	UAS-dzyC_GFP 9 ØPhiC31	X	srp-Gal4	No macrophages detected; autofluorescence salivary glands, gastrointestinal tract

	Effector line		Activator line	
E	UAS-dzyGFP (Boettner, 2007)	X	srp-Gal4	Macrophages were clearly visible.
F	UAS-Stinger	X	srp-Gal4	Macrophages were visible
G	UAS-dzyC_GFP 1 Ø PhiC31	X	h-Gal4	7 stripes were faintly visible in individual embryos

4. DISCUSSION

4.1 The PDZ-GEF Dzy regulates cell adhesion during macrophage migration

Cell migration is an essential element of morphogenesis during embryonic development of the animal organism and contributes significantly to the formation of its organs. We aim to contribute to the elucidation of the molecular mechanisms that trigger and control cell migration in the organism using the migration of mature macrophages in the *Drosophila* embryo as a model. Our analysis focuses on the function of the G-nucleotide exchange factor Dzy. In an EP-screen, *dzy* was identified as an essential gene for the regulation of cell shape and cell migration of macrophages in the *Drosophila* embryo. The loss-of-function phenotype shows that macrophages lacking function of *dzy* have smaller protrusions and migrate less efficiently (see Introduction; Huelsmann *et al.* 2006). Complementary, the gain-of-function phenotype also demonstrates that macrophages overexpressing Dzy from a single copy of the gene have larger protrusions, and macrophages overexpressing Dzy from two copies do not migrate efficiently. Thus, the motility of macrophages is not significantly affected when Dzy is overexpressed by one copy of dzy^{EP}, although the cell shape changes dramatically (Huelsmann *et al.* 2006). However, if *dzy* expression is further increased to two copies of dzy^{EP}, macrophage migration is slowed down. The dose of Dzy expression is therefore crucial for the regulation of cell shape and macrophage migration in the *Drosophila* embryo. On the one hand, these Dzy-induced effects require the function of the small GTPase Rap1 during macrophage migration: in *rap1* mutants, Dzy activity has no effect on the migrating macrophages (Huelsmann *et al.* 2006). These data suggest that Dzy may be a GEF for Rap1. The finding that Dzy activity requires Rap1 is consistent with mammalian cell culture experiments, as well as with other studies from *C.elegans* to humans (Rooij *et al.* 1999; Rebhun *et al.* 2000; Gao *et al.* 2001; Liao *et al.* 2001; Lee *et al.* 2002; Kuiperij *et al.* 2003; Pellis-van Berkel *et al.* 2005). On the other hand, the activity of Dzy and Rap1 requires the function of βPS integrins (Huelsmann *et al.* 2006; Siekhaus *et al.* 2010), suggesting that the PDZ-GEF Dzy regulates cell shape changes and cell migration via modulation of integrin-dependent adhesion. The finding that reduced RhoA function enhances the effect of Dzy is consistent with the fact that Dzy promotes integrin-mediated adhesion, as RhoA is thought to regulate the disassembly of integrin-containing adhesion complexes during cell migration (Worthylake *et al.* 2001; Ridley *et al.* 2003; Huelsmann *et al.* 2006). RhoA thus suppresses the function of Dzy in promoting adhesion. These data provide the first evidence for a signaling pathway in which Dzy regulates integrin-dependent adhesion via Rap1, which is suppressed by the function of RhoA during embryogenesis. What is interesting here is that the regulation of cell adhesion pathways via

Rap1 and integrins is similarly involved in human leukocyte migration (Sebzda *et al.* 2002; Katagiri *et al.* 2004). This suggests potentially conserved mechanisms regulating macrophage migration in the *Drosophila* embryo. This leads to the promising conclusion that in understanding the mechanisms of macrophage migration in *Drosophila*, new information on cell migration in all organisms will be uncovered. Many questions remain open: Our analysis focuses on the function of the G-nucleotide exchange factor Dzy, which is formed in three splice isoforms (*dzyA*, *dzyB* and *dzyC*). During this work, we addressed two main questions: (1) Do the different isoforms of Dzy have different functions? (2) What is the function of the conserved PDZ domain and the proline-rich motifs of Dzy? Are they relevant for cell migration and for cell shape change in macrophages? To reveal the function of *dzy* during migration of embryonic macrophages, we analysed the gene locus and the different splice forms, generated mutants and described their macrophage phenotype.

4.2 Characterisation of the molecular structure of the *dzy* gene

This work provides the first detailed characterisation of the structure-function relationships of the PDZ-GEF protein Dzy. We have analyzed three different splice forms of *dzy* (*dzyA*, *dzyB* and *dzyC*), which have equivalent 5' ends and different 3' ends. We have also shown that the splicing of *dzy* may be developmentally regulated and that this splicing results in functionally distinct proteins. Furthermore, of the three isoforms, only the *dzyC* form is able to cause a change in cell shape when expressed in the macrophages; and only this isoform is sufficient to partially rescue the characteristic escaper phenotype of homozygous adult flies. The only difference between *dzyC* and the other splice forms (*dzyA* and *dzyB*) is the presence or absence of exon 5 in the different splice forms. The domain encoded by exon 5 (including the proline-rich motifs PRM2 and PRM3) interacts intramolecularly with the PDZ domain of Dzy and has a function-inhibiting effect.

<u>*dzy* has three different isoforms</u>

We have systematically analysed the *dzy* mRNAs and characterised the structure of the *dzy* transcripts. Based on various ESTs (see Results section 3.2), *dzy* gives rise to three different mRNA splice variants *dzyA*, *dzyB* and *dzyC*. As shown in the introduction, *dzy* shows alternative splicing at the 3' end of the gene. The different mRNAs are spliced in the common fashion from exon 0 to exon 4, and interestingly, they display unique ends from exon 5 to exon 7*/7. First, exon 5 is either included entirely (splice form *dzyA*), truncated (named exon 5S) (*dzyB*) or spliced out (*dzyC*). The second set of alternative splicing involves exons 6/6L, exon 7 and exon 7*. The mRNA sequence of the different variants can be continued either with exon 6 and 7 (*dzyA*), or with exon 6L (a longer version of exon 6) and exon 7L (exon 7* - exon 7)

(*dzyB* and *dzyC*). These sets are combined and result in the following three forms: *dzyA*, *dzyB* and *dzyC*.

Two *dzy* splice forms were identified in the *Drosophila* embryo

To characterise the molecular structure of the *dzy* gene and to get the tools to study its function, cDNAs of the 3' end of *dzy* were first synthesised. The *dzy* cDNAs were amplified by PCR using the primer pair exon 3 - exon 7* or exon 3 - exon 7. With these two primer combinations, all possible splice variants could be detected. Thus, we performed PCR experiments to analyse all possible variants of the 3' end. Surprisingly, only two of the three originally expected splice forms, the *dzyB* form and the *dzyC* form, could be detected in the *Drosophila* embryo with the described PCR method (see Results section 3.2). It is still unclear why the *dzyA* form could not be found, although a corresponding EST (EST AT08279, *Drosophila Genome Resource Center*) and other references exist in the literature (Wang *et al.* 2006). All *dzyB* and *dzyC* clones isolated from the PCR experiments ended with exon 7* (*4#1*, *dzyB; 4#4, 4#7* and *4#8*, *dzyC*) or with exon 7L (*3#6*, *dzyB*) (see Results section 3.2). However, the detailed C-terminal structure of the *dzyB* and *dzyC* form is not yet fully known. Additional isoforms consisting only exon 7* or exon 7 cannot yet be excluded. In addition, we have also identified two different 3' splice sites in exons 5 and 6, yielding a shorter version of exon 5 (5S), and a longer version of exon 6 (6L), respectively. A more detailed analysis of the sequenced *dzyB* and *dzyC* clones revealed that *dzyB* had the shorter exon 5S, while exon 5 was completely absent in the *dzyC* form. The *dzyB* and *dzyC* splice form contained exon 6L, a longer version of exon 6 due to an alternative splice site at its 3' end. Moreover, we have also shown that all cDNAs of the *dzyB* and *dzyC* forms continue after exon 6L with exon 7*(PR189) and exon 7L (PR190), respectively. In all PCR experiments, we did not find any other 3' end different from exon 7* or exon 7L. In summary, it can be assumed that the *dzyB* and the *dzyC* splice form contain exon 6L and 7L (exon 7*, intron 7*/7 and exon 7). EST EK292203 already gave an indication of the possibility of this specific 3' end. Due to the small number of cloned and sequenced samples (cDNA PR231/PR189 (exon 3/exon 7)), we cannot yet completely exclude the existence of individual forms containing only exon 7. Other combinations, such as exon 6 - exon 7 or exon 6L - exon 7, are hypothetically possible, but have not been found. We have thus identified two splice forms of *dzy* that differ only in the presence of exon 5S, but not in their C-terminal ends (exon 6L + exon 7*/7L).

dzyA could not be detected in the *Drosophila* embryo

It is important to briefly mention here that, based on ESTs and other references in the literature, there should be three different splice forms *dzyA*, *dzyB* and *dzyC*, but only two splice forms were found in the described experiment described. There are several indications for the

existence of the *dzyA* form. Firstly, EST AT08279 was obtained from the testes of adult *Drosophila* flies and shows a sequence with exons 5, exon 6, and exon 7. In addition, EST EK183201 also gives an indication of *dzyA*. This is a slightly modified variant of *dzyA*, with exon 5, intron 5 - 6, exon 6L and exon 7* (referred here as *dzyA**). Secondly, Wang *et al.* studied the expression of the Gef26 protein in the testes of *Drosophila*. They used a polyclonal anti-Gef26 (*dzyA* according to NCBI) antibody to detect the protein. In wild-type testes, Gef26 was highly concentrated at the hubGSC interface and between the hub cells (Wang *et al.* 2006). In summary, Wang and colleagues produced a specific antibody against the *dzyA* isoform and detected the protein in the *Drosophila* testes. This is clear evidence for the existence of a *dzyA* form. Since the *dzyA* form, in contrast to the other two isoforms *dzyB* and *dzyC*, could not be detected with the PCR method described above, several further detection experiments were performed. On the one hand, we tried to detect the *dzyA* form using a *dzyA*-specific primer (PR183) or to increase the amount of transcript with a Nested PCR approach. On the other hand, we tried to detect the missing isoform by explicitly focusing on the original location of *dzyA*, the testes of adult *Drosophila* flies (see Results section 3.2). Despite these different approaches, the *dzyA* form could not be detected even with these alternative methods. Another possibility for detection would be to use the specific DzyA antibody of Wang and colleagues. As mentioned in the section above, Wang and colleagues were able to detect a *dzyA* variant in *Drosophila* testes using a specific *dzyA* antibody (Wang *et al.* 2006). It would be interesting to investigate whether we can also detect the *dzyA* form using this antibody and whether a difference between the signal in the *Drosophila* embryo and the testis of adult animals is detectable. Since there are also other sources for the existence of this splice form, the *dzyA* form was included in the further experiments for the sake of completeness.

Developmental regulation of *dzy* splice forms

We next wanted to know whether the expression of the two splice forms is differentially regulated during the life cycle of *Drosophila*. To investigate this question, we performed experiments with total RNA from embryos (E), larvae (L), pupae (P) and adult flies (A). We tested different methods of tissue collection, RNA isolation, cDNA synthesis and primer combinations to obtain the best results (see Results section 3.2). These data provide initial evidence that the two splice forms, *dzyB* and *dzyC*, are differentially expressed during the *Drosophila* life cycle.

Indeed, we have shown that the two isoforms (*dzyB* and *dzyC*) present in the embryo are both also expressed in the larva, pupa and adult fly. In the embryo and the adult fly, the *dzyC* form appears to be either equally or more strongly expressed than the *dzyB* form. In comparison, the *dzyB* form was significantly more strongly expressed in larvae and pupae. As this is not a quantitative PCR, no definitive conclusions can be drawn; the results merely indicate a pattern

of expression. A semi-quantitative RT-PCR analysis using tubulin as a loading control would have been a much better choice for this endeavor but was not available to us at the time of the experiments. Although our data only allow a relatively rough quantification of mRNA abundance, they can provide information about the existence of the two *dzy* splice forms in the different developmental stages. Thus, we conclude that the two identified splice variants, *dzyB* and *dzyC*, are expressed in all developmental stages. Furthermore, of the different splice forms, only the *dzyC* form is particularly able to cause a change in cell shape when expressed in macrophages (see Results section 3.3); and only this isoform *dzyC* is able to partially rescue the adult phenotype of the adult escaper flies (see Results section 3.5). Despite the presence of the *dzyB* form in both the embryo and the adult fly, no such effects can be observed. This is a very interesting result which sheds light on the posttranscriptional regulation of *dzy*, but at the same time raises some questions. So far, nothing is known about the tissue specificity und spatially variable expression of the individual splice forms. In our research group, we have previously shown through performing an *in situ* hybridization experiment using a probe specific for exon 3 that *dzy* is ubiquitously expressed in the *Drosophila* embryo (Huelsmann *et al.* 2006). Whether a tissue-specific expression exists for the splice forms remains an open question. Indeed, due to the combinatorial nature of the splicing, it is extremely difficult to develop an isoform-specific probe for an *in situ* hybridization analysis. In order to test the expression of the single splice forms, a probe for exon 5S would mark the splice forms *dzyA* and *dzyB*, but not the *dzyC* form. *dzyC* does not have any unique regions that would not also be present in *dzyA* and *dzyB*.

4.3 Structure-function analysis of Dzy

With regard to the different isoforms of *dzy* produced by alternative splicing, the relationship between structure and function of the protein will be clarified. All three isoforms, *dzyA*, *dzyB* and *dzyC*, were introduced into flies as Gal4-controllable transgenes in order to initially answer the following three questions: (i) Can overexpression of one or more isoforms in haemocytes cause the same change in cell shape as observed with the *dzy*[EP] allele? (ii) Can one or more isoforms rescue the migration phenotype of macrophages in *dzy* mutants? Which isoform is sufficient for Dzy function in macrophages? Which isoforms is important for early function in the embryo? (iii) Which isoform is sufficient to rescue the semi-lethality of *dzy* mutants and their defects in eye, wing and genital apparatus development?

The *dzyC* isoform is able to induce a cell shape change when specifically expressed in the migrating macrophages

To study the cell shape and motility of macrophages in the *Drosophila* embryo, we used a *srph-Gal4* driver that allows the expression of the different *UAS-dzy*splice form constructs in

156

macrophages. We generated transgenic animals for the *UAS-dzy_{splice form}* constructs (see Appendix Tab. S1) and expressed the different *dzy* isoforms in macrophages by crossing these animals with a fly stain carrying the macrophage-specific driver (*srph-Gal4*) coupled with *UAS-cd2* (Dunin-Borkowski & Brown 1995), which allowed detection of cell shape and position by antibody staining directed against CD2 (Huelsmann *et al.* 2006). Macrophage-specific expression of the *dzyC* form of the *UAS-dzyC* construct (see Results section 3.3) showed the formation of long cellular protrusions, resulting in the formation of the same characteristic cell network phenotype that we have already shown in the *dzy*^{EP} line. The observed protrusions were 2 - 3 times larger than those of wild-type macrophages. Accurate measurement of the protrusions from the microscope images would have been beneficial here. In particular, for a possible difference between splice forms that at first sight do not show a recognisable extension of the protrusions. In contrast to the *dzyC* form, overexpression of *dzyA* and *dzyB* has no effect on the cell shape of the macrophages: the macrophages appear roundish and with short protrusions. Thus, only the *dzyC* splice form causes a change in cell shape when specifically expressed in the macrophages, whereas the other splice forms, *dzyA* and *dzyB*, cannot influence macrophage morphology under the same conditions, demonstrating a differential functionality of the three splice forms in the *Drosophila* embryo. The main difference between the three isoforms is the presence or absence of exon 5/5S. Which motifs are contained in exon 5/5S and could contribute to functionally different proteins? All domains typical of a PDZ-GEF are encoded in exon 3 and are equally present in all forms. The only stretches in the variable domains are three proline-rich motifs (PRM1: exon 4 and PRM2/PRM3: exon 5/5S), of which the *dzyA* and *dzyB* isoforms have all three and *dzyC* has only the motif in exon 4. These proline-rich motifs are thought to play a role in protein-protein interactions. What functions the protein segments encoded by exon 6/6L, 7*, 7 and 7L might have remains completely open.

<u>The functions of Dzy are regulated by an intramolecular interaction</u>

The proteins DzyA, DzyB and DzyC contain six conserved domains and binding motifs (from the N- to the C-terminus): the cNMP binding motif (also CAP/ED), the N-terminal GEF domain (GEFN) and the PDZ domain are located at the N-terminus of the protein, the RA domain and the GEF domain are located in the central part, and the proline-rich motifs (PRMs) are located at the C-terminus. All domains and their arrangements have been reported from known PDZ-GEFs, except for the C-terminal proline-rich motifs, which are not found in any PDZ-GEFs. The presence of the proline-rich region at the C-terminus varies within PDZ-GEFs and within different isoforms of one protein. For example, human PDZ-GEF2A has the proline-rich region, whereas the region is absent in the hPDZ-GEF2B isoform (Kuiperij *et al.* 2003). The three isoforms of Dzy differ in their C-terminus; two isoforms (DzyA and DzyB) have three proline-

rich motifs, while the short DzyC lacks two of the three proline-rich motifs (PRM2 and PRM3). The orthologue Dzy proteins of *Drosophila pseudoobscura* and *Drosophila ananassae* have a similar structure with the proline-rich regions at the C-terminus (see Results section 3.2). So far, however, it is not known whether alternative splicing occurs in the *dzy* loci of the *Drosophila* relatives. Functional analysis of the different domains of Dzy will allow us to understand how the protein mediates its function and will lead to the identification of new components that interact with Dzy. From our data, it appears that the C-terminal region of Dzy plays an important role in regulating the function of the splice forms. The main difference between the splice forms resides in the presence/absence of the exon 5, which specifies the A, B and C classes. The *dzyC* form is the only one capable of causing a cell shape change when expressed in the macrophages and is sufficient to partially rescue the phenotype of homozygous adult *dzy* mutants. Thus, the domain encoded in exon 5 is the key component in the regulation of the activity of the different splice forms. We hypothesised that the domain region encoded by exon 5 interacts intramolecularly with the Dzy PDZ domain and has a functionally inhibitory effect.

We showed that the *dzyB* splice form is also expressed in all developmental stages of the *Drosophila* life cycle. Therefore, it is possible that although *dzyB* is expressed, masking of the PDZ domain by the PRMs in exon 5 prevents the protein from acting in signaling pathways or entering into protein-protein interactions. Whether a single PRM or both (PRM2 and PRM3) are responsible remains to be seen. The regulation of specific protein activity mediated by a splice form-dependent intramolecular interaction has already been described in the case of formins (Zeller *et al.* 1999; Tanaka *et al.* 2004; Schirenbeck *et al.* 2005). We thus hypothesize that the intramolecular interaction is a mechanism by which Dzy can prevent undesirable interactions or change its partner specificity, as has been described for the formins protein (Olson 2003; Goode & Eck 2007; Kühn & Geyer 2014). The details of these intramolecular interactions are still unclear; further analyses to characterise the fine structure of the different proteins will shed light on the structural basis of this intramolecular binding.

The PDZ (PSD-95/Discs-large/ZO-1 homology) domain is a protein-protein interaction domain (Nourry *et al.* 2003). Proteins with a PDZ domain are implicated in protein targeting and protein complex assembly (Hung & Sheng 2002). Evidence for the PDZ domain as an interaction partner for the C-terminal PRMs in exon 5/5S is the fact that the conserved PDZ domain, characteristic for all PDZ-GEFs, is a protein interaction module that frequently recognises short amino acid motifs at the C-termini of proteins (Lee & Zheng 2010). Therefore, we hypothesise that an interaction occurs between the N-terminal PDZ domain within exon 3 and the C-terminal PRMs encoded by exon 5/5S. We expect that the possible intramolecular interaction leads to reduced accessibility of the PDZ domain and the exon 5 derived motifs to their respective partners in other protein molecules, thus affecting the functionality of the Dzy protein. Therefore, in the A and B splice forms of Dzy, but not in the DzyC form, there is an

158

intramolecular interaction between the PDZ domain of exon 3 and the PRMs in exon 5/5S. This interaction results in a conformational change and renders the two domains within the DzyA and DzyB forms inaccessible. To confirm this model and to investigate the function of the PDZ domain and the PRMs as well as their interaction, PRM2 and PRM3 in exon 5 on the one hand and the PDZ domain on the other hand were completely removed from the DNA sequence. To investigate whether these domains are critical for Dzy function, deletion constructs containing protein deletions of the PDZ (ΔPDZ) and the PRMs (ΔPRMs) were generated and tested for their ability to change cell shape in macrophages or to rescue the escaper phenotype. Functional analysis of the different domains of the PDZ-GEF will allow us to understand how Dzy mediates its function and potentially lead to the identification of new components that interact with Dzy. A Dzy isoform with a non-functional PDZ domain (*dzyCΔPDZ*), has already been cloned in the pUAST transformation vector and is available as a transgenic fly strain. The proline-rich motifs PRM2 and 3 were also deleted, but the constructs *UAS-dzyAΔPRM2* and *UAS-dzyAΔPRM3* could not be successfully introduced into the flies. Despite multiple injection attempts, no red-eyed flies could be identified. The following experiments were therefore carried out only with the *UAS-dzyCΔPDZ* strains. While the macrophage-specific expression of *dzyC* leads to a pronounced elongation of the cell extensions, this influence on the shape of the macrophages could not be observed with the *dzyCΔPDZ* form (see Results section 3.4). Expression of the *dzyCΔPDZ* form results in short cellular protrusions and more round-looking macrophages. The *dzyC* form, but not the *dzyCΔPDZ* form, is sufficient to cause a dramatic change in cell shape, demonstrating a functional role for the PDZ domain. The two constructs, *UAS-dzyC* and *UAS-dzyCΔPDZ,* differ solely in the presence of the PDZ domain. Thus, the PDZ domain of the Dzy splice form C is necessary to induce a change in cell shape. How the influence of the PDZ domain looks in detail in this process still needs to be investigated in more detail. In addition to the deletion constructs *UAS-dzyAΔPRM2* and *UAS-dzyAΔPRM3*, a form with two deleted PRMs (*UAS-dzyAΔPRM2/3*) is to be cloned. Since the two regions are short sequences that are relatively close to each other, the construction of the deletion primers was considerably more difficult. A preliminary cloning strategy has already been worked out. Using these three *UAS-dzyAΔPRM* forms, we want to investigate whether the PRMs, like the PDZ domain, are also involved in the process of cell migration. Does the deletion of one or both PRMs lead to a reversal of the inhibitory effect of the intramolecular interaction and thus to the formation of the characteristic *dzy*[EP] and *dzyC* phenotype with elongated protrusions? To further investigate the intramolecular interaction between the PDZ domain and the PRMs, it would also be interesting to clone a *dzyA* form containing the three PRMs and an inactive PDZ domain (*UAS-dzyAΔPDZ*). To support our hypothesis, we would expect the *UAS-dzyAΔPRM* and *UAS-*

dzyAΔPDZ constructs to have their interaction with the PDZ domain and the PRMs disrupted and thus the cells to show long extensions.

Another good approach to confirming our hypothesis of the intramolecular interaction taking place between the exon 5 encoded domain via its PRMs and the PDZ domain is the Y2H assay. So, we wondered whether the exon 5 encoded domain acts as an inhibitory element that interacts intramolecularly with other parts of the protein and changes conformation. One idea to answer this question would be to use a Y2H assay to test the interaction of all different Dzy C-termini ((*dzyA*, *dzyB* and *dzyC* (exon 4 – exon 7*/7)) with different truncated versions of the Dzy N-terminus. However, if the interaction occurs via an intramolecular interaction between the PRMs encoded by exon 5/5S and the PDZ domain of exon 3, we would expect an interaction between the *dzyA* and *dzyB* splice form with all truncations of Dzy containing the PDZ domain. This experiment would not only show that the exon 5 encoded domain can interact, but also that the exon 4 encoded domain is not involved in the interaction (*dzyC*).

The different *dzy* isoforms play different roles in adult morphogenesis

The *dzyC* form is important in the macrophages since it is the only one sufficient to induce cell shape changes in these cells, and we hypothesised that this is due to an intramolecular interaction between the exon 5 encoded domain and the PDZ domain. As explained in the Results section 3.5 of this PhD thesis, we wondered whether the *dzyA* and *dzyB* forms are important for other functions or play a role at later stages of development. Indeed, *dzy* is known to play a role in adult fly morphogenesis (Lee *et al.* 2002). Lee and colleagues demonstrated in previous studies that homozygosity of *dzy* is lethal, but that there is some fluctuation in lethality (semi-lethality). Indeed, we were able to obtain the escapers of the lethal phenotype of *dzy* homozygotes between the *dzy/CyO* and *dzy/TM3* parents, distinguished by the dominant markers Cy and Sb. These *dzy* homozygous mutants display striking features: the wing edges are rolled downwards (wing⁻), the eyes become small and rough (eye⁻), and they exhibit sterility with no egg laying. Both mutant male and female flies are sterile (Lee *et al.* 2002; Wang *et al.* 2006). To test the functional relevance of the individual splice forms in adult fly morphogenesis and their ability to rescue the *dzy* mutant phenotype (wing⁻, eye⁻), we performed rescue experiments and expressed the different *dzy* isoforms into a *dzy* mutant background. For the expression of transgenic Dzy, we used either the heat-inducible *hs-Gal4* driver or the *dzy promotor-Gal4* construct. The *hs-Gal4* driver gave the strongest and clearest result in the preliminary experiments and offered the advantage of temporal regulation of expression. In comparison, the *dzy* promotor allowed expression of the gene at a level closest to the natural expression level of *dzy*. The possibility of distorting the results due to excessive overexpression was thus prevented. Rescue experiments carried out with the *pdz-Gal4* driver showed no rescue of any aspect of the mutant phenotype or significant changes in the number

of escapers. Presumably, the expression level of the *dzy* promoter was too low to achieve a visible effect.

Similar to the expression of *dzy* splice forms in embryonic macrophages, the expression of a single splice form, *dzyC*, in the mutant background under the control of the *hs-Gal4* driver was sufficient to at least partially rescue the mutant phenotype. The escapers of this cross no longer showed the typical downward bent wings. Instead, the flies showed straight wings (wing$^+$, eye$^-$), like the wings of the wild-type flies (see Results section 3.5). Furthermore, the genitalia of the male straight-winged flies were examined more closely, and we found that their appearance resembled that of the wt flies (see Results section 3.5). Compared to the escaper flies, the examined flies no longer showed destroyed, modified genitalia and the sterility of the flies had also changed. Thus, partial rescue could also be achieved in this area of the adult phenotype. The effects of this partial rescue were strongly dependent on the timing of the heat shock. In many preliminary experiments, it was found that HS before day 4 AEL did not lead to any rescue effect. Interestingly, *dzyC* and the positive control (*dzyGFP)* did not show complete rescue at any heat shock time point. *dzyC* and *dzyGFP* are sufficient to rescue the wing and genital phenotype of the *dzy* mutant, but not the eye phenotype. The partially rescued escapers continue to exhibit the small, rough eye phenotype. Next, we further investigated the function of Dzy through eye-specific overexpression. The *UAS-dzy*splice forms made it possible to induce *dzy* expression by using a tissue-specific Gal4 driver. To explicitly rescue the rough eye phenotype of the *dzy* homozygous mutants, an *eyeless-* and a *gmr-Gal4* driver were used. None of the splice forms showed a rescue of the rough eye phenotype. One possible explanation for this would be the strong overexpression of *dzy* in the eye. It has been shown that overexpression of *dzy* induced by the *gmr-Gal4* driver, which controls expression of the gene in the developing eye, showed the same rough eye phenotype with some fused clusters of single ommatidia (Lee *et al.* 2002). It would thus be difficult to distinguish the *dzy* mutants from the *gmr-Gal4* gof phenotype. As we have shown, the splice forms have different function in the adult, as only the *dzyC* form is able to partially rescue the mutant phenotype (wing$^+$, eye$^-$), whereas the *dzyA* and *dzyB* form are unable to rescue any defect of the mutant phenotype. Interestingly, rescue with the *dzyA* form significantly increases the number of escapers. Thus, the *dzyA* form may decrease the *dzy*$^-$ lethality rates. Expression of the *dzyB* form failed to rescue hemizygous *dzy*$^-$ flies; we observed neither partial rescue nor increased numbers of escapers. Since the *dzyB* form is presumably increased in expression in the *Drosophila* larva and pupa (see Results section 3.2), this isoform could possibly play an important role at these developmental stages. According to this experiment, the model of intramolecular interaction as an inhibitor for the PDZ-GEF protein is valid not only in the embryonic macrophages but also in the adult fly. It is therefore possible that other forms are also expressed, but that the masking of the PDZ domain prevents the protein from interacting

with other proteins. Interestingly, in contrast to *dzyC*, expression of *dzyCΔPDZ* in the mutant background under the control of the *hs-Gal4* driver was not sufficient to partially rescue the mutant phenotype. Since *dzyC* and *dzyCΔPDZ* differ only in the presence of the PDZ domain, it appears that the PDZ domain plays an important role not only in the process of cell shape change and cell migration in *Drosophila* embryos, but also in this context. Since *dzyC* lacks an inhibitory intramolecular interaction due to the absence of the two PRMs, the loss of Dzy function could occur due to the limited interaction with PDZ-binding interaction partners.

<u>Which splice form is able to rescue the macrophage migration phenotype of *dzy* mutants?</u>

We have shown that the expression of the individual *dzy* splice forms in macrophages has a very specific impact on cell morphology. Overexpression of the *dzyC* form alone was sufficient to cause a change in cell shape and the formation of the cell network phenotype (see Results section 3.3). We suggest that *dzyC* is the relevant form of Dzy that acts in the migratory cycle of macrophages and is involved in regulating cell shape and adhesion. Therefore, we tested whether *dzyC* or possibly one of the other *dzy* splice forms (*dzyA* and *dzyB*) are specifically required for the process of macrophage migration. However, due to the combinatorial nature of *dzy* mRNA splicing, there is no straight-forward way to generate a splice form-specific knockout of *dzy*, e.g. by RNA silencing, and test such a requirement directly. Therefore, we used an alternative approach and asked whether any of the single splice forms would be sufficient to rescue the macrophage migration phenotype of *dzy* mutants in the *Drosophila* embryo. At stage 13 and 14, macrophages of *dzy* homozygous mutant embryos show a marked delay in macrophage migration, especially in the migration along the ventral nerve cord (VNC). In *dzy* mutant embryos, macrophages are not evenly distributed and there are fewer macrophages in the posterior-ventral part of the embryo than in the corresponding area of a wild-type embryo. This results in a gap of a few neuromeres in the posterior region of the VNC (Huelsmann *et al.* 2006). Thus, the activity of *dzy* is required within the macrophages for proper cell motility. The involvement of the different splice forms and their ability to rescue this mutant phenotype are not yet clear.

To answer this question, an "embryonal rescue experiment" was performed focusing on macrophage migration along the VNC midline, since other migrations, such as migration along the dorsal epidermis, are not affected to the same extent in *dzy* mutants (Huelsmann *et al.* 2006). To investigate the ability of the different splice forms to rescue the migration defect and close the "cell gap", we expressed the individual *UAS-dzy* isoforms into the *dzy* mutant background *dzy^{Δ8}/Df(2L)ED380*. The expression was performed under the control of the *srph-Gal4* driver. To identify the hemizygous *dzy^{Δ8}/Df(2L)ED380* embryos in the progeny and distinguish them from the heterozygous embryos (*dzy^{Δ8}/CyO,GFP* and *Df(2L)ED380/CyO,GFP*), we used so-called "green balancers" (Casso *et al.* 1999), in this case

a modified CyO balancer chromosome (CyO, GFP). Green fluorescent embryos carrying the balancer (*dzy$^{\Delta 8}$/CyO,GFP* and *Df(2L)ED380/CyO,GFP*) should therefore be excluded from further investigations. Only the non-fluorescent embryos (*dzy$^{\Delta 8}$/ Df(2L)ED380*) will be analysed for a possible rescue of the cell migration phenotype by the different splice forms. Surprisingly, no fluorescence signal was detected when the transgenic *Df(2L)ED380 (CyO,GFP)/UAS-dzy* animals were crossed with flies carrying *dzy$^{\Delta 8}$ (CyO,*GFP*)* and the macrophage-specific *srph-Gal4* driver coupled with *UAS-cd2*. According to the crossing scheme (see Results section 3.6) only 1/3 of all embryos should not carry CyO,GFP and thus show no fluorescence signal. Further studies of the different fly strains involved are therefore necessary to give an accurate answer to this question. In parallel to the examination of the original CyO,GFP strain (Fly strain collection stock 1101), deposits of the parental strains (*Df(2L)ED380 (CyO,GFP)/UAS-dzy*) and (*dzy$^{\Delta 8}$ (CyO,GFP)/srph-Gal4*) should also be prepared and examined for fluorescent embryos. If the original CyO,GFP strain proves unsuitable, it must be replaced by another strain and the experiment repeated. An alternative would be to distinguish between homozygous and heterozygous embryos on the basis of a ftz::LacZ transgene contained in the balancer.

Target specific localisation via the PhiC31 integrase system

A major goal in the present era of genomics is the identification and functional characterisation of all genes relevant to a particular biological process. The multicellular model organism *Drosophila melanogaster*, with its powerful repertoire of genetic tools, has played a prominent role in this endeavour (St Johnston 2002; Bischof *et al.* 2007). One method for identifying relevant genes is the use of P-element-mediated germ-line transformation (Rubin & Spradling 1982; Spradling & Rubin 1982), especially in combination with tools such as the UAS-Gal4 expression system (Brand & Perrimon 1993). A feature of P-elements is their random integration behaviour. Although this "randomness" has been advantageous in performing an EP-Screen (Huelsmann *et al.* 2006), it is generally not ideal for transgene analysis. The random integration of P-elements necessitates considerable effort to map insertions. Genomic position effects complicate transgene analysis and make precise structure-function analyses almost impossible.

We have shown that the macrophage-specific expression of the different *dzy* splice forms (*dzyA*, *dzyB* and *dzyC*) has very specific influence on cell morphology. The *dzyC* form alone is sufficient to cause changes in cell shape and the formation of the characteristic cell network. In order to rule out the possibility that the observed effects are due to random integration and the associated genomic position of the different *dzy* splice forms in the genome influencing *dzy* transgene expression, a number of different studies were devised and in some cases carried out. To test the expression levels of the individual protein isoforms in the different lines

expressing *dzy* splice forms, the production of a specific antibody against a N-terminal fragment of Dzy was originally planned. However, it has not been possible to produce a reliable anti-Dzy antibody up to this point. Therefore, an analysis of the expression level was carried out using in situ hybridization and a specific dzy probe (see Results section 3.3). Our data showed that especially the dzyC and the dzyGFP form, which affect cell shape and migration, had a slightly stronger signal with the dzy probe. However, it was very difficult to make an accurate statement comparing the different expression levels of the splice forms. Since the dzy splice form constructs were randomly integrated into the genome and in situ hybridization analysis could not provide an accurate statement about the expression levels, we wanted to take an alternative approach to introduce the different splice forms directionally into the genome and thus be able to exclude a position effect and different expression levels. In 1998, another method for genome integration was developed based on the site-specific PhiC31 integrase (Thorpe & Smith 1998) and subsequently applied to *Drosophila (Groth et al. 2004)*. To circumvent the problem of randomness, we used this site-specific PhiC31 integrase integration system (Bischof *et al.* 2007) and generated *Drosophila* transgenes for *dzy_GFP*. To generate *dzy_GFP in pUASTattB* constructs, ORFs encoding the three different *dzy* splice forms were amplified via PCR and ligated into the digested *pUASTattB Drosophila* transformation vector. The UAS-controlled isoforms of *dzy* were fused with GFP to facilitate visualisation of macrophages and to allow detection *in vivo* after targeted expression. The *dzy_GFP* constructs were injected into embryos containing the desired attP landing site (*yw C31; +; 86 FB*; integration on the third chromosome). In contrast to the *dzy in pUAST* constructs, the new constructs (*dzy_GFP in pUASTattB*) were thus introduced at a specific chromosomal position and additionally fused with GFP. Surprisingly, the embryos of the injection strain itself, the resulting *dzy_GFP* strains and the different crosses with different Gal4-drivers showed a bright, fluorescent PNS. While in the *srph-Gal4/UAS-dzy_GFP* embryos only the PNS could be detected, in *prd-Gal4/UAS-dzy_GFP* the typical *prd-Gal4* pattern was visible in early embryos. Later, the PNS was also clearly visible. Interestingly, no signal can be detected in the macrophage-specifical expression of the *UAS-dzy_GFP* constructs even at early stages. It remains to be seen whether the two phenomena, the lack of visualisation of the macrophages and the fluorescent PNS, are related or whether they are two independent problems.

Unfortunately, despite intensive research in the literature, no reference to the fluorescent PNS phenomenon could be found. Since the injection strain already showed the fluorescent PNS, one idea was that this effect comes from the activity of the X-chromosomal PhiC31 integrase. To investigate whether the presence of PhiC31 integrase leads to the fluorescent PNS phenotype, *UAS-dzy_GFP* strains lacking PhiC31 integrase activity (ØPhiC31) were generated (see Results section 3.7). The transgenic fly strains: *UAS-dzyB_GFP ØPhiC31* and

UAS-dzyC_GFP ØPhiC31 were then crossed with animals carrying the macrophage-specific *srph-Gal4* driver, and the progeny were examined under the fluorescence microscope. Although the fluorescent nervous system was no longer observable, we still could not detect macrophages. Further research, experiments and examinations of the individual components as well as the injection strain are necessary.

4.4 Future perspectives

We are pursuing two goals with our project. On the one hand, we want to understand at the molecular and cellular level how PDZ-GEF Dzy acts during cell migration, which processes it controls and how it is regulated. To this end, we believe it is important to pursue the relationship of structure and function in Dzy and the relevance of alternative splicing and conserved domains. Furthermore, we want to deepen our phenotypic analysis and look for factors with which the Dzy protein interacts, other proteins that are either regulated by Dzy or in turn control Dzy in its activity. The role of the putative interactor of Dzy, SSCAM (Synaptic Scaffolding Cell Adhesion Moleculre) Magi (MAGuk with Inverted orientation) (Ohtsuka *et al.* 1999; Kawajiri *et al.* 2000; Mino *et al.* 2000; Sakurai *et al.* 2006; Kooistra *et al.* 2007), in the cell migration of macrophages will also be investigated.

The dzyN terminus and the alternative translation initiation sites

The canonical translation initiation site (TIS) of *dzy* is located in the central region of exon 1. Accordingly, what is the significance of exon 0, which is located 5' to the first exon, and the 5'-UTR region? Alternative TIS (altTIS) upstream of the canonical start codon can initiate the translation of different protein products: either an N-terminal extended isoform of the CDS-encoded protein or an unrelated protein. Do these protein products have a regulatory function? Detailed analysis of the N-terminus of Dzy, identified two alternative upstream translation initiation sites (uTIS1 and 2) in exon 0. Numerous studies have documented that translation begins not only at the canonical start codon, but also from alternative AUGs or even non-AUG start codons in the 5'-UTR of the transcripts. These alternative translation initiation sites are located upstream and represent unrelated upstream open reading frames (uORF type A) and CDS-overlapping uORFs (uORF type B (not in-frame) and uORF type C (in-frame)) that may have critical regulatory functions for gene expression. For example, N-terminal protein extensions may be important for the subcellular protein sorting (Touriol *et al.* 2003). During this work, we have discovered different sequence variants in the region between exon 0 and exon 1. Depending on which variant arrives, there is a shift in the uORF and thus new possible stop codons. The length of the proteins to be translated became longer or shorter depending on which variant was present and which stop codon ended the translation (see Results section 3.1). At this stage, it is difficult to make an accurate statement about the *dzy* sequence in the

exon 0 region. The isolation of further total RNA from flies is therefore necessary and should help to ensure that a tendency in one direction or a confirmation of both variants is possible. Interestingly, however, the experiment has already confirmed that there is no uORF type C among the different uORF variants. None of the overlapping uORFs are in-frame with the CDS and an N-terminal extension of the Dzy protein could not be found. However, the question of a regulatory function of the shorter AS sequences remains open. For efficient translation initiation, the nucleotide context of the AUG start codon plays an important role (Kozak 1997). However, if the context is suboptimal, some ribosomal subunits will recognize the AUG as a TIS, while others will omit it, continue scanning in 3' direction and initiate translation at a downstream AUG ("leaky scanning") (Kochetov 2008; Bazykin & Kochetov 2011). In a further step, we therefore want to investigate the nucleotide context of the newly identified alternative TIS (altTIS1 and altTIS2).

Subcellular localisation of Dzy

In addition to the temporal and spatial expression of a protein within the organism or individual tissues, its subcellular localisation is also of great interest, as it can be directly related to functional properties. For example, two proteins can only interact directly if they are located in the same cell compartment. With the help of a newly produced anti-Dzy antibody, the localisation of Dzy will be demonstrated by antibody staining directly in the *Drosophila* embryo. These studies will be complemented by efforts to express Dzy in combination with GFP or other fluorescent protein variants in the embryo and thus also to observe its intracellular localisation in living tissue, especially in migrating cells. Above all, it should be clarified whether this localisation depends on the state of the cell, for example its movement phase. What experience do we have so far about where Dzy acts in the cell? In the macrophages of the *Drosophila* embryo, Dzy seems to stabilise the tail of the migrating cells. In any case, lamellopodia are formed normally both in the mutants and after *dzy* overexpression, but the supernumerary cell protrusions seen both in fixed preparations and in living cells after *dzy* overexpression are apparently due to inadequately solubilised cell ends, according to live observations. This has no effect on the efficiency of cell migration when expression is intermediate (*dzy* overexpressed from one copy of *dzy^{EP}*), but when at the same time the function of RhoA is reduced, there is a very pronounced migration defect. The further enhancement of adhesion by the simultaneous expression of *dzy^{EP}* together with dominant negative RhoA^{N19} in macrophages disrupts their migration similarly to embryos expressing two copies of *dzy^{EP}* (Huelsmann *et al.* 2006). The small GTPase RhoA is known to be required for regulation of adhesion in migrating cells and it contributes to the retraction of the cell tail (Worthylake *et al.* 2001; Hogg *et al.* 2003; Ridley *et al.* 2003). Dzy may act antagonistically, which could explain the synergistic effect of Dzy overfunction and RhoA underfunction in

macrophage migration. Against this background, it is important to determine where Dzy acts in the cell and whether its localisation supports the implication of stabilising the cell tails.

<u>Interaction partners of Dzy</u>

Another important step in understanding how the PDZ-GEF Dzy acts in cell migration or cell adhesion is to identify proteins to which Dzy binds. Proteins that determine the localisation of Dzy in the cell, determine its activity or modify it. Vertebrate PDZ-GEF has been described to interact with the protein Magi (membrane-associated guanyl kinase) via its PDZ domain (Kooistra *et al.* 2007). Magi, also called SSCAM (synaptic scaffolding cell adhesion molecule), has 6 PDZ domains (Hirao *et al.* 1998; Ohtsuka *et al.* 1999), and is encoded in *Drosophila* by a gene located at 57C2-3 in the genome (Flybase; Beller *et al.* 2002). In preliminary experiments, the cDNA has already been cloned into the corresponding vectors to test the interaction ability of Magi. On the one hand, the interaction of the two proteins will be investigated using a Y2H approach. On the other hand, it will be tested whether Magi is important for the migration of macrophages. So, like *dzy*, Magi should be overexpressed in macrophages under the control of the *srph-Gal4* driver. The questions we want to answer are: Is Magi sufficient to cause a cell shape change similar to that observed for Dzy when expressed in migrating macrophages of the *Drosophila* embryo? Is there a functional interaction between Dzy and Magi in the regulation of cell shape in macrophages? Are both the PDZ domain of Dzy and one of the PDZ domains of MAGI required for this interaction? Is the interaction between Dzy and Magi splice form-dependent? Can only the *dzyC* isoform interact with Magi, both in yeast and in the *Drosophila* embryo? Conversely, does the intramolecular interaction in the other forms *dzyA* and *dzyB* prevent this interaction? The characterisation of protein-protein interactions is crucial for understanding protein functions. The functions of a protein can be extrapolated if the function of the binding partners is known. Identifying the interaction partners of Dzy would therefore bring us one step closer to understanding the specific function and regulation of this PDZ-GEF.

5. References

Arai A., Nosaka Y., Kanda E., Yamamoto K., Miyasaka N. & Miura O. (2001) Rap1 Is Activated by Erythropoietin or Interleukin-3 and Is Involved in Regulation of β1 Integrin-mediated Hematopoietic Cell Adhesion. *The Journal of biological chemistry,* **276**, 10453–62.

Asha H., Ruiter N.D. de, Wang M.G. & Hariharan I.K. (1999) The Rap1 GTPase functions as a regulator of morphogenesis in vivo. *The EMBO journal,* **18**, 605–15.

Barolo S., Carver L.A. & Posakony J.W. (2000) GFP and beta-galactosidase transformation vectors for promoter/enhancer analysis in Drosophila. *BioTechniques,* **29**, 726, 728, 730, 732.

Bazykin G.A. & Kochetov A.V. (2011) Alternative translation start sites are conserved in eukaryotic genomes. *Nucleic acids research,* **39**, 567–77.

Beller M., Blanke S., Brentrup D. & Jäckle H. (2002) Identification and expression of Ima, a novel Ral-interacting Drosophila protein. *Mechanisms of development,* **119 Suppl 1**, S253-60.

Bischof J., Maeda R.K., Hediger M., Karch F. & Basler K. (2007) An optimized transgenesis system for Drosophila using germ-line-specific phiC31 integrases. *Proceedings of the National Academy of Sciences of the United States of America,* **104**, 3312–7.

Boettner B. & van Aelst L. (2007) The Rap GTPase activator Drosophila PDZ-GEF regulates cell shape in epithelial migration and morphogenesis. *Molecular and cellular biology,* **27**, 7966–80.

Boettner B. & van Aelst L. (2009) Control of cell adhesion dynamics by Rap1 signaling. *Current opinion in cell biology,* **21**, 684–93.

Bökel C. & Brown N.H. (2002) Integrins in development: moving on, responding to, and sticking to the extracellular matrix. *Developmental cell,* **3**, 311–21.

Bos J.L. (2005) Linking Rap to cell adhesion. *Current opinion in cell biology,* **17**, 123–8.

Bos J.L., Bruyn K. de & Enserink J. *et al. (*2003) The role of Rap1 in integrin-mediated cell adhesion. *Biochemical Society transactions,* **31**, 83–6.

Bos J.L., Rehmann H. & Wittinghofer A. (2007) GEFs and GAPs: critical elements in the control of small G proteins. *Cell,* **129**, 865–77.

Bos J.L., Rooij J. de & Reedquist K.A. (2001) Rap1 signalling: adhering to new models. *Nature reviews. Molecular cell biology,* **2**, 369–77.

Brand A.H. & Perrimon N. (1993) Targeted gene expression as a means of altering cell fates and generating dominant phenotypes. *Development (Cambridge, England),* **118**, 401–15.

Brand M., Jarman A.P., Jan L.Y. & Jan Y.N. (1993) asense is a Drosophila neural precursor gene and is capable of initiating sense organ formation. *Development (Cambridge, England),* **119**, 1–17.

Brown N.H., Gregory S.L. & Martin-Bermudo M.D. (2000) Integrins as mediators of morphogenesis in Drosophila. *Developmental biology,* **223**, 1–16.

Brückner K., Kockel L., Duchek P., Luque C.M., Rørth P. & Perrimon N. (2004) The PDGF/VEGF receptor controls blood cell survival in Drosophila. *Developmental cell,* **7**, 73–84.

Caron E. (2003) Cellular functions of the Rap1 GTP-binding protein: a pattern emerges. *Journal of cell science,* **116**, 435–40.

Caron E., Self A.J. & Hall A. (2000) The GTPase Rap1 controls functional activation of macrophage integrin alphaMbeta2 by LPS and other inflammatory mediators. *Current biology : CB,* **10**, 974–8.

Casso D., Ramírez-Weber F.A. & Kornberg T.B. (1999) GFP-tagged balancer chromosomes for Drosophila melanogaster. *Mechanisms of development,* **88**, 229–32.

Cavener D.R. (1987) Comparison of the consensus sequence flanking translational start sites in Drosophila and vertebrates. *Nucleic acids research,* **15**, 1353–61.

Cho N.K., Keyes L. & Johnson E. *et al. (*2002) Developmental control of blood cell migration by the Drosophila VEGF pathway. *Cell,* **108**, 865–76.

Comber K., Huelsmann S. & Evans I. *et al. (*2013) A dual role for the βPS integrin myospheroid in mediating Drosophila embryonic macrophage migration. *Journal of cell science,* **126**, 3475–84.

Crozatier M. & Meister M. (2007) Drosophila haematopoiesis. *Cellular microbiology,* **9**, 1117–26.

Dunin-Borkowski O.M. & Brown N.H. (1995) Mammalian CD2 is an effective heterologous marker of the cell surface in Drosophila. *Developmental biology,* **168**, 689–93.

*Encyclopedia of Signaling Molecules (*2012). Springer, New York, NY.

Etienne-Manneville S. & Hall A. (2002) Rho GTPases in cell biology. *Nature,* **420**, 629–35.

Evans C.J., Hartenstein V. & Banerjee U. (2003) Thicker than blood: conserved mechanisms in Drosophila and vertebrate hematopoiesis. *Developmental cell,* **5**, 673–90.

Evans I.R. & Wood W. (2014) Drosophila blood cell chemotaxis. *Current opinion in cell biology,* **30**, 1–8.

Fauvarque M.-O. & Williams M.J. (2011) Drosophila cellular immunity: a story of migration and adhesion. *Journal of cell science,* **124**, 1373–82.

Fossett N., Hyman K., Gajewski K., Orkin S.H. & Schulz R.A. (2003) Combinatorial interactions of serpent, lozenge, and U-shaped regulate crystal cell lineage commitment during Drosophila hematopoiesis. *Proceedings of the National Academy of Sciences of the United States of America,* **100**, 11451–6.

Frische E.W. & Zwartkruis F.J.T. (2010) Rap1, a mercenary among the Ras-like GTPases. *Developmental biology,* **340**, 1–9.

Gao X., Satoh T. & Liao Y. *et al. (*2001) Identification and characterization of RA-GEF-2, a Rap guanine nucleotide exchange factor that serves as a downstream target of M-Ras. *The Journal of biological chemistry,* **276**, 42219–25.

García-Mata R. & Burridge K. (2007) Catching a GEF by its tail. *Trends in cell biology,* **17**, 36–43.

Ginsberg M.H. (2014) Integrin activation. *BMB reports,* **47**, 655–9.

Gloerich M. & Bos J.L. (2011) Regulating Rap small G-proteins in time and space. *Trends in cell biology,* **21**, 615–23.

Gold K.S. & Brückner K. (2014) Drosophila as a model for the two myeloid blood cell systems in vertebrates. *Experimental hematology,* **42**, 717–27.

Goode B.L. & Eck M.J. (2007) Mechanism and function of formins in the control of actin assembly. *Annual review of biochemistry,* **76**, 593–627.

Groth A.C., Fish M., Nusse R. & Calos M.P. (2004) Construction of transgenic Drosophila by using the site-specific integrase from phage phiC31. *Genetics,* **166**, 1775–82.

Guo X.-X., An S., Yang Y., Liu Y., Hao Q. & Xu T.-R. (2016) Rap-Interacting Proteins are Key Players in the Rap Symphony Orchestra. *Cellular physiology and biochemistry : international journal of experimental cellular physiology, biochemistry, and pharmacology,* **39**, 137–56.

Hazelett D.J., Bourouis M., Walldorf U. & Treisman J.E. (1998) decapentaplegic and wingless are regulated by eyes absent and eyegone and interact to direct the pattern of retinal differentiation in the eye disc. *Development (Cambridge, England),* **125**, 3741–51.

Heo K., Nahm M. & Lee M.-J. *et al. (*2017) The Rap activator Gef26 regulates synaptic growth and neuronal survival via inhibition of BMP signaling. *Molecular brain,* **10**, 62.

Hinz U., Giebel B. & Campos-Ortega J.A. (1994) The basic-helix-loop-helix domain of Drosophila lethal of scute protein is sufficient for proneural function and activates neurogenic genes. *Cell,* **76**, 77–87.

Hirao K., Hata Y. & Ide N. *et al. (*1998) A novel multiple PDZ domain-containing molecule interacting with N-methyl-D-aspartate receptors and neuronal cell adhesion proteins. *The Journal of biological chemistry,* **273**, 21105–10.

Hogg N., Laschinger M., Giles K. & McDowall A. (2003) T-cell integrins: more than just sticking points. *Journal of cell science,* **116**, 4695–705.

Holz A., Bossinger B., Strasser T., Janning W. & Klapper R. (2003) The two origins of hemocytes in Drosophila. *Development (Cambridge, England),* **130**, 4955–62.

Huelsmann S., Hepper C., Marchese D., Knöll C. & Reuter R. (2006) The PDZ-GEF dizzy regulates cell shape of migrating macrophages via Rap1 and integrins in the Drosophila embryo. *Development (Cambridge, England),* **133**, 2915–24.

Hummel T., Schimmelpfeng K. & Klämbt C. (1997) Fast and efficient egg collection and antibody staining from large numbers of Drosophila strains. *Development genes and evolution,* **207**, 131–5.

Hung A.Y. & Sheng M. (2002) PDZ domains: structural modules for protein complex assembly. *The Journal of biological chemistry,* **277**, 5699–702.

Hynes R.O. (1992) Integrins: versatility, modulation, and signaling in cell adhesion. *Cell,* **69**, 11–25.

Hynes R.O. (2002) Integrins: bidirectional, allosteric signaling machines. *Cell,* **110**, 673–87.

Hynes R.O. & Zhao Q. (2000) The evolution of cell adhesion. *The Journal of cell biology,* **150**, F89-96.

Ichiba T., Hashimoto Y. & Nakaya M. *et al. (*1999) Activation of C3G guanine nucleotide exchange factor for Rap1 by phosphorylation of tyrosine 504. *The Journal of biological chemistry,* **274**, 14376–81.

Jaśkiewicz A., Pająk B. & Orzechowski A. (2018) The Many Faces of Rap1 GTPase. *International journal of molecular sciences,* **19**.

Katagiri K., Hattori M., Minato N., Irie S.k., Takatsu K. & Kinashi T. (2000) Rap1 is a potent activation signal for leukocyte function-associated antigen 1 distinct from protein kinase C and phosphatidylinositol-3-OH kinase. *Molecular and cellular biology,* **20**, 1956–69.

Katagiri K., Maeda A., Shimonaka M. & Kinashi T. (2003) RAPL, a Rap1-binding molecule that mediates Rap1-induced adhesion through spatial regulation of LFA-1. *Nature immunology,* **4**, 741–8.

Katagiri K., Ohnishi N. & Kabashima K. *et al. (*2004) Crucial functions of the Rap1 effector molecule RAPL in lymphocyte and dendritic cell trafficking. *Nature immunology,* **5**, 1045–51.

Kawajiri A., Itoh N. & Fukata M. *et al. (*2000) Identification of a novel beta-catenin-interacting protein. *Biochemical and biophysical research communications,* **273**, 712–7.

Kay B.K., Williamson M.P. & Sudol M. (2000) The importance of being proline: the interaction of proline-rich motifs in signaling proteins with their cognate domains. *FASEB journal : official publication of the Federation of American Societies for Experimental Biology,* **14**, 231–41.

Kinbara K., Goldfinger L.E., Hansen M., Chou F.-L. & Ginsberg M.H. (2003) Ras GTPases: integrins' friends or foes? *Nature reviews. Molecular cell biology,* **4**, 767–76.

Kitayama H., Sugimoto Y., Matsuzaki T., Ikawa Y. & Noda M. (1989) A ras-related gene with transformation suppressor activity. *Cell,* **56**, 77–84.

Kiyokawa E., Mochizuki N., Kurata T. & Matsuda M. (1997) Role of Crk oncogene product in physiologic signaling. *Critical reviews in oncogenesis,* **8**, 329–42.

Knox A.L. & Brown N.H. (2002) Rap1 GTPase regulation of adherens junction positioning and cell adhesion. *Science (New York, N.Y.),* **295**, 1285–8.

Kochetov A.V. (2008) Alternative translation start sites and hidden coding potential of eukaryotic mRNAs. *BioEssays : news and reviews in molecular, cellular and developmental biology,* **30**, 683–91.

Kooistra M.R.H., Dubé N. & Bos J.L. (2007) Rap1: a key regulator in cell-cell junction formation. *Journal of cell science,* **120**, 17–22.

Korbie D.J. & Mattick J.S. (2008) Touchdown PCR for increased specificity and sensitivity in PCR amplification. *Nature protocols,* **3**, 1452–6.

Kozak M. (1978) How do eucaryotic ribosomes select initiation regions in messenger RNA? *Cell,* **15**, 1109–23.

Kozak M. (1980) Evaluation of the "scanning model" for initiation of protein synthesis in eucaryotes. *Cell,* **22**, 7–8.

Kozak M. (1997) Recognition of AUG and alternative initiator codons is augmented by G in position +4 but is not generally affected by the nucleotides in positions +5 and +6. *The EMBO journal,* **16**, 2482–92.

Kühn S. & Geyer M. (2014) Formins as effector proteins of Rho GTPases. *Small GTPases,* **5**, e29513.

Kuiperij H.B., Rooij J. de & Rehmann H. *et al. (*2003) Characterisation of PDZ-GEFs, a family of guanine nucleotide exchange factors specific for Rap1 and Rap2. *Biochimica et biophysica acta,* **1593**, 141–9.

Lauffenburger D.A. & Horwitz A.F. (1996) Cell migration: a physically integrated molecular process. *Cell,* **84**, 359–69.

Lebestky T., Chang T., Hartenstein V. & Banerjee U. (2000) Specification of Drosophila hematopoietic lineage by conserved transcription factors. *Science (New York, N.Y.),* **288**, 146–9.

Lee H.-J. & Zheng J.J. (2010) PDZ domains and their binding partners: structure, specificity, and modification. *Cell communication and signaling : CCS,* **8**, 8.

Lee J.H., Cho K.S. & Lee J. *et al. (*2002) Drosophila PDZ-GEF, a guanine nucleotide exchange factor for Rap1 GTPase, reveals a novel upstream regulatory mechanism in the mitogen-activated protein kinase signaling pathway. *Molecular and cellular biology,* **22**, 7658–66.

Liao Y., Kariya K. & Hu C.D. *et al. (*1999) RA-GEF, a novel Rap1A guanine nucleotide exchange factor containing a Ras/Rap1A-associating domain, is conserved between nematode and humans. *The Journal of biological chemistry,* **274**, 37815–20.

Liao Y., Satoh T., Gao X., Jin T.G., Hu C.D. & Kataoka T. (2001) RA-GEF-1, a guanine nucleotide exchange factor for Rap1, is activated by translocation induced by association with Rap1*GTP and enhances Rap1-dependent B-Raf activation. *The Journal of biological chemistry,* **276**, 28478–83.

Meister M. & Lagueux M. (2003) Drosophila blood cells. *Cellular microbiology,* **5**, 573–80.

Mino A., Ohtsuka T., Inoue E. & Takai Y. (2000) Membrane-associated guanylate kinase with inverted orientation (MAGI)-1/brain angiogenesis inhibitor 1-associated protein (BAP1) as a scaffolding molecule for Rap small G protein GDP/GTP exchange protein at tight junctions. *Genes to cells : devoted to molecular & cellular mechanisms,* **5**, 1009–16.

Mitchison T.J. & Cramer L.P. (1996) Actin-based cell motility and cell locomotion. *Cell,* **84**, 371–9.

Nourry C., Grant S.G.N. & Borg J.-P. (2003) PDZ domain proteins: plug and play! *Science's STKE : signal transduction knowledge environment,* **2003**, RE7.

Ohtsuka T., Hata Y. & Ide N. *et al. (*1999) nRap GEP: a novel neural GDP/GTP exchange protein for rap1 small G protein that interacts with synaptic scaffolding molecule (S-SCAM). *Biochemical and biophysical research communications,* **265**, 38–44.

Olson M.F. (2003) Dispatch. GTPase signalling: new functions for Diaphanous-related formins. *Current biology : CB,* **13**, R360-2.

Ou M., Wang S. & Sun M. *et al. (*2019) The PDZ-GEF Gef26 regulates synapse development and function via FasII and Rap1 at the Drosophila neuromuscular junction. *Experimental cell research,* **374**, 342–52.

Paladi M. & Tepass U. (2004) Function of Rho GTPases in embryonic blood cell migration in Drosophila. *Journal of cell science,* **117**, 6313–26.

Pannekoek W.-J., Kooistra M.R.H., Zwartkruis F.J.T. & Bos J.L. (2009) Cell-cell junction formation: the role of Rap1 and Rap1 guanine nucleotide exchange factors. *Biochimica et biophysica acta,* **1788**, 790–6.

Parsons B. & Foley E. (2013) The Drosophila platelet-derived growth factor and vascular endothelial growth factor-receptor related (Pvr) protein ligands Pvf2 and Pvf3 control hemocyte viability and invasive migration. *The Journal of biological chemistry,* **288**, 20173–83.

Pellis-van Berkel W., Verheijen M.H.G. & Cuppen E. *et al. (*2005) Requirement of the Caenorhabditis elegans RapGEF pxf-1 and rap-1 for epithelial integrity. *Molecular biology of the cell,* **16**, 106–16.

Quilliam L.A., Rebhun J.F. & Castro A.F. (2002) A growing family of guanine nucleotide exchange factors is responsible for activation of Ras-family GTPases. *Progress in nucleic acid research and molecular biology,* **71**, 391–444.

Rebhun J.F., Castro A.F. & Quilliam L.A. (2000) Identification of guanine nucleotide exchange factors (GEFs) for the Rap1 GTPase. Regulation of MR-GEF by M-Ras-GTP interaction. *The Journal of biological chemistry,* **275**, 34901–8.

Reedquist K.A., Ross E. & Koop E.A. *et al. (*2000) The small GTPase, Rap1, mediates CD31-induced integrin adhesion. *The Journal of cell biology,* **148**, 1151–8.

Rehorn K.P., Thelen H., Michelson A.M. & Reuter R. (1996) A molecular aspect of hematopoiesis and endoderm development common to vertebrates and Drosophila. *Development (Cambridge, England),* **122**, 4023–31.

Ridley A.J. (2001) Rho family proteins: coordinating cell responses. *Trends in cell biology,* **11**, 471–7.

Ridley A.J., Schwartz M.A. & Burridge K. *et al. (*2003) Cell migration: integrating signals from front to back. *Science (New York, N.Y.),* **302**, 1704–9.

Rockwell A.L., Beaver I. & Hongay C.F. (2019) A Direct and Simple Method to Assess Drosophila melanogaster's Viability from Embryo to Adult. *Journal of visualized experiments : JoVE.*

Rooij J. de, Boenink N.M., van Triest M., Cool R.H., Wittinghofer A. & Bos J.L. (1999) PDZ-GEF1, a guanine nucleotide exchange factor specific for Rap1 and Rap2. *The Journal of biological chemistry,* **274**, 38125–30.

Rooij J. de, Rehmann H., van Triest M., Cool R.H., Wittinghofer A. & Bos J.L. (2000) Mechanism of regulation of the Epac family of cAMP-dependent RapGEFs. *The Journal of biological chemistry,* **275**, 20829–36.

Rooij J. de, Zwartkruis F.J. & Verheijen M.H. *et al. (*1998) Epac is a Rap1 guanine-nucleotide-exchange factor directly activated by cyclic AMP. *Nature,* **396**, 474–7.

Rørth P. (1996) A modular misexpression screen in Drosophila detecting tissue-specific phenotypes. *Proceedings of the National Academy of Sciences of the United States of America,* **93**, 12418–22.

Rørth P., Szabo K. & Bailey A. *et al. (*1998) Systematic gain-of-function genetics in Drosophila. *Development (Cambridge, England),* **125**, 1049–57.

Rubin G.M. & Spradling A.C. (1982) Genetic transformation of Drosophila with transposable element vectors. *Science (New York, N.Y.),* **218**, 348–53.

Ryder E., Ashburner M. & Bautista-Llacer R. *et al. (*2007) The DrosDel deletion collection: a Drosophila genomewide chromosomal deficiency resource. *Genetics,* **177**, 615–29.

Sakurai A., Fukuhara S. & Yamagishi A. *et al. (*2006) MAGI-1 is required for Rap1 activation upon cell-cell contact and for enhancement of vascular endothelial cadherin-mediated cell adhesion. *Molecular biology of the cell,* **17**, 966–76.

Schirenbeck A., Bretschneider T., Arasada R., Schleicher M. & Faix J. (2005) The Diaphanous-related formin dDia2 is required for the formation and maintenance of filopodia. *Nature cell biology,* **7**, 619–25.

Schmidt A. & Hall A. (2002) Guanine nucleotide exchange factors for Rho GTPases: turning on the switch. *Genes & development,* **16**, 1587–609.

Sebzda E., Bracke M., Tugal T., Hogg N. & Cantrell D.A. (2002) Rap1A positively regulates T cells via integrin activation rather than inhibiting lymphocyte signaling. *Nature immunology,* **3**, 251–8.

Shirinian M., Popovic M. & Grabbe C. *et al. (*2010) The Rap1 guanine nucleotide exchange factor C3G is required for preservation of larval muscle integrity in Drosophila melanogaster. *PloS one,* **5**, e9403.

Siekhaus D., Haesemeyer M., Moffitt O. & Lehmann R. (2010) RhoL controls invasion and Rap1 localization during immune cell transmigration in Drosophila. *Nature cell biology,* **12**, 605–10.

Sierralta J. & Mendoza C. (2004) PDZ-containing proteins: alternative splicing as a source of functional diversity. *Brain research. Brain research reviews,* **47**, 105–15.

Spahn P., Huelsmann S. & Rehorn K.-P. *et al. (*2014) Multiple regulatory safeguards confine the expression of the GATA factor Serpent to the hemocyte primordium within the Drosophila mesoderm. *Developmental biology,* **386**, 272–9.

Spahn P., Ott A. & Reuter R. (2012) The PDZ-GEF protein Dizzy regulates the establishment of adherens junctions required for ventral furrow formation in Drosophila. *Journal of cell science,* **125**, 3801–12.

Spradling A.C. & Rubin G.M. (1982) Transposition of cloned P elements into Drosophila germ line chromosomes. *Science (New York, N.Y.),* **218**, 341–7.

St Johnston D. (2002) The art and design of genetic screens: Drosophila melanogaster. *Nature reviews. Genetics,* **3**, 176–88.

Tanaka H., Takasu E., Aigaki T., Kato K., Hayashi S. & Nose A. (2004) Formin3 is required for assembly of the F-actin structure that mediates tracheal fusion in Drosophila. *Developmental biology,* **274**, 413–25.

Tanaka S., Morishita T. & Hashimoto Y. *et al. (*1994) C3G, a guanine nucleotide-releasing protein expressed ubiquitously, binds to the Src homology 3 domains of CRK and GRB2/ASH proteins. *Proceedings of the National Academy of Sciences of the United States of America,* **91**, 3443–7.

Tautz D. & Pfeifle C. (1989) A non-radioactive in situ hybridization method for the localization of specific RNAs in Drosophila embryos reveals translational control of the segmentation gene hunchback. *Chromosoma,* **98**, 81–5.

Tepass U., Fessler L.I., Aziz A. & Hartenstein V. (1994) Embryonic origin of hemocytes and their relationship to cell death in Drosophila. *Development (Cambridge, England),* **120**, 1829–37.

Thorpe H.M. & Smith M.C. (1998) In vitro site-specific integration of bacteriophage DNA catalyzed by a recombinase of the resolvase/invertase family. *Proceedings of the National Academy of Sciences of the United States of America,* **95**, 5505–10.

Touriol C., Bornes S. & Bonnal S. *et al. (*2003) Generation of protein isoform diversity by alternative initiation of translation at non-AUG codons. *Biology of the cell,* **95**, 169–78.

Wang H., Singh S.R. & Zheng Z. *et al. (*2006) Rap-GEF signaling controls stem cell anchoring to their niche through regulating DE-cadherin-mediated cell adhesion in the Drosophila testis. *Developmental cell,* **10**, 117–26.

Wang L., Kounatidis I. & Ligoxygakis P. (2014) Drosophila as a model to study the role of blood cells in inflammation, innate immunity and cancer. *Frontiers in Cellular and Infection Microbiology,* **3**, 113.

Wennerberg K., Rossman K.L. & Der C.J. (2005) The Ras superfamily at a glance. *Journal of cell science,* **118**, 843–6.

Wittchen E.S., Aghajanian A. & Burridge K. (2011) Isoform-specific differences between Rap1A and Rap1B GTPases in the formation of endothelial cell junctions. *Small GTPases,* **2**, 65–76.

Wood W., Faria C. & Jacinto A. (2006) Distinct mechanisms regulate hemocyte chemotaxis during development and wound healing in Drosophila melanogaster. *The Journal of cell biology,* **173**, 405–16.

Wood W. & Jacinto A. (2007) Drosophila melanogaster embryonic haemocytes: masters of multitasking. *Nature reviews. Molecular cell biology,* **8**, 542–51.

Worthylake R.A., Lemoine S., Watson J.M. & Burridge K. (2001) RhoA is required for monocyte tail retraction during transendothelial migration. *The Journal of cell biology,* **154**, 147–60.

Wunderlich Z., Bragdon M.D. & DePace A.H. (2014) Comparing mRNA levels using in situ hybridization of a target gene and co-stain. *Methods (San Diego, Calif.),* **68**, 233–41.

Zeller R., Haramis A.G. & Zuniga A. *et al. (*1999) Formin defines a large family of morphoregulatory genes and functions in establishment of the polarising region. *Cell and tissue research,* **296**, 85–93.

Zwartkruis F.J. & Bos J.L. (1999) Ras and Rap1: two highly related small GTPases with distinct function. *Experimental cell research,* **253**, 157–65.

<u>Literature</u>

Campos-Ortega, J., & Hartenstein, V. (1985). The embryonic development of *Drosophila melanogaster*. *Springer Verlag, Berlin, Heidelberg*.

Lindsley, D.L., & Zimm, G. (1992). *The genome of Drosophila melanogaster. Academic Press. San Diego, CA.*

Nguyen, H., & Quilliam, L.A. (2012). *Encyclopedia of Signaling Molecules (Choi, Sangdun. Editor.), Chapter Rap GEF Family (pp1590-1596). Springer Verlag, New York.*

Wittinghofer, A., (2014). *Ras Superfamily Small G Proteins: Biology and Mechanisms 1+2. Springer Verlag, Wien.*

6. Appendix

A
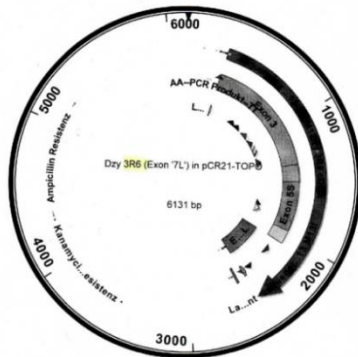
B
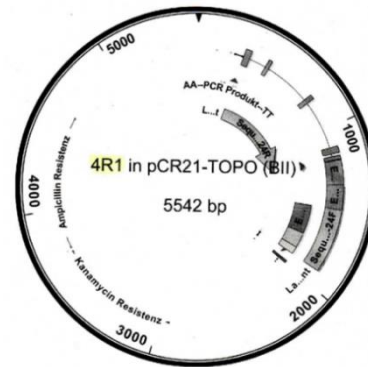
C

D
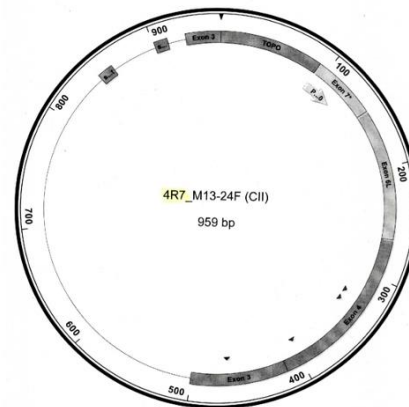
E
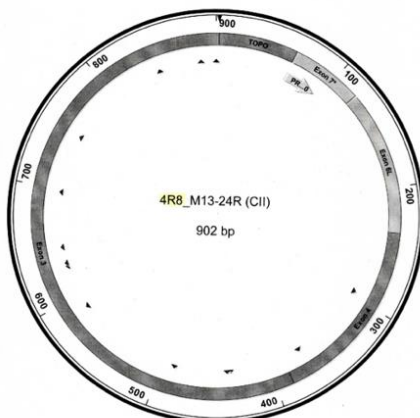
Fig. S1 Plasmid maps of the found *dzyB and dzyC in TOPO TA* constructs.
Production of *dzyB* clone *3#6* (A), *dzyB* clone *4#1* (B), *dzyC* clone *4#4 (C), dzyC* clone *4#7 (D)* and *dzyC* clone *4#8 (*E) gene constructs by total RNA isolation, cDNA synthesis, PCR and TOPO TA cloning. Plasmid map was generated by SeqBuilder software (DNASTAR).

Tab. S1 *UAS-dzyA*, *UAS-dzyB* and *UAS-dzyC* transgenic lines.
The three constructs *dzyA in pUAST, dzyB in pUAST* and *dzyC in pUAST* were injected into *w⁻* embryos. *UAS-dzyA* strain was commissioned externally from a *Drosophila* embryo injection service. The *UAS-dzyB* and the *UAS-dzyC* strains were produced by injection in the laboratory (Department of Animal Genetics). Fly strains were tested for the presence of the *dzy in pUAST* construct. The different *UAS-dzy* strains, including the position of their insertion, are listed in the table. The strains marked with the pink star were used for further experiments.

	UAS-dzyA line		Location
UAS-dzyA	UAS-dzyA 1	★	2nd Chromosome

	UAS-dzyB line		Location
N5_7 #1	UAS-dzyB 1	★	3rd Chromosome
N6/7_18 #1	UAS-dzyB 2		2nd Chromosome
N6/7_18 #3	UAS-dzyB 3	★	2nd Chromosome
N6/7_23 #1	UAS-dzyB 4	★	3rd Chromosome
N6/7_23 #2	UAS-dzyB 5		3rd Chromosome

	UAS-dzyC line		Location
Fly strain collection, 1303	UAS-dzyC 1	★	2nd Chromosome
Fly strain collection, 1307	UAS-dzyC 2		2nd Chromosome

A

dzyA in pUAST clone 4

14.296 kp
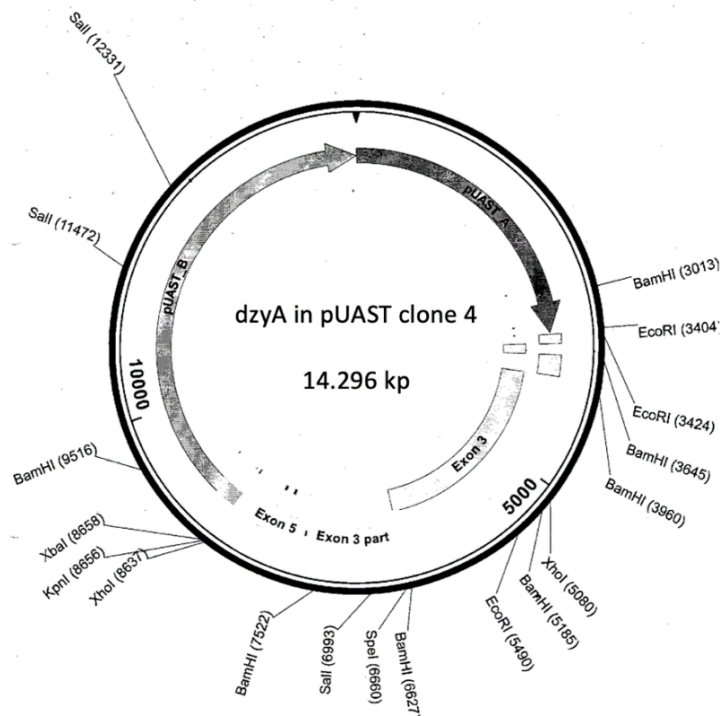
B
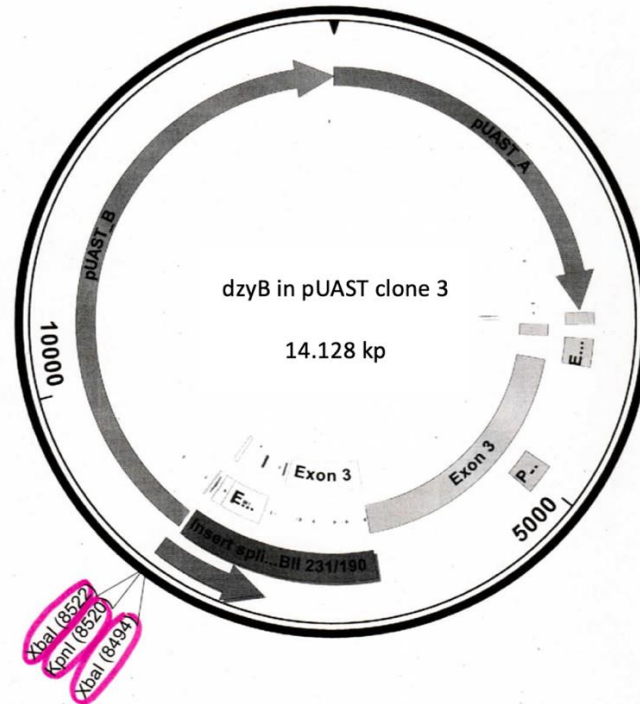
C
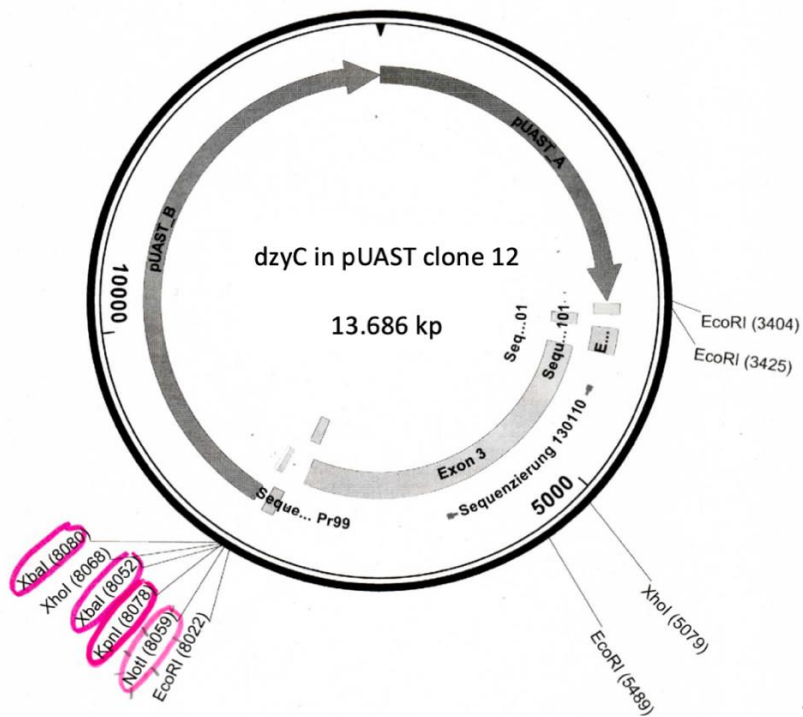
Fig. S2 Plasmid maps of the *dzy in pUAST* constructs.
Cloning of *dzyA in pUAST* clone 4 (A), *dzyB in pUAST clone 3* (B) and *dzyC in pUAST clone 12* (C) gene constructs via PCR and RE-digestion. *pUAST* vector and the *dzy* fragment, features and digestion restriction sites created by SeqBuilder software (DNASTAR).

Tab. S2 *UAS-dzyCΔPDZ* transgenic lines.

The constructs *dzyCΔPDZ in pUAST* was injected into *w⁻* embryos. *dzyCΔPDZ* strain was commissioned externally from a *Drosophila* embryo injection service (Fly Facility, France). Fly strains were tested for the presence of the *dzyCΔPDZ in pUAST* construct. The different *UAS-dzyCΔPDZ* strains, including the position of their insertion, are listed in the table. The strain marked with the pink star was used for further experiments.

	UAS-dzyCΔPDZ line		Location
14716-2-1M	UAS-dzyCΔPDZ 1	☆	2nd Chromosome
14716-2-2M	UAS-dzyCΔPDZ 2		3rd Chromosome
14716-2-3M	UAS-dzyCΔPDZ 3		2nd Chromosome
14716-2-4M	UAS-dzyCΔPDZ 4		3rd Chromosome
14716-2-5M	UAS-dzyCΔPDZ 5		X Chromosome
14716-2-6M	UAS-dzyCΔPDZ 6		3rd Chromosome
14716-2-7M	UAS-dzyCΔPDZ 7	☆	3rd Chromosome
14716-2-8M	UAS-dzyCΔPDZ 8		3rd Chromosome
14716-2-9M	UAS-dzyCΔPDZ 9		2nd Chromosome

A UAS-dzyA | 1228

P w; UAS-dzyA/SM1; + **X** w; Df(2L)ED380/CyO; +

F1 w; Df(2L)ED380/UAS-dzyA; +

B Recombination

104 w; Df(2L)ED380/UAS-dzyA; +

$$\frac{w}{w} \; ; \; \frac{Bl \; sp}{SM1} \; ; \; \frac{+}{+} \qquad \mathbf{X} \qquad \frac{w}{w} \; ; \; \frac{Df(2L)ED380 \qquad +}{+ \qquad UAS-dzyA} \; ; \; \frac{+}{+}$$

F2

$$\frac{w}{w} \; ; \; \frac{Df(2L)ED380 \qquad UAS-dzyA}{SM1} \; ; \; \frac{+}{+}$$ Select w+, CyO males (red eyes, curly wings)

$$\frac{w}{w} \; ; \; \frac{Df(2L)ED380 \qquad +}{SM1} \; ; \; \frac{+}{+}$$

$$\frac{w}{w} \; ; \; \frac{+ \qquad UAS-dzyA}{SM1} \; ; \; \frac{+}{+}$$

$$\frac{w}{w} \; ; \; \frac{+ \qquad +}{SM1} \; ; \; \frac{+}{+}$$

C Stock

Cross single ♂ with 4-5 ♀ 104:

		104
w; Df(2L)ED380 UAS-dzyA/ SM1; +	X	w; Bl sp/SM1; +

F3ₐ: w; Df(2L)ED380 UAS-dzyA/ SM1; + → Df(2L)ED380/UAS-dzyA line

D Complementation

Cross single ♂ (C) with 4-5 ♀ 660:

		660
w; Df(2L)ED380 UAS-dzyA/ SM1; +	X	w; dzy^Δ8/ CyO; +

F3_b:
w; Df(2L)ED380 UAS-dzyA/ dzy^Δ8; + ✝
w; Df(2L)ED380 UAS-dzyA/ CyO; + w⁺, CyO
w; dzy^Δ8/ SM1; + w⁻, CyO
w; SM1/ CyO; + ✝

Fig. S3 Crossing scheme for the generation of the *Df(2L)ED380/UAS-dzyA* effector line.
Recombination of *Df(2L)ED380* and *UAS-dzyA*. Both were recombined on the second chromosome. For recombination, the two alleles were crossed together and females without curly wings were selected among the progeny (A). These females were mated with second chromomsome balancer males and the progeny were selected for the red eye and curly wing phenotype (B). Single males were crossed with 4 - 5 second chromosome balancer virgin females to generate a Df(2L)ED380/UAS-dzyA strain (C). Positive recombinants, i.e. stocks that have both the *Df(2L)ED380* and the *UAS-dzyA* alleles on the same chromosome, were lethal over the *dzy^Δ8* mutant allele. To identify positive recombination, the single males from (C) were screened over *dzy^Δ8* for lethality (D). The identified recombinants were sequenced to confirm the recombination.
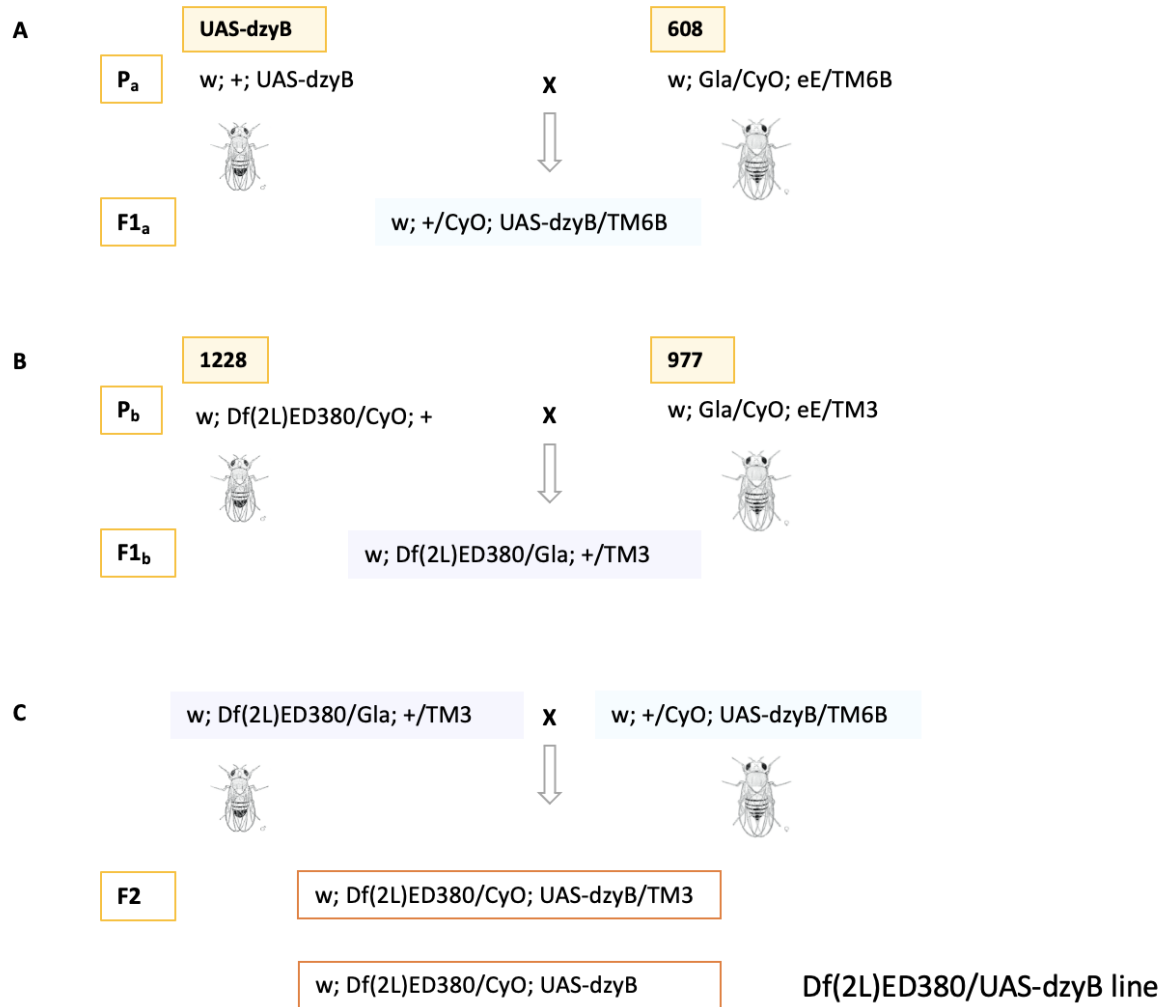
Fig. S4 Crossing scheme for the generation of the *Df(2L)ED380/UAS-dzyB* effector line.
(A) and (B) 5 males of the strains carrying *Df(2L)ED380* or the *UAS-dzyB* allele were mated with 20 virgin females of the multibalancer stocks 608 and 977. (C) Combination of *Df(2L)ED380* and *UAS-dzyB* to generate *the Df(2L)ED380/UAS-dzyB* effector line. Males carrying *Df(2L)ED380* on chromosome 2 balanced over Gla and virgin females carrying *UAS-dzyB* on chromosome 3 balanced over TM6B were crossed and the progeny was screened for flies with the two chromosomal markers Cy and Sb.
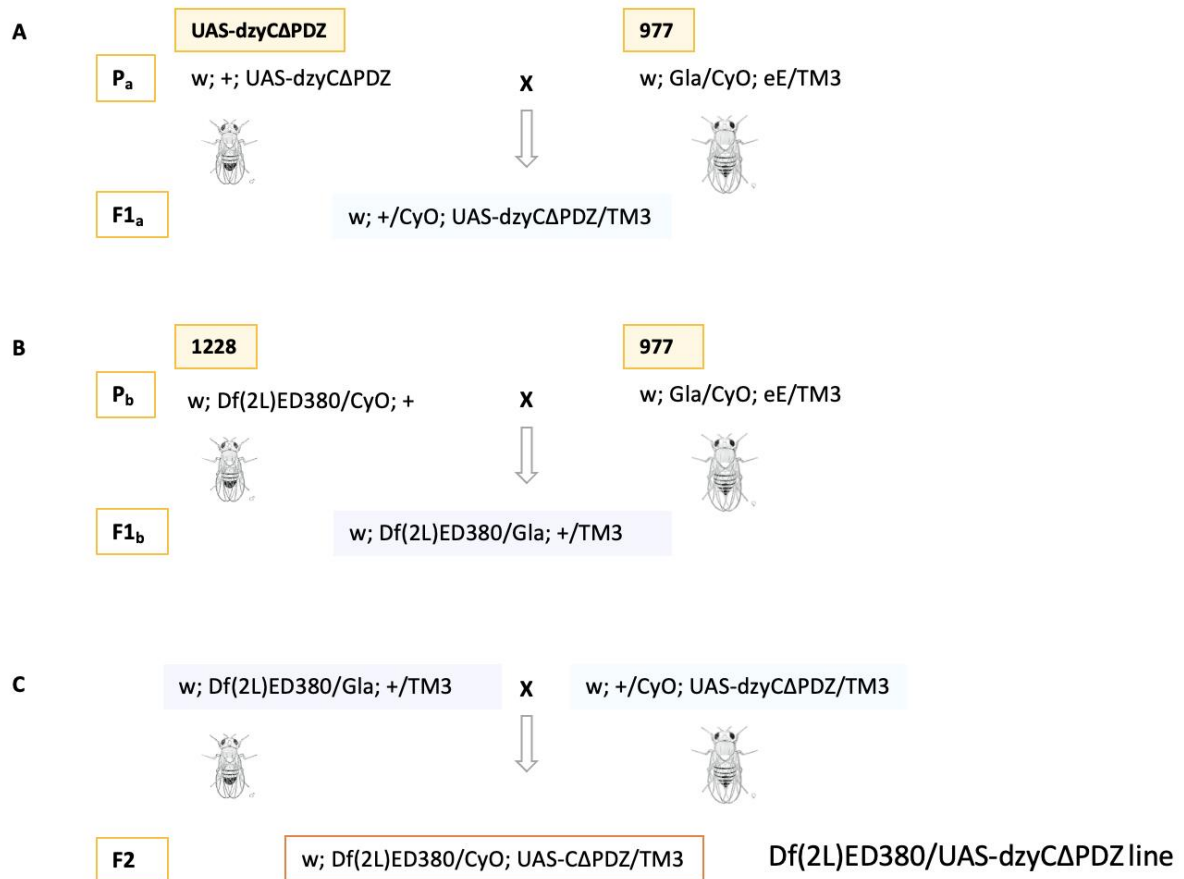
Fig. S5 Crossing scheme for the generation of the *Df(2L)ED380/UAS-dzyCΔPDZ* effector line.
(A) and (B) 5 males of the strains carrying *Df(2L)ED380* or the *UAS-dzyCΔPDZ* allele were mated with 20 virgin females of the multibalancer stock 977. (C) Combination of *Df(2L)ED380* and *UAS-dzyCΔPDZ* to generate the *Df(2L)ED380/UAS-dzyCΔPDZ* effector line. Males carrying *Df(2L)ED380* on chromosome 2 balanced over Gla and virgin females carrying *UAS-dzyCΔPDZ* on chromosome 3 balanced over TM3 were crossed and the progeny was screened for flies with the two chromosomal markers Cy and Sb.
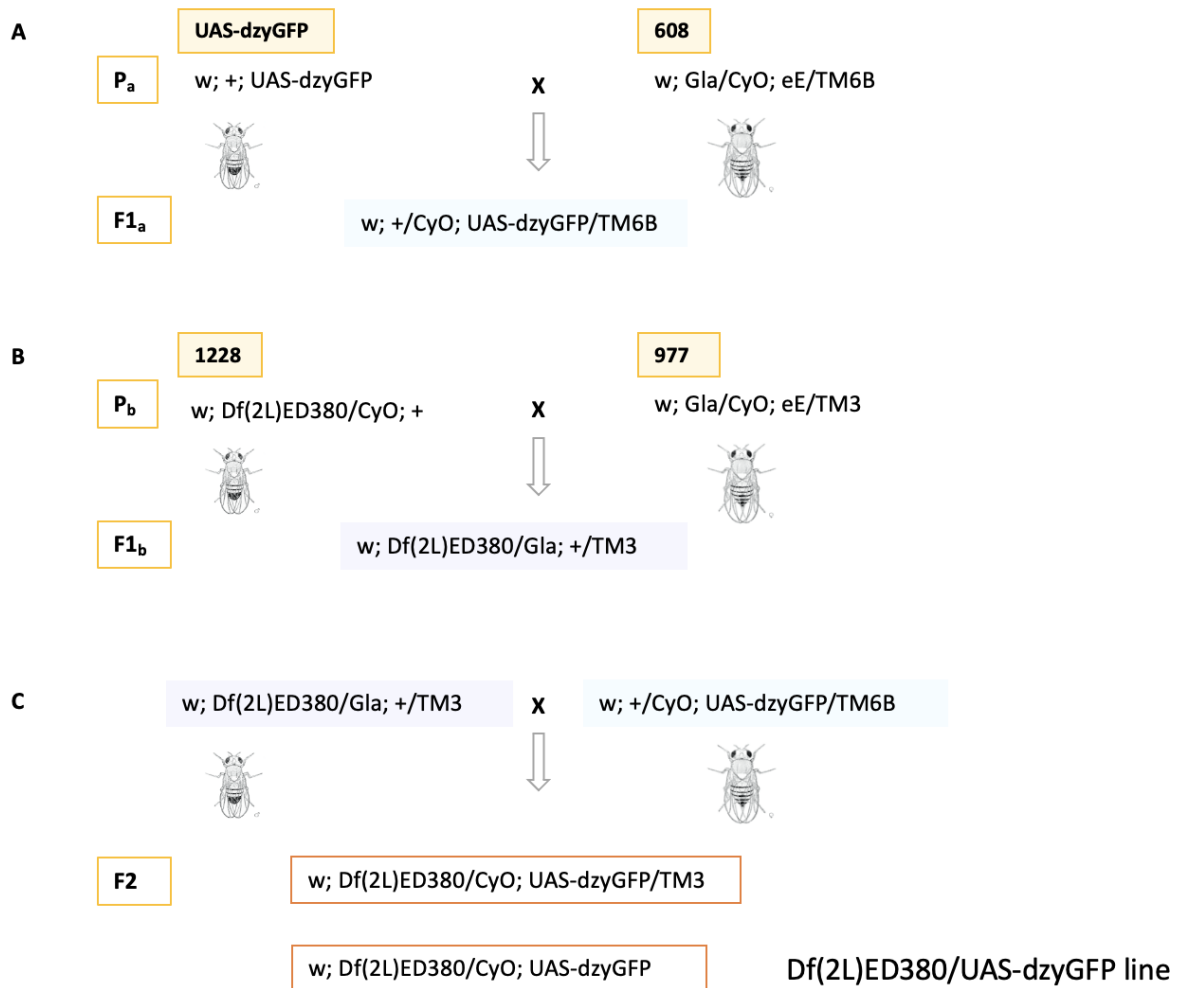
Fig. S6 Crossing scheme for the generation of the *Df(2L)ED380/UAS-dzyGFP* effector line.
(A) and (B) 5 males of the strains carrying *Df(2L)ED380* or the *UAS-dzyGFP* allele were mated with 20 virgin females of the multibalancer stocks 608 and 977. (C) Combination of *Df(2L)ED380* and *UAS-dzyGFP* to generate the *Df(2L)ED380/UAS-dzyGFP* effector line (positive control for further experiments). Males carrying *Df(2L)ED380* on chromosome 2 balanced over Gla and virgin females carrying *UAS-dzyGFP* on chromosome 3 balanced over TM6B were crossed and the progeny was screened for flies with the two chromosomal markers Cy and Sb.

A
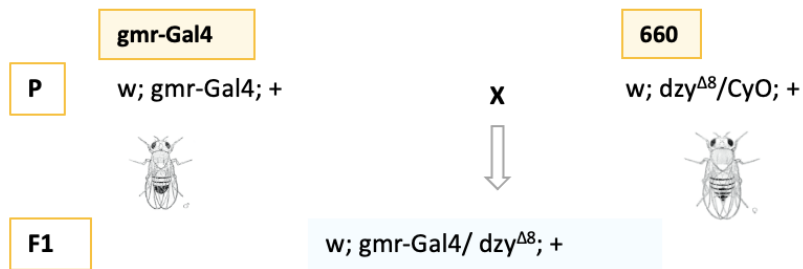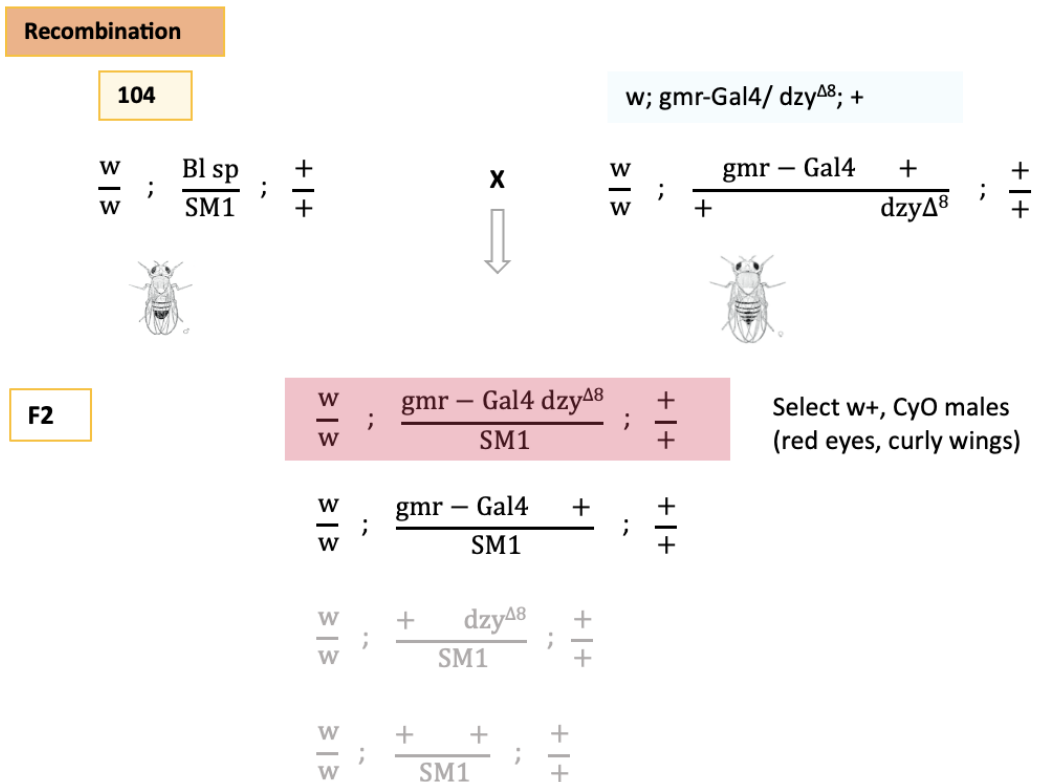
gmr-Gal4   660

P   w; gmr-Gal4; +   X   w; dzy$^{\Delta 8}$/CyO; +

F1   w; gmr-Gal4/ dzy$^{\Delta 8}$; +

B   Recombination

104   w; gmr-Gal4/ dzy$^{\Delta 8}$; +

$$\frac{w}{w} \; ; \; \frac{Bl\ sp}{SM1} \; ; \; \frac{+}{+} \qquad X \qquad \frac{w}{w} \; ; \; \frac{gmr-Gal4 \qquad +}{+ \qquad dzy\Delta^8} \; ; \; \frac{+}{+}$$

F2

$$\frac{w}{w} \; ; \; \frac{gmr-Gal4\ dzy^{\Delta 8}}{SM1} \; ; \; \frac{+}{+}$$ Select w+, CyO males (red eyes, curly wings)

$$\frac{w}{w} \; ; \; \frac{gmr-Gal4 \qquad +}{SM1} \; ; \; \frac{+}{+}$$

$$\frac{w}{w} \; ; \; \frac{+ \qquad dzy^{\Delta 8}}{SM1} \; ; \; \frac{+}{+}$$

$$\frac{w}{w} \; ; \; \frac{+ \qquad +}{SM1} \; ; \; \frac{+}{+}$$

183

C | Stock |

Cross single ♂ with 4-5 ♀ 104:

| 104 |

w; gmr-Gal4 dzy$^{\Delta 8}$/ SM1; +   **X**   w; Bl sp/SM1; +

| F3$_a$ | w; gmr-Gal4 dzy$^{\Delta 8}$/ SM1; +   **gmr-Gal4/dzy$^{\Delta 8}$ line**

D | Complementation |

Cross single ♂ (C) with 4-5 ♀ 660:

| 660 |

w; gmr-Gal4 dzy$^{\Delta 8}$/ SM1; +   **X**   w; dzy$^{\Delta 8}$/ CyO; +

| F3$_b$ |

w; gmr-Gal4 dzy$^{\Delta 8}$/ dzy$^{\Delta 8}$; +   †

w; gmr-Gal4 dzy$^{\Delta 8}$/ CyO; +   w$^+$, CyO

w; dzy$^{\Delta 8}$/ SM1; +   w$^-$, CyO

w; SM1/ CyO; +   †
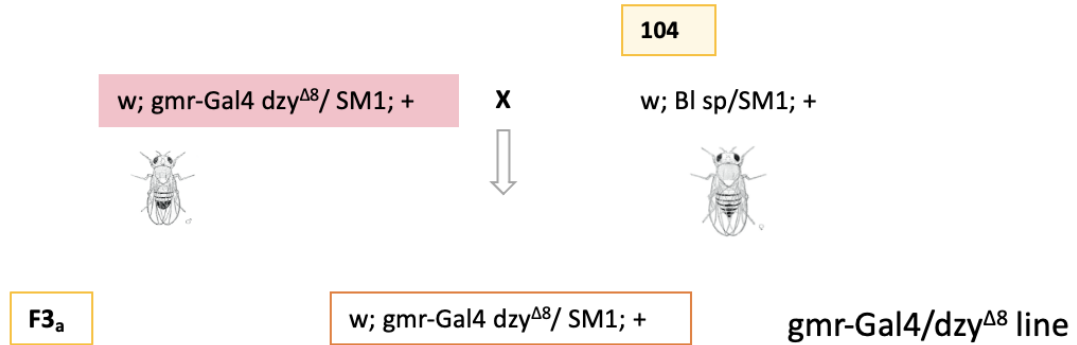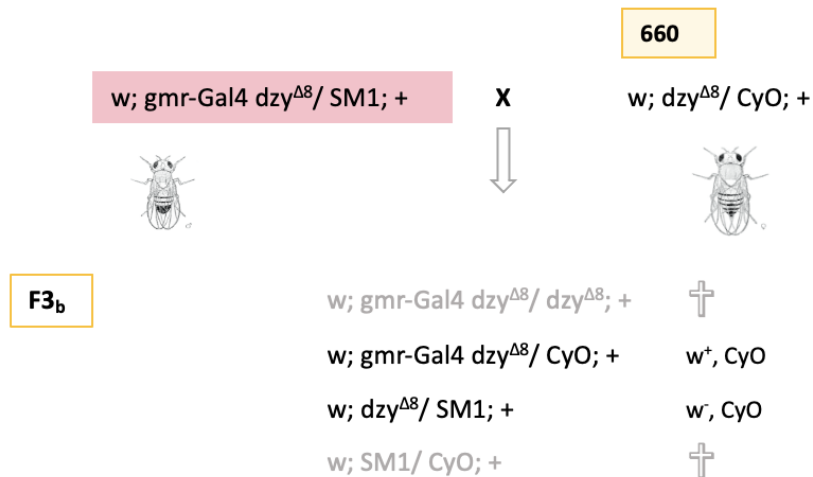
Fig. S7 Crossing scheme for the generation of the *dzy$^{\Delta 8}$/gmr-Gal4* activator line.
Recombination of *gmr-Gal4* and *dzy$^{\Delta 8}$*. Both were recombined on the second chromosome. For recombination, the two alleles were crossed together and females without curly wings were selected among the progeny (A). These females were mated with second chromomsome balancer males and the progeny were selected for the red eye and curly wing phenotype (B). Single males were crossed with 4 - 5 second chromosome balancer virgin females to generate a *dzy$^{\Delta 8}$/gmr-Gal4* strain (C). Positive recombinants, i.e. stocks that have both the *gmr-Gal4* and the *dzy$^{\Delta 8}$* alleles on the same chromosome, had to be lethal over the *dzy$^{\Delta 8}$* mutant allele. To identify positive recombination, the single males from (C) were screened over *dzy$^{\Delta 8}$* for lethality (D). The identified recombinants were sequenced to confirm the recombination.

A dzyA

P **Activator line** w; dzy^Δ8 gmr-Gal4/SM1; +   X   **Effector line** w; Df(2L)ED380 UAS-dzyA/SM1; +

F1 w; dzy^Δ8 gmr-Gal4 /Df(2L)ED380 UAS-dzyA; +

w; dzy^Δ8 gmr-Gal4 /SM1; +
w; Df(2L)ED380 UAS-dzyA /SM1; +

B dzyB

P **Activator line** w; dzy^Δ8 gmr-Gal4/SM1; +   X   **Effector line** w; Df(2L)ED380/CyO; UAS-dzyB

F1 w; dzy^Δ8 gmr-Gal4 /Df(2L)ED380; + /UAS-dzyB

w; dzy^Δ8 gmr-Gal4 /CyO; + /UAS-dzyB
w; Df(2L)ED380 /SM1; + /UAS-dzyB

C dzyC

P **Activator line** w; dzy^Δ8 gmr-Gal4/SM1; +   X   **Effector line** w; Df(2L)ED380/CyO; UAS-dzyC

F1 w; dzy^Δ8 gmr-Gal4 /Df(2L)ED380; + /UAS-dzyC

w; dzy^Δ8 gmr-Gal4 /CyO; + /UAS-dzyC
w; Df(2L)ED380 /SM1; + /UAS-dzyC

D dzyCΔPDZ

P **Activator line** w; dzy^Δ8 gmr-Gal4/SM1; +   X   **Effector line** w; Df(2L)ED380/CyO; UAS-dzyCΔPDZ/TM3

F1 w; dzy^Δ8 gmr-Gal4 /Df(2L)ED380; + /UAS-dzyCΔPDZ

w; dzy^Δ8 gmr-Gal4 /Df(2L)ED380; + /TM3
w; dzy^Δ8 gmr-Gal4 /CyO; + /UAS-dzyCΔPDZ
w; dzy^Δ8 gmr-Gal4 /CyO; + /TM3
w; Df(2L)ED380/SM1; + /UAS-dzyCΔPDZ
w; Df(2L)ED380/SM1; + /TM3

E dzyGFP

P **Activator line** w; dzy^Δ8 gmr-Gal4/SM1; +   X   **Effector line** w; Df(2L)ED380/CyO; UAS-dzyGFP

F1 w; dzy^Δ8 gmr-Gal4 /Df(2L)ED380; + /UAS-dzyGFP

w; dzy^Δ8 gmr-Gal4 /CyO; + /UAS-dzyGFP
w; Df(2L)ED380 /SM1; + /UAS-dzyGFP

F Δ

P **Activator line** w; dzy^Δ8 gmr-Gal4/SM1; +   X   **1228** w; Df(2L)ED380/CyO; +

F1 w; dzy^Δ8 gmr-Gal4 /Df(2L)ED380; +

w; dzy^Δ8 gmr-Gal4 /CyO; +
w; Df(2L)ED380 /SM1; +

Fig. S8 Crossing scheme for combining the activator line (*dzy^Δ8/gmr-Gal4*) and the effector lines. The depicted crossing scheme was used to obtain transgenic flies expressing the different *dzy* splice forms in a *dzy* mutant background (*dzy^Δ8/Df(2L)ED380*). 20 virgin females of the activator line (*dzy^Δ8/gmr-Gal4*) were mated with 5 males of the effector line (*Df(2L)ED380/UAS-dzyA* (A), *Df(2L)ED380/UAS-dzyB* (B), *Df(2L)ED380/UAS-dzyC* (C), *Df(2L)ED380/UAS-dzyCΔPDZ* (D) or *Df(2L)ED380/UAS-dzyGFP* (E)). A *Df(2L)ED380* line without UAS transgene (Δ, Fly strain collection stock 1228) was used as negative control (F). The F1 generation was screened for the different phenotypes with special focus on the eye phenotype. Flies carrying the dominant marker Cy (*dzy^Δ8*/CyO and *Df(2L)ED380*/CyO) were counted and discarded. Flies carrying *dzy^Δ8* and *Df(2L)ED380* on the 2nd chromosome and thus not showing curved wings were collected and examined for their eye-phenotypes: eye^+ and eye^- escaper.

A

ey-Gal4

660

P   w; gmr-Gal4/CyO; +   X   w; dzy$^{\Delta 8}$/CyO; +

F1   w; ey-Gal4/ dzy$^{\Delta 8}$; +

B

Recombination

104   w; ey-Gal4/ dzy$^{\Delta 8}$; +

$$\frac{w}{w} \; ; \; \frac{Bl \; sp}{SM1} \; ; \; \frac{+}{+} \qquad X \qquad \frac{w}{w} \; ; \; \frac{ey - Gal4 \quad +}{+ \qquad dzy\Delta^8} \; ; \; \frac{+}{+}$$

F2

$$\frac{w}{w} \; ; \; \frac{ey - Gal4 \; dzy^{\Delta 8}}{SM1} \; ; \; \frac{+}{+}$$ Select w+, CyO males
(red eyes, curly wings)

$$\frac{w}{w} \; ; \; \frac{ey - Gal4 \quad +}{SM1} \; ; \; \frac{+}{+}$$

$$\frac{w}{w} \; ; \; \frac{+ \quad dzy^{\Delta 8}}{SM1} \; ; \; \frac{+}{+}$$

$$\frac{w}{w} \; ; \; \frac{+ \quad +}{SM1} \; ; \; \frac{+}{+}$$

C Stock

Cross single ♂ with 4-5 ⚥ 104:

104

w; ey-Gal4 dzy^Δ8^/ SM1; +   X   w; Bl sp/SM1; +

F3_a_   w; ey-Gal4 dzy^Δ8^/ SM1; +   ey-Gal4/dzy^Δ8^ line

D Complementation

Cross single ♂ (C) with 4-5 ⚥ 660:

660

w; ey-Gal4 dzy^Δ8^/ SM1; +   X   w; dzy^Δ8^/ CyO; +

F3_b_

w; ey-Gal4 dzy^Δ8^/ dzy^Δ8^; +   †

w; ey-Gal4 dzy^Δ8^/ CyO; +   w+, CyO

w; dzy^Δ8^/ SM1; +   w-, CyO

w; SM1/ CyO; +   †
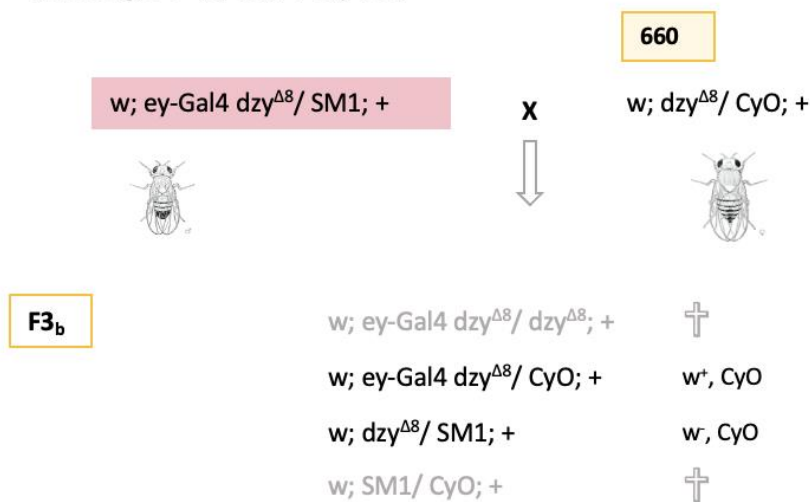
Fig. S9 Crossing scheme for the generation of the *dzy^Δ8^/ey-Gal4* activator line.
(A) Recombination of *ey-Gal4* and *dzy^Δ8^*. Both were recombined on the second chromosome. For recombination, the two alleles were crossed together and females without curly wings were selected among the progeny (A). These females were mated with second chromomsome balancer males and the progeny were selected for the red eye and curly wing phenotype (B). Single males were crossed with 4 - 5 second chromosome balancer virgin females to generate a *dzy^Δ8^/ey-Gal4* strain (C). Positive recombinants, i.e. stocks that have both the *ey-Gal4* and the *dzy^Δ8^* alleles on the same chromosome, were lethal over the *dzy^Δ8^* mutant allele. To identify positive recombination, the single males from (C) were screened over *dzy^Δ8^* for lethality (D). The identified recombinants were sequenced to confirm the recombination.

Fig. S10 Crossing scheme for combining the activator line (*dzy^Δ8/ey-Gal4*) with the different effector lines.

The depicted crossing scheme was used to obtain transgenic flies expressing the different *dzy* splice forms in a *dzy* mutant background (*dzy^Δ8/Df(2L)ED380*). 20 virgin females of the activator line (*dzy^Δ8/ey-Gal4*) were mated with 5 males of the effector line (*Df(2L)ED380/UAS-dzyA* (A), *Df(2L)ED380/UAS-dzyB* (B), *Df(2L)ED380/UAS-dzyC* (C), *Df(2L)ED380/UAS-dzyCΔPDZ* (D) or *Df(2L)ED380/UAS-dzyGFP* (E)). A *Df(2L)ED380* line without UAS transgene (Δ, Fly strain collection stock 1228) was used as negative control. The F1 generation was screened for the different phenotypes with special focus on the eye phenotype. Flies carrying the dominant marker Cy (*dzy^Δ8*/CyO and *Df(2L)ED380*/CyO) were counted and discarded. Flies carrying *dzy^Δ8* and *Df(2L)ED380* on the 2nd chromosome and thus not showing curved wings were collected and examined for their eye-phenotypes: eye^+ and eye^- escaper.

A dzyA

Activator line		Effector line
P	w; $dzy^{\Delta8}$ pdzy-3-Gal4/CyO; +	X	w; Df(2L)ED380 UAS-dzyA/SM1; +

F1: w; $dzy^{\Delta8}$ pdzy-3-Gal4 /Df(2L)ED380 UAS-dzyA; +
w; $dzy^{\Delta8}$ pdzy-3-Gal4 /SM1; +
w; Df(2L)ED380 UAS-dzyA/ CyO; +

B dzyB

P: w; $dzy^{\Delta8}$ pdzy-3-Gal4/CyO; + X w; Df(2L)ED380/CyO; UAS-dzyB

F1: w; $dzy^{\Delta8}$ pdzy-3-Gal4 /Df(2L)ED380; +/UAS-dzyB
w; $dzy^{\Delta8}$ pdzy-3-Gal4 /CyO; +/UAS-dzyB
w; Df(2L)ED380/ CyO; +/UAS-dzyB

C dzyC

P: w; $dzy^{\Delta8}$ pdzy-3-Gal4/CyO; + X w; Df(2L)ED380/CyO; UAS-dzyC

F1: w; $dzy^{\Delta8}$ pdzy-3-Gal4 /Df(2L)ED380; +/UAS-dzyC
w; $dzy^{\Delta8}$ pdzy-3-Gal4 /CyO; +/UAS-dzyC
w; Df(2L)ED380/ CyO; +/UAS-dzyC

D dzyCΔPDZ

P: w; $dzy^{\Delta8}$ pdzy-3-Gal4/CyO; + X w; Df(2L)ED380/CyO; UAS-dzyCΔPDZ/TM3

F1: w; $dzy^{\Delta8}$ pdzy-3-Gal4 /Df(2L)ED380; +/UAS-dzyCΔPDZ
w; $dzy^{\Delta8}$ pdzy-3-Gal4 /Df(2L)ED380; +/TM3
w; $dzy^{\Delta8}$ pdzy-3-Gal4 /CyO; +/UAS-dzyCΔPDZ
w; $dzy^{\Delta8}$ pdzy-3-Gal4 /CyO; +/TM3
w; Df(2L)ED380 /CyO; +/UAS-dzyCΔPDZ
w; Df(2L)ED380 /CyO; +/TM3

E dzyGFP

P: w; $dzy^{\Delta8}$ pdzy-3-Gal4/CyO; + X w; Df(2L)ED380/CyO; UAS-dzyGFP

F1: w; $dzy^{\Delta8}$ pdzy-3-Gal4 /Df(2L)ED380; +/UAS-dzyGFP
w; $dzy^{\Delta8}$ pdzy-3-Gal4 /CyO; +/UAS-dzyGFP
w; Df(2L)ED380 /CyO; +/UAS-dzyGFP

F Δ

Activator line   1228

P: w; $dzy^{\Delta8}$ pdzy-3-Gal4/CyO; + X w; Df(2L)ED380/CyO; +

F1: w; $dzy^{\Delta8}$ pdzy-3-Gal4 /Df(2L)ED380; +
w; $dzy^{\Delta8}$ pdzy-3-Gal4 /CyO; +
w; Df(2L)ED380 /CyO; +

Fig. S11 Crossing scheme for combining the activator line ($dzy^{\Delta8}$/pdzy-3-Gal4) with the different effector lines.
The depicted crossing scheme was used to obtain transgenic flies expressing the different *dzy* splice forms in a *dzy* mutant background ($dzy^{\Delta8}$/*Df(2L)ED380*). 20 virgin females of the activator line ($dzy^{\Delta8}$/*pdzy-3-Gal4*) were mated with 5 males of the effector line (*Df(2L)ED380/UAS-dzyA* (A), *Df(2L)ED380/UAS-dzyB* (B), *Df(2L)ED380/UAS-dzyC* (C), *Df(2L)ED380/UAS-dzyCΔPDZ* (D) *or Df(2L)ED380/UAS-dzyGFP* (E)). A *Df(2L)ED380* line without UAS transgene (Δ, Fly strain collection stock 1228) was used as negative control. The F1 generation was screened for the different phenotypes with special focus on the escaper phenotype. Flies carrying the dominant marker Cy ($dzy^{\Delta8}$/CyO and *Df(2L)ED380*/CyO) were counted and discarded. Flies carrying $dzy^{\Delta8}$ and *Df(2L)ED380* on the 2nd chromosome and thus not showing curved wings were collected and examined for their possible phenotypes: wing⁻, eye⁺ and wing⁺, eye⁻ escaper.

Tab. S3 *UAS-dzyB_GFP* and *UAS-dzyC_GFP* transgenic lines.
The two constructs *UAS-dzyB_GFP* and *UAS-dzyC_GFP* were injected into the attP-containing fly strain *yw, C31; +; 86 FB*. Progeny with red eyes were tested for the presence of the *dzy_GFP in pUASTattB* construct. The different *UAS-dzy_GFP* strains are listed in the two tables. The strains marked with the pink star were used to generate the *UAS-dzyB_GFP ØPhiC31* and *UAS-dzyC_GFP ØPhiC31* lines.

	UAS-dzyB_GFP line	
dzyB_GFP Platte 1,2,3,4,5,6 Nr. 1	UAS-dzyB_GFP 1	★
dzyB_GFP Platte 3 Nr. 3	UAS-dzyB_GFP 2	
dzyB_GFP Platte 3 Nr. 4	UAS-dzyB_GFP 3	
dzyB_GFP Platte 4,5 Nr. 7	UAS-dzyB_GFP 4	
dzyB_GFP #1	UAS-dzyB_GFP 5	
dzyC_GFP #5	UAS-dzyB_GFP 6	★
dzyC_GFP #8	UAS-dzyB_GFP 7	
dzyC_GFP #10	UAS-dzyB_GFP 8	
dzyC_GFP #12	UAS-dzyB_GFP 9	
dzyC_GFP #13	UAS-dzyB_GFP 10	

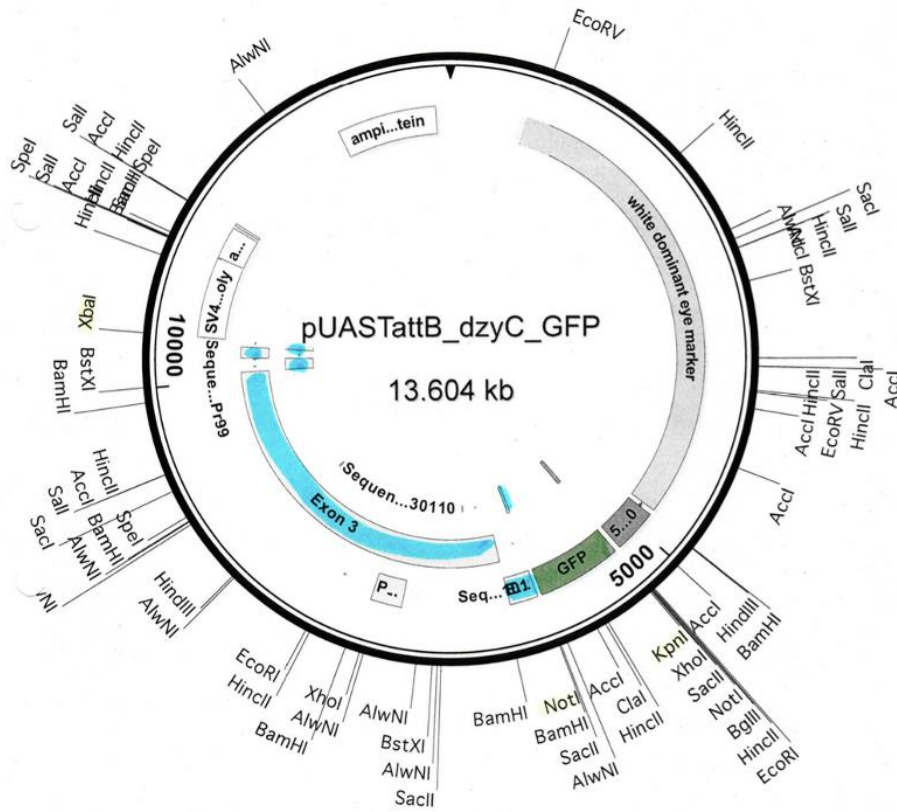|	UAS-dzyC_GFP line	
dzyC_GFP Platte 1,2,3,4 Nr. 3	UAS-dzyC_GFP 1	★
dzyC_GFP Platte 1,2,3,4 Nr. 5	UAS-dzyC_GFP 2	
dzyC_GFP Platte 1,2,3,4 Nr. 7	UAS-dzyC_GFP 3	
dzyC_GFP Platte 8 Nr. 7	UAS-dzyC_GFP 4	
dzyC_GFP Platte 8 Nr. 13	UAS-dzyC_GFP 5	
dzyC_GFP Platte 13 Nr. 5	UAS-dzyC_GFP 6	
dzyC_GFP #4	UAS-dzyC_GFP 7	
dzyC_GFP #9	UAS-dzyC_GFP 8	
dzyC_GFP #11	UAS-dzyC_GFP 9	★
dzyC_GFP #20	UAS-dzyC_GFP 10	

A

B

191
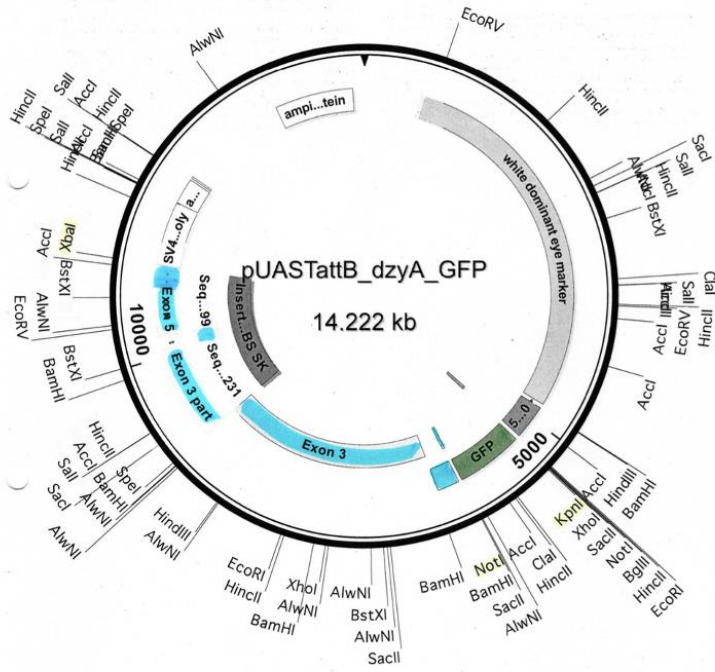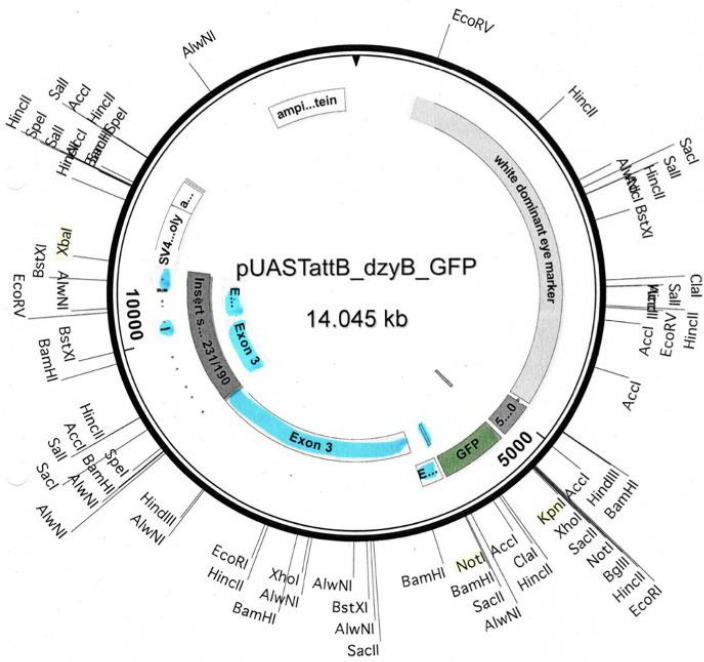
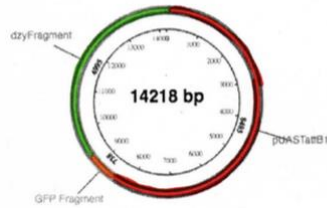**Fig. S12 Plasmid maps of the *dzy_GFP in pUASTattB* constructs (RE-digestion)**.
Cloning of *dzyA_GFP in pUASTattB* (A), *dzyB_GFP in pUASTattB* (B) and *dzyC_GFP in pUASTattB* (C) gene constructs via RE-digestion. *pUASTattB* vector with the *GFP* and the *dzy* fragment, features and digestion restriction sites created by SeqBuilder software (DNASTAR).

A   dzyA_GFP in pUASTattB

New Assembly
Created: 8/19/2019, 10:53:02 AM
Saved: not saved

Component Fragments

Name	Length	Produced by	5' End	3' End
pUASTattB1	8485	Restriction Digest	EcoRI-HF	EcoRI
GFP Fragment	768	PCR	Fwd Primer (auto)	Rev Primer (auto)
dzyFragment	5025	PCR	Fwd Primer (auto)	Rev Primer (auto)

Notes

- Any element of a construction that includes the 5 prime overhang of a restriction site will be altered upon assembly. For example, the essential cysteine codon at the N-terminus of the intein segment of IMPACT vectors is present in the 5 prime overhang of the SapI site in those vectors. The bases removed in the assembly reaction can be added back by including them in the PCR primers for the corresponding insert.
- Primer GFP Fragment_fwd contains a run of 4+ repeats of a mono/di/trinucleotide.
- Primer GFP Fragment_rev has %GC outside of desired range (35-65%) in the annealing segment.

Required oligos

Name	Primer 5' (overlap/spacer/ANNEAL) 3'	Len	%GC	3' %GC	3' Tm	3' Ta
GFP Fragment_fwd	actctgaatagggaattggg CAACATGAGTAAAGGAGAAGAACTTTTCACTGGAGTTG	58	41	40	70.7	71.7
GFP Fragment_rev	cggatccataGCGGCCGCGGAAGAGGAA	28	64	72	74.5	71.7
dzyFragment_fwd	ccgcggccgcTATGGATCCGTATCACCATATC	32	59	41	60.3	59.1
dzyFragment_rev	cggccgcagatctgttaacgAGCGTTTAAGGGAGTATG	38	53	44	58.1	59.1

Build Settings

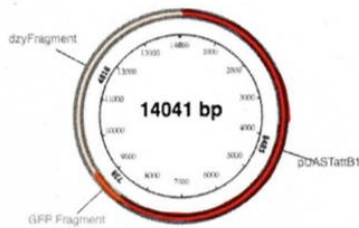| Property	Value
Product/Kit	#E5520 NEBuilder HiFi DNA Assembly Cloning Kit
Minimum Overlap	20 nt
Minimum Overlap Tm	48 °C
Circularize	Yes
PCR Polymerase/Kit	Q5 High-Fidelity DNA Polymerase
PCR Primer Conc.	500 nM

B   dzyB_GFP in pUASTattB

New Assembly
Created: 8/19/2019, 10:53:02 AM
Saved: not saved

Component Fragments

Name	Length	Produced by	5' End	3' End
pUASTattB1	8485	Restriction Digest	EcoRI-HF	EcoRI
GFP Fragment	768	PCR	Fwd Primer (auto)	Rev Primer (auto)
dzyFragment	4848	PCR	Fwd Primer (auto)	Rev Primer (auto)

Notes

- Any element of a construction that includes the 5 prime overhang of a restriction site will be altered upon assembly. For example, the essential cysteine codon at the N-terminus of the intein segment of IMPACT vectors is present in the 5 prime overhang of the SapI site in those vectors. The bases removed in the assembly reaction can be added back by including them in the PCR primers for the corresponding insert.
- Primer GFP Fragment_fwd contains a run of 4+ repeats of a mono/di/trinucleotide.
- Primer GFP Fragment_rev has %GC outside of desired range (35-65%) in the annealing segment.

Required oligos

Name	Primer 5' (overlap/spacer/ANNEAL) 3'	Len	%GC	3' %GC	3' Tm	3' Ta
GFP Fragment_fwd	actctgaatagggaattggg CAACATGAGTAAAGGAGAAGAACTTTTCACTGGAGTTG	58	41	40	70.7	71.7
GFP Fragment_rev	cggatccataGCGGCCGCGGAAGAGGAA	28	64	72	74.5	71.7
dzyFragment_fwd	ccgcggccgcTATGGATCCGTATCACCATATC	32	59	41	60.3	61.3
dzyFragment_rev	cggccgcagatctgttaacgTTCTGATTGCTGGCGAAATTG	41	51	43	63.6	61.3

Build Settings

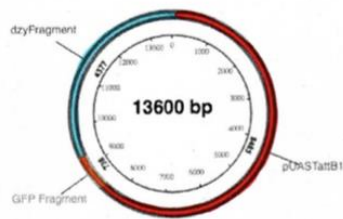| Property	Value
Product/Kit	#E5520 NEBuilder HiFi DNA Assembly Cloning Kit
Minimum Overlap	20 nt
Minimum Overlap Tm	48 °C
Circularize	Yes
PCR Polymerase/Kit	Q5 High-Fidelity DNA Polymerase
PCR Primer Conc.	500 nM

C   dzyC_GFP in pUASTattB

New Assembly
Created: 8/19/2019, 10:53:02 AM
Saved: not saved

Component Fragments

Name	Length	Produced by	5' End	3' End
pUASTattB1	8485	Restriction Digest	EcoRI-HF	EcoRI
GFP Fragment	768	PCR	Fwd Primer (auto)	Rev Primer (auto)
dzyFragment	4407	PCR	Fwd Primer (auto)	Rev Primer (auto)

13600 bp

Notes

- Any element of a construction that includes the 5 prime overhang of a restriction site will be altered upon assembly. For example, the essential cysteine codon at the N-terminus of the intein segment of IMPACT vectors is present in the 5 prime overhang of the SapI site in those vectors. The bases removed in the assembly reaction can be added back by including them in the PCR primers for the corresponding insert.
- Primer GFP Fragment_fwd contains a run of 4+ repeats of a mono/di/trinucleotide.
- Primer GFP Fragment_rev has %GC outside of desired range (35-65%) in the annealing segment.

Required oligos

Name	Primer 5' (overlap/spacer/ANNEAL) 3'	Len	%GC	3' %GC	3' Tm	3' Ta
GFP Fragment_fwd	actctgaataggggaattggg CAACATGAGTAAAGGAGAAGAACTTTTCACTGGAGTTG	58	41	40	70.7	71.7
GFP Fragment_rev	cggatccataGCGGCCGCGGAAGAGGAA	28	64	72	74.5	71.7
dzyFragment_fwd	ccgcggccgcTATGGATCCGTATCACCATATC	32	59	41	60.3	61.3
dzyFragment_rev	cggccgcagatctgttaacgTTCTGATTGCTGGCGAAATTG	41	51	43	63.6	61.3

Build Settings

Property	Value
Product/Kit	#E5520 NEBuilder HiFi DNA Assembly Cloning Kit
Minimum Overlap	20 nt
Minimum Overlap Tm	48 °C
Circularize	Yes
PCR Polymerase/Kit	Q5 High-Fidelity DNA Polymerase
PCR Primer Conc.	500 nM

Fig. S13 Required oligos and plasmid maps of the *dzy_GFP in pUASTattB* constructs (NEBuilder Assembly Mix).
Cloning of *dzyA_GFP in pUASTattB* (A), *dzyB_GFP in pUASTattB* (B) and *dzyC_GFP in pUASTattB* (C) constructs using NEBuilder HiFi DNA Assembly Mix. NEBuilder Assembly Tool was used to design primers with overlapping sequences for the NEBuilder HiFi DNA Assembly reaction. Plasmid maps of the final constructs and a summary of the primers used for cloning, created by NEBuilder Assembly Tool (nebulider.neb.com), are shown in (A), (B) and (C).

7. Acknowledgements

First of all, I would like to thank my PhD dissertation supervisor and group leader Prof. Dr. Rolf Reuter for giving me the opportunity to conduct my research in this lab and for providing me with an interesting and challenging scientific environment. I am very grateful to PD Dr. Bernard Moussian for giving me the opportunity to complete this PhD and for his helpful comments, advice and support. He provided the right encouraging environment. Furthermore, I would like to thank Dr. Uwe Irion for reading my thesis and writing the the secondary evaluation. I also want to thank all the staff members of the Department of Animal Genetics for their warm cooperation and pleasant working atmosphere. Special thanks go to Dr. Denise Dewald in particular, for her advice and support, and helpful and entertaining discussions about science, life and everything else. I would like to thank Dr. Sven Huelsmann for our lively biological debates and the intellectual stimulation during my time in the lab. I would like to thank Karin Henzler for her enduring cheerfulness and her continual help in every situation. My special thanks go to our technical staff, Nicole Gehring, Ulrike Engels-Bochtler and Linnea Ossenkop for making life in the lab a lot easier. I always felt welcome when asking for help. Last but not least, I want to thank my family and friends for supporting me, for being patient and persistent and never losing the faith in my ability to finish the thesis, even when it took some time.